EFFICIENCY ANALYSIS AND OPTIMAL CONTROL OF E-HAILING SERVICE UNDER DEMAND SURGE AFTER MASS GATHERING EVENTS

SU HANG

PhD

The Hong Kong Polytechnic University

This programme is jointly offered by The Hong Kong Polytechnic University and Tongji University

2025

The Hong Kong Polytechnic University

Department of Industrial and Systems Engineering

Tongji University

College of Transportation

Efficiency Analysis and Optimal Control of E-hailing Service under Demand Surge after Mass Gathering Events

Su Hang

A thesis submitted in partial fulfillment of the requirements for the degree of Doctor of Philosophy

January 2025

CERTIFICATE OF ORIGINALITY

I hereby declare that this thesis is my own work and that, to the best of my knowledge and belief, it reproduces no material previously published or written, nor material that has been accepted for the award of any other degree or diploma, except where due acknowledgement has been made in the text.

_____(Signed)

SU Hang (Name of student)

ABSTRACT

When mass gathering events (such as concerts or sports events) end, the demand for passenger flow in limited areas often increases sharply, which not only puts enormous pressure on the transportation system, but also brings significant safety risks. As an emerging mode of transportation, the introduction of e-hailing services not only enhances transportation capacity, but also provides a new approach for evacuating large passenger flows. However, despite a large amount of research in recent years focusing on the impact of e-hailing services on urban transportation, there is still little in-depth exploration of their application potential and control strategies in responding to large passenger flow events. In response to this research gap, innovative and systematic analysis has been conducted to improve the service efficiency of e-hailing services when large passenger flows happen.

This thesis focuses on how to make e-hailing services efficiently and reasonably serve the evacuation of passengers in urban transportation systems. The following three problems are addressed, to improve e-hailing service's management under demand surge conditions.

We first address the control problem of e-hailing vehicles in an evacuation system under demand surge case. A mathematical model with Trip-based Macroscopic Fundamental Diagram (MFD) representation is proposed to capture the dynamic passenger evacuation rates and traffic conditions within a bi-modal system. We adopt Logit model to determine passengers' mode choice between bus and e-hailing vehicles during evacuation. To accelerate passenger evacuation in such scenarios, we introduce two perimeter control strategies based on Proportional-Integral (PI) controller. These strategies regulate the total inflow rate of e-hailing vehicles and background traffic based on vehicle accumulation and the number of parked vehicles within the area, respectively.

The second part investigates the pricing problem of e-hailing services in a two-region evacuation system. We improve the above Trip-based MFD model to illustrate the time-varying evolution of e-hailing vehicles within a two-region transportation system. The model takes into account the bilateral dynamics of drivers' repositioning decisions, passengers' demand dynamics, and dispatching between the two parties. To assist the e-hailing platform in ensuring a balanced distribution of e-hailing vehicle supply within a two-region transportation system, we propose a region-dependent pricing strategy and compare it with the undifferentiated static

pricing strategy. This strategy adjusts e-hailing drivers' per unit time wages in different regions, guiding passengers' and drivers' behaviors in the market effectively.

Furthermore, we explore the design of boarding space in a bi-modal evacuation system, considering both efficiency and safety under demand surge case. The evacuation dynamics are captured utilizing three-dimensional macroscopic fundamental diagram (3D-MFD). We model the total generalized cost including users' cost, operating cost and safety cost. Passengers' mode choice between bus and e-hailing vehicles is also determined by Logit model. Two types of safety cost are mainly considered, including both pedestrian-vehicle conflicts and pedestrian-pedestrian conflicts. Four transport scenarios with different boarding space design are modeled and compared.

The effectiveness of the models and control methods proposed for the three problems are all validated by respective extensive numerical experiments. Managerial insights are also derived for relevant stakeholders.

PUBLICATIONS ARISING FROM THE THESIS

Journal Papers

1. **Su, H.**, Wang X., Liu, W, Zhang X., Xu, M., 2024. Modelling and accelerating the passenger evacuation process in a bi-modal system with bus and e-hailing modes after mass gathering events. *Travel Behaviour and Society*, 35, 100713.
2. **Su, H.**, Xu, M., Wang X., Zhang X., 2024. A region-dependent e-hailing service pricing strategy for rapid massive evacuation. *Transportation Research Part D*, 136, 104399.
3. **Su, H.**, Wang X., Xu, M., Zhang X., 2025. Boarding space design for passenger evacuation with bus and e-hailing services under a surge in traffic demand. *Travel Behaviour and Society*, 40, 101021.

Conference Presentations

1. **Su, H.**, Xu, M., Wang X., Zhang X., 2024. A region-dependent e-hailing service pricing strategy for rapid massive evacuation. *Presentation at the 2024 INFORMS Annual Meeting*.
2. **Su, H.**, Xu, M., Wang X., Zhang X., 2024. A region-dependent e-hailing service pricing strategy for rapid massive evacuation. *Presentation at the PolyU ISE Research Student Conference 2024*. (Best presenter of EML session)
3. **Su, H.**, Wang X., Liu, W, Zhang X., Xu, M., 2023. Modelling and accelerating the passenger evacuation process in a bi-modal system with bus and e-hailing modes after mass gathering events. *Presentation at the 13th Production and Operations Management Society - Hong Kong Chapter International Conference*.
4. **Su, H.**, Wang X., Liu, W, Zhang X., 2021. Perimeter control of e-hailing vehicle inflow rate under demand surge after mass gathering events. *Presentation of the Annual Conference of Traffic Flow and Data Science Committee of Shanghai Society of Mechanics*.

ACKNOWLEDGMENTS

Firstly, I want to convey my heartfelt thanks and admiration to my supervisor, Prof. Xu Min, for her immense support, encouragement, and invaluable mentorship during my PhD studies at The Hong Kong Polytechnic University. Her profound expertise, insightful wisdom, and unwavering passion for research have significantly influenced my ideas, refined my research methods, and motivated me to strive for excellence. I am profoundly grateful to Prof. Xu for fostering an intellectual environment of freedom and autonomy, while simultaneously challenging me to think critically, creatively, and meticulously. Her insightful comments, helpful advice, and professional mentorship have significantly influenced my research and empowered me to unlock my full capabilities. I am also grateful to Prof. Zhang Xiaoning from Tongji University for providing me with the opportunity for joint training, which has greatly contributed to my personal and academic development.

Furthermore, I express my gratitude to the members of my thesis committee for their perceptive insights, constructive criticisms, and continuous encouragement throughout the evolution of my research. Their expert guidance has significantly elevated the quality and reach of my work. Additionally, I am deeply thankful to the faculty members and researchers in the Department of Industrial and Systems Engineering for their mentorship, collaborative efforts, and valuable feedback, which have been instrumental in the development and refinement of my research endeavor.

I also want to acknowledge the support, understanding, and encouragement of my colleagues and friends during the various phases of my PhD journey. Especial thanks want to give my research team members—Dr. Wu Ting, Dr. Yan Xiaoyuan, Dr. Peng Shouguo, Dr. Huang Jiangyan, Dr. Ji Rumei, Dong Pingping, Ren Qiaoqiao, Wang Yilun, Chen Xiaohua, Ran Tanghong, Tu Lin, Xiong Ya, Rong Donglei. Heartfelt thanks are extended to my office colleagues of VA335—Dr. Zhao Dongning, Dr. Hu Yusha, Dr. Cui Yanqing, Dr. Cai Xing, Dr. Zhu Yongyang, Dr. Bai Wuliyasu, Zhu Ruonan, Liu Lingrui, Chen Xuanlai. Their companionship and joy have made this path more enjoyable and rewarding.

Lastly, but importantly, I offer my profound thanks to my parents and my husband for their unwavering dedication, steadfast support, and immense love. I am deeply grateful for the love and support they have given me.

CONTENTS

LIST OF FIGURES

LIST OF TABLES

CHAPTER 1 INTRODUCTION

This chapter gives an introduction of this thesis, covering the following key areas: (i) background (Section 1.1); (ii) research scope and objectives (Section 1.2) and (iii) thesis organization (Section 1.3).

1.1 Background

1.1.1 Urban emergency management towards special events

With the rapid advancement of urbanization in our country, the scale of cities continues to expand, and various special traffic incidents are becoming more frequent. These events are often influenced by multiple factors such as extreme weather, special events, or social events. For example, after a large-scale event (such as a concert, sports event, or celebration), the surge in passenger flow often leads to overcrowding, pushing, and disorderly movement, posing serious safety risks to passengers in densely populated areas, and may even pose a serious threat to people's lives and property safety. Tragedies of the crowd disasters have occurred many times over the past years. According to Hsieh et al. (2009), from 1980 to 2007, a total of 215 human stampedes is recorded in all geographical regions, and they resulted in 7069 deaths and at least 14,078 injuries. Table.1.1 lists some of the serious crowd safety accidents both domestically and internationally since 2010.

From Table.1.1, it can be seen that these safety incidents typically have the following characteristics: (1) large crowds gathering due to specific activities; (2) The organizer has oversight in management and failed to effectively guide the crowd, resulting in delayed evacuation of passengers. The cumulative effect of multiple factors is like a domino effect, affecting more people through a chain reaction and causing serious impacts on the road transportation system. This situation indicates that effectively managing the evacuation process after large-scale events and ensuring passenger safety has become an important issue that urgently needs to be addressed in urban emergency management.

In the research field of crowd management and evacuation, mass gathering events are usually not defined as disasters due to their limited scale and impact. Instead, they are typically regarded as management challenges, where the primary concern is efficiency rather than fairness and humanitarianism. These challenges can be analyzed and optimized through scientific methods

Table 1.1 Serious crowd safety accidents both domestically and internationally since 2010

Time	Location	Casualties	Causes
2010-07	Duisburg, Germany	21 deaths, 342 injuries	”Love Parade” electronic music festival carnival(Helbing and Mukerji, 2012; Krausz and Bauckhage, 2012)
2010-11	A suspension bridge on Diamond Island in Phnom Penh, Cambodia	456 deaths, over 700 injuries	”Water Festival” celebration event, bridge shaking triggers panic(BBC, 2010)
2013-10	Ratangar Temple in Wakaz City, Madhya Pradesh, India	At least 115 deathes, over 100 injuries	Rumors sparked panic(Smith, 2013)
2014-12	Chen Yi Plaza on the Bund in Shanghai, China	36 deaths, 49 injuries	New Year’s Eve event, crowded and trampled by tourists(ChinaDaily, 2015)
2017-11	Sidib Alaram in southwestern Morocco	15 deaths, dozens injuries	Crowds during the Ramadan supplies distribution event caused stampede(BBC, 2017)
2019-08	Algiers Music Festival in Algeria	5 deathes, over 20 injuries	During the festival, the venue was overcrowded, the exits were narrow, and the order was chaotic(Reuters, 2019)
2021-04	Israel Mellon Music Festival	At least 45 deaths, hundreds injuries	Large crowds rushing into narrow passages causing crowding and stampede(Kershner et al., 2021)
2021-11	Astro Music Festival in Houston, USA	10 deaths, over 300 injuries	Overcrowding during the concert, improper management leading to stampede(TheGuardian, 2021)
2022-10	Kagaruhan Stadium in Malang City, East Java Province, Indonesia	132 deaths	Clashes between fans and police, with police using tear gas to try to control the situation, causing panic(BangkokPost, 2022)
2022-10	Itaewon, Seoul, South Korea	154 deathes, more than 100 injuries	Stampede during Halloween party(Kim, 2022)
2023-04	Sana’a, the capital of Yemen	At least 85 deaths, over 300 injuries	Ramadan charity event, cramped venue leading to overcrowding and stampede(AFP, 2023)
2024-07	Hathras, Uttar Pradesh, India	130 deaths, over a hundred injuries	The number of attendees exceeded the venue capacity, resulting in severe stampede (Shandilya, 2024)

in many academic papers and industry standards (Fruin, 1971; Still, 2000; Code, 2012). City managers also have been developing emergency management policies to address such special events. The concept of urban emergency management was proposed by the RAND Institute in New York in 1966 and has been developed for more than 60 years (Green and Kolesar, 2004). Later on, the communication of emergency public warnings was studied in Mileti and Sorensen (1990) from a social science perspective. Perry and Lindell (2003) provided guidance on building a rapid-response emergency planning process. As an indispensable and important part of urban emergency management, emergency traffic management has the characteristics of urgency and large-scale, requiring rapid response and close cooperation of various transportation-related departments, to reliably and effectively organize and implement evacuation operations. The issue of rapid massive evacuation has received continued attention from governments, emergency management agencies, related industries, and academia.

Risks and disruptions induced by evacuation activities

Due to the time-sensitive nature of rapid massive evacuation, longer staying times will double the personal injury and property damage. The ability to evacuate people swiftly can be the deciding factor between life and death, highlighting the importance of efficient evacuation in saving lives. As a result, how to transport people out of the area as quickly as possible after events has become a big concern for mass-gathering event organizers, for sake of avoiding crown disasters. Given that pedestrian evacuation is often the first or last option in escaping a sudden event, transportation agencies around the world are working on how to develop pedestrian emergency plans (Ercolano, 2008). Therefore, in order to avoid serious crowd disasters, how to evacuate people out of the country as soon as possible after the event has become a major concern for organizers of mass gathering activities. Recently, Vermuyten et al. (2016) reviewed the optimisation models for pedestrian evacuation and design problems. Aalami and Kattan (2020) modeled and simulated fairness and efficiency in pedestrian emergency evacuation. Chen et al. (2021b) conducted pedestrian evacuation simulations in indoor emergency situations. However, most pedestrian evacuation studies are limited to indoor scenarios such as buildings, stadiums, and bus stops, rather than urban transportation networks (Shiwakoti et al., 2013). From the perspective of urban networks, personnel evacuation always relies on vehicular evacuation. Rapid vehicle evacuation can accelerate personnel evacuation. Therefore, it would be an important research topic to conduct evacuation analysis from the perspective of

the dynamic evolution of vehicles in urban networks.

Unconventional traffic accidents are likely to increase vehicle mileage, exacerbate traffic congestion, increase energy use and carbon emissions, and increase noise and air pollution. Proper traffic management measures are required to mitigate these negative externalities. Vehicles in urban traffic areas are the main source of many urban air pollutant emissions (HEI, 2010; Bharadwaj et al., 2017; Wang et al., 2024a). The gas emissions they produce will significantly increase the content of harmful gases in the air, contributing up to 45%, 50% and 90% of total Nitrogen Oxides (NOx), Hydrocarbon (HC) and Carbon Monoxide (CO) emissions. Especially when there is traffic congestion and vehicles start to idle in long queues, the content of harmful gases significantly deteriorating air quality (Choudhary and Gokhale, 2016; Mascia et al., 2017). In addition to emissions, traffic congestion leads to increased fuel consumption and increased social costs. To deal with the emergency cases in the urban traffic network, many traffic management policies have been formulated to ensure efficient and reliable operation of urban traffic networks, by considering different control measures (such as traffic signal optimization (Chen et al., 2007; Jahangiri et al., 2011; Parr and Kaisar, 2011; Ren et al., 2013; Marcianò et al., 2015), speed control (Li et al., 2018), route guidance (Chen et al., 2014; Ikeda and Inoue, 2016; Shahparvari et al., 2019; Tamakloe et al., 2021), etc.).

The impact of unconventional traffic accidents will spread from the central area to surrounding adjacent areas, which will further cause vehicle delays, increase congestion, and undermine the stability of traffic flow in the entire urban environment. Saberi et al. (2020) used a simple contagion process to describe spreading of traffic jams in urban networks. In general, the spread of urban traffic emergencies will have a wide-ranging impact on different areas of the city, and the impact will vary depending on the nature of the event and the urban structure. Therefore, it is crucial for urban planning and emergency management to understand and respond to this contagiousness. So far, some of the main types of practical traffic control plans are managed to reduce the traffic impact of special events, such as signal control, dedicated public transit service and subway station-skipping strategy. The primary objective of these control measures is to prioritize the evacuation of passengers within the special event area and distribute the traffic pressure to the surrounding areas. As a crucial aspect of passenger transport studies, dedicated shuttle bus services and/or additional public transport services are typically organized. These measures are designed to swiftly transport passengers out of the event area to nearby stations (Matherly et al., 2014, 2015; Amini et al., 2016).

Mitigation strategies facing evacuation-induced impacts

To mitigate the negative impacts of demand-surges, research problems and studies can be divided into two mainstreams according to the time point of occurrence, which are simulations and facility planning before the occurrence, and responses and treatments during the occurrence.

(1) Simulations and facility planning before the occurrence: Various pedestrian models have been proposed to simulate passenger movements within the demand-surge areas (Kim et al., 2015; Seriani and Fernandez, 2015; Chen et al., 2017; Shahhoseini and Sarvi, 2019; Yi et al., 2020; Xie et al., 2021), so as to investigate the crowd evacuation dynamics features and examine the efficiencies of different pedestrian flow control strategies inside the demand-surge area. Furtherly, combined with facility location and the influence of exit planning, pedestrian evacuation simulations are proposed to improve emergency evacuation effectiveness under the limitations like high-density urban areas (Liu, 2018; Zuo et al., 2021). In the view of a broader perspective, urban space between different modes are redistributed to maximize passenger flows for idealized networks (Zheng and Geroliminis, 2013).

(2) Responses and treatments during the occurrence: Extensive investigations have been conducted on bus bridging services and optimization for passenger evacuation (e.g. Kepaptsoglou and Karlaftis, 2009; Ibeas et al., 2010; Szeto and Wu, 2011; Jin et al., 2014, 2016); real-time traffic signals at the local level are also proposed to provide bus priority with an objective to maximize passenger flows (Christofa et al., 2013, 2016a; Hu et al., 2016); routing optimizations are also proposed for passenger and vehicles to improve the effectiveness of evacuation (He et al., 2021; Zeng et al., 2021); behaviors and performances of crowds under evacuation urgency are investigated to help reduce casualties (Haghani et al., 2020; Chen et al., 2021a).

Ongoing challenges in evacuation strategies making

However, above measures to alleviate transportation pressure always follow the same decision-making model, which is based on evaluating the current event scenario and replicating successful experiences from past events to more effectively address current related issues. However, in special events, traffic pressure relief measures face higher requirements and require more flexible and easy to implement methods to provide real-time decision-making basis.

Looking at the response measures to the above special events, we find that in order to achieve large-scale efficient evacuation of personnel, it is still necessary to rely on the efficient operation

of transportation modes, and the rapid evacuation of personnel always depends on the efficient scheduling and orderly operation of vehicles. Rapid vehicle evacuation not only significantly reduces the time it takes for people to leave, but also reduces the safety risks that can arise due to stranded people. In addition to the traditional bus and metro services, the introduction of new service models and the realization of multimodal transport are critical. Based on this, it will become an important topic to study the dynamic evolution law of vehicles and the synergistic characteristics of traffic flow in urban transportation network, and to propose strategies and methods to accelerate evacuation accordingly. At present, some scholars are no longer limited to a single mode of transportation when studying the issue of bus bridging services. They are starting to explore multimodal transport networks by integrating transportation modes such as highways, railways, aviation, and water transportation. Chen and Miller-Hooks (2012) considered the emergency linkage of multiple traffic modes (highway, railway and aviation) when studying the container transport problems after disasters. The model establishes a multi-layer network, each layer represents a single traffic mode, and establishes virtual nodes and connection arcs in the multimodal transport hub to connect multiple networks. Recently, Sun et al. (2017) put forward the new concept of Temporary Multiple Airport Region (MAR) based on travel time, which includes five ground transportation modes of private car, taxi, bus, subway and light rail, and analyzed the network topology characteristics, similarity clustering and destination overlap within the MAR. This new type of temporary MAR offers valuable insights into optimizing traffic connectivity, operational efficiency, and capacity resource scheduling between multiple airports during emergencies and natural disasters. It also contributes to the development of rapid recovery strategies for multi-modal, three-dimensional transportation systems.

However, due to the short history of e-hailing services, there is currently a lack of literature studying their impact on passenger evacuation during demand surges. Therefore, it is necessary to combine traditional bus and subway services with flexible new modes of transportation, such as shared mobility and e-hailing services. Through technological empowerment, multi-mode collaborative operations can be achieved, enhancing the responsiveness and resource scheduling efficiency of the transportation system, thereby comprehensively improving the effectiveness and efficiency of evacuation.

1.1.2 E-hailing service's management in an urban transportation system

In recent years, the rising prevalence of smartphones, coupled with the rapid advancements in global positioning systems, data repositories, and wireless communication technology, has given rise to the widespread use of smartphone-based online car-hailing applications, exemplified by platforms like Uber and Didi. E-hailing services allow passengers to book rides via mobile apps, offer features like convenience, dynamic pricing, and safety measures such as real-time tracking and user ratings. The integration of advanced information technology has significantly diminished the information barrier between passengers and drivers.

Review of e-hailing service development

Over the past two decades, e-hailing services have experienced remarkable growth and evolution. Originating around 2010 with Uber's pioneering model in San Francisco, e-hailing quickly gained traction as a convenient and real-time transportation option. Uber's success catalyzed global expansion, leading to the rise of competitors like Lyft, Didi, and Ola, and diversification into sectors such as food delivery and freight transportation. However, this rapid growth also brought regulatory challenges, prompting governments to enact measures ensuring safety and fairness. Despite hurdles, technological advancements, including GPS, big data analysis, and AI, have enhanced the efficiency and user experience of e-hailing services. In recent years, there has been a notable shift towards sustainability, with a focus on promoting electric vehicles to reduce emissions and align with urban sustainability goals. Overall, the journey of e-hailing services reflects a dynamic landscape of innovation, competition, and adaptation, shaping urban transportation and providing users with convenient travel solutions.

E-hailing services have revolutionized urban transportation with their smartphone-based apps, enabling passengers to request rides, track vehicles, and pay electronically. Unlike traditional taxis, vehicles are typically privately owned, and pricing is transparent, based on time, distance, and demand. Users can rate drivers and provide feedback, ensuring service quality. With global coverage and innovative technologies like GPS, e-hailing platforms offer efficient, real-time travel solutions. This model has profoundly impacted urban mobility, providing users with flexible options and driving changes in travel behaviors.

E-hailing service's relationship with other transportation modes

There is a complex relationship between e-hailing services and other transportation modes, which involves their mutual influence and competition in the urban transportation system. Initially, e-hailing services caused dissatisfaction in the traditional taxi industry. Traditional taxi companies believe that e-hailing services enter the market in a more flexible and convenient way, leading to competition. This has led to a tense relationship between the traditional taxi industry and e-hailing services in some cities, sometimes even triggering demonstrations and protests. A plenty of studies compare the differences between these two modes from different perspectives or under different cases (He and Shen, 2015; Wang et al., 2022; Hu et al., 2022; Zhai et al., 2023; Jaydarifard et al., 2024). However, e-hailing services are considered a supplement to public transportation. In some areas, public transportation may not be able to meet all travel needs, and e-hailing services fill this gap, providing users with more flexible choices. The fast development of smartphone-based e-hailing services offers an attractive alternative to passengers, so that a number of passengers may choose e-hailing service, rather than buses, to leave the event area. Such a substitutive effect of e-hailing service to public transit for daily travel has been reported in many previous literature. For example, Schaller (2017) finds that the bus ridership in NYC declined at the same time as the ridesourcing trip began to grow; when some of subway stations in NYC are closed, an increase of over 30% in the use of ridesourcing services were observed (Hoffmann et al., 2016). From a comprehensive travel and residential survey deployed in seven major U.S. cities, in two phases from 2014 to 2016, Clewlow and Mishra (2017) reports a 6% reduction of transit use among Americans in major cities after using e-hailing. More studies about the interrelationship between public transit and e-hailing service can refer to Paudel and Das (2023), Ribeiro et al. (2024) and Pereira et al. (2024).

With the development of autonomous driving technology, e-hailing services may become one of the main application scenarios for autonomous vehicles. This may further alter the relationship between e-hailing services and other modes of transportation, as it will involve interaction between autonomous vehicles and traditional modes of transportation. Interesting studies related to this topic can refer to Irannezhad and Mahadevan (2022) and Wang et al. (2024b). Overall, the relationship between e-hailing services and other transportation modes is dynamic, influenced by various factors such as urban size, user demand, regulatory policies, and technological innovation.

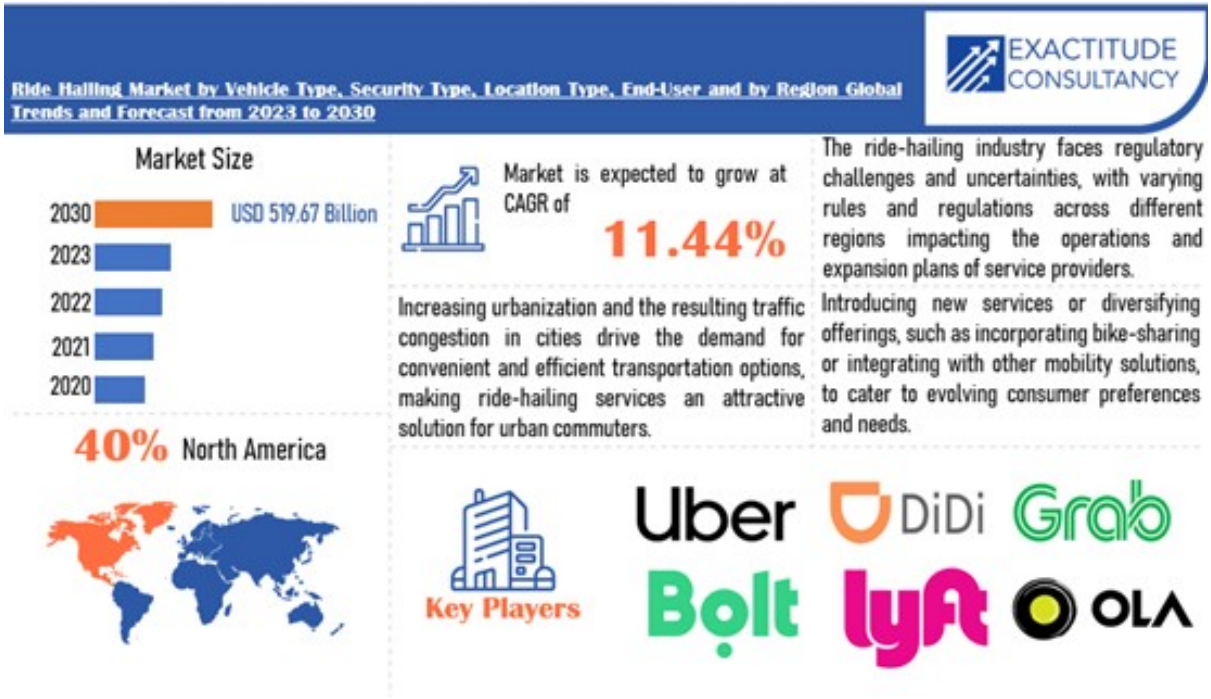

Source:Exactitude Consultancy (2024)

Figure 1.1 Outlook for the e-hailing market in 2030

Global outlook of e-hailing service

The global e-hailing market is fiercely competitive, with key players including companies like Didi, Uber, Grab, Lyft, Ola, Yandex, Bolt, and others. Didi stands as the largest online car-hailing platform in the world, operating across countries such as Mainland China, Australia, Brazil, Chile, Colombia, Costa Rica, Japan, Mexico, and more, boasting over 500 million users and 31 million drivers. Uber, recognized as the most prominent e-hailing platform globally, operates in regions including the United States, Canada, Europe, Latin America, Africa, the Middle East, and Asia Pacific, with over 110 million monthly active users and 5 million drivers. Grab is the largest e-hailing platform in Southeast Asia, covering countries such as Singapore, Malaysia, Indonesia, the Philippines, Thailand, and Vietnam, with over 210 million users and 9 million drivers. Figure 1.1 shows the outlook for the e-hailing market in 2030. The global e-hailing market is expected to continue to rise, growing from $24.347 billion in 2023 to $51.967 billion in 2030, with a compound annual growth rate (CAGR) of 11.44% over the forecast period..

The evolution of China's e-hailing industry dates back to 2009, when a shortage of taxis in the country made it difficult for many passengers to find a ride. The introduction of online taxi-

hailing services, which connect passengers with drivers through Internet technology, helped address the imbalance between supply and demand in the taxi market. This innovation leveraged private vehicles as additional sources of transportation, providing urban residents with a more convenient and comfortable travel option. According to the 53th Statistical Report on China's Internet Development in 2024, as of December 2023, the number of ride hailing users has reached 528 million, an increase of 90.57 million from 2022, with a growth rate of 20.7%, accounting for 48.3% of the total number of Internet users. Especially after the end of large-scale events or when extreme events occur, the demand for e-hailing vehicles' appointment usually increases sharply. In recent years, urban transportation has developed rapidly. The innovation of the new generation of information technology has injected power into the city, and at the same time, the comprehensive transportation system has made leapfrog progress. Urban transportation has gradually entered the era of intelligent transportation. The change of transportation mode not only facilitates the masses, but also provides a new method for studying how to efficiently transport passengers and alleviate congestion in the event of sudden large passenger flow.

In 2023, China's e-hailing industry saw significant recovery and growth, with a market size maintaining high-speed year-on-year growth, reaching 317.6 billion yuan with a 24.5% increase in 2024. Recently, according to the statistics of the online ride hailing regulatory information exchange system, as of October 31, 2024, a total of 362 online ride hailing platform companies in China have obtained operating licenses for online ride hailing platforms, an increase of 2 compared to the previous month; A total of 7.483 million ride hailing driver's licenses and 3.206 million vehicle transportation licenses were issued in various regions, with a month on month increase of 1.4% and 2.1% respectively. The online ride hailing regulatory information exchange system received a total of 1.007 billion orders in October, an increase of 1.9% compared to the previous month. It can be seen that the online ride hailing industry is continuously improving people's travel efficiency. Besides, the competitive landscape of China's e-hailing market is relatively stable. Didi Chuxing, as the largest e-hailing platform, has already occupied the vast majority of the market share, followed by platforms such as Meituan Taxi, Caocao Chuxing, and Shouqi e-hailing.

Necessity of studying e-hailing services in evacuation scenarios

The development process of e-hailing services demonstrates the dynamic innovation of trans-

portation vehicles and modes, which not only profoundly reshapes the urban transportation system, but also plays an important role in the event of emergencies and surging demand. Its flexible scheduling and precise matching characteristics can effectively compensate for the shortcomings of traditional transportation methods and provide more efficient travel services for passengers. In today's society, e-hailing services have become widely popular and frequently integrated into people's daily travel scenes. As the public's dependence on e-hailing services deepens, transportation planners and event organizers must be aware of the profound impact of this service on the efficiency of passenger evacuation in special events. Through rational design and meticulous management, e-hailing services can serve as a core component of multimodal transportation coordination mechanisms. This can ensure that passengers leave the scene quickly and safely with its support, thereby significantly improving the responsiveness and efficiency of urban emergency traffic management.

1.2 Research Scope and Objectives

Given the above background, this study aims to assist e-hailing services in efficiently and reasonably serving passenger evacuation issues in high passenger flow situations from the following three aspects, explore service efficiency analysis and management improvement, and expand the traffic management theory of collaborative evacuation of e-hailing services in special events. Fig.1.2 depicts the research issues to be covered by this study. These research topics are divided into three parts, corresponding to management suggestions for three aspects of e-hailing services.

Part I: E-hailing vehicles' flow control problem considering evacuation efficiency.

This thesis models the evacuation process and proposes a flow control strategy for e-hailing service under mass gathering events. Decision-making basis is expected to be provided for traffic management departments, helping them to handle traffic flow issues more efficiently after large-scale events, ensuring that passengers can quickly leave the activity area, and avoiding traffic congestion and chaos. **Part I** will be explored in Chapter 3.

Part II: E-hailing vehicles' pricing strategy considering platform's response efficiency.

This thesis further assist e-hailing platforms in pricing strategy, to effectively allocate transportation capacity and manage traffic conditions, especially during large gatherings. This

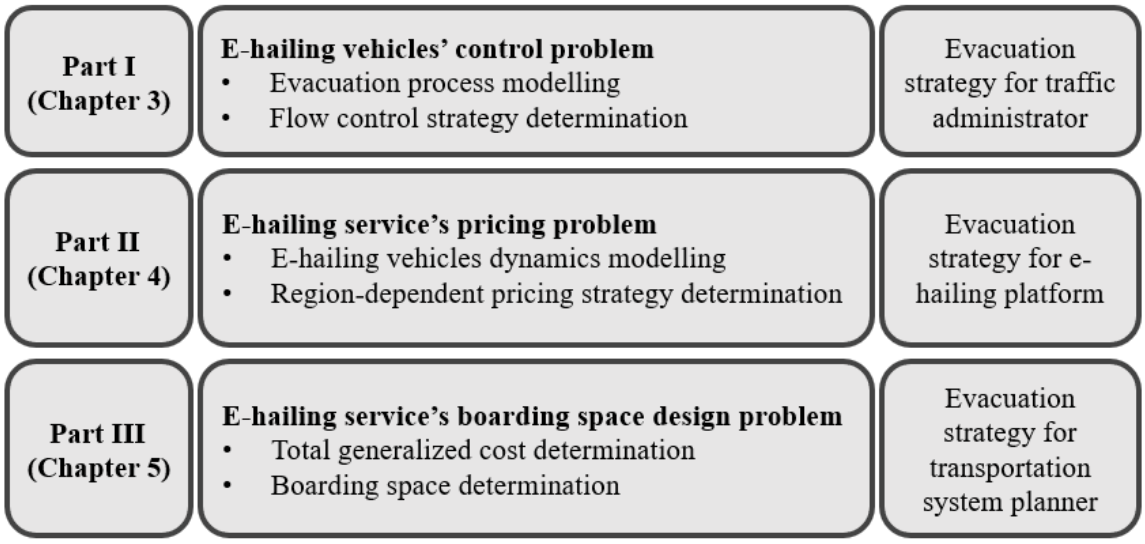

Figure 1.2 Research topics addressed by this study

can significantly improve the response speed of e-hailing platforms to passenger demand and thereby enhancing transportation efficiency. This part of the work helps design appropriate pricing strategies to achieve supply-demand balance between drivers and passengers during peak hours. **Part II** will be explored in Chapter 4.

Part III: E-hailing vehicles' boarding space design considering passengers' safety.

The study explores the design of boarding space in the bi-modal transportation system of buses and e-hailing services. This helps transportation system planners understand the impact of boarding space design on system performance, and thus improve passenger boarding efficiency through reasonable design. The findings of the study can provide decision support for transportation planning and design departments, helping them to design efficient, safe, and economical bi-modal transportation systems in special events. **Part III** will be explored in Chapter 5.

These three research topics collectively tackle key decision-making challenges related to e-hailing service's application in the context of large-scale passenger surges. For each decision-making problem, both mathematical models and solutions will be proposed, which contribute to building a more adaptive, efficient, and sustainable urban mobility framework for emergency scenarios.

1.3 Thesis Organization

The contents of each chapter in this thesis are provided as follows:

Chapter 1 introduces the research background and points out the current situation of urban emergency management and e-hailing service management for special events. It emphasizes the importance of analyzing and improving e-hailing service efficiency in the context of a surge in demand after large-scale gatherings. Meanwhile, this chapter clarifies the main content and objectives of the research.

Chapter 2 summarizes the literature on various traffic control strategies based on MFD models, the characteristics and time-varying strategies of e-hailing services, and the bi-modal transportation system of bus and e-hailing services. Subsequently, the gaps and shortcomings in the research were identified.

Chapter 3 investigates the traffic situation and passenger evacuation dynamics based on MFD models in a bi-modal system that includes both bus and e-hailing service. To alleviate congestion, two perimeter control strategies have been proposed: one based on the number of vehicles entering the direction, and the other based on the number of parking spaces, aimed at improving passenger evacuation efficiency.

Chapter 4 is also based on the MFD model, depicting the evolution of e-hailing vehicles over time in a two-region transportation system composed of high passenger flow areas and their surrounding areas. The study considered bilateral dynamic factors such as driver repositioning decisions, dynamic changes in passenger demand, and matching rates. To this end, a region-dependent pricing strategy has been proposed, which adjusts the unit time wages of e-hailing drivers in different regions to motivate them to improve their service willingness, thereby helping e-hailing platforms manage vehicle capacity reasonably and achieve rapid evacuation.

Chapter 5 explores the design of boarding space in the bi-modal transportation system of bus and e-hailing service. The study characterizes the traffic dynamics of e-hailing and bus services. The generalized cost of evacuating passengers is modelled, taking into account users' cost, operating cost and safety cost. Through numerical examples, this study compared and analyzed four different scenarios of boarding space design, aiming to find a design scheme that minimizes the total cost of the bi-modal transportation system.

Chapter 6 summarizes the research results of this thesis, analyze the shortcomings and propose directions for further research.

CHAPTER 2 LITERATURE REVIEW

This chapter systematically reviews the pertinent literature of the thesis in a sequenced manner, covering the following key areas: (i) multi-types of traffic control strategies with MFD representations (Section 2.1); (ii) e-hailing service's properties and times-varying strategies (Section 2.2) and (iii) multi-modal transportation system (Section 2.3). Besides, the research gaps regarding these dimensions (Section 2.4) are also pointed out.

2.1 Multi-Types of Traffic Control Strategies with Macroscopic Fundamental Diagram Representations

This section reviews the literature of multi-types of traffic control strategies with MFD representations, covering the following key areas: (i) basic concepts and categories of MFD (Subsection 2.1.1); (ii) traffic control strategies based on MFD representations (Subsection 2.1.2) and (iii) transportation network heterogeneity analysis based on MFD representations (Subsection 2.1.3).

2.1.1 Basic concepts and categories of macroscopic fundamental diagram

The macroscopic fundamental diagram (MFD) of networks is always served as a convenient tool to model the dynamic traffic conditions and design appropriate real-time control strategies. An MFD captures the collective traffic flow dynamics of an urban region and relates the vehicle accumulation (or density) to the space-mean speed and trip completion rate within an area. The concept of MFD dates back to Godfrey (1969), but its existence is verified until Geroliminis and Daganzo (2008). This aggregated network-level traffic model (MFD) is demonstrated to have the feature that can connect the traffic variables including space-mean flow, density and speed for urban areas if they are homogeneously congested across space. It proves that under the condition that if congestion is uniformly homogeneous in the region, the MFD of urban traffic provides a unimodal, low-scatter, and demand-insensitive relationship between network vehicle density and network space-mean flow (or outflow). As a result, numerous studies using the MFD approach have assumed that network outflow is directly related to travel production and trip length (Geroliminis, 2015; Ramezani et al., 2015; Liu and Geroliminis, 2016; Saeedmanesh and Geroliminis, 2016). Since then, the properties of analytically tractable of the MFD

has made it an convenient tool for traffic modeling and control strategy design in large scale networks (e.g., Knoop et al. (2012) and Yildirimoglu et al. (2015) for route guidance management, Geroliminis et al. (2012), Haddad et al. (2013) and Haddad (2017b) for boundary traffic control, Zheng and Geroliminis (2016) for parking management, Wei et al. (2020) for multimodal traffic management).

Two classic MFD models were presented in Fig.2.1, namely the Accumulation-based MFD model and the Trip-based MFD model. Accumulation-based MFD model, which is presented in Fig.2.1(a), requires the existence of an outflow-MFD (or speed-MFD and production-MFD). The traffic status within the system is given by a clear relationship between traffic production P (unit: [m/s]) and the number of vehicles $n(t)$, with a unimodal, low dispersion relationship between traffic productivity and the number of vehicles, as shown in Fig.2.1(a). The maximum system productivity P_{max} under a specific number of vehicles n_{cr} exists within the system. When the number of vehicles in the system is between$n_{cr} \leq n(t) \leq n_{max}$, the system productivity P will monotonically decrease. These models assume a steady-state relationship between traffic productivity (the number of kilometers traveled by vehicles per unit time in a region) and vehicle outflow, i.e., a constant average travel length without memory. The basic principle is that the urban road system can be described in an aggregated manner, characterized by its number of vehicles $n(t)$, which is the number of cyclic vehicles at time t (in units of [veh]). At each time t, the average speed V of travelers (in [m/s]) is given by $V(n(t)) = P(n(t))/n(t)$. The travel length L is the same for all travelers and satisfies the following equation:

$$O(n) = \frac{P(n)}{L}, \tag{2.1}$$

where $O(n)$ is the system outflow (in [veh/s]). It may represent the end of a journey in the system or the area of a journey leaving the system. The total demand $\lambda(t)$ for internal or transit travel is always lower than the network capacity, therefore it is not affected by system entry or supply functions. Based on these assumptions, the evolution of the number of vehicles $n(t)$ is given by the following equation:

$$\frac{dn}{dt} = \lambda(t) - O(n(t)) \tag{2.2}$$

If we use the travel time formula based on outflow, that is

$$n(t - T(t)) = N_{\text{out}}(t) - N_{\text{out}}(t - T(t)) = \int_{t-T(t)}^{t} O(n(s))ds \tag{2.3}$$

And when combined with Eq.(2.1), we have,

$$n(t - T(t)) = \int_{t-T(t)}^{t} \frac{P(n(s))}{L} ds. \tag{2.4}$$

Therefore, in the Accumulation-based MFD model, we obtain the following expression for L:

$$L = \frac{1}{n(t - T(t))} \int_{t-T(t)}^{t} P(n(s))ds \tag{2.5}$$

The accumulation-based MFD approach assumes a steady-state relationship between production (veh.km traveled per unit of time in a region) and outflow, which implies a constant average trip length with no memory. However, this assumption may be problematic in certain cases, as the memoryless trip length assumption may not be valid. Therefore, in Mariotte et al. (2017), inconsistent lags for information propagation were observed between boundaries with the traditional accumulation-based MFD model. Overreaction of outflow may lead to unrealistic results, which is due to the inaccuracy of the accumulation-based approach when the demand varies rapidly. Different from accumulation-based MFD model acts in a macro way, the trip-based model acts in a micro way to track the trip length at each moment and to record the dynamic memory. It follows the principle of First In First Out to construct the trip start step function and trip exit step function respectively, as shown in Fig.2.1(b). The driving distance L entered by the driver at time $t - T(t)$ should meet the following requirements:

$$L = \int_{t-T(t)}^{t} V(n(s))ds \tag{2.6}$$

In the trip-based MFD model, we replace $V(n(s))$ with $P(n(s))/n(s)$, and the equation can be changed to:

$$L = \int_{t-T(t)}^{t} \frac{P(n(s))}{n(s)} ds \tag{2.7}$$

It can be seen that the accumulation-based MFD considers the number of vehicles $n(s)(s \in [t - t(t), t])$ as a constant $n(t - t(t))$ for the duration of travel $[t - T(t), t]$, and is used for calculating the length of travel. In contrast, the trip-based model considers the evolution of the number of vehicles over the same time period, making it more realistic. This comparison shows

Table 2.1 Comparison of Characteristics between Accumulation based MFD and Trip based MFD

Features	Accumulation based MFD	Trip based MFD
Definition	MFD based on traffic flow density and flow relationship within the region	MFD based on completed travel quantity and average travel time relationship within the region
Research object	The relationship between the total density (number of vehicles) and traffic flow within the region	The relationship between the trip completion rate and average travel time completed within the region
Data type	Using static data such as traffic density, flow, and speed to construct a relatively smooth and continuous MFD curve	Using dynamic data such as travel volume and average travel time, which do not change continuously in real time, resulting in the image appearing as discrete points rather than completely continuous curves
Applicable scenarios	Suitable for studying long-term road traffic evolution, etc.	Suitable for analyzing short-term road traffic evolution
Advantages	Easy to obtain data from existing traffic perception systems (such as traffic flow detectors)	More intuitive reflection of travel efficiency, but high data demand
Focus	The relationship between vehicle density, flow, and speed within the region	The completion status and average travel time of trips within the region

that the two methods are equivalent in steady-state conditions or when demand changes gradually and the number of vehicles changes slowly. However, in situations like peak hours, the cumulative traffic-based model is expected to be less accurate during the transition phase. We provide a comprehensive comparison of the Accumulation-based MFD and Trip-based MFD methods in various aspects in Table.2.1.

Due to the properties of computationally demanding and problematic to integrate with control, trip-based MFD representation also faces much dilemma when adopted to different cases. A newly developed MFD model, named M-model, provides a decent approximation of trip-based models (Lamotte et al., 2018; Murashkin, 2021; Sirmatel and Geroliminis, 2021). The M-model is an intermediate approach designed to address the limitations of the accumulation-based model by summarizing past events into the total remaining distance, which is then used to update the exit function. In comparison, trip-based models track individual remaining distances, while accumulation-based models do not retain any record of this information. This model provides useful insights and presents an appealing compromise for control applications. Sirmatel et al. (2021) provided a multi-region formulation of the M-model and integrated it successfully in a perimeter control framework.

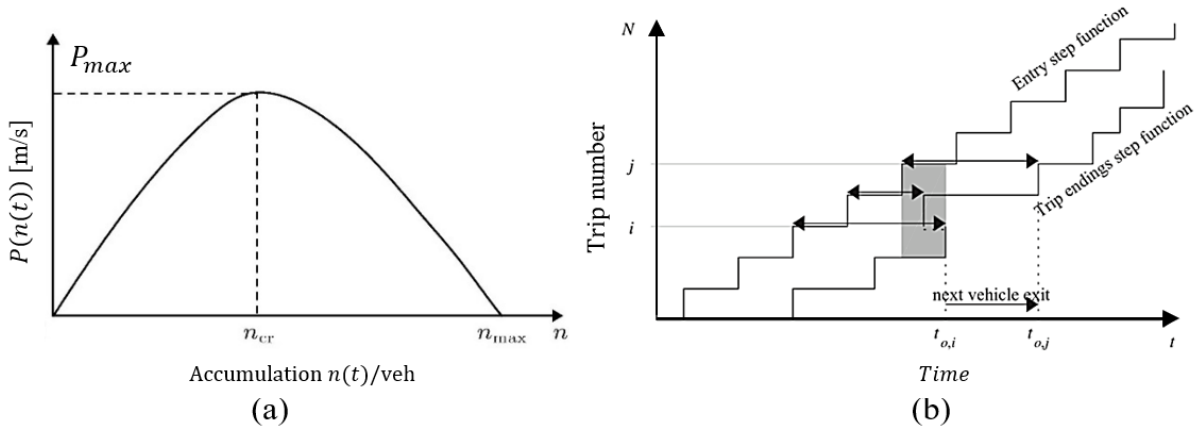

Figure 2.1 Schematic diagram of two classic MFD models

Similar to the studies of Arnott (2013), Fosgerau (2015), Leclercq et al. (2017), Mariotte et al. (2017), and Lamotte and Geroliminis (2018), this research adopts a trip-based approach to reproduce the evacuation process of car traffic on roads and trip state transition. A discrete-time approximation for the trip-based approach was adopted in our numerical studies.

2.1.2 Traffic control strategies based on MFD representations

Different control strategies utilizing the concept of the MFD have been introduced for urban networks. A practical tool, frequently employed against hyper-congested of significant or sensitive links, arteries or urban network parts, is gating-based feedback perimeter control framework (Bretherton et al., 2002; Wood et al., 2002; Austroads, 2010), which is a closed-loop of the problem. Recent works have introduced perimeter feedback-control strategies for a homogeneous urban region in Daganzo (2007) and Keyvan-Ekbatani et al. (2012), or multiple urban regions in Aboudolas and Geroliminis (2013) with the help of the Macroscopic Fundamental Diagram (MFD) representation. In the above studies, a pre-determined set-point is selected carefully, ensuring it falls within a range in the uncongested regime of the MFD, where the slope is positive and near the critical state of the MFD function, i.e. the critical total time spent in Keyvan-Ekbatani et al. (2012) or the critical accumulations in Aboudolas and Geroliminis (2013). Since the first work on MFD-based control considering a single region (see Daganzo (2007), recently many methods for the analysis, modeling, and control via MFD-based traffic modeling have been proposed: Proportional–integral control (e.g. Keyvan-Ekbatani et al., 2012; Aboudolas and Geroliminis, 2013; Keyvan-Ekbatani et al., 2015; Ding et al., 2018; Ingole et al., 2020), optimal control (e.g. Haddad, 2017a,b; Aalipour et al., 2019), robust control (e.g. Haddad and Shraiber, 2014; Haddad, 2015; Ampountolas et al., 2017; Zhong et al., 2018a; Mo-

hajerpoor et al., 2020), adaptive control (e.g. Kouvelas et al., 2014; Haddad and Mirkin, 2016; Haddad and Zheng, 2020; Tsitsokas et al., 2023), control with route choice (Menelaou et al., 2017, 2019), hierarchical control (Fu et al., 2017). Detailed literature reviews of MFD-based modeling and control can be found in Haddad (2017a) and Sirmatel and Geroliminis (2020).

Among these studies, MPC controller has been widely used to optimize an objective function at each time step, to predict the optimal control input for a period of time in the future, which can refer to Kouvelas et al. (2017). Then, the optimized control input is applied to the system and re-optimized in the next time step to form an open-loop optimal control scheme. The advantage lies in that such open-loop control needs no real-time feedback information. However, open-loop control is highly sensitive to changes in system parameters and external disturbances, and increases complexity and computational costs. The performance of the control system greatly depends on the accuracy and fine-tuning of the model used(Tsitsokas et al., 2023). What's more, similarly focusing on capturing the supply-demand relationship and traffic flow dynamics in ride-sharing systems at the aggregated network level, a recent work used the MPC method, which mainly optimized the matching and scheduling control strategies in ride-sharing service, and didn't integrate with price optimization problem(Shen et al., 2023). MPC itself does not directly provide pricing decisions, but influences prices by optimizing scheduling strategies. Therefore, when using MPC for pricing problem design, it further needs combining with other pricing models and algorithms to determine the optimal pricing strategy, which further increases methods' complexity. However, close-loop control can make adjustments based on the actual output and feedback information of the system, compensate for changes in system parameters and external disturbances, which is not only easy and simple to be adopted, but also has good performance in improving system performance and stability.

2.1.3 Transportation network heterogeneity analysis based on MFD representations

The MFD offers a analytically simple and computationally efficient framework for modeling the dynamics of urban traffic networks at an aggregate level. This is because it does not require detailed information about individual links to describe congestion levels and their evolution. Thanks to this advantage, the control problem associated with MFDs can be easily extended from homogeneous regions to more complex, heterogeneous networks. The purpose of dividing into multiple regions is to better model each region's specific traffic flow, which can more accurately describe the traffic flow between different regions. This helps traffic regula-

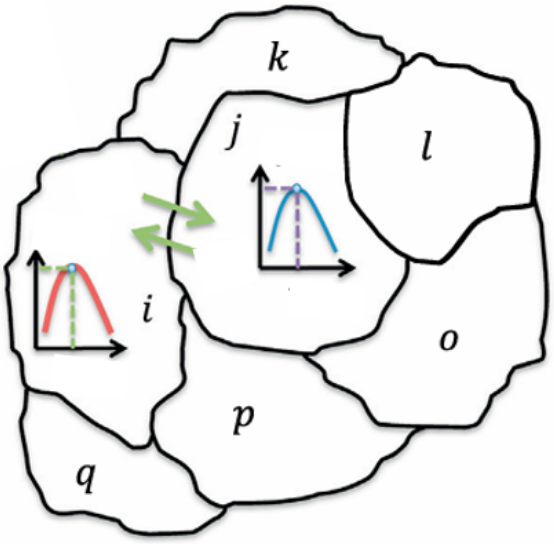

Figure 2.2 A multi-reservoir network based on MFD representation

tors better understand and analyze the dynamic characteristics of urban transportation systems, provides more reliable insights and decisions and achieves more precise traffic management and optimization. By using the MFD approach, urban traffic dynamics can be modeled through the traffic conservation law along with MFDs for a heterogeneous network, provided the network can be divided into several homogeneous subregions (Geroliminis et al., 2012; Haddad and Geroliminis, 2012; Aboudolas and Geroliminis, 2013; Haddad et al., 2013; Haddad, 2015). In the multi-region model, each region has its own independent MFD curve describing its own traffic flow characteristics, as shown in Fig.2.2. The network is modeled as a multi-reservoir system, where each reservoir i follows its own macroscopic fundamental diagram. Each destination reservoir i can be accessed from multiple origin reservoirs, either from the perimeter or boundary of the network.

The control problem connected with MFDs can also be extended from homogeneous region to different heterogeneous networks. Daganzo et al. (2011) proposed a Two-Bin model, exploring the optimal control in a homogeneous traffic network. Dividing the city as a core region and a remote region, Haddad and Geroliminis (2012) conducted a mathematical model to realize the two regions perimeter flow control. Geroliminis et al. (2012) extended the boundary flow control problem of the two regions and solved it by using the model predictive control method to maximize the number of vehicles arriving at the destination. Aboudolas and Geroliminis (2013) divided the city into multiple regions and established a multi-region boundary flow control method. The urban area of San Francisco is divided into three areas in this work and

the simulation results show that after the adoption of control strategy, the number of vehicles waiting in the peripheral area increases, but the traffic volume can still be kept high during peak hours. Haddad et al. (2013) studied the cooperative control problem of two regions and one expressway hybrid network. Hajiahmadi et al. (2015) divided the city into multiple homogeneous regions, established a mixed integer optimization model, and carried out boundary flow control on the regional boundary. The mathematical model of boundary flow control for multiple regions is investigated in Haddad (2015), and the robust constrained boundary flow control for two regions is proposed. Ramezani et al. (2015) divided the city into multiple subregions, established a MFD model based on sub regions, proposed hierarchical boundary flow control, increasing the flow of network traffic, and reducing hysteresis. Ding et al. (2018) proposed a boundary hybrid control method. Zhong et al. (2018a) used a two-state two-region MFDs system model to design a robust continuous-time control Lyapunov function(CLF) based controller. In Zhong et al. (2018b), one-, two-, and multi-region MFD system models are explored, establishing links between the system boundary conditions, inflow demand levels, and the existence of equilibrium points.

2.2 E-hailing Service's Properties and Time-varying Strategies

With the popularity of e-hailing services around the world, studies of e-hailing services and its debatable impacts on urban traffic conditions have attracted abundant research interest in recent years (see Wang and Yang (2019) for a comprehensive review). This section reviews the literature of e-hailing service's properties and time-varying strategies, covering the following key areas: (i) e-hailing service's management strategies design (Subsection 2.2.1); (ii) e-hailing service's impact on transportation network and passengers' travel behavior (Subsection 2.2.2) and (iii) modelling of e-hailing service's time-varying dynamics using the non equilibrium model (Subsection 2.2.3).

2.2.1 E-hailing service's management strategies design

E-hailing platforms are actively implementing management strategies to drive their expansion into new markets (Nie, 2017). These strategies can generally be grouped into one or more of the following categories: pricing, fleet sizing, empty vehicle routing (rebalancing), and dispatching passengers to drivers. Some typical studies mainly focus on the platform's pricing and wage scheme design (e.g. Wang et al., 2016; Castillo et al., 2017; Yang et al., 2020; Lei et al.,

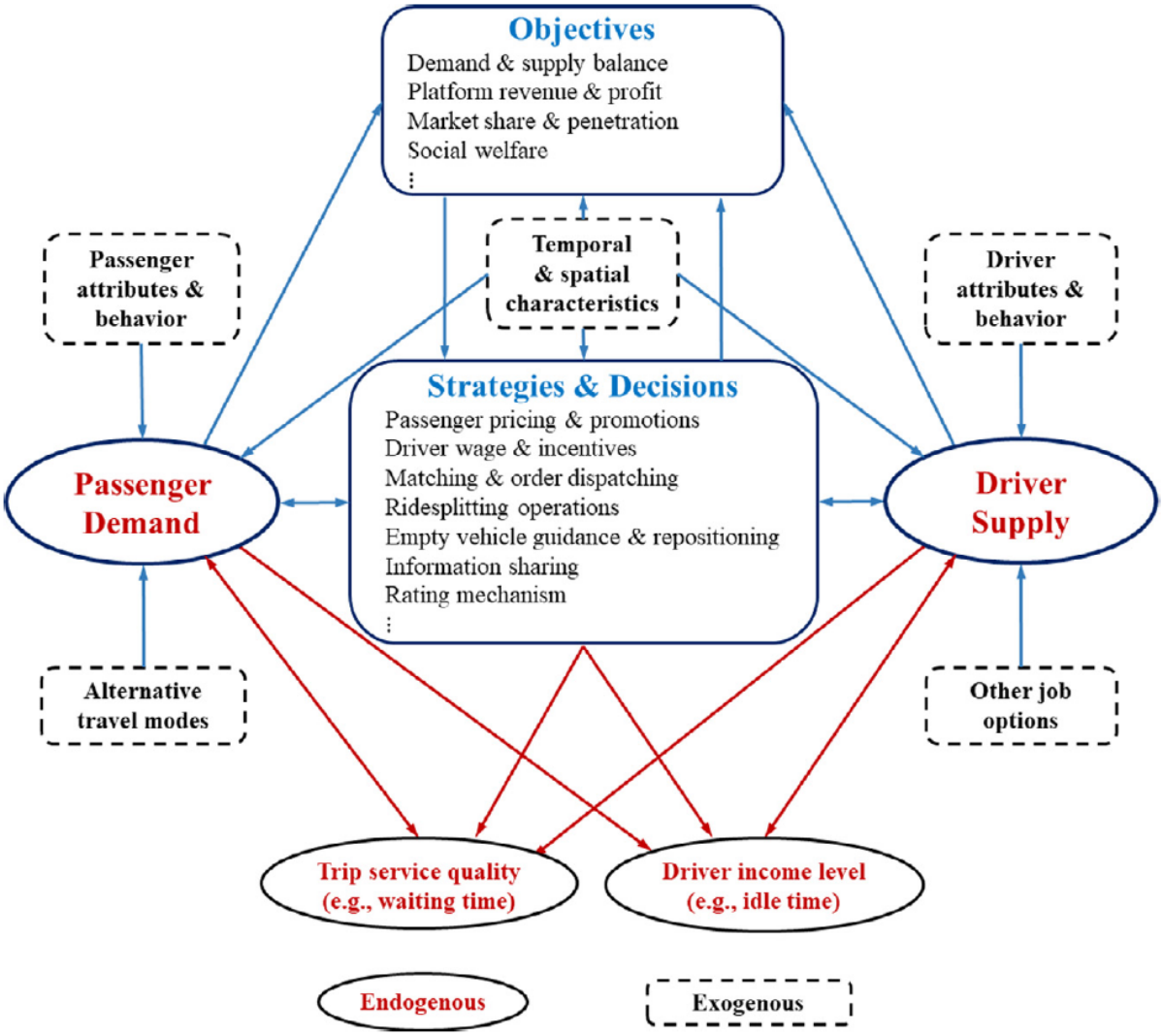

Source:Wang and Yang (2019)

Figure 2.3 General research framework for e-hailing systems

2020), vehicle dispatching strategy design (e.g., Santos and Xavier, 2013; Wang et al., 2018; Ke et al., 2019; Li and Liu, 2021; Shen et al., 2023), and customers'/drivers' behavior study (e.g. Ke et al., 2017; Wang et al., 2020).

As a bilateral service, e-hailing platforms form a bilateral market by connecting passengers and drivers. A specific research framework of ride-sourcing service was proposed in Wang and Yang (2019), as shown in Fig.2.3, which clearly illustrates the intrinsic relationships between variables and factors of relevant stakeholders and institutions. This two-sided market connects two major players–passengers (demand side) and drivers (supply side). E-hailing platforms attract more passengers and drivers into the system through network effects, forming a self-reinforcing cycle. More passengers attract more drivers, and in turn more drivers attract

more passengers. E-hailing platforms can regulate the relationship between supply and demand through pricing and other means. Wang et al. (2016) investigated pricing strategies for taxi-hailing platforms and contributes by developing models that optimize pricing to balance demand, supply, and platform revenue. Castillo et al. (2017) investigated the impact of surge pricing in ride-sharing markets, demonstrating that it reduces inefficiencies and improves allocation by minimizing the time drivers spend searching for passengers. He et al. (2018) investigated pricing and penalty/compensation strategies for taxi-hailing platforms and proposes models to optimize these strategies for improved efficiency and service quality. Yang et al. (2020) explored the integration of reward schemes and surge pricing in a ridesourcing market, proposing a model to optimize these strategies for better market efficiency and balance. Lei et al. (2020) investigated path-based dynamic pricing for vehicle allocation in ridesharing systems with fully compliant drivers, presenting a model to enhance operational efficiency and service allocation. Another most significant research direction for platforms is to improve their operational efficiency by minimizing the spatio-temporal mismatch between supply and demand (e.g. Yang et al., 2010; Agatz et al., 2011; He and Shen, 2015; Zha et al., 2016; Djavadian and Chow, 2017; Najmi et al., 2017; He et al., 2018; Long et al., 2018; Lu and Quadrifoglio, 2019; Lei et al., 2020; Zuniga-Garcia et al., 2020). Interactions between driver supply and passenger demand under static equilibrium conditions are frequently analyzed to balance the supply and demand of taxi services. Although it can provide valuable strategic decision-making insights, it is limited in its ability to account for stochasticity and time-dependency.

Under special events, surge-pricing is always used to manage the operation of e-hailing service. Surge-pricing strategy can help e-hailing platforms to boost driver supply, as drivers are motivated to work more to earn higher wages, as noted in Uber (2018). However, this strategy is not always effective during peak demand periods. During such times, platforms often raise commission rates to attract more drivers to meet the sudden surge in demand. Nevertheless, working in high-traffic areas may not be appealing to drivers due to the significant time cost involved. Additionally, there is no definitive proof that surge pricing effectively attracts drivers to high-demand areas in the short term, as indicated by an experimental study conducted by Lyft (Nicholas, 2016). Interestingly, Nourinejad and Ramezani (2020) even suggested allowing driver wages to exceed the fares collected from riders during peak periods. Although this might seem counter-intuitive for short-term planning, it has been shown to enhance overall profitability in the long run.

2.2.2 E-hailing service's impact on transportation network and passengers' travel behavior

Considering e-hailing services as a part of the urban transportation system, there have also been an increasing number of studies that model the impacts of e-hailing services on urban road traffic conditions.

Some literatures study the traffic congestion with ridesharing by assuming that travelers follow the user equilibrium (UE) principle (Wardrop, 1952), which postulates that the travel times (congestion costs) in all the used paths are equal and not more than those that would be experienced by a vehicle on any unused path. Modelling ridesharing as a traffic network equilibrium dated back to the carpooling equilibrium developed by Daganzo (1981). Previous studies (Yang and Wong, 1998; Wong et al., 2001; Yang et al., 2002; Wong et al., 2008; Yang et al., 2010; Yang and Yang, 2011) that have developed network models describing urban street-hailing taxi services in a stable equilibrium state. With the recent proliferation of taxi hailing apps, a main branch of these studies focuses on modeling travelers' mode and route choices on general networks when e-hailing services are available, and predict the traffic flow pattern at user equilibrium for the purpose of transportation planning (e.g. Di et al., 2018a; Li et al., 2020a,b; Wang et al., 2021; Li and Liu, 2021).

Among these, Xu et al. (2015a) introduced an optimization model for the ridesharing traffic assignment problem under the assumption of no detours for passenger pick up and drop off. Later, Xu et al. (2015b) relaxed this assumption and allow matching a driver with one or multiple riders from different OD pairs. Liu and Li (2017) studied a dynamic bottleneck model where congestion evolves over time and the commuters' choices of departure time and role (among solo driver, ridesharing driver and rider) are explained as dynamic UE. Ban et al. (2019a) proposed a traffic assignment model for transportation systems with ride-sourcing services and flow congestion, which modeled the interactions of solo driving, e-hailing taxis, and TNC services. Di and Ban (2019) developed a more generic network equilibrium framework which accounts for the interactions among different types of travel modes (ride-hailing services in particular). Later, Xu et al. (2019) extended taxi network models, which describes the equilibrium state that results from the interactions between background regular traffic, and occupied, idle and deadheading ride-sourcing vehicles. The above works contribute to understanding how shared mobility operations impact network flow and traffic congestion, providing valuable insights to assist transportation planners in making policy and regulatory decisions concerning shared

mobility services.

The situation of demand surge has great particularity. In general, the strategy of surge pricing is often adopted for demand surge areas to suppress demand. With the increase in fare, the drivers' wage will naturally increase. At the same time, during peak demand periods, the platform may increase the commission rate to attract more drivers to provide services to address the sudden emergence of huge demand. But in reality, it's not the case. Serving areas with high passenger flow is not necessarily a good choice for drivers, as there is a high time cost. Similarly, there is no clear evidence that surge pricing attracts drivers to areas with high demand, at least within the short time frame during the surge. This finding appears to be supported by an experimental study conducted by Lyft (Nicholas, 2016). What's even worse, inappropriate pricing or fleet sizing strategy may result in inefficient e-hailing service and additional congestion (Beojone and Geroliminis, 2021). Attracting more vehicles to areas with surging demand may not accelerate evacuation speed, but rather worsen traffic conditions. Moreover, this situation will further deteriorate the service efficiency of e-hailing platform, affecting their reputation and sustainable development.

In addition, the introduction of e-hailing services has added new complexity and risks. When high passenger flow conditions happen, an increase in the number of vehicles often occurs together to deal with the unmet passenger demand. With the distance between vehicles becomes smaller, and the interference between them increases, making the traffic environment more complex. This can easily lead to driver psychological tension, fatigue, and operational errors, thus increasing the probability of traffic accidents, which can be validated in continuous related studies (e.g. Hakkert and Mahalel, 1978; Abdel-Aty and Radwan, 2000; Xiao et al., 2024). E-hailing services, characterized by their relatively low passenger capacity per vehicle, substantially increase the total number of vehicles on the road. This proliferation of vehicles intensifies traffic congestion and complexity (Ban et al., 2019b), thereby elevating the likelihood of traffic accidents within the entire transportation system.

2.2.3 Modelling of e-hailing service's time-varying dynamics using the non equilibrium model

Recently, time-varying e-hailing dynamics attract increasing focus, especially on modelling the dispatching, pricing, scheduling and relocating and any other problems exist in e-hailing service's management issue. Because it can better study short-term changes and capture real-time

characteristics of dynamic traffic flow. This is more suitable for making short-term responses and adjustments facing special events, while time-invariant static equilibrium models are not capable of analyzing such policies. The importance of time dynamics has been emphasized in recent papers that design time-dependent demand/supply management strategies(Ramezani and Nourinejad, 2018). Assuming that the urban region can be partitioned into several homogeneous sub-regions with well-defined MFDs, they modeled the evolutionary traffic conditions with vacant and occupied taxis movements among regions, and proposed a model predictive control approach to optimize the taxi dispatch rates between the regions. Wang et al. (2019) introduced a dynamic user equilibrium approach to determine the optimal time-varying driver compensation rate. Later, a dynamic model was developed to investigate pricing strategies; this model accommodates pricing strategies that may result in short-term losses for the platform (when driver wages exceed trip fares). They highlighted that time-invariant static equilibrium models are insufficient for analyzing such policies (Nourinejad and Ramezani, 2020). A controller adopting model predictive control approach is proposed to maximize the service provider's profit by controlling the fare requested from passengers and the wage offered to drivers. Recently, Beojone and Geroliminis (2021) adopted trip-based MFD model to model the impacts of ride-sourcing service on urban congestion. Their experiment confirmed that ridesourcing operators may not be directly interested in congestion, as they observed that larger fleet sizes, while reducing waiting times, exacerbate congestion and extend total travel time. Xu et al. (2022) discussed the impact of time-dependent order cancellation behavior on the efficiency of ridesourcing platforms and examines strategies for ridesourcing platform operation, considering taxis as an alternative mode. The model takes into account factors such as time dependent order cancellation behavior, dynamic pricing strategies, and limitations on price fluctuations, with the goal of maximizing platform profits for optimization. Beojone and Geroliminis (2023a) presented a dynamic multi-region macroscopic fundamental diagram (MFD) model for ride-sourcing with ridesplitting, used the non equilibrium model to more accurately capture the dynamic evolution of the system under transient conditions. The development of this model can pave the way for real-time feedback-based management policies and regulations for ride-sourcing in congested areas. What's more, Beojone and Geroliminis (2023b) also studied the time-varying dynamic strategy existed in carpooling system, by proposing a path oriented revenue prediction strategy based on Markov chain model, aiming to evaluate the driver's repositioning response when providing guidance. This strategy provides personalized recent income estimates for drivers

by predicting their activities and income, guiding them to make repositioning decisions that are more likely to maximize their income. Su et al. (2024a) discussed the impact of e-hailing services on passenger evacuation efficiency in a bi-modal transportation system. A mathematical model was proposed to depict the dynamic evacuation rates and traffic conditions in such a system and suggests two feedback-based perimeter control strategies to improve evacuation efficiency. The paper contributed to the understanding of the impacts of e-hailing services on passenger evacuation and proposes practical control strategies to enhance the efficiency. Later on, a mathematical model was proposed in Su et al. (2024b) to characterize the time-varying evolution of e-hailing services in a two-region transportation system, and management methods were provided to improve the evacuation process. This study considers the repositioning decisions of drivers and the dynamic demands of passengers, and develops a region-dependent pricing strategy for rapid and large-scale evacuation. The region-dependent e-hailing pricing strategy proposed in this study can significantly shorten the total evacuation time and bring more stable traffic conditions.

2.3 Multi-Modal Transportation System

This section reviews the literature of multi-modal transportation system, covering the following key areas: (i) bus bridging services and optimization (Subsection 2.3.1); (ii) impacts of different transport modes on traffic performance and on each other (Subsection 2.3.2) and (iii) design of transportation system (Subsection 2.3.3).

2.3.1 Bus bridging services and optimization

In the context of multi-modal traffic dynamics, the number of buses actively deployed in service is typically a more straightforward decision variable, while the frequency is determined endogenously based on traffic conditions, given the dispatched fleet size. Numerous studies have explored bus bridging services and optimization strategies for passenger evacuation (e.g. Kepaptsoglou and Karlaftis, 2009; Ibeas et al., 2010; Szeto and Wu, 2011; Jin et al., 2014, 2016) or under multi-modal and multi-directional transportation system (Zhang and Liu, 2020). With the improvement of peoples' income level, there is an increasing demand of urban residents to use e-hailing service during travel. However the effect on the overall performance of them both on a transportation system still remains a challenge. Understanding the cooperation and competition among modes can effectively help to implement the management strategies in an urban

transportation system. By implementing effective multimodal joint transportation strategies, resource allocation can be optimized, service quality can be improved, and traffic congestion can be alleviated. Accurately modeling the dynamic characteristics of multimodal transportation systems can provide a basis for urban traffic managers to formulate more precise policies. On the basis of single mode MFD research, further exploration of the dynamic characteristics of multi-mode networks will bring far-reaching theoretical and practical value to the design and management of transportation systems, thus helping to cope with increasingly complex urban transportation challenges.

2.3.2 Impacts of different transportation modes on traffic performance and on each other

There has been significant progress in understanding the impact of e-hailing services or bus bridging service on road traffic conditions which has been introduced in aforementioned studies, resulting in a wealth of literature in this field. However, the comprehensive impact of both e-hailing service and bus on the performance of the entire transportation system remains a complex challenge. The dynamics of traffic flow in bi-modal networks are more complicated due to the operational characteristics of both modes. They share the common transport facilities and influence the flow interactions. Variances in passenger occupancy, driving behaviors, and travel durations further compound the complexity. In addition to transportation network design(e.g. Tong et al., 2015; Di et al., 2018b) and traffic signal optimization(e.g. Christofa and Skabardonis, 2011; Christofa et al., 2016b), the design of boarding spaces for each mode plays a crucial role in system functionality. In urban environments, all vehicles experience stops related to traffic congestion, which in turn causes delays to the overall transportation system. For example, buses stop at bus stops to board and alight passengers (30-50 seconds), e-hailing vehicles frequently and randomly stop while searching for or picking up passengers (5-15 seconds), and cars may stop or maneuver when searching for a parking spot (Zheng and Geroliminis, 2013). These service-related stops across various modes (taxis, buses, delivery vehicles) create both static and moving bottlenecks of varying severity. Vehicles may queue behind a stopped vehicle, forming a local queue that can be analyzed using standard shockwave theory, or they may change lanes to bypass the service-related stop (Barmpounakis and Geroliminis, 2020). This explains why a great amount of studies focus on modelling the cruising for parking and parking(e.g. Shoup, 2006; Ommeren et al., 2012; Geroliminis, 2015; Zakharenko,

2016; Leclercq et al., 2017; Liu and Geroliminis, 2017; Arnott and Williams, 2017; Gu et al., 2020; Zhao et al., 2021; Ommeren et al., 2021; Gu et al., 2023). Unreasonable parking arrangements can easily lead to congestion and low efficiency. The impact of this phenomenon on the overall performance of transportation system remains a challenge, especially in situations of passenger demand surge. While intuitively we would expect these stops to be almost negligible in situations of low demand, the temporal and spatial frequency of such stops is very high in situations of surges in demand. Su et al. (2024a) use numerical experiments to verify that without control, the time spent on cruising for parking and waiting for passengers to get on board takes up a large part of the entire trip. This period of time is dependent on the distribution and number of vehicles and passengers within the area. As more vehicles accumulate and the more disorderly they are dispersed, the time period will be lengthened and congestion will inevitably occur. Furthermore, the design of parking spaces of different modes in transportation system not only affects vehicle dynamics, but also has an impact on crowds due to the process of pedestrian-vehicle conflicts. This not only affects the boarding time of the crowd, but also poses risks to pedestrians. This risk not only includes vehicle-pedestrian crashes, but also pedestrian-pedestrian crashes. In related studies, the risks of accidents and casualties during this process are always served as a motivation for speedy passenger evacuation. However, considering the integration of different modes in a transportation system, the focus should not only lie on how to transport passengers more efficiently, but also on how to deal with the safety danger bringing to passengers by different modes of transportation in the system. Building on the knowledge of single-mode analysis, there is considerable potential for developing an understanding of bi-modal networks. By grasping the interplay of cooperation and competition among different modes of transportation, effective management strategies can be implemented in urban transportation systems.

Recent studies have made progress in considering the interaction between automobiles and the transit system in bi-modal urban networks. Traditional two-dimensional relationship of MFD only describes the cumulative number of vehicles and traffic flow, ignoring diverse regional traffic flow characteristics such as vehicle heterogeneity (e.g. private cars and buses). To address these shortcomings, scholars proposed a three-dimensional Macroscopic Fundamental Diagram (3D-MFD), which links the network accumulation of cars and public transport vehicles to the network's travel production, whether for vehicles or passengers. Geroliminis et al. (2014) extended the modeling and the application of the single-mode MFD to a bi-modal (bus

and cars) one, with the consideration of passenger flows and traffic performance of each mode. The dynamics of traffic flow in bi-modal networks are more complicated due to the operational characteristics of both modes. Buses have scheduled service stops in addition to those caused by traffic congestion and signals, which results in lower speeds and flow rates compared to cars. On the other hand, buses carry a significantly larger number of passengers. Therefore, it is not enough to solely consider vehicle flows when developing management strategies for a multimodal network. 3D-MFD is particularly suitable for networks with significant traffic differences, in order to conduct high-density, multi-mode traffic network research and improve the ability of multi-mode traffic coordination. In terms of deriving relevant management strategies for multimodal transportation networks, adopting 3D-MFD relationship is a necessary attempt. It can not only compensate for the shortcomings of two-dimensional MFD in multimodal and spatiotemporal dynamic modeling, but also provide more accurate decision support for collaborative management of multimodal systems. For example, the initial applications of the 3D-MFD (and its three-dimensional variant for passenger flows, 3D-pMFD) are related to urban space allocation (Zheng and Geroliminis, 2013) and parking (Zheng and Geroliminis, 2016). Loder et al. (2017) proposed a statistical model of the 3D-MFD, which estimates the effects of the vehicle accumulation on car and public transport speeds under multi-modal traffic conditions. Furthermore, some works extend the single-mode MFD to a bi-modal one, where cars and buses share the same infrastructure, while also considering passenger flow dynamics alongside vehicular dynamics (e.g. Zheng and Geroliminis, 2013; Chiabaut et al., 2014; Geroliminis et al., 2014; Chiabaut, 2015). Through appropriate dynamic modeling of flows in a bi-modal system, regulations and policies can be proposed to guide decision-making.

2.3.3 Design of transportation system

After effectively accounting the impact of different transport modes on traffic performance, it makes it available to design a bi-modal transportation system with different objectives. To optimize the infrastructure of a transit system with elastic demand, Daganzo et al. (2012) focused on maximizing the system's social welfare while accounting for multiple user classes. Sivakumaran et al. (2014) improved the system's efficiency by enhancing the mobility of feeder services and optimizing the land-use patterns around the trunk sections. Similarly, Amirgholy and Gonzales (2016) optimized the operation of demand-responsive transit systems with time-varying demand by minimizing the combined generalized cost to users and the operating cost of

the service provider. Amirgholy et al. (2017) proposed an analytical model for transit systems that incorporates the impact of congestion on service quality and system performance using the MFD model. This model is used to estimate the generalized cost experienced by transit users during their trips. A numerical example is provided to compare the optimal designs of the transit system across various network allocation scenarios.

However, transit system typically encompasses public transportation services within a city or region, such as buses, subways, and light rail. It is usually managed and operated by the government or specialized transportation agencies. Extending the analysis to a transportation system that includes both cars and public transit, Gonzales and Daganzo (2012) investigated system-optimal solutions for the morning commute problem. The authors addressed both user and system optimality for the bottleneck model and system optimality for the network model, using an MFD representation. Their model accounts for the fact that the network capacity for cars is reduced when transit operations are allocated dedicated space.

E-hailing services (such as Uber and Lyft) are generally classified as private transportation services. They utilize online platforms to match passengers with drivers, deviating from the traditional realm of public transit. In regions with a large passenger flow waiting to evacuate, a significant number of e-hailing vehicles will be attracted to pick up passengers. There is a growing demand to integrate e-hailing services within the framework of transit system to enhance overall transportation system's efficiency and coverage. What's more, it is important to note that the presence of e-hailing services introduces additional complexities. E-hailing services operate in an online-matching and offline-meeting pattern. The offline passenger-driver bilateral searching process (for their assigned vehicles/passengers) in crowded areas, with dense traffic and population, can be notably more dangerous than usual. As waiting passengers navigate the area to find their designated vehicles, pedestrian movements become more complex and chaotic, potentially increasing the risk of crowd-related incidents. This case has received considerable attention by passenger safety related studies. Rashidi et al. (2016) discussed the effect of installing sidewalks and crosswalks on the safety and usability of a transportation network. The objective of the study is to minimize the safety hazard for pedestrians and the total transportation cost of the network. What's more, a significant amount of research has been conducted to assess pedestrian safety during interactions with vehicles (e.g. Osama and Sayed, 2017; Kraidi and Evdorides, 2020; Amini et al., 2022; Su and Sze, 2022; Ihssian and Ismail, 2023). Amini et al. (2022) developed a conflict risk evaluation model to evaluate pedestrian

safety when conflict events between pedestrians and vehicles occur. This model helps assess the level of safety for pedestrians in relation to other road users. Pedestrians, as well as lighter road users such as two- or three-wheel vehicles, generally have more freedom of movement compared to heavier users like passenger cars or heavy goods vehicles. This greater mobility allows pedestrians to change their movement trajectories on the road. Consequently, predicting the next actions of users and the associated risks becomes complex due to the diverse range of user types and the various evasive maneuvers they can undertake to avoid conflict situations. Therefore, considering safety will be another important factor while designing an integrated transportation system.

2.4 Research Gaps

From the above literature review, three significant issues in e-hailing service's management problem under mass gathering events that have received little attention can be identified. The three issues are described as follows.

(1) E-hailing service's impact on passenger evacuation's efficiency has not been systematically considered

Existing mitigation measures adhere to a decision-making paradigm that relies on assessing event scenarios and replicating approaches used in prior special events to better comprehend current challenges. Nonetheless, mitigating traffic pressure during special events demands a heightened level of emergency preparedness, necessitating a more adaptable and easily adoptable approach for real-time decision-making. This becomes crucial, especially in overcoming the hurdle posed by a lack of reference scenarios. Furthermore, expanding the range of transportation modes is a vital initiative to complement traditional methods such as buses and subways, enhancing the overall efficiency of passenger evacuation during special events.

The aforementioned studies primarily focus on modeling e-hailing services in regular scenarios, where the matching time and pick-up time decrease as the number of waiting passengers and vacant vehicles increases. However, when a substantial number of e-hailing vehicles converge on a small area for pick-ups, the inverse tends to happen during the pick-up process. As more vehicles accumulate in the area, the time for an e-hailing vehicle to reach its assigned passenger lengthens, and the time for a passenger to locate their designated vehicle amidst a large number of options also increases. Therefore, using e-hailing services is a double-edged sword. On the one hand, e-hailing services supplement buses by providing more transportation

supplies; On the other hand, the large influx of e-hailing services and the time-consuming offline passenger driver search process can lead to a large accumulation of vehicles in the area, thereby reducing vehicle speed and reducing the evacuation efficiency of other bus. It is in urgent need to enhance our understanding towards the impacts of e-hailing vehicles on passenger evacuation efficiency during demand-surge events.

(2) E-hailing service's supply distribution under time-varying traffic conditions has hardly been studied

Under the case of passenger demand surge, only the non-equilibrium model can effectively account for stochasticity and time-dependency, instead of time-invariant equilibrium model. The equilibrium model presumes a stable system state, reaching equilibrium at each time point or interval, making it apt for long-term planning and policy formulation. However, it falls short in studying short-term changes and capturing real-time characteristics of dynamic traffic flow. In the context of the sudden high passenger flow, a transportation system's modelling and analysis based on a non-equilibrium model is more suitable for making short-term responses and adjustments facing special events, while time-invariant static equilibrium models are not capable of analyzing such policies.

In instances of demand surges or large-scale aggregation events, the passenger flow and traffic performance of each mode become more unpredictable. During the evacuation of a large number of passengers from a region experiencing significant flow, this region becomes a focal point for attracting numerous e-hailing vehicles to pick up passengers. Given the imperative need to efficiently and safely evacuate a substantial passenger flow during such events, spatio-temporal decisions become critical. Incorrect decisions in this context can result in wasted space or valuable time. In the dynamic environment of the region where sudden traffic incidents occur and its surrounding regions, the availability of e-hailing services are constantly changing. The formulation of pricing strategies requires accurate understanding of the distribution of e-hailing supply and demand dynamics in different regions. There are still gaps in the design of time-dependent demand/supply management strategies, in order to effectively assist e-hailing services in adapting to constantly changing traffic conditions in a region-based manner.

(3) E-hailing service's integration with the design of a transportation system has scarcely been investigated

It is in urgent need to design an efficient transportation system that integrates both e-hailing and bus services as a bi-modal system. This integration involves analyzing the operational and

financial characteristics of different modes to design and plan a comprehensive transportation system. Under the setting of passenger demand surge, it should consider boarding space design of different modes in the transportation system. We especially aim to take the effect of this vehicle-passenger offline boarding process into consideration, because this critical process plays an important part in deciding the transportation system's efficiency and transportation modes' performance. The primary objective during such a massive evacuation is to efficiently and safely move the large passenger flow out of the demand surge region. This can facilitate the synergistic operation of various transportation modes, offering a more inclusive range of transportation choices.

Risks of accidents and casualties resulting from pedestrian accumulation should be emphasized under expeditious passenger evacuation. Previously, the risk of accidents and casualties due to pedestrian congestion was a key motivator for quick passenger evacuation. Exploring how e-hailing services increase the risk of crowd disasters is a compelling research topic that warrants further investigation. In the case of evacuation after mass gathering events, pedestrian movements could be more complicated and disordered, potentially leading to increasing danger. What's more, the availability of e-hailing services introduces new risks. Therefore, when designing systems for mass gathering events, decisions should prioritize not only efficiency but also safety.

2.5 Summary

This chapter comprehensively reviewed studies on (1) multi-types of traffic control strategies with MFD representations, (2) e-hailing service's properties and times-varying strategies and (3) multi-modal transportation system. Subsequently, three significant issues that remain to be addressed were identified. The first issue is the consideration of e-hailing service's impact on passenger evacuation's efficiency. To close this research gap, Chapter 3 will investigates the dynamics of traffic conditions and passenger evacuation process in a bi-modal system with both buses and e-hailing vehicles can be chosen for passengers' evacuation. The second issue is the consideration of e-hailing service's supply distribution under time-varying traffic conditions. Therefore, Chapter 4 will investigate the time-varying evolution of e-hailing vehicles within a two-region transportation system. To assist the e-hailing platform in managing a reasonable level of vehicle supply for rapid evacuation, a region-dependent pricing strategy by adjusting e-hailing drivers' per unit time wages in different regions is proposed to motivate their service

willingness. The third issue is the consideration of e-hailing service's integration with the design of a transportation system. Therefore, Chapter 5 will design the boarding space within a bi-modal evacuation system to minimize the generalized cost, which includes users' cost, operating cost, and safety cost. We propose four prevalent scenarios within the transportation system and compare them using a numerical example. Overall, the primary objective of the thesis is to address the decision-making challenges faced by e-hailing platforms due to demand surge situations.

CHAPTER 3 PASSENGER EVACUATION PROCESS MODELLING AND VEHICLE FLOW CONTROL PROBLEM IN A BI-MODAL SYSTEM WITH BUS AND E-HAILING MODES

With the acceleration of urbanization and the continuous expansion of urban scale, the problem of transportation capacity gap in the transportation system is becoming increasingly serious. In this context, integrating e-hailing services into the transportation system can effectively enhance transportation supply capacity. Through smartphone applications, e-hailing services provide users with a convenient way to pre-book taxis, reducing information barriers between passengers and drivers, and bringing new travel options and more comfortable travel experiences to urban residents. In recent years, the academic community has conducted extensive research on the impact of e-hailing services on urban transportation. However, during the evacuation process in areas with high passenger flow, e-hailing services present a double-edged sword effect. On the one hand, e-hailing services provide additional options for quickly evacuating passengers and have become an important supplement to public transportation such as buses and subways; on the other hand, the large inflows of e-hailing vehicles and the time-consuming passenger-driver (offline) searching process would lead to a huge vehicle accumulation within the area, thus lower vehicle speed and reduce the efficiency of bus evacuation.

This chapter describes the duration of each state in the evacuation process using Trip-based MFD and the passenger mode choice using Logit model in a transportation system that can utilize both bus and e-hailing modes simultaneously, and provides the evolution of passenger evacuation rates and traffic conditions. To accelerate passenger evacuation, this chapter further proposes two feedback based perimeter control strategies, which control the total inflow rate of e-hailing and background traffic vehicles by regulating the number of vehicles in the area. The simulation results have verified the effectiveness of these two control strategies in improving evacuation efficiency under the participation of e-hailing services, as well as their sensitivity under different total passenger demands, bus headway, and total parking spaces.

The remainder of this chapter is organized as follows. Section 3.1 states the assumptions and problem descriptions. Section 3.2 describes the model for the dynamic evacuation process in a bi-modal transportation system, and demonstrates the impacts of e-hailing services on the passenger evacuation efficiency through numerical examples. Section 3.3 introduces two

feedback-based perimeter control strategies and Section 3.4 demonstrates their effectiveness. And finally Section 3.5 concludes the chapter.

3.1 Assumptions and Problem Description

This section provides the assumptions and problem descriptions from duration of each state in a trip-based process (Subsection 3.1.1) and passenger mode choice (Subsection 3.1.2).

3.1.1 Duration of each state in a trip-based process

Consider a small area where passenger travel demand surges after a mass gathering event or metro disruption. At time $t = 0$, a total number of Q passengers are accumulated within the area and waiting for transportation. They can choose bus shuttle service to nearby stations, or hail for-hire vehicles through an e-hailing platform. All passengers stay within pedestrian zones to wait for buses or e-hailing vehicles.

There are three types of vehicles that contribute to the traffic within the area: buses, e-hailing vehicles and background traffic. The arrival rate of the three types of vehicles at the demand surge area are indicated by $u_p(t)$,$u_r(t)$ and $u_b(t)$ respectively. The maximal inflow rate to the area is subject to the boundary capacity C_{max}, which is determined by the capacity of roads leading to the area. For simplicity, we assume the total arrival rates of the three types of vehicles is always smaller than C_{max}. As shown in Figure 3.1, after entering the study area, vacant buses and e-hailing vehicles first move towards passengers to stop and load passengers, and then drive out of the area with passengers on board, while background traffic traverses the area without stop. Within the area, the average driving distances of buses (/e-hailing vehicles) in vacant and occupied states are indicated by l_p^v and l_p^o ($/l_r^v$ and l_r^o) respectively, and the average travelling distance of background traffic is l_b. And without loss of generality, we assume all background vehicles that are during the initial θ ($0 < \theta < 1$) proportion of their trips (i.e., when their travel distance within the area is less than θl_b) within the area are approaching the passenger waiting area, and background vehicles in the remaining proportion of their trips within the area are getting away from the passenger waiting area, as shown in Figure 3.1.

As there are a large number of passengers waiting for transport in the demand-surge area, every e-hailing vehicle will get immediately dispatched to pick up a designated passenger when it enters the searching radius of the platform. And then every driver-passenger pair needs to search and meet each other offline. In this study, we suppose the streets within the area are all

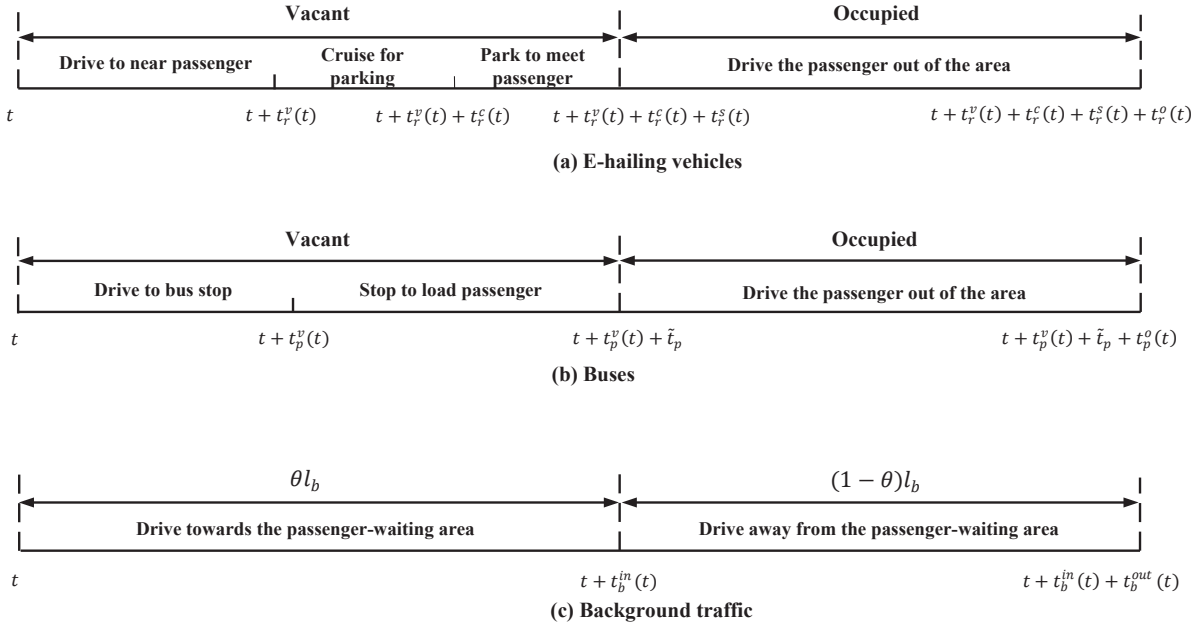

Figure 3.1 The trip duration of each type of vehicles

multi-lane. When e-hailing vehicles get close to the passenger waiting area, they first cruise to search for a temporary curbside parking space and then park at the space to wait for their passengers. The cruising distance for parking space is dependent on the occupancy ratio of parking spaces (Shoup, 2006; Ommeren et al., 2012; Geroliminis, 2015; Arnott and Williams, 2017). The higher the occupancy ratio, the longer time it takes for a vehicle to find a parking space. Let N^{pk} be the total number of curbside parking spaces within the area, and n_r^{pk} be the number of parked e-hailing vehicles. For simplicity, in this study we assume that buses have dedicated parking spaces, and all curbside parking spaces are used only by e-hailing vehicles during the study period. Then the occupancy ratio of curbside parking spaces follows

$$q = \frac{n_r^{pk}}{N^{pk}}. \tag{3.1}$$

The same as in Geroliminis (2015), we assume the searching-for-parking space process for each vehicle can be approximated by a number of independent Bernoulli trials that stop until finding a vacant parking space, and the probability of success in each trial is q. Then following Geroliminis (2015), the cruising for parking distance l_r^c can be approximated by

$$l_r^c = \frac{d}{1-q}, \tag{3.2}$$

where d is the average spacing between two neighbouring parking spaces.

After successfully parking, e-hailing drivers contact their passengers to give a vague description of their locations (e.g., the street name), and the passengers start to search. So it takes time for each driver-passenger pair to search and meet each other offline. As passengers need to check the license plate of every parked vehicle on the street until meeting their designated vehicles, we assume their average searching time is increasingly dependent on the number of parked vehicles. Let t_{chk} be a constant that indicates the average time it takes for passengers to check one vehicle, then the average passenger searching time when there are n_r^{pk} parked vehicles can be approximated by

$$t_r^s(n_r^{pk}) = \alpha \cdot n_r^{pk} \cdot t_{chk}, \tag{3.3}$$

where α is a constant parameter whose value is dependent on the distribution of vehicles and passengers within the area and the way passengers adopt to check these vehicles.[3.1]

Assuming that the relationship between the number of vehicles and their speed in the region follows a well-defined Macroscopic Fundamental Diagram (MFD) relationship, and that the changes in the proportion of vehicle types caused by different types of vehicles do not undermine the assumption of uniformity in traffic conditions, thus not causing significant changes in the shape of MFD. Furthermore, we consider two-directional traffic flows in the area: 1) the flow that moves towards the passenger waiting area, including all vacant buses and e-hailing vehicles and all background vehicles that are during the initial θ proportion of their trips within the area; and 2) the flow that moves away from the passenger-waiting area, including all occupied buses and e-hailing vehicles, and all background vehicles that are in the remaining $(1-\theta)$ proportion of their trip within the area. Those two-directional flows for all three types of vehicles can be clearly represented in Figure 3.1. Traffic in different directions can have different speeds (this treatment is similar to that in Zhang and Liu (2020), which helps capture the heterogeneity in the system, especially under imbalanced demand and traffic for different directions). Let $n^{in}(t)$ and $n^{out}(t)$ respectively be the vehicle accumulation (in unit of passenger car equivalent (PCE)) that into and out of the passenger-waiting area at time t, $v^d(t)$ be the speed of vehicles driving in direction $d \in \{in, out\}$ at time t. The vehicle speed and vehicle accumulation within the

[3.1] We note that $\alpha \geq \frac{1}{2}$ usually holds. To see this, taking each vehicle as a node, if there is a Hamilton cycle to visit each vehicle once and only once, and all passengers (starting from different vehicle nodes) follow the Hamilton cycle before meeting their designated vehicles, then the average number of vehicles that passengers have to check before meeting their designated ones are $\frac{1}{2}n_r^{pk}$, and we thus have $\alpha = \frac{1}{2}$ in this case. However, if there does not exist a Hamilton cycle for the vehicle checking problem, and/or passengers do not follow the Hamilton cycle, then some vehicles would be visited twice or more, and the average number of vehicles that passengers have to check before meeting their designated ones would be larger than $\frac{1}{2}n_r^{pk}$, and $\alpha > \frac{1}{2}$ in this case.

area in direction d follows a well-defined MFD, i.e.,

$$v^d(t) = V(n^d(t)), d \in \{in, out\}. \tag{3.4}$$

In this chapter, we assume the arrival rates of buses and background traffic vehicles at any time t, i.e., $u_p(t)$ and $u_b(t)$, $t \geq 0$, are exogenously given. The e-hailing vehicles' arrival rate $u_r(t)$ is endogenously determined by passengers' mode choice and e-hailing vehicles' arrival rate at the platform's searching radius $A_r(t)$, which will be introduced in the next subsection. The total number of passengers who leave the area by bus and by e-hailing vehicles are determined by the number of buses and e-hailing vehicles flowed into the area before the end of the evacuation. Meanwhile, let $o_r(t), o_p(t)$ and $o_b(t)$ respectively indicate the outflow rates of e-hailing vehicles, buses and background traffic at time t, $b_r(t)$ and $b_p(t)$ respectively be the boarding rates of e-hailing vehicles and buses at time t, $b_b(t)$ be the completion rate of background traffic for the first θ proportion of their trip within the area, and $p_r(t)$ be the parking rate of e-hailing vehicles at time t. As show in Figure 3.2, the arrival rates of different types of vehicles at the boundary at any moment, together with the dynamic travelling time, cruising time for parking spaces and the passenger-driver meeting time, determine the parking, boarding and outflow rates of different types of vehicles in the subsequent periods; and the vehicle parking, boarding and outflow rates in turn affects the dynamic vehicle speed and vehicle travelling time within the area through its impact on vehicle accumulation in each direction.

3.1.2 Passenger mode choice

We now model passengers' dynamic mode decisions between bus and e-hailing vehicles. Let $Q^{rm}(t)$ be the number of waiting passengers who haven't been assigned vacant vehicles or gotten on buses. Under dynamic traffic conditions, such passengers may frequently change their mode choices according to the generalized trip costs of the two modes. Let $P_r(t)$ and $P_p(t)$ respectively be passengers' choice probability of e-hailing and bus modes at time t, and $W_r(t)$ and $W_p(t)$ respectively represent the perceived generalized trip cost of taking e-hailing vehicle and bus at time t, which will be modeled in the following. In this study, we assume $P_r(t)$ and bus $P_p(t)$ can be approximated by the following Logit model:

$$P_r(t) = \frac{e^{-\eta \cdot W_r(t)}}{e^{-\eta \cdot W_r(t)} + e^{-\eta \cdot W_p(t)}}, \tag{3.5}$$

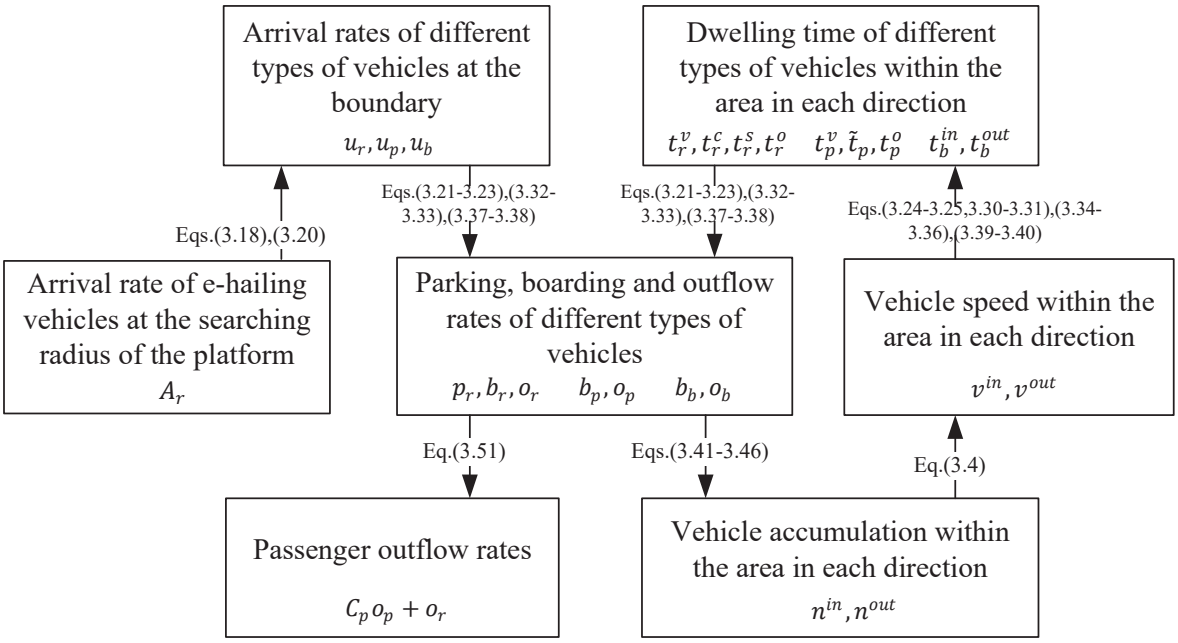

Figure 3.2 The modelling framework

$$P_p(t) = \frac{e^{-\eta \cdot W_p(t)}}{e^{-\eta \cdot W_r(t)} + e^{-\eta \cdot W_p(t)}}, \tag{3.6}$$

where η is the dispersion parameter reflecting passengers' uncertainty towards these two modes of transportation.

Let $Q_r^{rm}(t)$ be the intended passengers number of e-hailing at time t, $Q_p^{rm}(t)$ be the intended passengers number of bus at time t. Then we have

$$Q_r^{rm}(t) = Q^{rm}(t) \cdot P_r(t), \tag{3.7}$$

$$Q_p^{rm}(t) = Q^{rm}(t) \cdot P_p(t). \tag{3.8}$$

In Eqs. (3.5) and (3.6), the passengers' perceived generalized costs $W_r(t)$ and $W_p(t)$ include the passengers' perceived time cost for response and for rest duration of the trip, the perceived average trip payment and the additional perceived discomfort cost for bus users. Let $w_r^{rp}(t)$ be the e-hailing passengers' perceived waiting time for response at time t, $w_r^{rt}(t)$ be the perceived time for rest duration of the trip, f_r be the average trip payment for the e-hailing service. The total generalized perceived cost of e-hailing $W_r(t)$ can be formulated as:

$$W_r(t) = \beta \cdot (w_r^{rp}(t) + w_r^{rt}(t)) + f_r. \tag{3.9}$$

Let $A_r(t)$ be the vacant e-hailing vehicles' arrival rate at the platform's searching radius at time t, which is exogenously given, $\bar{A}_r(t)$ be the average vacant e-hailing vehicles' arrival rate during the past k minutes. Therefore the e-hailing passengers' perceived waiting time for 'response' at time t $w_r^{rp}(t)$ can be formulated as:

$$w_r^{rp}(t) = \frac{Q_r^{rm}(t)}{2 \cdot \bar{A}_r(t)}. \tag{3.10}$$

As long as the e-hailing vehicles have been matched, they will drive towards the demand surge area to pick up the waiting passengers. We assume the fixed driving time from being assigned an order to arriving the boundary of the demand surge area as $\tilde{t}_r$. Together with the vacant driving time $t_r^v(t)$, cruising for parking time $t_r^c(t)$, checking time $t_r^s(t)$ within the demand surge area and the occupied driving time with passenger on board $t_r^o(t)$, the 'rest' trip time of e-hailing vehicle $w_r^{rt}(t)$ can be formulated as:

$$w_r^{rt}(t) = \tilde{t}_r + t_r^v(t) + t_r^c(t) + t_r^s(t) + t_r^o(t), \tag{3.11}$$

where the determination of $t_r^v(t), t_r^c(t), t_r^s(t)$ and $t_r^o(t)$ will be elaborated in detail in the following section.

Similarly, let $w_p^{av}(t)$ be the bus headway of arriving the boundary of the demand surge area, $w_p^{rt}(t)$ be the passengers' rest trip time, f_p be the average payment for bus. Besides, we also consider the discomfort cost of taking bus as θ_p. Therefore the total bus's generalized cost $W_p(t)$ can be formulated as:

$$W_p(t) = \beta \cdot (w_p^{av}(t) + w_p^{rt}(t)) + f_p + \theta_p. \tag{3.12}$$

Given the bus arrival rate at the boundary of the demand surge area at time t, i.e., $u_p(t)$, we let $\bar{u}_p(t)$ be the average bus arrival rate at the boundary of the demand surge area during the past k minutes. Let C_p be the bus's passenger capacity when it is fully loaded. Therefore the bus headway of 'arriving' the boundary of the demand surge area $w_p^{av}(t)$ can be formulated as:

$$w_p^{av}(t) = \frac{Q_p^{rm}(t)}{2 \cdot C_p \cdot \bar{u}_p(t)}. \tag{3.13}$$

We assume the vacant driving time within the demand surge area as $t_p^v(t)$, fixed passenger loading time as $\tilde{t}_p(t)$ and the occupied driving time with passenger on board as $t_p^o(t)$, the 'rest'

trip time of bus $w_p^{rt}(t)$ can be formulated as:

$$w_p^{rt}(t) = t_p^v(t) + \tilde{t}_p(t) + t_p^o(t), \tag{3.14}$$

where the determination of $t_p^v(t)$, $\tilde{t}_p(t)$ and $t_p^o(t)$ will be elaborated in detail in the following section.

As soon as the e-hailing passengers have been assigned an driver or the bus passengers have gotten on board, they will stop re-updating their mode choice. Let $m_r(t)$ and $m_p(t)$ denote the matching rate of e-hailing passenger and the boarding rate of bus passenger at time t. Therefore up to time t, with the objective of evacuating a total number of Q passengers, the remaining waiting passenger number $Q^{rm}(t)$, the cumulative number of passengers successfully matched by e-hailing $M_r(t)$ and the cumulative number of passengers successfully on boarded by bus $M_p(t)$, can be respectively modeled as:

$$Q^{rm}(t) = Q - M_r(t) - M_p(t), \tag{3.15}$$

$$M_r(t) = \int_0^t m_r(t)dt, \tag{3.16}$$

$$M_p(t) = \int_0^t m_p(t)dt. \tag{3.17}$$

We now firstly discuss the e-hailing matching rate $m_r(t)$. As we have modeled the passengers' mode choice process based on the perceived cost variation, it is critical to note that the evacuation dynamics will also be determined by the vehicle(/transportation) supply. When a event of passenger demand surge occurs, the demand/supply pattern varies rapidly and the system may not be able to attain the steady-state equilibrium conditions. Both of the waiting passenger number for each mode and the supply restriction for each mode determine the vehicle-passenger matching process. From the passengers' perspective, they intuitively tend to leave the crowded area as soon as possible in order to get rid of the potential danger. Therefore, the waiting passenger will choose to get on board as long as there are available vacant vehicles. From the e-hailing drivers' perspective, each e-hailing vehicle usually can only carry one passenger. Due to the great difference between the huge passenger demand and limited transportation supply, a vacant e-hailing vehicle can always be dispatched as soon as possible. From above two-sided perspectives, it is reasonable to assume that, the successful driver-passenger matching pairs $m_r(t)$ at time t is determined by the smaller value of the number of vacant e-

hailing vehicles available for dispatching at time t and the number of passengers waiting for dispatching at time t, which is given as follow:

$$m_r(t) = \min\left\{Q_r^{rm}(t), A_r(t)\right\}, \tag{3.18}$$

where $m_r(t)$ is usually determined by the number of vacant e-hailing vehicles available for dispatching in most cases.

As bus can only accommodate a maximum of fully loaded passengers number, its overall transportation capacity at time t can be represented as $C_p \cdot b_p(t)$. Following the similar manner as e-hailing, the passenger number that successfully on boarded at time t, i.e.,$m_p(t)$ should be determined as follow:

$$m_p(t) = \min\left\{Q_p^{rm}(t), C_p \cdot b_p(t)\right\}. \tag{3.19}$$

Given the e-hailing vehicles' driving time from being assigned an order to arriving the boundary of the demand surge area $\tilde{t}_r$, together with matching rare $m_r(t)$ at time t, the e-hailing arrival rate of the boundary of the demand surge area at time t can be formulated as:

$$u_r(t) = m_r(t - \tilde{t}_r). \tag{3.20}$$

3.2 Modelling the Dynamic Evacuation Process in a Bi-modal Transportation System

In the following, under arrival rates $u = (u_r(t), u_p(t), u_b(t), t \geq 0)$, we first model the boarding, parking and outflow rates of each type of vehicles within the area based on a trip-based MFD model, and then trace the dynamic traffic conditions within the area, so as to determine the passenger outflow rate.

3.2.1 Determining the parking, boarding and outflow rates based on a trip-based MFD model

As shown in Figure 3.1(a), for an e-hailing vehicle that enters the area at time point t, let $t_r^v(t)$ be the time it takes to complete an average distance l_r^v to get near its passenger, $t_r^c(t)$ be the time it takes to cruise until finding a parking space, $t_r^s(t)$ be the time it takes for the passenger to check and successfully find the parked vehicle, and $t_r^o(t)$ be the time it takes to drive a distance l_r^o to leave the area with passenger on board. Suppose e-hailing vehicles within the area follow

first-in-first-board and first-in-first-out assumptions, then provided the inflow rate $u_r(t)$ of e-hailing vehicles at time t, we have

$$p_r(t + t_r^v(t) + t_r^c(t)) = u_r(t), \tag{3.21}$$

$$b_r(t + t_r^v(t) + t_r^c(t) + t_r^s(t)) = u_r(t), \tag{3.22}$$

$$o_r(t + t_r^v(t) + t_r^c(t) + t_r^s(t) + t_r^o(t)) = u_r(t). \tag{3.23}$$

From the definition of $t_r^v(t)$ and $t_r^o(t)$, they must satisfy the following conditions:

$$\int_t^{t+t_r^v(t)} v^{in}(s)ds = l_r^v, \tag{3.24}$$

$$\int_{t+t_r^v(t)+t_r^c(t)+t_r^s(t)}^{t+t_r^v(t)+t_r^c(t)+t_r^s(t)+t_r^o(t)} v^{out}(s)ds = l_r^o. \tag{3.25}$$

Meanwhile, with a parking rate $p_r(t)$ and a boarding rate $b_r(t)$, the number of parked e-hailing vehicles within the area at time t can be formulated as:

$$n_r^{pk}(t) = \int_0^t b_r(s) - p_r(s)ds. \tag{3.26}$$

According to Eqs. (3.1)–(3.2), we then define the parking occupancy $q(t)$ of this area at time t and the cruising distance for parking spaces for vehicles that start searching at time t as follows:

$$q(t) = \frac{n_r^{pk}(t)}{N^{pk}}, \tag{3.27}$$

$$l_r^c(t) = \frac{d}{1 - q(t)}. \tag{3.28}$$

As drivers would usually slower their speed when they are cruising for parking spaces, we assume the vehicle cruising speed at time t , denoted by $v^{cr}(t)$, is a proportion of the vehicle speed of the 'in' direction, i.e.,

$$v^{cr}(t) = \gamma \cdot v^{in}(t), \tag{3.29}$$

with γ being a discount parameter satisfying $0 \leq \gamma \leq 1$. Then for a vehicle that enters the demand-surge area at time t and starts cruising for parking space at time $t + t_r^v(t)$, the time it takes to successfully find a parking space, i.e., $t_r^c(t)$, must satisfy the following condition:

$$\int_{t+t_r^v(t)}^{t+t_r^v(t)+t_r^c(t)} v^{cr}(s)ds = l_r^c(t+t_r^v(t)). \tag{3.30}$$

And from Eq. (3.3), for an e-hailing vehicle that enters the area at t, its passenger-searching time $t_r^s(t)$ then follows:

$$t_r^s(t) = \frac{1}{2} \cdot n_r^{pk}(t+t_r^v(t)+t_r^c(t)) \cdot t_{chk}, \tag{3.31}$$

where $n_r^{pk}(t+t_r^v(t)+t_r^c(t))$ is the number of parked vehicles at time $t+t_r^v(t)+t_r^c(t)$. In a trip-based model, we track the travel distance of e-hailing vehicle entering the area at time t, so as to determine the value of $t_r^v(t)$, $t_r^c(t)$ and $t_r^o(t)$ that satisfy Eqs. (3.24), (3.30) and (3.25).

On the other hand, for a vacant bus that enters the area at time t, let $t_p^v(t)$ be the time it takes to complete an average distance l_p^v and reach the bus stop, $\tilde{t}_p(t)$ be the passenger loading time, and $t_p^o(t)$ be the time it takes to drive an average distance $l_p^o(t)$ with passengers on-board to leave the area, as shown in Figure 3.1(b). Similar to Eqs. (3.22) and (3.23), suppose buses within the area follow first-in-first-board and first-in-first-out assumptions, then provided the bus inflow rate $u_p(t)$, the bus boarding rate and bus outflow rate can be formulated as:

$$b_p(t+t_p^v(t)+\tilde{t}_p(t)) = u_p(t), \tag{3.32}$$

$$o_p(t+t_p^v(t)+\tilde{t}_p(t)+t_p^o(t)) = u_p(t). \tag{3.33}$$

Suppose bus speed is the same as e-hailing vehicle speed, then the same as in Eqs. (3.24) and (3.25), the values of $t_p^v(t)$ and $t_p^o(t)$ in Eqs. (3.32) and (3.33) must satisfy the following conditions:

$$\int_{t}^{t+t_p^v(t)} v^{in}(s)ds = l_p^v, \tag{3.34}$$

$$\int_{t+t_p^o(t)+\tilde{t}_p(t)}^{t+t_p^o(t)+\tilde{t}_p(t)+t_p^o(t)} v^{out}(s)ds = l_p^o. \tag{3.35}$$

And in this chapter, we assume all buses will be fully loaded, so that the bus loading time $\tilde{t}_p(t)$ is a constant, depending on bus capacity, i.e.,

$$\tilde{t}_p(t) = \phi \cdot C_p, \tag{3.36}$$

where C_p indicates bus capacity, and ϕ is a constant of passenger boarding speed. And in a

trip-based model, the same as we do for $t_r^v(t)$ and $t_r^o(t)$, we track the travel distance of each bus entering the area at time t, so as to determine the value of $t_p^v(t)$ and $t_p^o(t)$ that satisfy Eqs. (3.34) and (3.35).

All background traffic drive an average distance l_b to traverse the area without stopping. As shown in Figure 3.1(c), for a background vehicle that enter the area at time t, let $t_b^{in}(t)$ be the time it takes to complete the initial θ proportion of the distance l_b, which is assumed in the direction of towards the passenger-waiting area, and $t_v^{out}(t)$ be the time it takes to complete the rest distance, which is in the direction of out of the passenger-waiting area. Assuming that all background traffic within the area follow first-in-first-out assumptions, then provided the inflow rate of background traffic at time t, the completion rate $b_b(t)$ of background traffic for the initial θ proportion of their trip within the area, and the outflow rate $o_b(t)$ of background traffic can be formulated as:

$$b_b(t + t_b^{in}(t)) = u_b(t), \tag{3.37}$$

$$o_b(t + t_b^{in}(t) + t_b^{out}(t)) = u_b(t). \tag{3.38}$$

And similar as Eqs. (3.34) and (3.35), $t_b^{in}(t)$ and $t_b^{out}(t)$ must satisfy the following conditions:

$$\int_t^{t+t_b^{in}(t)} v^{in}(s)ds = \theta l_b, \tag{3.39}$$

$$\int_{t+t_b^{in}(t)}^{t+t_b^{in}(t)+t_b^{out}(t)} v^{out}(s)ds = (1-\theta) l_b. \tag{3.40}$$

We track the travel distance of each background vehicle entering the area at time t, so as to determine the value of $t_b^{in}(t)$ and $t_b^{out}(t)$ that satisfy Eqs. (3.39) and (3.40).

As can be seen from Eqs. (3.23)–(3.40), the parking, boarding and outflow rates of each type of vehicles at any time t are dependent on the inflow rates and their trip duration in each direction within the area, and the trip duration of vehicles that enter the area at different time t is governed by the dynamic vehicle speed $v^{in}(t)$ and $v^{out}(t)$ within the area. From Eq. (3.4), to determine the vehicle speed of each direction at any time t, we then proceed to figure out the vehicle accumulations $n^{in}(t)$ and $n^{out}(t)$ at any time t in the next subsection.

3.2.2 Traffic dynamics within the area

Let $n_r^d(t), n_p^d(t), n_b^d(t)$ respectively be the numbers of e-hailing vehicles, buses, and background traffic in direction $d \in \{in, out\}$ at time t. All buses and e-hailing vehicles change their

direction to leave the area after passengers get on-board, so the evolution of the numbers of buses and e-hailing vehicles in each direction follows:

$$n_r^{in}(t) = \int_0^t [u_r(s) - b_r(s)]ds, \tag{3.41}$$

$$n_r^{out}(t) = \int_0^t [b_r(s) - o_r(s)]ds, \tag{3.42}$$

$$n_p^{in}(t) = \int_0^t [u_p(s) - b_p(s)]ds, \tag{3.43}$$

$$n_p^{out}(t) = \int_0^t [b_p(s) - o_p(s)]ds, \tag{3.44}$$

where $b_r(t), o_r(t), b_p(t)$ and $o_p(t)$ are given by Eqs. (3.22), (3.23), (3.32), and (3.33) respectively.

For the background traffic, they are in the 'in' direction during the first θ proportion of the trip within the area, and turn into the 'out' direction afterwards. So the evolution of the number of background traffic in each direction follows:

$$n_b^{in}(t) = \int_0^t [u_b(s) - b_b(s)]ds, \tag{3.45}$$

$$n_b^{out}(t) = \int_0^t [b_b(s) - o_b(s)]ds, \tag{3.46}$$

where $b_b(t), o_b(t)$ are given by Eqs. (3.37) and (3.38).

Assuming that each bus is equivalent to 2.5 private-car units, the total accumulation in direction d within this area follows:

$$n^d(t) = n_r^d(t) + 2.5n_p^d(t) + n_b^d(t), d \in \{in, out\}, \tag{3.47}$$

And the total accumulation within this area is

$$n(t) = n^{in}(t) + n^{out}(t). \tag{3.48}$$

Furthermore, as in Geroliminis and Daganzo (2008), we define $P^d(t)$ as the production of vehicles within the demand-surge area in direction d at time t, which follows:

$$P^d(t) = n^d(t) \cdot v^d(t), d \in \{in, out\}. \tag{3.49}$$

And the total production of the area is defined as:

$$P(t) = P^{in}(t) + P^{out}(t). \tag{3.50}$$

3.2.3 Passenger dynamics within the area

As buses and e-hailing vehicles get loaded, the number of waiting passengers within the area decreases. Let $e(t)$ be the passenger evacuation rate at time t. Since we assume each e-hailing vehicle serves one passenger and each bus takes C_p passengers, $e(t)$ follows

$$e(t) = C_p \cdot o_p(t) + o_r(t), \tag{3.51}$$

and it represents the passenger evacuation efficiency during a time period. Let $Q_r(t)$ and $Q(t)$ be the cumulative number of e-hailing passengers and total passengers that have been transported out of the area at time t, i.e.,

$$Q_r(t) = \int_0^t o_r(s)ds, \tag{3.52}$$

$$Q(t) = \int_0^t e(s)ds, \tag{3.53}$$

and T be the total time it takes for all passengers to be evacuated out of this area, then T satisfies

$$Q(T) = Q. \tag{3.54}$$

Accordingly, $Q_r(T)$ denotes the passenger number transported by e-hailing when the total evacuation has been completed at time T. Therefore we denote the proportion of passengers evacuated by e-hailing vehicles at time t as $S_r(t)$. When total evacuation has been completed at time T, we have the overall proportion of passengers evacuated by e-hailing vehicles modeled as:

$$S_r(T) = \frac{Q_r(T)}{Q(T)}. \tag{3.55}$$

Based on the above dynamic passenger evacuation model, we can simulate the dynamic traffic conditions and passenger evacuation process to demonstrate the impacts of e-hailing services on the passenger evacuation efficiency. Note that while the above Eqs. are all described in continuous-time form, we divide time into discrete units with time interval Δt, i.e., $t = \{0, \Delta t, 2\Delta t, ..., k\Delta t, ...\}$ in our simulation experiment. The integration of any function $f(x)$

from 0 to t is then approximated by

$$\int_0^{k\Delta t} f(s)ds = \sum_0^k f(k\Delta t)\Delta t. \tag{3.56}$$

Let $n^{in}(0)$ and $n^{out}(0)$ be the initial vehicle accumulation within the area at $k = 0$. From the above discussion, given $n^{in}(k\Delta t)$ and $n^{out}(k\Delta t)$ at the beginning of the kth interval, we can determine the vehicle speed $v(k\Delta t)$ from Eq. (3.4). The product $v(k\Delta t)\Delta t$ gives the travel distance of vehicles within a time interval Δt. By taking record of the total travel distance of vehicles entering the area at the beginning of the kth interval, we can determine the parking rate, boarding rate and outflow rate of each type of vehicles at the end of the kth interval (or equivalently, the beginning of the $(k+1)$th interval) according to Eqs. (3.22)–(3.40), and the number of passengers evacuated according to Eq. (3.53). And based on the value of $u_i((k+1)\Delta t), b_i((k+1)\Delta t)$ and $o_i((k+1)\Delta t), i = \{r, p, b\}$ we can further determine the vehicle accumulation $n_i^d((k+1)\Delta t), i = \{r, p, b\}$ of each type in each direction $d = \{in, out\}$ in the $(k+1)$th interval from Eqs. (3.41)–(3.46).

3.2.4 Numerical example

Assume that there are $Q = 6000$ passengers waiting for transportation at time t within the demand-surge area. Background traffic arrives at the boundary of the area with a constant rate $u_p(t) = 0.033$ veh/s since $t = 0$; dedicated buses and e-hailing vehicles start to arrive at the boundary since $t = 120s$. Buses keep entering with a mean rate $u_b(t) = 1$ veh/s. As mentioned above, e-hailing vehicles' arrival rate $u_r(t)$ is determined by the matching rate $m_r(t)$, which is further determined by the e-hailing vehicles' supply by the platform. Both of these two types of vehicles will keep arriving until the total vehicle supply is sufficient to transport all passengers out of the area. E-hailing vehicles will go through a period of driving time from being assigned an order to arriving the boundary of the demand surge area with $\tilde{t}_r$=120 s. The average bus driving distances l_p^v and l_p^o within the area are both set to be 500 m. And with a bus capacity 50 psgr/veh, and the average bus loading time is a constant $\widetilde{t}_p$=180 s. For background traffic, their average distance within the area is $l_b = 1000$ m, and a proportion $\theta = 50\%$ of the distance is of the 'in' direction. The speed of each direction follows

$$v^d(n^d) = v_f^d \cdot \exp\left\{-0.6 \times \left(\frac{n^d}{n_{opt}^d}\right)^2\right\}, d \in \{in, out\}. \tag{3.57}$$

Table 3.1 Parameter setting in the numerical analysis

Parameter	Value	Unit
Total passenger evacuation demand (Q)	6000	person
Bus arrival rate (u_p)	0.033	veh/s
Background traffic arrival rate (u_b)	1	veh/s
Free flow speed (v_f^d)	12.5	m/s
Driving distance of vacant e-hailing vehicles within the area (l_r^v)	500	m
Driving distance of occupied e-hailing vehicles within the area (l_r^o)	500	m
Driving distance of vacant buses within the area (l_p^v)	500	m
Driving distance of occupied buses within the area (l_p^o)	500	m
Bus capacity (C_p)	50	psgr/veh
Average bus loading time ($\tilde{t}_p$)	180	s/veh
Driving distance of background traffic within the area (l_b)	1000	m
The proportion of distance in in direction (θ)	50	%
Distance of two neighbouring parking spaces (d)	6	m
Total number of parking spaces (N^{pk})	200	spot
The discount of vehicles' cruising for parking speed (γ)	60	%
Per vehicle checking time(t_{chk})	3	s
Boundary capacity (C_{max})	1.75	veh/s
Value of time(β)	60	¥/hour
E-hailing driving time from being assigned an order to arriving the boundary of the demand surge area ($\tilde{t}_r$)	120	s
Average trip payment for e-hailing service (f_r)	30	¥
Average trip payment for bus service (f_p)	5	¥
Discomfort cost of taking bus (θ_p)	5	¥
The coefficient in the Logit-model(η)	0.15	
Sampling time	60	s

where $v_f^d = 12.5$ m/s is the free flow speed of direction $d = \{in, out\}$ and $n_{opt}^d = 170$ veh is the optimal vehicle accumulation that can maximize the vehicle production of each direction $d = \{in, out\}$. The setup of parameters is summarized in Table 3.1.

Under the above setting, we simulate the passenger evacuation process and dynamic traffic conditions within the area under different arrival rates of e-hailing vehicles at the platform's searching radius $A_r = 0, 0.25, 0.5, 0.75, 1$ veh/s. When $A_r = 0$, it corresponds to the bus-only case (hereinafter, we use 'BO' for short), where there are only buses and background traffic entering the area (in this special case, all the 6000 passengers would be served by buses). And when $A_r > 0$, all passengers will be shared by both two modes[3.2]. After entering the area, e-hailing vehicles drive an average distance $l_r^v = 500$ m to park near their passengers. There are 200 parking spaces within the area, the vehicle cruising speed $v_{cr}(t)$ is 60% of the vehicle speed $v^{in}(t)$, and the average distance between two neighbouring parking spaces is 6 m. In the passenger searching time function (3.3), we set $t_{chk} = 3$ s and $\alpha = \frac{1}{2}$. After passengers get on

[3.2]The inflow rate of e-hailing vehicles is set to be zero when the buses and e-hailing vehicles flowed into the area have been sufficient to take all passengers.

board, e-hailing vehicles then drive an average distance $l_r^o = 500$ m to leave the area. In each simulation, all variables are updated every one minute.

The passenger evacuation efficiency under different e-hailing arrival rates at the boundary are presented in Figure 3.3. As we can see from Figure 3.3(a), the arrival rate of e-hailing vehicles plays a significant role in determining the passenger evacuation efficiency. With the increase of e-hailing vehicles' arrival rate, the total evacuation time will firstly be sightly shortened and then greatly extended. When $A_r = 0.25$ veh/s, the number of parked vehicles and the number of cruising-for-parking vehicles are small, so the small arrival rate of e-hailing vehicles would not cause dense vehicle accumulation within the area, and the total passenger evacuation time 3472s is shorter in comparison with 3982s in the 'BO' case. However, when A_r increases to 0.5 veh/s or more, the existence of e-hailing services slows down rather than speeding up the evacuation process. And the higher the e-hailing vehicle arrival rates, the longer the passenger evacuation time. When $A_r = 1$ veh/s, the total evacuation time 7846s is more than twice as much as the evacuation time in the 'BO' case. In these cases, a large number of vehicles are accumulated in the 'in' direction (as shown in Figure 3.3(b), and the passengers evacuation time is significantly prolonged. Figure 3.3 (b) and (c) depict the vehicle accumulation $n^{in}(t)$ and the number of parked e-hailing vehicles $n_r^{pk}(t)$ at each moment under different e-hailing arrival rates. Similar with the trend of total evacuation time, with the increase of e-hailing vehicles' arrival rate, both the vehicle accumulation $n^{in}(t)$ and the number of parked vehicles $n_r^{pk}(t)$ have obvious larger quantities compared with normal state. As we can see from the two figures, when $A_r = 0$ or 0.25 veh/s, both $n^{in}(t)$ and $n_r^{pk}(t)$ keep at low levels during the whole evacuation period. However, when $A_r \geq 0.5$veh/s, both the vehicle accumulation $n^{in}(t)$ and the number of parked vehicles increase quickly after the start of the evacuation, and then $n^{in}(t)$ stay at a very high level ($\geq 400 vehs$), while $n_r^{pk}(t)$ drops quickly to between 10 and 40 vehs. It's worth mentioning that when the evacuation process approaches the end, $n_r^{pk}(t)$ has sharps when $A_r \geq 0.5$veh/s in Figure 3.3(c). Due to the excessive e-hailing vehicles' inflow without perimeter control strategy, traffic congestion lasts almost whole evacuation process. During this process, huge amount of vehicles is accumulated in the 'in' direction and the traffic speed is low. The vehicles accumulated in 'in' direction are unable to reach the passenger waiting area to start cruising for parking and park to wait for passengers. With the vehicles keep on outflowing of this demand surge area, traffic congestion is relieved in the final process and traffic speed returns to normal state. Huge amount of congested vehicles becomes able to cruise

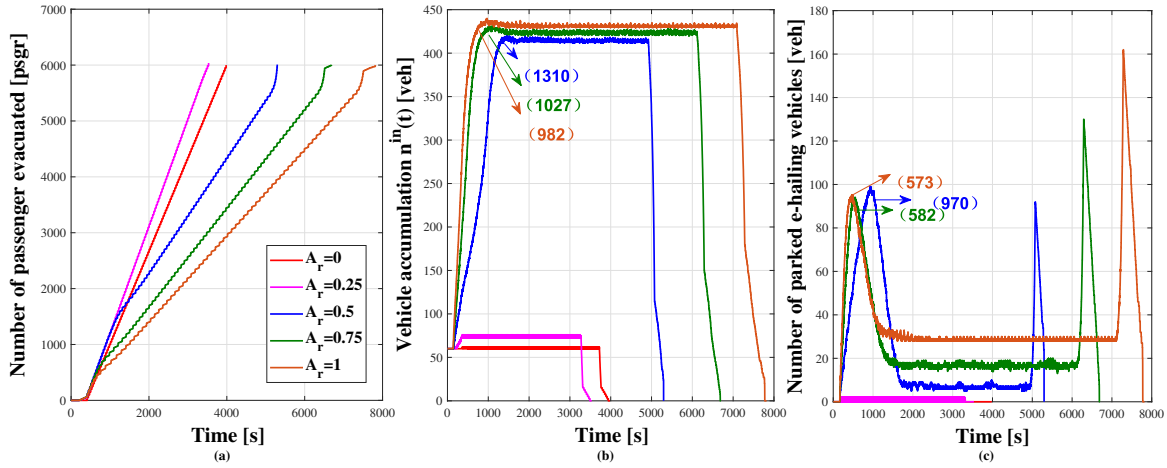

Figure 3.3 The dynamic passenger evacuation process and traffic conditions under different e-hailing arrival rate without perimeter control

for parking and park the vehicle. The high turnover efficiency of the parked vehicles when the evacuation approaches the end results a sharp in the number of parked vehicle.

To further understand how the large arrival rate of e-hailing vehicles slows down the passenger evacuation process, Figure 3.4(a)–(c) present the dynamic passenger evacuation process,vehicle accumulation and vehicle speed when $A_r = 0$ and $A_r = 0.5$ veh/s, and Figure 3.4 (d) depicts the trip duration time of e-hailing vehicles entering the area at different time points when $A_r = 0.5$ veh/s. In the figure, 'BO' stands for the case when $A_r = 0$, and 'UC' stands for the case when $A_r = 0.5$ veh/s and the e-hailing inflow rates to the area is uncontrolled. As shown in Figure 3.4(a) and (b), in the 'BO' case, it takes 3982 s (66.4 min) to transport all passengers out of the area, and the 'in' and 'out' direction accumulation within the area keeps at around 60 veh and 45 veh from $t = 500$s to $t = 3780$s. Under the given arrival rate of buses and background traffic in this example, the congestion effect within the area in the 'BO' case is insignificant. As can been seen from Figure 3.4(c), the vehicle speeds of the 'in' and 'out' directions are around 11.0 m/s and 11.5 m/s during almost the entire evacuation period because of the relatively few total vehicle accumulation within the area.

However, when $A_r = 0.5$ veh/s, it takes 5292 s (that is 88.2 min, being 21.8 min longer than 66.4 min in the 'BO' case) to evacuate all passengers out from this area. As can been seen from Figure 3.4(d), starting from $t = 500s$, the e-hailing vehicle's driving time to the passenger goes through a sharp increase from $50s$ to $500s$. From $t = 1239s$ to $t = 4325s$, for every e-hailing vehicle entering the area during this period, it takes more than $510s$ to drive to the passenger waiting area and then around $50s$ to cruise for parking. This is apparently due to

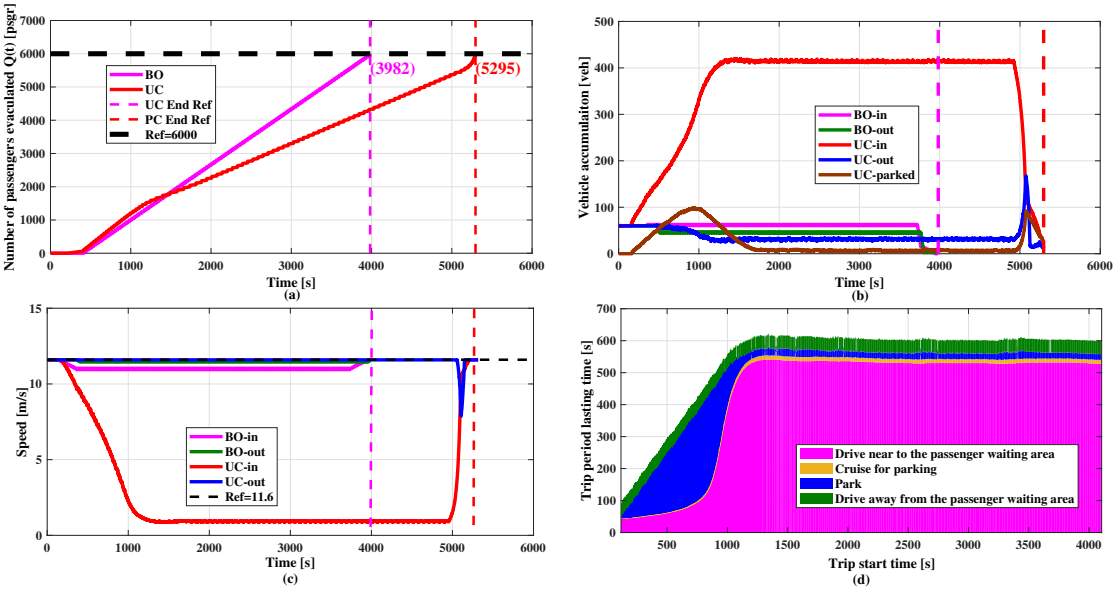

Figure 3.4 The dynamic passenger evacuation and traffic condition curves when $A_r = 0.5$ veh/s

the dense vehicle accumulation $v^{in}(t)$ and consequently slow vehicle speed $v^{in}(t)$ during the period. As shown in Figure 3.4(b) and (c), the vehicle accumulation $n^{in}(t)$ has a rapid increase from the start of this evacuation to $t = 1239s$, which leads to the rapid decrease of the vehicle speed. From $t = 1239s$ to $t = 4950s$, there are more than 400 vehicles accumulated in the 'in' direction, and the resulting vehicle speed $v^{in}(t)$ is less than 2m/s[3.3]. Meanwhile, the vehicle speed of the 'out' direction is almost constantly at $12m/s$ during the entire evacuation process, and the vehicle travel time within the area after picking up passengers is around $42s$ during the whole evacuation period. So the long evacuation time in this case is generally due to the dense vehicle accumulation of the 'in' direction. However, the rise of vehicle accumulation $n^{in}(t)$ is due to the increase of the number of parked vehicles $n_r^{pk}(t)$. As shown in Figure 3.4(b) and (d), with e-hailing vehicles flowing into the area since $t = 50s$, the number of parked vehicles increases quickly from $t = 200s$ to $t = 926s$, and the passenger searching time for their designated vehicles thus increases quickly. At $t = 926s$, around half of the vehicles in the 'in' direction are parked vehicles. The increasing number of parked vehicles $n_r^{pk}(t)$ leads to a quick

[3.3] We note that the vehicle speed does not drop to completely zero because in this example we assume the boundary capacity is decreasing with vehicle accumulation $n^{in}(t)$ within the area when accumulation is larger than the optimal accumulation, i.e.,

$$C(t) = \begin{cases} C_{max} & 0 \le n^{in}(t) \le n_{opt}^{in} \\ C_{max} \times \dfrac{n_{jam}^{in} - n^{in}(t)}{n_{jam}^{in} - n_{opt}^{in}} & n_{opt}^{in} \le n^{in}(t) \le n_{jam}^{in} \end{cases} \tag{3.58}$$

where C_{max} is the upper bound of the boundary capacity, determined by the capacity of roads leading to the area, n_{jam}^{in} represents the jam accumulation of the 'in' direction and n_{opt}^{in} represents the optimal accumulation of the 'in' direction that maximizes the production. In this example, we set $C_{max} = 1.75$ veh/s (or equivalently, 105 veh/min), $n_{jam}^{in} = 500$ veh, and $n_{opt}^{in} = 170$ veh.

increase of $n^{in}(t)$, and slows down the vehicle speed $v^{in}(t)$. And with the decrease of $v^{in}(t)$, e-hailing vehicles have to spent longer time to cruise for parking, so that the parking rate of e-hailing vehicles decreases, and the number of parked vehicles thus decreases. Since $t = 1750s$, $n_r^{pk}(t)$ is stabilized at around $9veh$ because the parking rate and boarding rate become almost equal. As we can see from this example, the dense vehicle accumulation of the 'in' direction is the major reason that prolongs the passenger evacuation process, and the initial increase of the number of parked vehicles serves as an inducement.

In the above, to make the impact of e-hailing arrival rate on evacuation process much clearer, we only examine the evacuation performance under the fixed bus arrival rate. However, in reality, passengers' mode choice will be deeply impacted by the transportation supply, which includes the buses capacity supply and e-hailing vehicles' supply. The supply of each mode of transportation during this process will influence the proportion of passengers evacuated by each mode, as well as the total evacuation time. To offer a more comprehensive perspective of this bi-modal system instead of only focusing on e-hailing service, we further explore the passenger evacuation performance with variable bus and e-hailing arrival rates. We provide a discussion of the impact of transportation supply on the proportion of passengers evacuated by each mode and total evacuation time, in which we test different combinations of bi-modal arrival rates.

We conduct the simulation with the objective of evacuating $Q = 6000$ passengers and take the bus arrival rate with the value 0.017 veh/s, 0.02 veh/s, 0.025 veh/s, 0.033 veh/s, 0.05 veh/s and 0.1 veh/s (the corresponding bus headway takes the value 60s, 50 s, 40 s, 30 s, 20 s, and 10 s). From Figure 3.3, we can easily figure out a reversed effect from speeding up the evacuation efficiency when $A_r = 0.25veh/s$ to slowing down the evacuation efficiency when $A_r = 0.5veh/s$. Interested in exploring the effect e-hailing vehicles' arrival rate on evacuation efficiency, we test the e-hailing vehicles' arrival rate with the value 0.2 veh/s, 0.25 veh/s, 0.3 veh/s, 0.35 veh/s, 0.4 veh/s, 0.45 veh/s, 0.5 veh/s. Shown in Figure 3.5, we can intuitively find that under the combinations of high bus arrival rate and low e-hailing vehicle arrival rate, the total evacuation time will be short and averagely below 3000s, which can be figured out in the dark blue part in Figure 3.5. On the contrary, under the combinations of high e-hailing vehicle arrival rate and low bus arrival rate, the total evacuation time will be long and averagely above 5000s, which can be figured out in the light yellow part in Figure 3.5. The corresponding data of total evacuation time can be found in Table 3.2. Under the fixed e-hailing vehicles' arrival rate, the total evacuation time will be shortened as the bus arrival rate increases from 0.017 veh/s to 0.1 veh/s. This

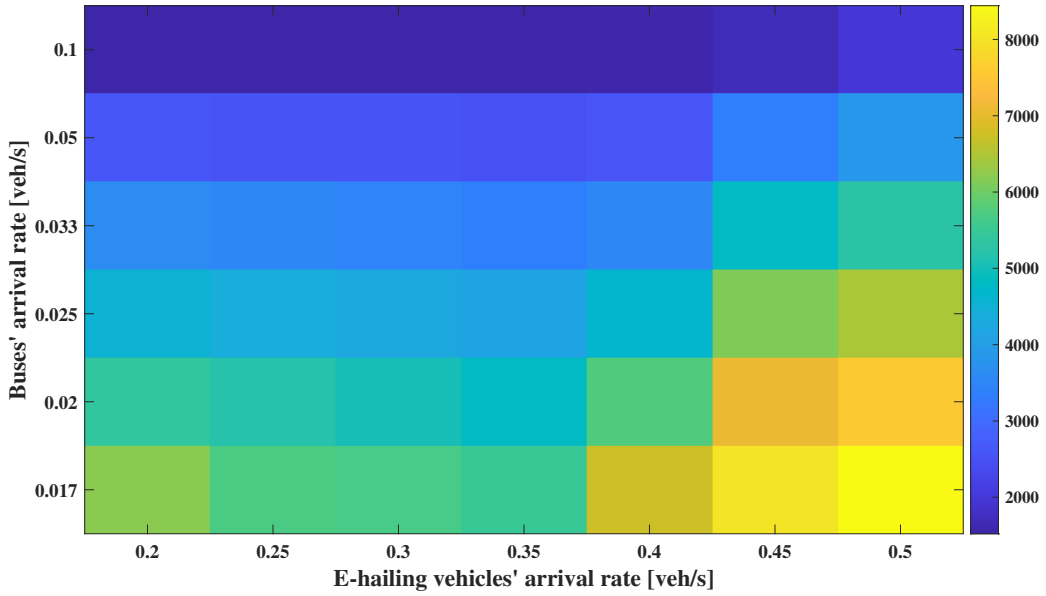

Figure 3.5 Total evacuation time under different combinations of bus and e-hailing vehicles arrival rates

shows the bus's completely positive impact on evacuation speed. It is highlighted that bus is a mode of intensive and efficient transportation under huge passenger demand, which explains its popularity in relevant studies. However under the fixed bus arrival rate, the total evacuation time will first sightly decrease and then largely increase with the e-hailing vehicles' arrival rate increases from 0.2 veh/s to 0.5 veh/s. The e-hailing vehicles' positive impact on evacuation is mostly utilized when $A_r = 0.35veh/s$ because at this point, the minimum evacuation time can be achieved. When $A_r > 0.35veh/s$, the positive effect of e-hailing service is weakened. In light of the findings, it is worthy to note that higher e-hailing vehicle arrival rate will not definitely lead to a reduction in the total evacuation time. In order to prevent the congestion effect caused by the excessive amount of vehicles during evacuation process, an appropriate range of e-hailing vehicles' arrival rate needs to be identified to maximize the evacuation efficiency.

As e-hailing's supply is an critical influential factor on passengers' mode choice, we also examine the proportion of passengers evacuated by e-hailing vehicles under various combinations of arrival rates, which uses the same parameter settings as above. As shown in Figure 3.6 and Table 3.3, under the fixed bus arrival rate, the proportion of passengers evacuated by e-hailing vehicles will increase as the e-hailing vehicles' arrival rate increases from 0.2 veh/s to 0.5 veh/s. Similarly, under the fixed e-hailing vehicles' arrival rate, the proportion of passengers evacuated by e-hailing vehicles will decrease as the bus arrival rate increases from 0.017 veh/s to 0.1 veh/s. A competitive relationship between these two modes can be figured out.

Table 3.2 Total evacuation time under different combinations of bus and e-hailing vehicles arrival rates

u_p \ A_r	0.2	0.25	0.3	0.35	0.4	0.45	0.5
0.017	6202	5692	5665	5482	6741	8028	8442
0.02	5382	5182	5032	4832	5761	7084	7568
0.025	4541	4382	4262	4142	4633	6131	6466
0.033	3623	3533	3443	3356	3529	4793	5295
0.05	2624	2566	2544	2504	2603	3353	3871
0.1	1549	1539	1530	1522	1562	1688	1993

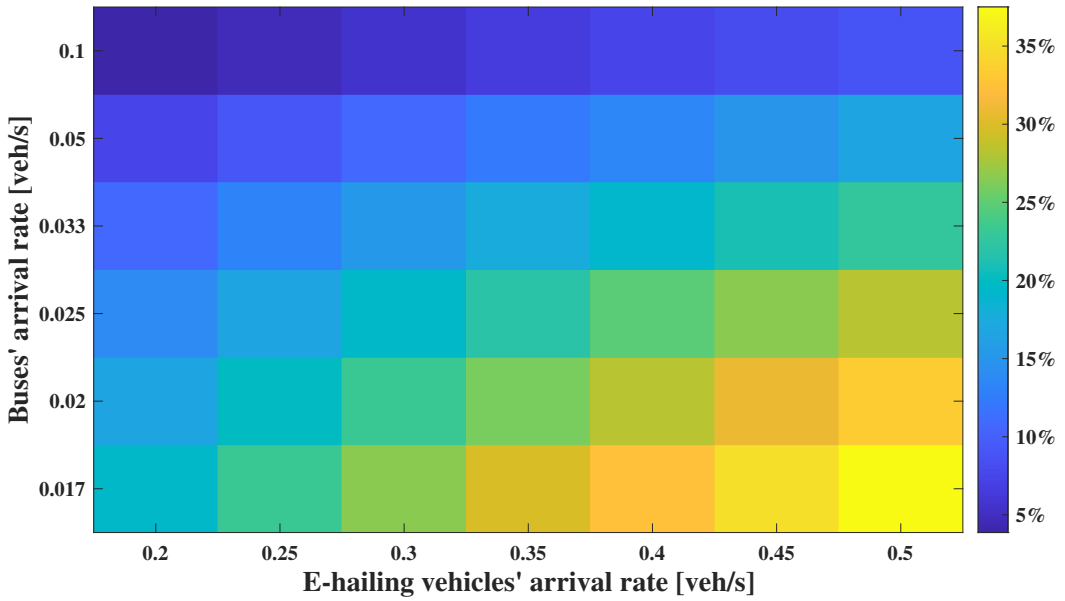

Figure 3.6 The proportion of passengers evacuated by e-hailing vehicles under different combinations of bus and e-hailing vehicles arrival rates

Table 3.3 The proportion of passengers evacuated by e-hailing vehicles under different combinations of bus and e-hailing vehicles arrival rates

u_p \ A_r	0.2	0.25	0.3	0.35	0.4	0.45	0.5
0.017	0.194	0.2325	0.2667	0.2975	0.325	0.3502	0.375
0.02	0.1667	0.2	0.2325	0.2595	0.2835	0.3083	0.3333
0.025	0.1387	0.1667	0.1938	0.2192	0.2481	0.2667	0.2833
0.033	0.108	0.1312	0.153	0.175	0.1917	0.2095	0.2268
0.05	0.0747	0.0917	0.108	0.1237	0.1353	0.15	0.1667
0.1	0.0387	0.0478	0.057	0.0658	0.0747	0.082	0.0887

Both of the two modes follow a rule that as long as more transportation capacity is provided, more passengers will choose this mode of transportation. We can intuitively find that under the combinations of high bus arrival rate and low e-hailing vehicle arrival rate, the proportion of passengers evacuated by e-hailing vehicles will be low and averagely below 10%, which can be figured out in the dark blue part in Figure 3.6. On the contrary, under the combinations of high e-hailing vehicle arrival rate and low bus arrival rate, the proportion of passengers evacuated by e-hailing vehicles will be high and averagely over 30%, which can be figured out in the light yellow part in Figure 3.6. The corresponding data of total evacuation time can be found in Table 3.3. Comparing Figure 3.5 with Figure 3.6, proportion of passengers evacuated by e-hailing vehicles has a similar trend with total evacuation time. Therefore, it is reasonable to infer that when proportion of passengers evacuated by e-hailing vehicles is too high, it may negatively affect evacuation efficiency. Thereby the necessity of controlling the e-hailing arrival rate can be effectively confirmed to help improve the evacuation efficiency.

3.3 The Feedback Perimeter Control Strategy

The numerical example in the previous section shows that in case of large arrival rates of e-hailing vehicles, the availability of e-hailing service may seriously deteriorate the traffic conditions within the demand-surge area, slow down not only e-hailing outflow rate but also bus transport efficiency, and prolong the passenger evacuation process. To mitigate the negative impacts of e-hailing services on the evacuation process, it is essential to control the inflow rate of e-hailing vehicles, so as to avoid over-congestion within the area. So this section is devoted to find out an effective perimeter control strategy. Note that since it is difficult (if not impossible) to differentiate background traffic from e-hailing vehicles, we propose a gating strategy that is imposed on the two types of vehicles indifferently at the boundary. A discussion of the perimeter control strategy when e-hailing vehicles and background traffic are differentiable will be provided in the following. The bus inflow rate is not subject to control, but it would be influenced by the perimeter control strategy due to the queuing background traffic and e-hailing vehicles at the boundary.

Let $I(t)$ be the maximally allowed inflow rate of e-hailing vehicles and background traffic under the perimeter control strategy, and $\bar{u}_r(t)$, $\bar{u}_b(t)$ and $\bar{u}_p(t)$ respectively be the actual inflow rates of e-hailing vehicles, background traffic and buses under the perimeter control strategy at time t. When the total arrival rates of e-hailing vehicles and background traffic exceeds the

maximally allowed inflow rate for the two types of vehicles, there will be waiting vehicles on the roads leading to the boundary of the area. In this case, the arrival rate of vehicles to the gating position at the boundary will be restrained by the boundary capacity. And since we assume buses share lanes with the other two types of vehicles, the boundary capacity constraint is effective on all types of vehicles, including buses. So we may observe waiting buses at the boundary, although the perimeter control strategy is not intentionally imposed on buses. Let $W_r(t), W_b(t)$ and $W_p(t)$ be the number of waiting e-hailing vehicles, background traffic and buses at the boundary at time t, then we have

$$W_r(t) = \int_0^t u_r(t) - \bar{u}_r(t)dt, \tag{3.59}$$

$$W_b(t) = \int_0^t u_b(t) - \bar{u}_b(t)dt, \tag{3.60}$$

$$W_p(t) = \int_0^t u_p(t) - \bar{u}_p(t)dt. \tag{3.61}$$

The boundary capacity constraint determines the arrival rates of the three types of vehicles to the gating position. When it is activated, we assume the boundary capacity proportionally distributed to the three types of vehicles according to their queue length. Let $\widetilde{u}_r(t), \widetilde{u}_b(t)$ and $\widetilde{u}_p(t)$ be the arrival rates of e-hailing vehicles, background traffic and buses at the gating position, then we have

$$\widetilde{u}_r(t) = \begin{cases} C(t)\frac{W_r(t)}{W_r(t)+W_b(t)+2.5W_p(t)}, & \text{if } W_r(t)+W_b(t)+2.5W_p(t) > 0 \\ \min\left\{C(t)\frac{u_r(t)}{u_r(t)+u_b(t)+2.5u_p(t)}, u_r(t)\right\}, & \text{otherwise} \end{cases} \tag{3.62}$$

$$\widetilde{u}_b(t) = \begin{cases} C(t)\frac{W_b(t)}{W_r(t)+W_b(t)+2.5W_p(t)}, & \text{if } W_r(t)+W_b(t)+2.5W_p(t) > 0 \\ \min\left\{C(t)\frac{u_b(t)}{u_r(t)+u_b(t)+2.5u_p(t)}, u_b(t)\right\}, & \text{otherwise} \end{cases} \tag{3.63}$$

$$\widetilde{u}_p(t) = \begin{cases} C(t)\frac{2.5W_p(t)}{W_r(t)+W_b(t)+2.5W_p(t)}, & \text{if } W_r(t)+W_b(t)+2.5W_p(t) > 0 \\ \min\left\{C(t)\frac{2.5u_b(t)}{u_r(t)+u_b(t)+2.5u_p(t)}, u_p(t)\right\}, & \text{otherwise} \end{cases} \tag{3.64}$$

where 2.5 is the passenger car unit of buses.

At the gating position, all buses will flow into the area without stopping, i.e.,

$$\bar{u}_p(t) = \widetilde{u}_p(t). \tag{3.65}$$

But the e-hailing vehicles and background traffic will be subject to perimeter control. As it is difficult to differentiate e-hailing vehicles with private cars, we assume the maximally allowed inflow rate $I(t)$ is proportionally distributed to the arrived e-hailing vehicles and background traffic at the gating position. Specifically, if there are waiting e-hailing vehicles and background traffic at the boundary at time t, then the allowed inflow rate at time t is distributed to the two types of vehicles according to their number of waiting vehicles; and if there are no waiting vehicles at the boundary at time t, but the total arrival rate of e-hailing vehicles and background vehicles is larger than the allowed inflow rate at time t, then $I(t)$ is proportionally distributed to the two types of vehicles according to their arrival rates. So with $I(t), W_r(t), W_b(t), \widetilde{u}_r(t)$ and $\widetilde{u}_b(t)$, the actual inflow rates of e-hailing vehicles and background traffic at time t, follow

$$\bar{u}_r(t) = \begin{cases} I(t)\frac{W_r(t)}{W_r(t)+W_b(t)}, & \text{if } W_r(t)+W_b(t) > 0 \\ \min\left\{I(t)\frac{\widetilde{u}_r(t)}{\widetilde{u}_r(t)+\widetilde{u}_b(t)}, \widetilde{u}_r(t)\right\}, & \text{otherwise} \end{cases} \tag{3.66}$$

$$\bar{u}_b(t) = \begin{cases} I(t)\frac{W_b(t)}{W_r(t)+W_b(t)}, & \text{if } W_r(t)+W_b(t) > 0 \\ \min\left\{I(t)\frac{\widetilde{u}_b(t)}{\widetilde{u}_r(t)+\widetilde{u}_b(t)}, \widetilde{u}_b(t)\right\}, & \text{otherwise} \end{cases} \tag{3.67}$$

Ideally, the objective of the control problem is to find out the optimal inflow rate $I(t)$ which minimizes the total evacuation time T, i.e.,

$$I(t) \in arg\min_{I(t)} T \tag{3.68}$$

s.t.

$$\int_0^T [C_p o_p(s) + o_r(s)]ds = Q, \tag{3.69}$$

$$p_r(t + t_r^v(t) + t_r^c(t)) = \bar{u}_r(t), \tag{3.70}$$

$$b_r(t + t_r^v(t) + t_r^c(t) + t_r^s(t)) = \bar{u}_r(t), \tag{3.71}$$

$$o_r(t + t_r^v(t) + t_r^c(t) + t_r^s(t) + t_r^o(t)) = \bar{u}_r(t), \tag{3.72}$$

$$b_p(t + t_p^v(t) + \tilde{t}_p(t)) = \bar{u}_p(t), \tag{3.73}$$

$$o_p(t + t_p^v(t) + \tilde{t}_p(t) + t_p^o(t)) = \bar{u}_p(t), \tag{3.74}$$

$$b_b(t + t_b^{in}(t)) = \bar{u}_b(t), \tag{3.75}$$

$$o_b(t + t_b^{in}(t) + t_b^{out}(t)) = \bar{u}_b(t), \tag{3.76}$$

$$n_i^{in}(t) = \int_0^t [\bar{u}_i(s) - b_i(s)]ds, i \in \{p, r, b\}, \tag{3.77}$$

$$n_i^{out}(t) = \int_0^t [b_r(s) - o_r(s)]ds, i \in \{p, r, b\}, \tag{3.78}$$

$$v^d(t) = V(n^d(t)), \tag{3.79}$$

where $\bar{u}_i(t), i \in \{p, r, b\}$ is subject to Eqs. (3.59)–(3.67), $t_r^v(t)$, $t_r^c(t)$, $t_r^s(t)$ and $t_r^o(t)$ are subject to Eqs. (3.24)–(3.31), $t_p^v(t), t_p^o(t)$ and $\tilde{t}_p(t)$ are subject to Eqs. (3.34)–(3.36), and $t_b^{in}(t)$ and $t_b^{out}(t)$ are subject to Eqs. (3.39)–(3.40).

However, as the arrival rate of different types of vehicles at any subsequent time points are generally unknown to traffic regulators, it is impossible to obtain such optimal inflow control rates by solving Eqs. (3.68)–(3.79). As we observed in the numerical examples in Subsection 3.2.4, the dense vehicle accumulation of the 'in' direction is the major reason that slows down the passenger evacuation efficiency, and the increase of the number of parked vehicles serves as an inducement. So in this study, we propose to achieve the minimal evacuation time approximately by keeping either the vehicle accumulation of the 'in' direction $n^{in}(t)$ or the number of parked vehicles $n_r^{pk}(t)$ within the area at appropriately levels. In order to achieve this target, we propose to adopt the classical Proportional-Integral-type (PI) controller, which was adopted in many previous traffic control literature (e.g., Keyvan-Ekbatani et al. (2012), Aboudolas and Geroliminis (2013), Haddad and Shraiber (2014), Ingole et al. (2020)) for its simplicity and cost-efficiency. Two PI controllers, which respectively control the inflow rates $I(t)$ based on observations of $n^{in}(t)$ and $n_r^{pk}(t)$ are introduced and compared in the following.

In the first PI controller, we let $\bar{n}^{in}$ be the desired vehicle accumulation of the 'in' direction. Gating is activated when the vehicle accumulation $n^{in}(t)$ within the area exceeds a threshold $\sigma\bar{n}^{in}$ and is de-activated when $n(t)$ drops to below $\sigma\bar{n}^{in}$, i.e.,

$$\text{PC-1: } I(t) = \begin{cases} \widehat{I}_1(t), \text{if } n^{in}(t) \geq \sigma\bar{n}^{in} \\ +\infty, \text{otherwise} \end{cases} \tag{3.80}$$

where $\widehat{I}_1(t)$ follows

$$\widehat{I}_1(t) = \max\left\{K_P\left[\bar{n}^{in} - n^{in}(t)\right] + K_I\int_0^t \left\{\bar{n}^{in} - n^{in}(s)\right\}ds, 0\right\}. \tag{3.81}$$

In Eq. (3.81), K_P is the non-negative proportional gain applied to the error between the current

accumulation $n^{in}(t)$ and the optimal accumulation $\bar{n}^{in}$, and K_I is the non-negative integral gain applied to the integral of the error. When $n^{in}(t) < \bar{n}^{in}$ ($n^{in}(t) > \bar{n}^{in}$), the error term $\bar{n}^{in} - n^{in}(t)$ is positive (negative), and the integral of the error $\int_0^t \{\bar{n}^{in} - n^{in}(s)\}\, ds$ increases (decreases) as the time that the system spent in state $n^{in}(t) < \bar{n}^{in}$ ($n^{in}(t) > \bar{n}^{in}$) increases. Therefore, the allowed inflow rate $\hat{I}_1(t)$ increases (decreases) with the gap $|\bar{n}^{in} - n^{in}(t)|$ and the time that the system spent in state $n^{in}(t) < \bar{n}^{in}$ ($n^{in}(t) > \bar{n}^{in}$), so as to increase (decrease) the vehicle accumulation $n^{in}(t)$ and push it towards $\bar{n}^{in}$. In the following numerical examples, we set $\bar{n}^{in}$ to be the optimal vehicle accumulation n^{in}_{opt} that maximizes the vehicle production of the 'in' direction, i.e.,

$$n^{in}_{opt} = arg\max_{n} P^{in}(n) = n^{in} \cdot V(n^{in}). \tag{3.82}$$

And based on numerical tests in the following, we suggest to set $K_P = 0.5, K_I = 0.3, \sigma = 85\%$ for PC-1.

In the second PI controller, we let $\bar{n}^{pk}_r$ be the target level for the number of parked vehicles within the area. Gating is activated when the number of parked vehicles $n^{pk}_r(t)$ exceeds a threshold $\sigma\bar{n}^{pk}_r$ and de-activated when $n^{pk}_r(t)$ drops to below $\sigma\bar{n}^{pk}_r$, i.e.,

$$\text{PC-2: } I(t) = \begin{cases} \widehat{I}_2(t), \text{if } n^{in}(t) \geq \sigma\bar{n}^{pk}_r \\ +\infty, \text{otherwise} \end{cases} \tag{3.83}$$

where $\widehat{I}_2(t)$ follows

$$\widehat{I}_2(t) = \max\left\{K_P\left[\bar{n}^{pk}_r - n^{pk}_r(t)\right] + K_I \int_0^t \left\{\bar{n}^{pk}_r - n^{pk}_r(s)\right\} ds, 0\right\}. \tag{3.84}$$

Based on numerical tests in the following, we suggest to set $K_P = 0.06$, $K_I = 0.0001$ and $\sigma = 85\%$ for PC-2.

3.4 Numerical Examples

In this section, keeping all parameters unchanged as in Subsection 3.2.4, we first conduct simulation experiments to examine the efficiency of the two perimeter control strategies, and then provide sensitivity analysis to show how the bus headway, passenger demand and the number of parking spaces affect the effectiveness of the two perimeter control strategies. Finally, we test the different combinations of bi-modal arrival rates, to examine the effectiveness of perimeter control strategy on reducing the proportion of passengers evacuated by e-hailing ve-

hicles and shortening total evacuation time. For the first PI controller based on observation of $n^{in}(t)$, according to the space-mean speed-accumulation relationship (3.57), the target vehicle accumulation $\bar{n}^{in} = n^{in}_{opt}$ is set to be $170 veh s$; for the second PI controller based on observation of $n^{pk}_r(t)$, according to our observation from Figure 3.3, the target $\bar{n}^{pk}_r$ is set to be $10 veh s$.

3.4.1 Effectiveness of the two perimeter control strategies

Figures 3.7 and 3.8 respectively depict the dynamic passenger evacuation process and traffic conditions under the first and second PI controllers. And the resulting passenger evacuation time at different e-hailing arrival rates are depicted in Figure 3.9, where 'BO' indicates the case with 'bus-only' service, 'UC' is for the 'uncontrolled' case when both bus and e-hailing services are available, and 'PC-1' and 'PC-2' are respectively for the cases with the first and second PI controllers. As can be seen from Figure 3.7 and Figure 3.8, when the mean arrival rates of e-hailing vehicles are small, i.e., $A_r = 0.25$ veh/s, and the impact of e-hailing services on passenger evacuation efficiency is positive, both perimeter control strategies would not be activated; but when the mean arrival rates of e-hailing vehicles become larger, i.e., $A_r \geq 0.5$ veh/s, both PI controllers would be activated after a short period of uncontrolled inflow. And then the first PI controller would keep the vehicle accumulation $n^{in}(t)$ at around the target 170 vehs, and the second PI controller would keep the number of parked vehicles $n^{pk}_r(t)$ at around 10 vehs. Clearly as shown in Figure 3.9, both perimeter control strategies can effectively reduce the passenger evacuation time, and the second perimeter control strategy leads to a shorter passenger evacuation time. When $A_r = 0.5$ veh/s, the passenger evacuation time with e-hailing service under both perimeter control strategies can be reduced to be less than that in the 'BO' case. When $A_r = 1$ veh/s, the passenger evacuation time under the first PI controller is only 58.4% of the time in the 'UC' case, and evacuation time under the second PI controller is 283s less. The necessity of control strategy can be well confirmed from the fact that the total evacuation time under 'UC' case has the fastest increase with the increase of e-hailing vehicle's arrival rate.

The above discussion shows the effectiveness of the two PI controllers when we set $\bar{n}^{in} = 170 veh$ and $\bar{n}^{pk}_r = 10 veh$ respectively for PC-1 and PC-2. Figures 3.10 and 3.11 present the results when we change the control targets $\bar{n}^{in}$ and $\bar{n}^{pk}_r$ respectively. As can be seen from the two figures, the effectiveness of both PI controllers are not very sensitive to the choice of targets. When $\bar{n}^{in}$ varies between 150 and 190, and $\bar{n}^{pk}_r$ increases from 10 from 50, the vehicle

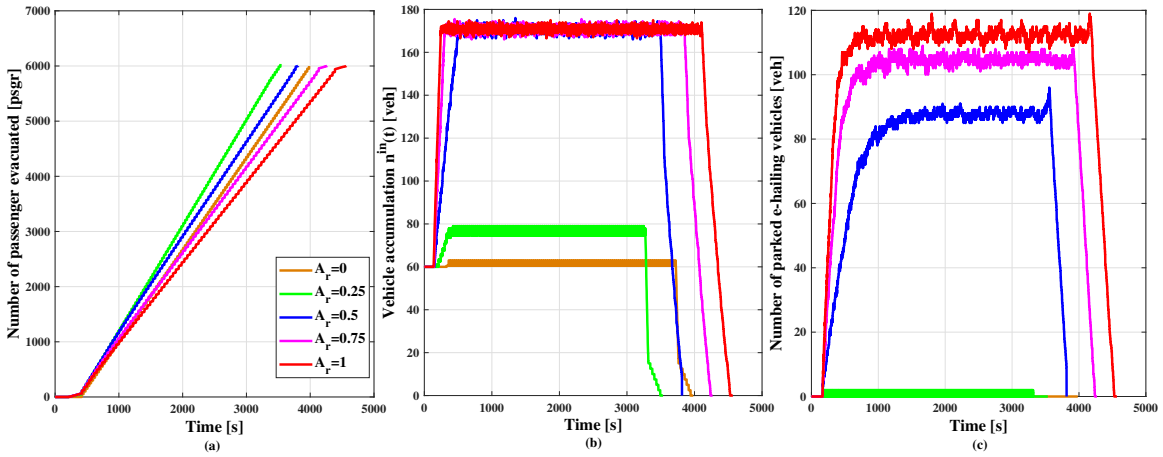

Figure 3.7 The dynamic passenger evacuation process and traffic conditions under the first PI controller based on $n^{in}(t)$

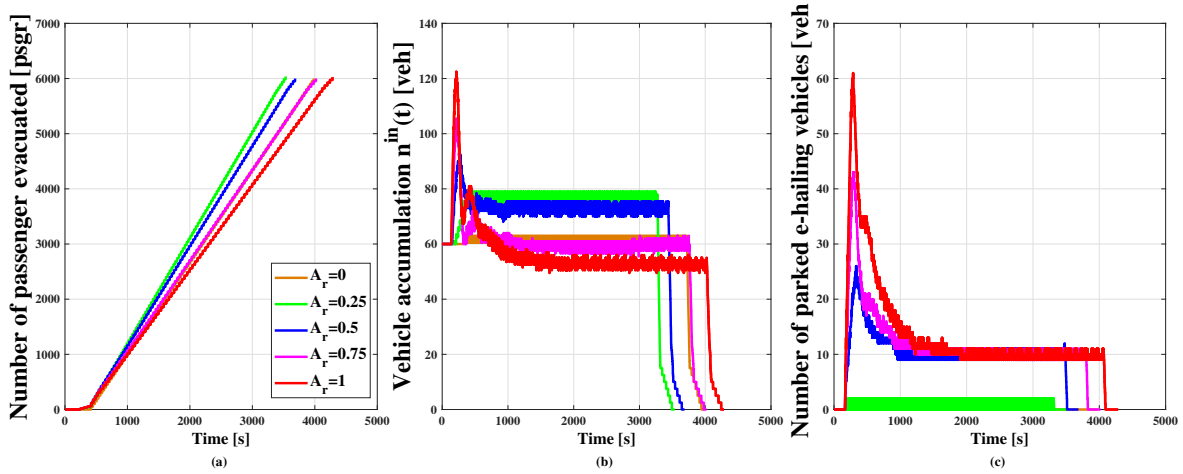

Figure 3.8 The dynamic passenger evacuation process and traffic conditions under the second PI controller based on $n_r^{pk}(t)$

accumulation and the number of parked vehicles would stabilize at different levels during the evacuation process, but the required evacuation time is only slightly changed. However, if we set $\bar{n}_r^{pk} = 100$, then the perimeter control strategy is not effective, as the controller is not activated at all during the whole evacuation process.

3.4.2 Sensitivity analysis

3.4.2.1 Impacts of bus headway

Keeping all parameters unchanged as in Subsection 3.4.1, and setting $A_r = 0.5$ veh/s, we re-conduct the simulation experiments when the bus headway takes the value 20 s, 30 s, 40 s, 50 s, and 60 s (the corresponding bus arrival rate takes the value 3 veh/min, 2 veh/min, 1.5 veh/min, 1.2 veh/min and 1 veh/min), and the results are presented in Figure 3.12. As we can see from

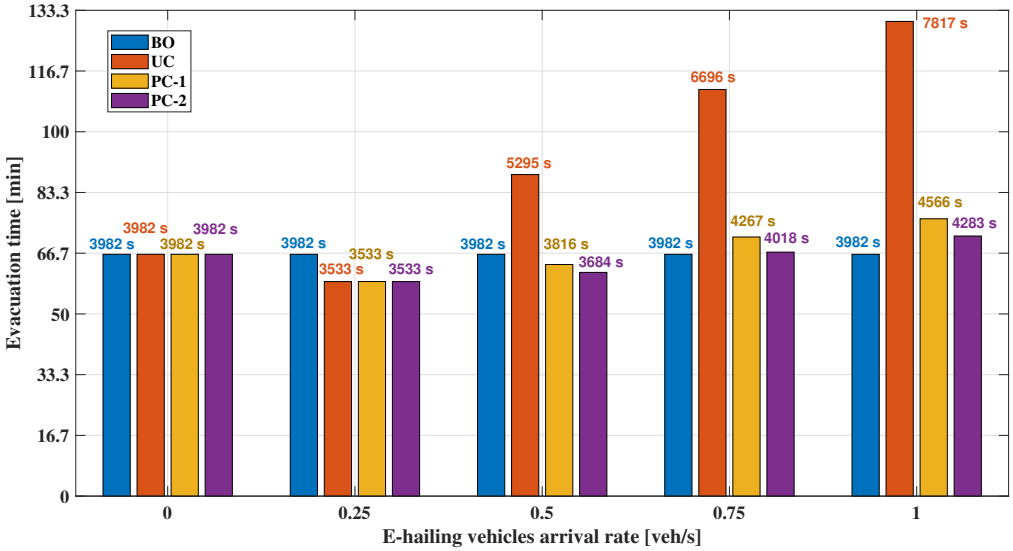

Figure 3.9 The passenger evacuation time under different e-hailing arrival rates with and without perimeter control

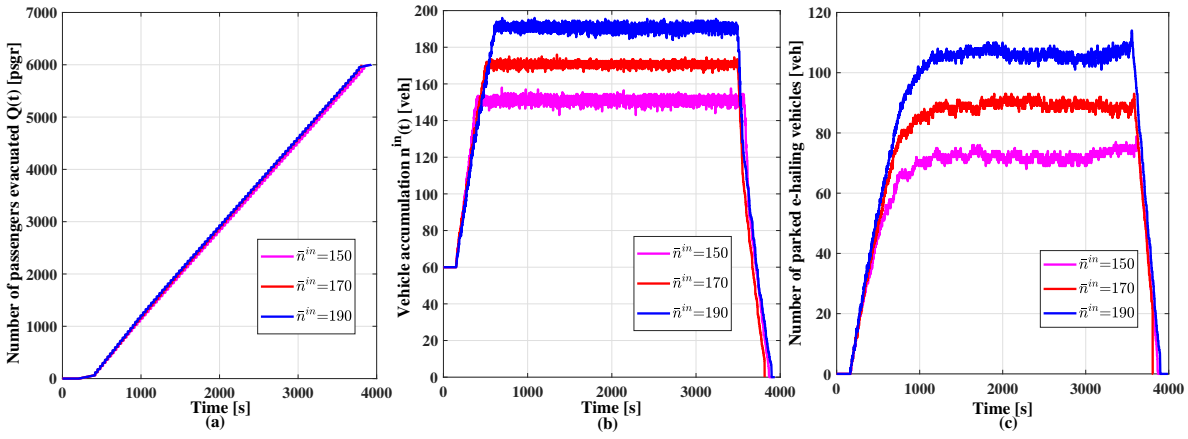

Figure 3.10 The passenger evacuation process and dynamic traffic conditions under the first PI controller with different $\bar{n}^{in}$

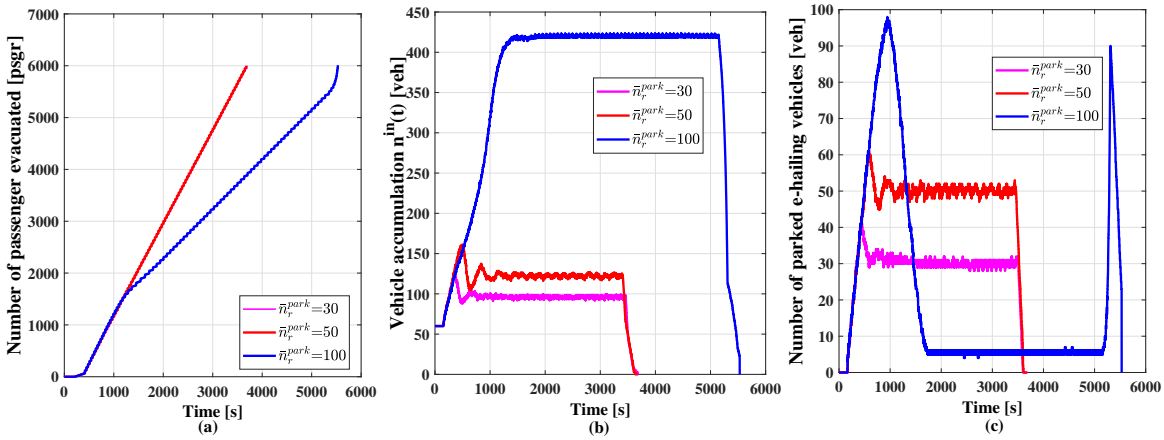

Figure 3.11 The passenger evacuation process and dynamic traffic conditions under the second PI controller with different $\bar{n}_r^{pk}$

the figure, when the bus headway increases, the passenger evacuation time increases in all the four cases. If there is no perimeter control, the presence of e-hailing vehicles always lead to a longer total evacuation time than in the 'BO' case, but the increase is less significant when the bus headway is longer. However, if either of the perimeter control strategies is imposed, the total evacuation time in the presence of e-hailing vehicles can be effectively reduced. When the bus headway is 20 s, the total evacuation time under 'PC-1' is slightly shorter than that in the 'BO'case, and the evacuation time under 'PC-2' is slightly larger than the time in the 'BO' case. When the bus headway is 30 seconds or more, both perimeter control strategies can lead to shorter total evacuation time in comparison with the 'BO' case, and the reduction is more significant when the second PI controller is imposed. When the bus headway is 60 s, the total evacuation time under the second PI controller is 6142s, being 1440s (24 min) less than the evacuation time in the 'BO' case. So when there are sufficient buses, the adoption of e-hailing vehicles is not a wise idea for passenger evacuation; but if there are not sufficient buses, we can effectively speed up the evacuation process by allowing e-hailing vehicles to take passengers and imposing a inflow control at the perimeter.

3.4.2.2 Impacts of total passenger demand

Keeping all parameters unchanged as in Subsection 3.4.1, and setting $A_r = 0.5$ veh/s, we re-conduct the simulation when the total passenger demand Q varies from 3,000 to 10,000. The total evacuation times under different Q are depicted in Figure 3.13. As we can see from the figure, with the increase of total passenger demand, the total evacuation time increases in all the three scenarios, but the increasing speed in the 'UC' case is the fastest. When $Q = 10000$,

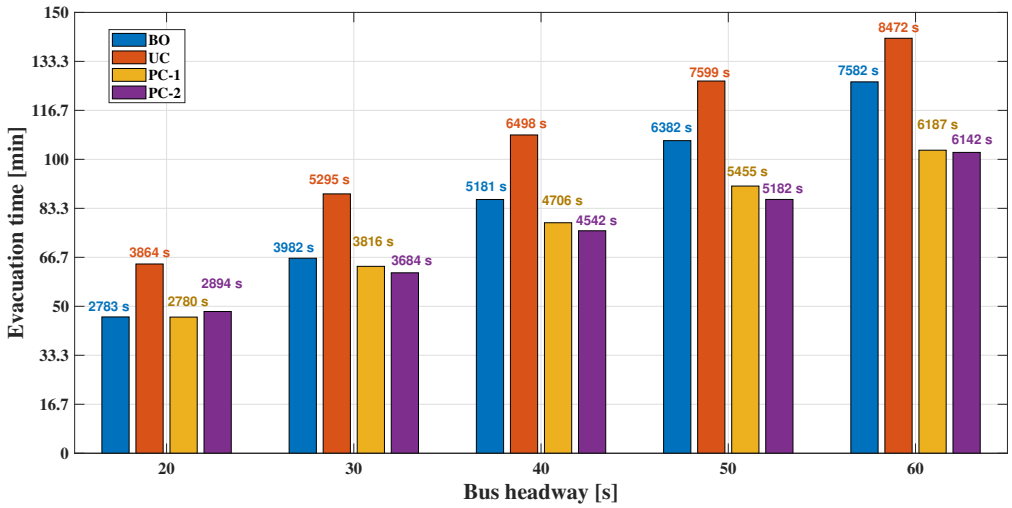

Figure 3.12 Passenger evacuation time under different bus headway

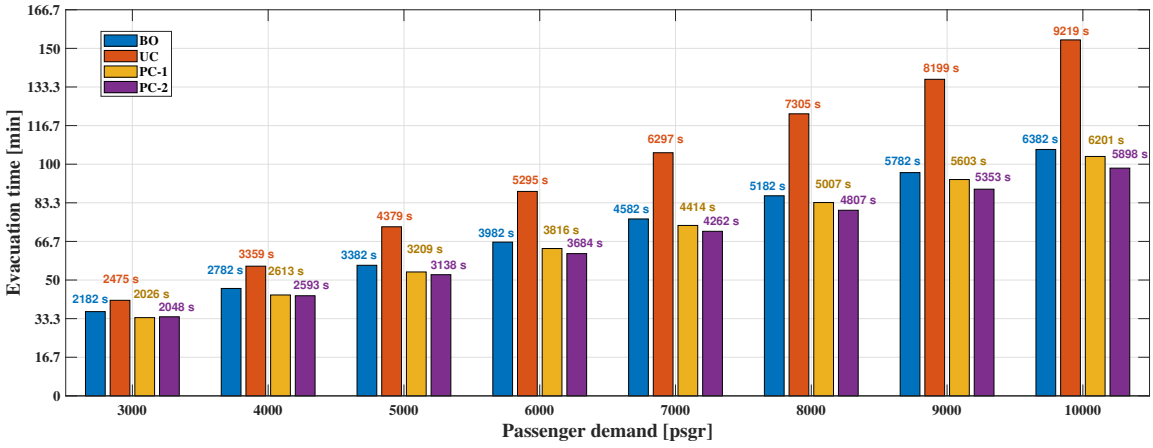

Figure 3.13 Passenger evacuation time under different passenger demand

the total evacuation time in the 'UC' case is almost 1.5 times of the evacuation time in the 'BO case. This highlights the necessity of regulation when the total number of passenger demand is high. Indeed, as shown in Figure 3.13, both of our proposed perimeter control strategies can effectively reduce the evacuation time, and the shortest evacuation time is achieved under the second PI controller. At all passenger demand levels, the evacuation time in the 'PC-1' and 'PC-2' cases are shorter than that in the 'BO' case, the difference between the evacuation time in the 'UC' and 'PC' cases is larger when the passenger demand is higher.

3.4.2.3 Impacts of the number of parking spaces

As the number of parking spaces plays a critical role in determining the cruising time of e-hailing vehicles for parking spaces, we also examine the passenger evacuation efficiency when the number of parking spaces N^{pk} increases from 50 to 300 when $A_r = 0.5veh/s$. As shown in Figure 3.14, in the 'UC' case, when the total number of parking spaces is small, the presence of e-hailing vehicles would significantly prolong the total evacuation time. This is not surprising, as e-hailing vehicles have to spend much longer time to cruise for parking when the number of parking spaces is small. However, with the second perimeter controller, the total evacuation times can be effectively reduced to around 3700s when N^{pk} takes different values, which is shorter than in the 'BO' case. So the effectiveness of the second perimeter controller is not sensitive to the total number parking spaces. The first perimeter control strategy can also effectively reduce the evacuation time in comparison with the 'UC' case, but the reduction is less significant when the number of parking spaces is small. When $N = 50$ and 100, the evacuation time in the 'PC-1' case is longer than that in the 'BO' case. This is because under the first PI controller, the number of parked vehicles would not be restricted to a sufficiently small level, and the vehicle cruising time for parking spaces is thus long when the number of parking spaces is small.

3.4.3 Impact of perimeter control strategy on the proportion of passengers evacuated by e-hailing vehicles and total evacuation time

In Subsection 3.2.4, we examine the evacuation performance under different arrival rates combinations without control. As adopting perimeter control strategy, passengers' accessibility towards the transportation will be changed. Therefore we examine the total evacuation time and proportion of passengers evacuated by e-hailing vehicles under different arrival rates combinations with perimeter control strategy.

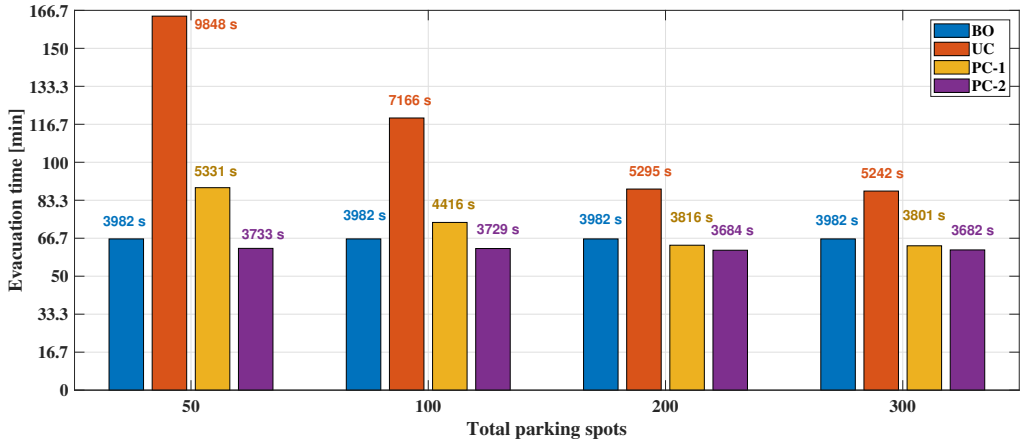

Figure 3.14 Passenger evacuation time under different number of parking spaces

Table 3.4 Total evacuation time under different combinations of bus and e-hailing vehicles arrival rates with control

u_p \ A_r	0.2	0.25	0.3	0.35	0.4	0.45	0.5
0.017	6202	5692	5665	5482	5609	5853	5982
0.02	5382	5182	5032	4833	5082	5235	5266
0.025	4541	4382	4262	4142	4283	4432	4560
0.033	3623	3533	3443	3356	3514	3620	3684
0.05	2624	2566	2544	2504	2594	2696	2750
0.1	1549	1539	1530	1522	1554	1614	1659

We conduct the simulation under the same arrival rate setting under the 'PC-2' strategy due to its better performance proven in Section 3.4.2. As shown in Figure 3.15 and Table 3.4, when $A_r \leq 0.35$ veh/s, the total evacuation time keeps the same as the uncontrolled case, as the perimeter control strategy is not activated. The minimal evacuation time is still achieved when $A_r = 0.35$ veh/s. However when $A_r > 0.35$ veh/s, the perimeter control is activated and the total evacuation time is effectively reduced almost 20% compared with the uncontrolled case, which can be found in Table 3.2 and Table 3.4. The positive impact of incorporating e-hailing service into evacuation can be greatly retained because of the perimeter control. Its effectiveness on effectively preventing the congestion caused by the excessive amount of vehicles' inflow is well proven.

We further examine the proportion of passengers evacuated by e-hailing vehicles under various combinations of arrival rates under case 'PC-2', using the same parameter settings as above.

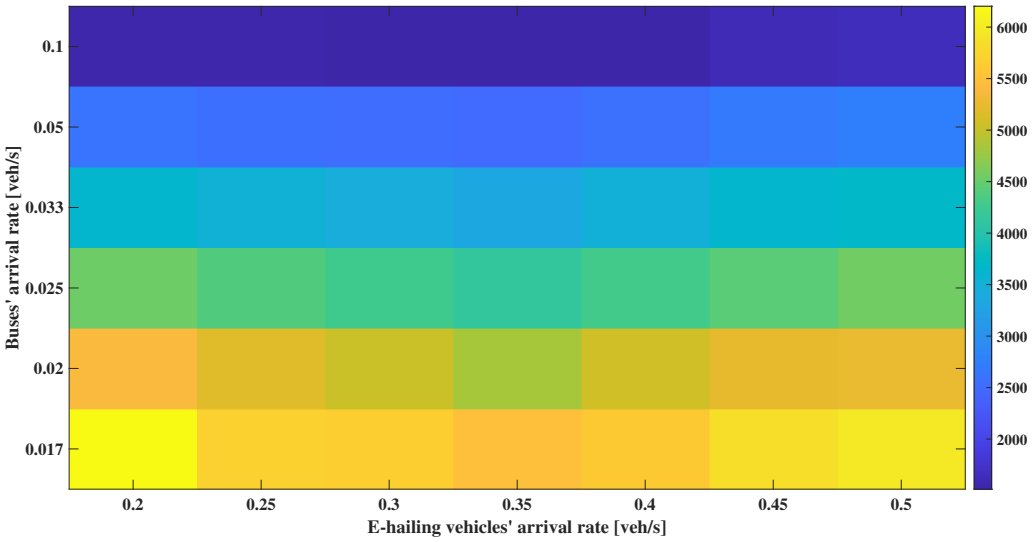

Figure 3.15 Total evacuation time under different combinations of bus and e-hailing vehicles arrival rates with control

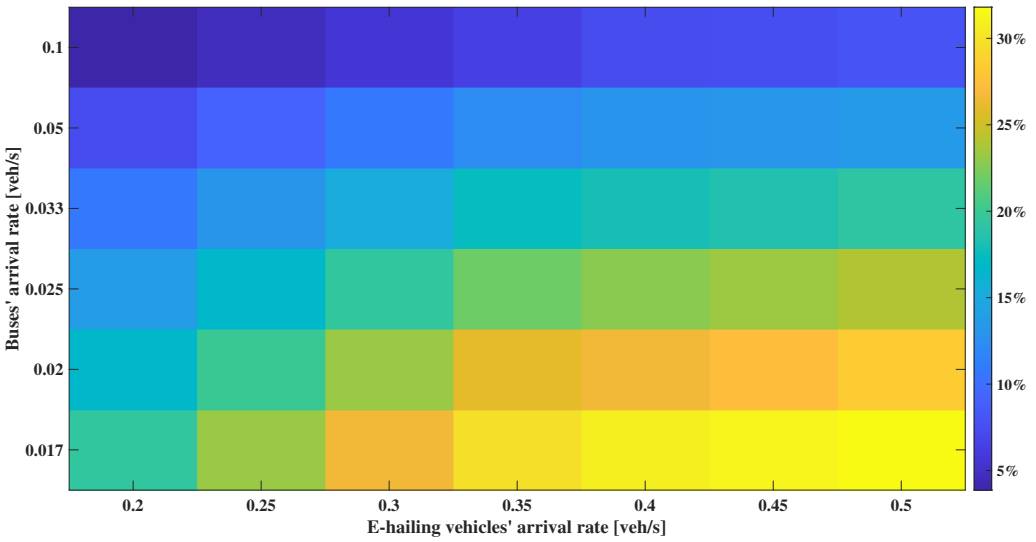

Figure 3.16 The proportion of passengers evacuated by e-hailing vehicles under different combinations of bus and e-hailing vehicles arrival rates with control

Table 3.5 The proportion of passengers evacuated by e-hailing vehicles under different combinations of bus and e-hailing vehicles arrival rates with control

u_p \ A_r	0.2	0.25	0.3	0.35	0.4	0.45	0.5
0.017	0.194	0.2325	0.2667	0.2975	0.3083	0.3135	0.318
0.02	0.1667	0.2	0.2325	0.2595	0.2667	0.2743	0.2833
0.025	0.1387	0.1667	0.1938	0.2192	0.2283	0.2333	0.2402
0.033	0.108	0.1312	0.153	0.175	0.1805	0.1843	0.1917
0.05	0.0747	0.0917	0.108	0.1237	0.1293	0.1322	0.1355
0.1	0.0387	0.0478	0.057	0.0658	0.074	0.0767	0.0799

As shown in Figure 3.16 and Table 3.5, when $A_r \leq 0.35$ veh/s, the proportion of passengers evacuated by e-hailing vehicles keeps the same as the uncontrolled case, as the perimeter control strategy is not activated. However when $A_r > 0.35$ veh/s, the perimeter control is activated and the proportion of passengers evacuated by e-hailing vehicles is effectively reduced almost 10% compared with the uncontrolled case, which can be found in Table 3.3 and Table 3.5. The negative effect of high proportion of passengers evacuated by e-hailing vehicles on evacuation efficiency can also be figured out from Figure 3.15 and Figure 3.16. Therefore by adopting the perimeter control strategy, the restriction effect influences the passengers' mode choice, thereby restricts the proportion of passengers evacuated by e-hailing vehicles so as to speed up the evacuation efficiency.

In the above result, we find that the perimeter control well optimize the traffic condition and help it back to the optimal condition without congestion, when there are excessive amount of vehicles inflowing the demand surge area. However, our perimeter control is unable to maintain the evacuation performance around the optimal condition when $A_r = 0.35$ veh/s, even though the 'PC-2' which has a better control performance. It is because its objective is just to keep the vehicle accumulation(/production) around the most desirable value. This objective may not be completely consistent with minimizing the total passenger evacuation time, due to the potential errors between vehicles dynamics and passenger evacuation dynamics. Fortunately, through our simulation results, we successfully find this optimal inflow rate $A_r = 0.35$ veh/s, which don't activate the perimeter control as well as maximally utilize the positive effect of e-hailing service on evacuation efficiency. However in reality, it requires precise and strict control because the inflow amount of vehicles is always higher than this. Thereby our proposed control strategy can be widely reproduced in most of the real cases to optimize the traffic condition. In our

following work, we are interested in exploring how to sustain the e-hailing arrival rate around the optimal condition, regardless of control strategy.

3.4.4 Differentiated perimeter control of background traffic and e-hailing vehicles

In Section 3.3, we assume e-hailing vehicles and background traffic are indistinguishable from their appearance, so the maximally allowed vehicle inflow rate is proportionally distributed to the two types of vehicles according to the number of waiting/arrived e-hailing vehicles and background traffic. In this appendix, we assume e-hailing vehicles and background traffic are distinguishable, and examine the efficiency of two different perimeter control strategies: 'e-hailing priority control' and 'background traffic-priority control'. Under the 'e-hailing-priority control' strategy, all the allowed inflow rates are assigned to e-hailing vehicles if there are waiting e-hailing vehicles at the boundary or the arrival rate of e-hailing vehicles exceeds the maximally allowed inflow rate. The actually inflow rates of e-hailing vehicles and background traffic under this control strategy thus follows

$$\bar{u}_r(t) = \begin{cases} I(t), & \text{if } W_r(t) > 0 \\ \min\left\{I(t), u_r(t)\right\}, & \text{otherwise} \end{cases} \tag{3.85}$$

$$\bar{u}_b(t) = \begin{cases} I(t) - \bar{u}_r(t), & \text{if } W_b(t) > 0 \\ \min\left\{I(t) - \bar{u}_r(t), u_b(t)\right\}, & \text{otherwise} \end{cases} \tag{3.86}$$

On the contrary, under the 'background traffic priority control' strategy, all the allowed inflow rates are assigned to background traffic if there are waiting background traffic at the boundary or the arrival rate of background traffic exceeds the maximally allowed inflow rate. The actually inflow rates of e-hailing vehicles and background traffic under this control strategy thus follows

$$\bar{u}_b(t) = \begin{cases} I(t), & \text{if } W_b(t) > 0 \\ \min\left\{I(t), u_b(t)\right\}, & \text{otherwise} \end{cases} \tag{3.87}$$

$$\bar{u}_r(t) = \begin{cases} I(t) - \bar{u}_b(t), & \text{if } W_r(t) > 0 \\ \min\left\{I(t) - \bar{u}_b(t), u_r(t)\right\}, & \text{otherwise} \end{cases} \tag{3.88}$$

Keeping the same parameter settings as in Subsection 3.4.1, and setting $A_r = 0.5$ veh/s, we re-conduct the simulation experiment under PC-1 and PC-2 when inflow priorities are given to e-hailing vehicles or background traffic, and the results are presented in Figures 3.17–3.20. In

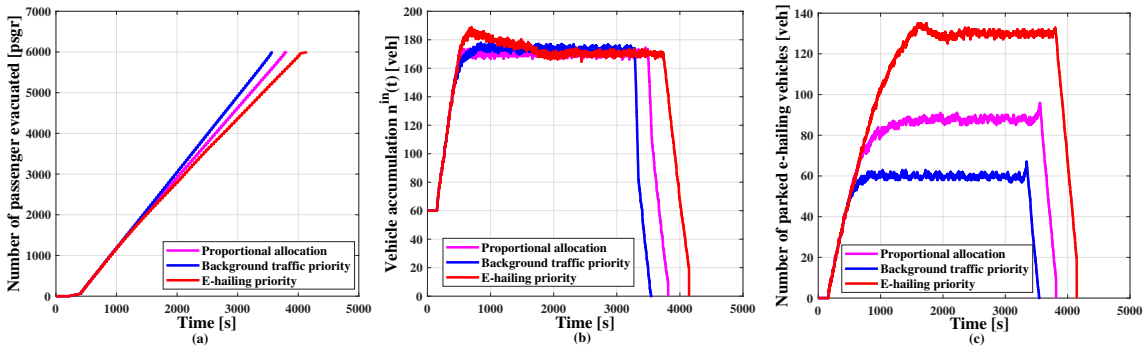

Figure 3.17 The dynamic passenger evacuation process and traffic conditions under PC-1 with different priority rules

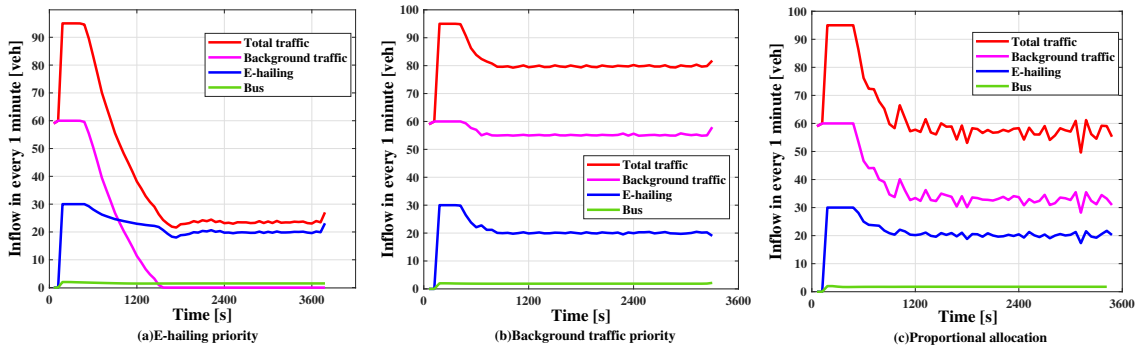

Figure 3.18 Vehicle inflow rates under PC-1 with different priority rules

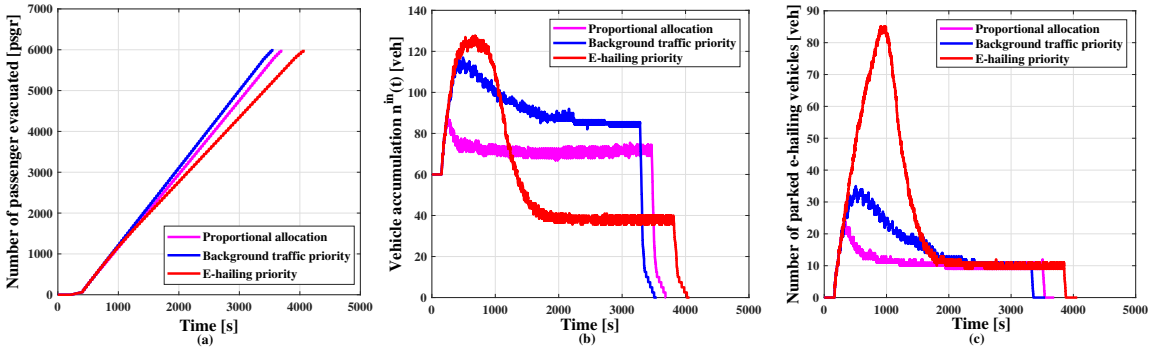

Figure 3.19 The dynamic passenger evacuation process and traffic conditions under PC-2 with different priority rules

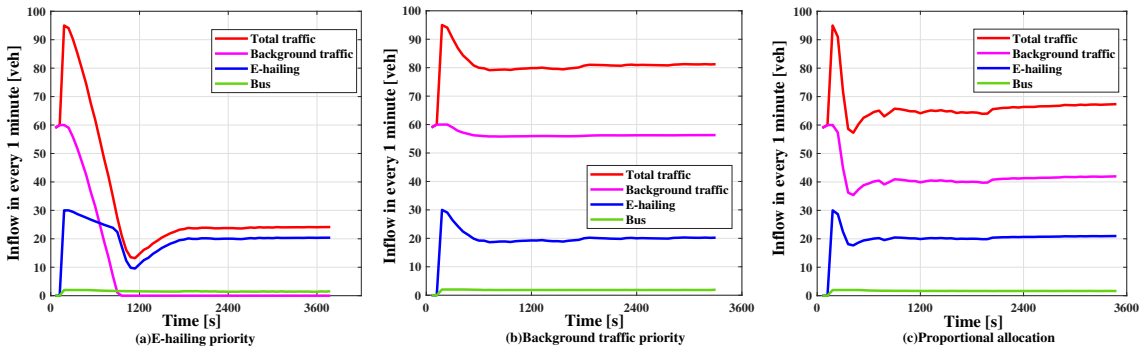

Figure 3.20 Vehicle inflow rates under PC-2 with different priority rules

the figures, 'proportional allocation', 'background traffic priority' and 'e-hailing priority' respectively refer to the cases in which the allowed inflow rates are distributed to e-hailing vehicles and background traffic following Eqs. (3.66)–(3.67), Eqs. (3.85)–(3.86) and Eqs. (3.87)–(3.88). Interestingly, as we can see from Figure 3.17 and Figure 3.19, under both perimeter control strategies, the passenger evacuation time is the shortest when inflow priorities are given to background traffic. The reason is as follows. Under PC-1, after the PI controller being activated at $t = 455s$, the vehicle accumulation $n^{in}(t)$ decrease immediately and stabilize at $\bar{n}^{in}$ in the case of 'proportional allocation' and 'background traffic priority'; but if the inflow priority is assigned to e-hailing vehicles, the number of parked vehicles would keep increasing until $t = 1750$s, and as a result $n^{in}(t)$ would keep increasing to 190 veh and then decrease to $\bar{n}^{in}$ slowly until $t = 1950s$. Figure 3.18 depicts the inflow rates of different types of vehicles from $t = 0$ to the time point when the number of e-hailing vehicles and buses is sufficient to carry all waiting passengers[3.4]. As we can see from Figure 3.18, due to the slow decrease of $n^{in}(t)$ after the controller being activated, the controlled inflow rate ($I(t)$) would keep decreasing and stabilize at the lowest level in the 'e-hailing priority' case. Due to the lowest allowed inflow rate $I(t)$, the allowed inflow rate of background traffic drops to zero since $t = 1400$s in the 'e-hailing priority' case. And this leads to a long queue of background traffic at the boundary. As mentioned in Section 3.3, when there are queues at the boundary, the inflow rates of different types of vehicles would be affected by not only the perimeter control strategy, but also the boundary capacity constraint. The boundary capacity is proportionally allocated to three types of vehicles according to their number of waiting vehicles, so with the large accumulation of waiting background traffic at the boundary, the bus inflow rate drops to 1.5 veh/min (0.025veh/s) since $t = 1050$s. The drop of bus inflow rate is much less significant in the 'pro-

[3.4] After that, the arrival rate of e-hailing vehicles and buses become zero, while background traffic keeps arriving.

portional allocation' and 'e-hailing priority' cases, because the total inflow rates in these cases are much larger than in the 'e-hailing priority' case. The lowest bus inflow rate then leads the longest total passenger evacuation time in the 'e-hailing priority' case.

Under PC-2, similarly as under PC-1, from $t = 120$s to $t = 1100$s, when inflow priorities are assigned to e-hailing vehicles, the number of parked vehicles would surge to the highest level 95 veh, as shown in Figure 3.19(c). And due to the largest integral of error $|n_r^{pk}(t) - \bar{n}_r^{pk}(t)|$ when $t \leq 1800s$, the maximally allowed inflow rate $I(t)$ would stabilize at the lowest level in the 'e-hailing priority' case, as shown in Figure 3.20. As a result, the allowed inflow rate of background traffic drops to zero since $t = 1000s$, which leads to a large accumulation of background traffic at the boundary. And the same as under PC-1, the increasing accumulation of background traffic at the boundary lowers the bus inflow rate, and prolongs the passenger evacuation time. In the 'background traffic-priority' case, the maximally allowed inflow rate is the highest, so the vehicle accumulation at the boundary is the smallest. As a result, the bus inflow rate is the highest, such that the passenger evacuation time is shortest in the 'background traffic-priority' case.

In summary, from the above example, we can see that when e-hailing vehicles and background traffic are distinguishable, giving entry priority to e-hailing vehicles would not speed up the passenger evacuation process. This is because with the proposed PI controllers, the maximally allowed inflow rate would be kept at the lowest level in the 'e-hailing priority' case. The large number of waiting vehicles at the boundary would lower the bus inflow rate, thus prolong the passenger evacuation time. Instead, the traffic regulator should give the entry priority to background traffic. This could lead to the fastest decrease of $n^{in}(t)$ and/or $n_r^{pk}(t)$ after the controllers being activated, such that the maximally allowed inflow rate would stabilize at the highest level, while the allowed inflow rate of e-hailing vehicles is almost the same as in the 'e-hailing priority' case. With the fewest number of vehicles waiting at the queue, the bus inflow rate would be least affected, and the passenger evacuation time is thus the shortest in the 'background traffic-priority' case.

3.5 Concluding Remarks

While previous studies have explored the impact of e-hailing services on urban congestion in normal traffic conditions, this chapter delves into a unique scenario where a significant passenger demand accumulates within a small area, awaiting evacuation by both buses and e-hailing

vehicles. In a bi-modal system where passengers can choose between buses and e-hailing vehicles for evacuation, this chapter models the dynamics of traffic conditions and the passenger evacuation process. It proposes two perimeter control strategies—one based on observations of vehicle accumulation in the 'in' direction and the other based on observations of the number of parked vehicles—to enhance passenger evacuation efficiency. Our model demonstrates that, in the absence of perimeter control, the dense traffic within the area, induced by a large number of parked vehicles when numerous e-hailing vehicles flow into the area, can decelerate all types of traffic. While e-hailing services offer an attractive travel option for passengers leaving the area, they often deteriorate rather than improve passenger evacuation efficiency. The deterioration is more pronounced when the bus headway is shorter, the total passenger demand is higher, and/or the number of parking spaces is limited. Testing different combinations of bi-modal arrival rates further allows for a discussion of the impact of transportation supply on the proportion of passengers evacuated by e-hailing vehicles and the total evacuation time. The results underscore the necessity of reducing the e-hailing arrival rate, which significantly decreases the proportion of passengers evacuated by e-hailing vehicles and shortens the total evacuation time. The promising aspect is that two convenient perimeter control strategies, dynamically adjusting the total inflow rate of e-hailing vehicles and background traffic based on vehicle accumulation in the 'in' direction and the number of parked vehicles, can effectively mitigate the impact of e-hailing services. Implementation of such perimeter control strategies results in an observable acceleration of the passenger evacuation process (compared to the bus-only case), with higher efficiency under the latter control strategy—especially in situations with insufficient bus fleets, a large number of passengers, and/or limited parking spaces for e-hailing vehicles. Through simulations with varying combinations of bi-modal arrival rates, the results indicate that perimeter control strategies effectively restrict the proportion of passengers evacuated by e-hailing vehicles, accelerating the evacuation process while preserving the positive impact of incorporating e-hailing services.

CHAPTER 4 E-HAILING VEHICLES DYNAMICS MODELLING AND REGION-DEPENDENT PRICING PROBLEM IN A TWO-REGION SYSTEM

The short-term increase in travel demand will prompt e-hailing platforms to dispatch some empty vehicles to high demand areas to assist passengers in evacuating. However, excessive influx of vehicles into crowded areas may cause traffic congestion, thereby reducing overall evacuation efficiency. At the same time, the randomness of e-hailing scheduling may weaken the supply of transportation capacity in other regions, unable to meet normal travel needs, and thus affect the stability of the spatial distribution of e-hailing vehicles. In addition, due to the bilateral characteristic of e-hailing services, unreasonable traffic control strategies may further disrupt the supply-demand balance, leading to an imbalance in the allocation of spatiotemporal resources. Therefore, it is urgent to develop differentiated vehicle pricing and scheduling strategies for specific regions to achieve efficient evacuation in peak areas while ensuring normal operations in other areas.

This chapter is based on the Trip-based MFD traffic dynamics model in Chapter 3, and characterizes the dynamics of e-hailing trips in a two-region transportation system consisting of high passenger flow areas and their surrounding areas. The model comprehensively considers the bilateral dynamics of drivers' repositioning decisions, passengers' demand dynamics, and the dispatching process between the two parties. In order to aid the e-hailing platform in effectively managing a reasonable level of vehicle supply for swift evacuation and ensuring a well-balanced distribution of e-hailing vehicle supply within the two-region transportation system, we propose a region-dependent pricing strategy. This strategy involves adjusting e-hailing drivers' per unit time wages in different regions, positioning e-hailing service providers as leaders to guide drivers' and passengers' behaviors within the e-hailing market as followers. Through simulation experiments, our proposed integrated model and region-dependent pricing strategy are tested across varying levels of passenger demand and vehicle supply. The study investigates their impact on both traffic conditions and bilateral dynamics within the e-hailing service market. The results demonstrate the effectiveness of the region-dependent pricing strategy, emphasizing its role in ensuring a more appropriate distribution and effective management of transportation supplies, particularly in the application of e-hailing services during mass gath-

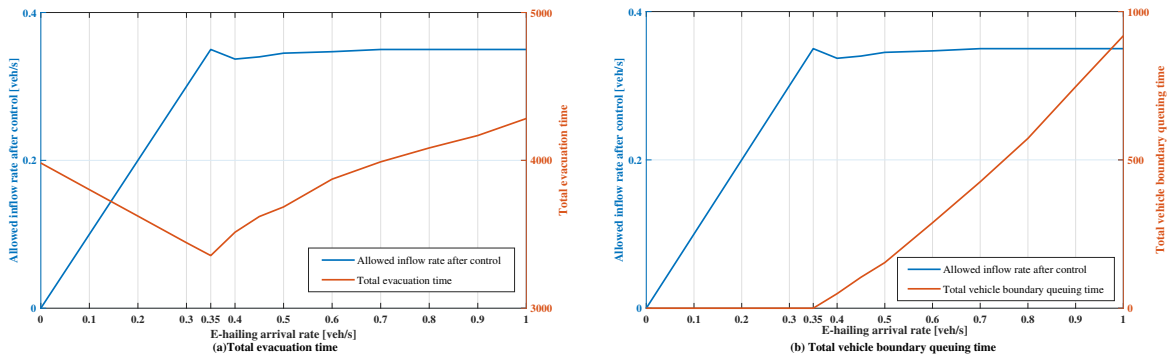

Figure 4.1 Total evacuation time and total vehicle boundary queuing time under different e-hailing vehicles' arrival rates and allowed inflow rates

ering events.

The remainder of this paper is organized as follows. Section 4.1 starts from the interrelated results between e-hailing vehicles' arrival rate and total evacuation time. Based on the empirical evidence and assumptions, Section 4.2 models the e-hailing vehicles dynamics in a two-region transportation system. Section 4.3 derives the e-hailing demand-supply bilateral dynamics. Serving as guidance, the above methodology framework paves the way for Section 4.4 to make region-dependent pricing optimization to find the price that can realize the optimal traffic condition. Section 4.5 demonstrates its effectiveness. And finally Section 4.6 concludes this chapter.

4.1 Problem Setup and Assumptions

4.1.1 Empirical Evidence for Problem Setup

It has been verified in Chapter 3 that when unconstrained number of e-hailing vehicles inflowing into the passenger demand region, the traffic condition may seriously deteriorate the passenger evacuation process may be prolonged. To mitigate the negative impacts of e-hailing services on the evacuation process, they propose an effective perimeter control strategy.

Based on this, we conduct a new set of numerical experiments, where we measure the arrival rate of e-hailing services in units of 0.1 from 0 to 1 vehicle per second. Figure 4.1 demonstrates the change of total evacuation time in (a) and the total vehicle boundary queuing time in (b) with respect to different e-hailing vehicles' arrival rates and allowed inflow rates. In this case, as the arrival rate increases from 0 to 0.35, the total evacuation time decreases from 3982s to 3384s, and the total vehicle queuing time at demand surge region boundary keeps at 0. When the arrival rate exceeds 0.35, the perimeter control is activated and the total evacuation time

will be extended from 3384s to 4283s. The total vehicle queuing time at demand surge region boundary increases sharply from 0 to almost 1000h.

As we have verified the strong inefficiency brought to e-hailing service under traffic control strategy conducted by traffic regulators, we attempt to utilize a more moderate and effective control pattern, which can maintain the system at the optimal e-hailing inflow rate. In this way, both of speedy evacuation and minimal negative impact on external regions can be ensured. It has been observed that a minimal total evacuation time of 3384s can be achieved when the arrival rate of e-hailing vehicles is 0.35 veh/s, and the total vehicle queuing time at the demand surge region boundary remains at 0, indicating no activation of perimeter control. Such an optimal e-hailing vehicles' arrival rate can be served as guidance for regulating e-hailing dispatching rate in a two-sided market.

4.1.2 Model Assumptions

Simulating the same problem setting as in Chapter 3, we consider a small area where passenger travel demand surges following a mass gathering event or metro disruption. Due to the distinct differences between the demand surge region and the surrounding area, we partition the urban scale into two regions, as shown in Figure 4.2(a). At time $t = 0$, a total of Q_{ij} passengers are accumulated within region i and are waiting to be transported to their destinations.

Region i, the demand surge region, occupies the central area, while region j, the normal region, occupies the periphery. When mass gathering events occur in region i, the primary objective is to efficiently evacuate the large passenger demand from the region to reduce danger. We assume that no passengers attempt to enter the demand surge region during this period. Both regions i and j have passengers who wish to reach normal region j. Passengers can choose between bus shuttle services or other available modes to leave the area. However, since our focus is on e-hailing services, we specifically model the trip and operational dynamics of e-hailing services and assume a constant passenger sharing rate for all other modes.

Regarding vacant e-hailing vehicle supply, we assume the platform has the capability to directly schedule necessary amount of vacant e-hailing vehicles for sake of effectively solving the vehicle resources and spatiotemporal imbalance. During this demand surge period, there are no vacant e-hailing vehicles in normal region i and all of the vacant e-hailing vehicles are dispatched from normal region j. These vacant vehicles can be dispatched to both regions i and j, as Figure 4.2(a) shows. Based on these assumptions, we proceed to model the dynamics of

e-hailing vehicles in both the demand surge and normal regions.

We assume each vehicle has four distinct operating phases: (a) cruising with empty seats to look for the next passenger (vacant state), (b) on the way to pick up the passenger (dispatched state), (c) boarding state and (d)carrying a passenger on board (occupied state). The transformation relationship among these three states can be explained as follow: the state that an e-hailing vehicle has not been assigned an order is 'vacant'. Once an idle e-hailing vehicle has been assigned an order by the platform, its state will switch from 'vacant' to 'dispatched'. Once the e-hailing vehicle has arrived the passenger's nearby area and starts cruising for parking, its state will switch from 'dispatched' to boarding. Once the e-hailing vehicle has picked up the passenger, its state will switch from 'boarding' to 'occupied'. If the e-hailing vehicle has finished the order, its state will switch from 'occupied' to 'vacant'. Every working e-hailing vehicle will cycle through these four phases to continuously transport passengers.

Similar to Chapter 3, this chapter assumes that the changes in the proportion of vehicle types caused by different types of vehicles will not undermine the assumption of uniformity in traffic conditions, and therefore will not cause significant changes in the shape of MFD. The vehicle accumulation and speed within both regions follow a well-defined MFD, which allows each trip follows first-in-first-board and first-in-first-out assumptions. In the e-hailing market, passengers and drivers are assumed to be price-sensitive. Passengers choose travel modes based on perceived cost, while e-hailing drivers decide whether to enter the market and which regions to serve based on perceived utility. The measurement of travel costs is based on the sum of monetary and time costs.

4.2 Modelling E-hailing Vehicles Dynamics in a Two-region Transportation System

4.2.1 Determining e-hailing trips' phases based on a trip-based MFD model

In the following, we use v, d, b and o to respectively represent vacant, dispatched, boarding and occupied state of the vehicle. As for the vacant state of e-hailing vehicles is dependent on the demand and supply relationship in the e-hailing market, this will be elaborated in the next section. In this section, we mainly model the evolution of dispatched, boarding and occupied states, which are highly connected with the traffic dynamics. The adoption of trip-based MFD model makes the vehicle follow first-in-first-board and first-in-first-out assumptions, enabling

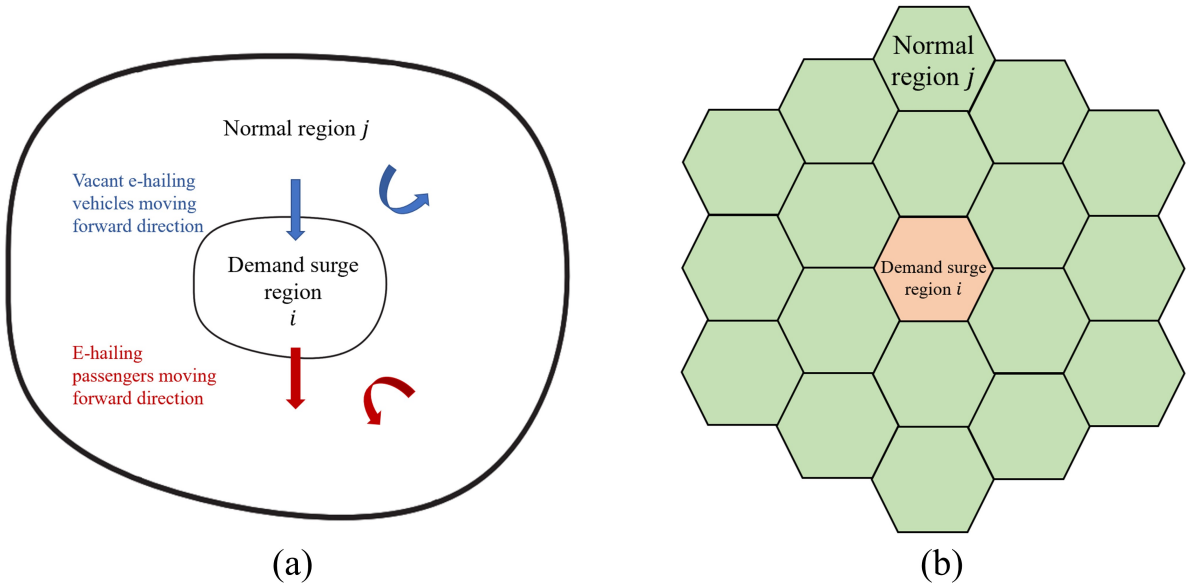

Figure 4.2 Schematic diagram of the research region.

us to trace the dynamic traffic conditions, so as to determine the trip phase.

Figure 4.3 illustrates how each one of these above phases communicates to each other to account for a trip's transitions, with (a) representing the e-hailing trip that transfers between regions i and j and (b) representing the e-hailing trip that only traverses region j. As illustrated in Figure 4.3, Phase 1 models the dispatched state, Phase 2 models the boarding state and Phase 3 models the occupied state. In the next subsections, we detail the dynamics for each phase.

4.2.1.1 Phase 1: Dispatched state

Once finishing the last order assigned from the platform, the occupied e-hailing vehicle's state will switch to 'vacant' and it will be ready to serve for the next passenger with waiting a period of vacant time for dispatching.

Figure 4.3 shows each phase of the trip by its time, which will be affected by its regional mean speed, for sake of recording its trip state. In Phase 1, we define $t^d_{jij}(t)$ as the e-hailing driving time of the trips that is dispatched from region j and drives towards region i at time t, which has not crossed the border and currently is driving in region j. Similarly, $t^d_{jii}(t)$ is denoted as the e-hailing driving time of the trips that is dispatched from region j and drives towards region i at time t, which has crossed the border and currently is driving in region j. Furthermore, $t^d_{jj}(t)$ is the e-hailing driving time of the trips that is dispatched from region j and drives towards region j to pick up passengers at time t. We denote the driving length with 'dispatched' state('dispatched trip length' for short) in region j and heading to region i with a

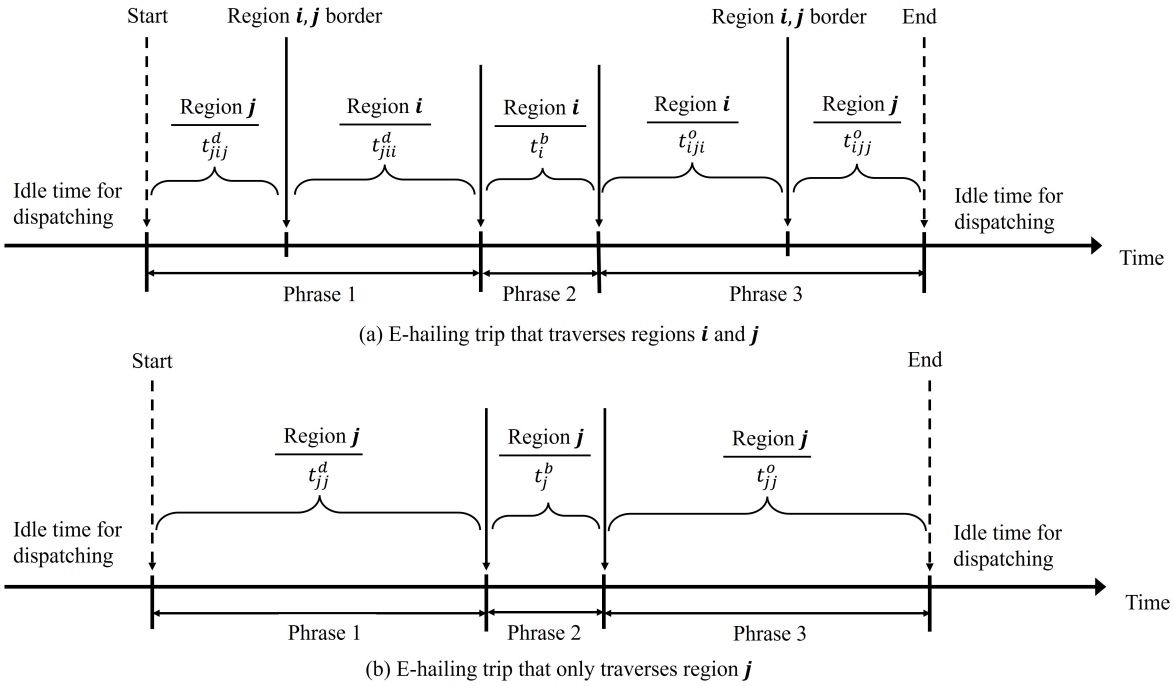

Figure 4.3 Illustration of e-hailing trip's phases and its relation with the regional reposition in the timeline.

mean value of $l_j^{d_1}$, heading to region j with a mean value of $l_j^{d_2}$. The dispatched trip length in region i is assumed with a mean value of l_i^d. All of the variational values of trip distance are assumed to be independently and identically distributed with a Gumbel probability distribution function. With $v_i(t)$ and $v_j(t)$ being the speed of vehicles driving in regions i and j at time t, in a trip-based model, we track the cumulative travel distance of each e-hailing vehicle being assigned an order at time t, so as to determine the trip time. The following conditions must be satisfied:

$$\int_0^{t^d_{jij}(t)} v_j(s)ds = l_j^{d_1}, \tag{4.1}$$

$$\int_{t^d_{jij}(t)}^{t^d_{jij}(t)+t^d_{jii}(t)} v_i(s)ds = l_i^d, \tag{4.2}$$

$$t^d_{ji}(t) = t^d_{jij}(t) + t^d_{jii}(t), \tag{4.3}$$

$$\int_0^{t^d_{jj}(t)} v_j(s)ds = l_j^{d_2}. \tag{4.4}$$

In Eq. (4.3), $t^d_{ji}(t)$ is denoted as the total time of driving from region j to i with dispatched state.

4.2.1.2 Phase 2: Boarding state

And following we model the process of driver's cruising for parking and driver-passenger offline meeting behavior. As shown in Figure 4.3(a), in Phase 2, when e-hailing vehicles get close to the passenger waiting area in region i, they will first cruise to search for a temporary curbside parking space and then park at the space to wait for their passengers. This part follows the same pattern as Subsection 3.1.1 in Chapter 3. Let $t_i^{cr}(t)$ and $t_i^{pk}(t)$ denote the time it needs to successfully find a parking space and the average driver parking time in region i. So the total boarding time of e-hailing vehicles in region i at time t can be defined as $t_i^b(t)$, which includes two processes of cruising for parking and parked, and should be formulated as:

$$t_i^b(t) = t_i^{cr}(t) + t_i^{pk}(t). \tag{4.5}$$

As for the e-hailing trips that traverse region j may experience little effect by boarding process, we assume it is a constant $\hat{t_j^b}$.

4.2.1.3 Phase 3: Occupied state

After successfully getting on board, the vehicle drives within the 'occupied' state. Here we also make the similar assumption with dispatched trip length that the driving length with 'occupied' state('occupied trip length' for short) has low variation, because it is always the case that an e-hailing order is supposed to cover a distance around 10-15km to finish the order. So here we assume that the occupied trip length would not generate great differences on occupied trip time. As shown in Figure 4.3, in Phase 3, we denote the occupied trip lengths in region i have a mean value of l_i^o, the occupied trip length in region j from i has a mean value of $l_j^{o_1}$, the occupied trip length in region j from j has a mean value of $l_j^{o_2}$. We denote $t_{iji}^o(t)$ as the occupied driving time of e-hailing vehicle in region i and heading towards region j at time t, which has not crossed the border and currently in region i. We denote $t_{ijj}^o(t)$ as the occupied driving time of e-hailing vehicle in region i and heading towards region j at time t, which has crossed the border and currently in region j. $t_{jj}^o(t)$ is define as the occupied driving time of the trips that starts from region j and heading to region j at time t.

From the definitions above, similar as in Eqs. (4.1)–(4.4), the following conditions must be satisfied:

$$\int_{t_{ji}^d(t)+t_i^b(t)}^{t_{ji}^d(t)+t_i^b(t)+t_{iji}^o(t)} v_i(s)ds = l_i^o, \tag{4.6}$$

$$\int_{t_{ji}^d(t)+t_i^b(t)+t_{iji}^o(t)}^{t_{ji}^d(t)+t_i^b(t)+t_{iji}^o(t)+t_{ijj}^o(t)} v_j(s)ds = l_j^{o_1}, \tag{4.7}$$

$$t_{ij}^o(t) = t_{iji}^o(t) + t_{ijj}^o(t), \tag{4.8}$$

$$\int_{t_{jj}^d(t)+\hat{t_j^b}}^{t_{jj}^d(t)+\hat{t_j^b}+t_{jj}^o(t)} v_j(s)ds = l_j^{o_2}. \tag{4.9}$$

In Eq. (4.8), $t_{ij}^o(t)$ denotes the total driving time from region i to j in occupied state at time t. As each period of time is timely variant, so we represent each period of time by calculating the average time of every past three trips that have been finished this period of time.

4.2.1.4 Deriving phase transitions and relations

As described in the previous sections, there are several forms of transition processes. We start from denoting $d_j(t)$ as the total dispatching rate in region j, in which $d_{ji}(t)$ and $d_{jj}(t)$ as the dispatching rate distributed to regions i and j respectively. All of the vacant e-hailing vehicles will be assigned an order in region j. Assuming that all vehicles within the region i follow first-in-first-out assumptions, then provided the dispatching rate of e-hailing vehicles $d_{ji}(t)$, the border arrival rate from region j to i[4.1], cruising for parking rate, parking rate, boarding rate in region i and the border arrival rate from region i to j at time t should be respectively modeled as:

$$a_{ji}(t + t_{jij}^d(t)) = d_{ji}(t), \tag{4.10}$$

$$r_i(t + t_{ji}^d(t)) = d_{ji}(t), \tag{4.11}$$

$$p_i(t + t_{ji}^d(t) + t_i^{cr}(t)) = d_{ji}(t), \tag{4.12}$$

$$b_i(t + t_{ji}^d(t) + t_i^b(t)) = d_{ji}(t), \tag{4.13}$$

$$a_{ij}(t + t_{ji}^d(t) + t_i^b(t) + t_{iji}^o(t)) = d_{ji}(t). \tag{4.14}$$

Assuming that all vehicles within the region j follow first-in-first-out assumptions, then provided the dispatching rate of e-hailing vehicles $d_{jj}(t)$, the passenger pick-up point arrival

[4.1] We note that as we don't impose perimeter control strategy, the border arrival rate will equal the actual inflow rate. We would like to clarify that if there is excessive amount of vehicles staying in a region, the boundary constraint effect will start to work, which denotes the capacity of roads leading to the area will be reduced to prevent the congested region from the gridlock situation. Both of regions i and j will follow this pattern. However in our proposed case, this situation will not occur according to our problem setting. Therefore we only provide a brief explanation instead of providing a specific model expansion.

rate and boarding rate within region j at time t can be formulated as:

$$s_j(t + t^d_{jj}(t)) = d_{jj}(t), \tag{4.15}$$

$$b_j(t + t^d_{jj}(t) + \hat{t^b_j}) = d_{jj}(t). \tag{4.16}$$

Let o denote the outflow rate to record how many occupied trips have left both regions[4.2]. Then the outflow rate of the trips that starts from region i and region j at time t an be formulated as:

$$o_i(t + t^d_{ji}(t) + t^b_i(t) + t^o_{ij}(t)) = d_{ji}(t), \tag{4.17}$$

$$o_j(t + t^d_{jj}(t) + \hat{t^b_j} + t^o_{jj}(t)) = d_{jj}(t). \tag{4.18}$$

In the above Eqs. (4.11)–(4.14) and (4.17), time periods are merged for simplicity according to the Eqs. (4.3), (4.5) and (4.8).

In this subsection, we can see that the parking, boarding and outflow rates at any time t are dependent on the dispatching rates and their trip duration in each region, and the trip duration of vehicles that enter the area at different time t is determined by the dynamic regional speed $v_i(t)$ and $v_j(t)$. To determine the vehicle speed of each region at any time t, we then proceed to figure out the vehicle accumulations of different state at any time t in the next subsection.

4.2.2 Traffic dynamics within a two-region transportation system

Based on the modelling of the traffic dynamics within this two-region transportation system, we first model the vehicle accumulation that will transfer within both two regions with state switching. Let $n^d_{jij}(t)$ denote the number of dispatched vehicle in region j that has been dispatched to region i, which has not crossed the border and currently in region j. Let $n^d_{jii}(t)$ denote the number of dispatched vehicle at time t in region j that has been dispatched to region i, which has crossed the border and currently in region i. With all of the rates defined above in

[4.2]In real situations, it is always the case that an e-hailing order is supposed to cover a distance more than 10 km. Therefore the e-hailing vehicle will switch to vacant state in a relatively far region from the studied two regions. As a result, we only account the vehicle outflow rate instead of trip completion rate, which requires a complex modeling and precise tracking of a relatively large area. In this chapter, we focus on these two regions and appropriately simplify and omit the dynamics of distant regions, which aims to avoid overlooking the presence of this demand surge region within a larger city scale. We choose to study these two regions is to clearly account the impact of demand surge region on the near-surrounding region, which is the most directly affected area. This near-surrounding region owns the most direct comparative relationship with the demand surge region, and always serves as a supply offering necessary amount of vacant e-hailing vehicles to help solve the problem of surged passenger evacuation in the central region. The traffic regulator should firstly ensure the rapid evacuation of the demand surge region, and then ensure balanced spatial distribution of e-hailing vehicle supply in the near-surrounding region. Although, this surged demand will also have an impact on the far-surrounding regions, but as this impact will be much smaller than the two regions we studied.

Eqs. (4.10)–(4.14) and (4.17), the evolution of the above types of vehicle should follow:

$$n_{jij}^{d}(t) = \int_0^t [d_{ji}(s) - a_{ji}(s)]ds, \tag{4.19}$$

$$n_{jii}^{d}(t) = \int_0^t [a_{ji}(s) - r_i(s)]ds. \tag{4.20}$$

Meanwhile, with cruising rate $r_i(t)$ and boarding rate $b_i(t)$ within region i, the parked and total boarding e-hailing vehicles number $n_i^{pk}(t)$ and $n_i^b(t)$ in region i at time t can be formulated as:

$$n_i^{pk}(t) = \int_0^t [p_i(s) - b_i(s)]ds, \tag{4.21}$$

$$n_i^{b}(t) = \int_0^t [r_i(s) - b_i(s)]ds. \tag{4.22}$$

Let $n_{iji}^{o}(t)$ denote the number of occupied vehicle in region i and drives towards region j at time t, which has not crossed the border and currently in region i. Let $n_{ijj}^{o}(t)$ denote the number of occupied vehicle in region i and drives towards region j at time t, which has crossed the border and currently in region j. So the evolution of the above types of vehicle should follow:

$$n_{iji}^{o}(t) = \int_0^t [b_i(s) - a_{ij}(s)]ds, \tag{4.23}$$

$$n_{ijj}^{o}(t) = \int_0^t [a_{ij}(s) - o_i(s)]ds. \tag{4.24}$$

Then we model the vehicle accumulation that only switches from different states within region j. Let $l_j(t)$ denote the exogenous total e-hailing vehicle supply rate to this two-region system at time t. We assume $l_j(t)$ can be directly scheduled by the e-hailing platform. A more extended large-scale model is needed to study more comprehensive pricing and supply decision issues. However, this work is not within the scope of this chapter and is a future research direction. The total supply rate is independent of e-hailing dynamics yet time-varying, while the number of vacant e-hailing vehicle in region j is subject to the total dispatching rate in region j, $d_j(t)$. Let $n_j^v(t)$ denote the number of vacant vehicle supply in region j at time t, which can be formulated as:

$$n_j^{v}(t) = \int_0^t [l_j(s) - d_j(s)]ds. \tag{4.25}$$

Let $n_{jj}^{d}(t)$ denote the number of dispatched vehicle starting from region j and keeping run-

ning in region j, $n_j^b(t)$ denote the number of boarding state vehicles in region j, $n_{jj}^o(t)$ denote the number of occupied vehicle starting from region j and keeping running in region j at time t. With all of the rates defined above in Eqs. (4.15), (4.16) and (4.18), the evolution of the above types of vehicle follows:

$$n_{jj}^d(t) = \int_0^t [d_{jj}(s) - s_j(s)]ds, \tag{4.26}$$

$$n_j^b(t) = \int_0^t [s_j(s) - b_j(s)]ds, \tag{4.27}$$

$$n_{jj}^o(t) = \int_0^t [b_j(s) - o_j(s)]ds. \tag{4.28}$$

To better show the accumulation of vehicles in different state and different region, we define the number of dispatched vehicles and occupied vehicles at time t in region j as $n_j^d(t)$ and $n_j^o(t)$, then we have

$$n_j^d(t) = n_{jj}^d(t) + n_{jij}^d(t), \tag{4.29}$$

$$n_j^o(t) = n_{jj}^o(t) + n_{ijj}^o(t). \tag{4.30}$$

Similarly, the number of dispatched vehicles at time t in region i, i.e., $n_i^d(t)$, which is same as $n_{jii}^d(t)$. The number of occupied vehicles at time t in region i, i.e., $n_i^o(t)$, which is same as $n_{iji}^o(t)$. We denote $n_i(t)$ and $n_j(t)$ as the total number of e-hailing vehicles in regions i and j at time t, which ensure that all states of e-hailing vehicles have been taken into consideration. Then we have

$$n_i(t) = n_i^d(t) + n_i^b(t) + n_i^o(t), \tag{4.31}$$

$$n_j(t) = n_j^v(t) + n_j^d(t) + n_j^b(t) + n_j^o(t). \tag{4.32}$$

It is important to note that there is no vacant state e-hailing vehicles in region i because all of the vacant e-hailing vehicles will be assigned an order before driving into region i. Let n_i^{other} and n_j^{other} denote the total number of other types of vehicle besides e-hailing vehicles in regions i and j, such as background traffic. Then the total vehicle accumulation in regions i and j $N_i(t)$ and $N_j(t)$ at time t should follow:

$$N_i(t) = n_i^{other} + n_i(t), \tag{4.33}$$

$$N_j(t) = n_j^{other} + n_j(t). \tag{4.34}$$

As we have defined $v_i(t)$ and $v_j(t)$ as the space mean speed in regions i and j at time t, the relationship between vehicle speed and vehicle accumulation within both regions i and j follow a well-defined MFD, i.e.,

$$v_i(t) = V(N_i(t)), \tag{4.35}$$

$$v_j(t) = V(N_j(t)). \tag{4.36}$$

4.3 E-hailing Service Bilateral Dynamics of Both Regions

E-hailing platform plays an important role in ensuring transportation capacity during large-scale gatherings and enhance the stability of dispatching efficiency. In order to better understand and solve practical problems in carpooling systems and provide more effective solutions, some studies assumed the drivers are fully compliant and studied the pricing and scheduling decisions of MSPs (Mobility Service Providers) in one-sided market to manage carpooling systems(Lei et al., 2020). However, in actual bilateral markets, the perceived utility of e-hailing drivers is usually considered to ensure their job satisfaction and income. Drivers may have a preference for choosing their own path and may even refuse to follow scheduling instructions especially under the extreme case. In this situation, the platform needs to clearly consider the driver's decision-making and adopt corresponding strategies to balance supply and demand. The platform may take measures such as offering higher wages, flexible working hours, and route choices to attract and retain drivers, and improve their perceived utility. The platform needs to determine the driver's wage strategy based on market demand, supply, and competitive environment to ensure that the driver's income can match their workload and contribution. This can increase the enthusiasm and satisfaction of drivers, promote the stability and sustainable development of e-hailing services. Therefore, under our proposed situation, we proceed to approximate the dispatching rate of two regions using e-hailing service bilateral dynamics. This section discusses the decision for drivers to reposition in Subsection 4.3.1, the passengers' demand dynamics in Subsection 4.3.2 and the driver passenger dispatching in Subsection 4.3.3.

4.3.1 Drivers' repositioning decision

From drivers' perspective, we denote $n^v_{ji}(t)$ and $n^v_{jj}(t)$ as the number of vacant e-hailing vehicles in region j and has the serving willingness of regions i and j respectively. Therefore the waiting time of vacant vehicles to be dispatched a new passenger from region j to region i

or j at time t, i.e., $w^e_{ji}(t)$ and $w^e_{jj}(t)$, should be formulated as:

$$w^e_{ji}(t) = \frac{n^v_{ji}(t)}{d_{ji}(t)}, \tag{4.37}$$

$$w^e_{jj}(t) = \frac{n^v_{jj}(t)}{d_{jj}(t)}. \tag{4.38}$$

Referring to the dynamic model proposed in Section 4.2, which can give all periods of time that e-hailing drivers will experience in a trip, i.e., $t^d_{ji}(t), t^d_{jj}(t), t^b_i(t), t^o_{ij}(t), t^o_{jj}(t)$ in Eqs. (4.1)–(4.9), we can capture the realistic and time-variant traffic dynamics and serve for the e-hailing market. Driver can rely on these information to make determination like which region to serve. In order to practically estimate the trip cost from a whole trip's perspective, we add a term t^{rm} to represent the average remaining trip time in the outside region after the e-hailing vehicle has left region j. The e-hailing driver's total driving time of per trip that picks up passenger from regions i and j at time t, $t^e_i(t)$ and $t^e_j(t)$, can be formulated as:

$$t^e_i(t) = w^e_{ji}(t) + t^d_{ji}(t) + t^b_i(t) + t^o_{ij}(t) + t^{rm}, \tag{4.39}$$

$$t^e_j(t) = w^e_{jj}(t) + t^d_{jj}(t) + \hat{t^b_j} + t^o_{jj}(t) + t^{rm}. \tag{4.40}$$

It is intuitive that the attractiveness of serving two regions are different. We define $C^e_{ji}(t)$ and $C^e_{jj}(t)$ as the trip utility of serving regions i and j at time t, which can reflect the serving attractiveness to drivers or generalized benefit. It will positively depend on expected revenue incurred by the occupied trips and negatively depend on the time cost incurred by the whole trip. We denote $g_{ji}(t)$ and $g_{jj}(t)$ as the wage rate offered to the drivers who serve regions i and j's passenger per unit time. Let σ^e denote the drivers' time-unit operating cost, and we do not distinguish it between occupied and vacant states. We assume it includes monetary value of time, fuel cost, vehicle depreciation, and all other indirect costs. With having defined all periods of time that e-hailing drivers' will experience on the trip as above, the trip utility of serving regions i and j at time t, i.e., $C^e_{ji}(t)$ and $C^e_{jj}(t)$, can be formulated as:

$$C^e_{ji}(t) = g_{ji}(t) \cdot (t^o_{ij}(t) + t^{rm}) - \sigma^e \cdot t^e_i(t), \tag{4.41}$$

$$C^e_{jj}(t) = g_{jj}(t) \cdot (t^o_{jj}(t) + t^{rm}) - \sigma^e \cdot t^e_j(t). \tag{4.42}$$

Each idle driver in region j can either remain in current region or cruise to region i to search

for the next passenger. Drivers make re-positioning decisions by comparing his/her per unit time earning in each region. Drivers' per unit time earning of serving regions i and j at time t, i.e., $e_{ji}(t)$ and $e_{jj}(t)$, are formulated as:

$$e_{ji}(t) = C^e_{ji}(t) \cdot \frac{t^o_{ij}(t) + t^{rm}}{t^e_i(t)}, \tag{4.43}$$

$$e_{jj}(t) = C^e_{jj}(t) \cdot \frac{t^o_{jj}(t) + t^{rm}}{t^e_j(t)}. \tag{4.44}$$

Due to the scale difference between region i and region j, here we denote a size difference coefficient Z, which represents the multiple of the area of region j relative to region i. Therefore, region j can be partitioned into Z subregions[4.3], and each subregion $z \in \mathcal{Z}$, $\mathcal{Z} = \{1, 2, ..., Z\}$. We denote $e_{jj}(t)$ as the attractiveness of serving any subregion $z \in \mathcal{Z}$ in region j and $e_{jj}(t)$ can also be rewritten as $e^z_{jj}(t)$. Note that a simple serving region(/subregion) choice model is integrated, where the probabilities are calculated by a logit model according to the expected earnings per unit time of serving this subregion. η is the dispersion parameter reflecting e-hailing drivers' uncertainty towards the utility of serving different region(/subregion). The re-positioning probability $P_{ji}(t)$ and $P^z_{jj}(t)$ of idle drivers serving region i and Z subregions in j at time t can be formulated as:

$$P_{ji}(t) = \frac{exp(-\eta \cdot e_{ji}(t))}{exp(-\eta \cdot e_{ji}(t)) + \sum_{z \in \mathcal{Z}} exp(-\eta \cdot e^z_{jj}(t))}, \tag{4.45}$$

$$P^z_{jj}(t) = \frac{exp(-\eta \cdot e^z_{jj}(t))}{exp(-\eta \cdot e_{ji}(t)) + \sum_{z \in \mathcal{Z}} exp(-\eta \cdot e^z_{jj}(t))}. \tag{4.46}$$

The sum of $P_{ji}(t)$ and $\sum_{z \in \mathcal{Z}} P^z_{jj}(t)$ should equal to 1, i.e.,

$$P_{ij}(t) + \sum_{z \in \mathcal{Z}} P^z_{jj}(t) = 1. \tag{4.47}$$

Given $n^v_j(t)$ representing the vacant vehicle number in region j at time t, the vacant e-hailing number that intends to serve regions i and j, $n^v_{ji}(t)$ and $n^v_{jj}(t)$ can be formulated as:

$$n^v_{ji}(t) = n^v_j(t) \cdot P_{ji}(t), \tag{4.48}$$

[4.3] We don't further define the heterogeneity of the Z partitioned subregions in region j and they are only used here to represent the relative area size of regions i and j. To keep this model simple and clear, we don't include the partition of Z subregions in other sections such as demand and dispatching rate. It is because those variables can be treated both integrally or separately, which will not generate critical impact to the model. Due to the incomplete expansion of modelling subregions in region j, we keep naming this system as a two-region system instead of multi-region system. Exploring the heterogeneity of subregions and expanding it into a multi-region system are meaningful research topics to be investigated in future research.

$$n_{jj}^{v}(t) = n_{j}^{v}(t) \cdot \sum_{z \in \mathcal{Z}} P_{jj}^{z}(t). \tag{4.49}$$

4.3.2 Passenger demand dynamics

From passengers' perspective, we define $q_{ij}^{r}(t)$ and $q_{jj}^{r}(t)$ as the passenger demand for e-hailing in regions i and j. We define the passengers' expected waiting time in region i or j heading to region j at time t, i.e., $w_{ij}^{p}(t)$ and $w_{jj}^{p}(t)$, which can be formulated as:

$$w_{ij}^{p}(t) = \frac{q_{ij}^{r}(t)}{d_{ji}(t)}, \tag{4.50}$$

$$w_{jj}^{p}(t) = \frac{q_{jj}^{r}(t)}{d_{jj}(t)}, \tag{4.51}$$

where $d_{ji}(t)$ and $d_{jj}(t)$ are the dispatching rate distributed to regions i and j from region j respectively. In the similar way as e-hailing drivers, with having given all periods of time that passengers will experience on the trip for e-hailing, the passengers' average travel time $t_{i}^{r}(t)$ and $t_{j}^{r}(t)$ in regions i and j starting at time t can be formulated as:

$$t_{i}^{r}(t) = w_{ij}^{p}(t) + t_{ji}^{d}(t) + t_{i}^{b}(t) + t_{ij}^{o}(t) + t^{rm}, \tag{4.52}$$

$$t_{j}^{r}(t) = w_{jj}^{p}(t) + t_{jj}^{d}(t) + \hat{t}_{j}^{b} + t_{jj}^{o}(t) + t^{rm}, \tag{4.53}$$

where $t_{ji}^{d}(t)$, $t_{jj}^{d}(t)$, $t_{i}^{b}(t)$, $t_{ij}^{o}(t)$, $t_{jj}^{o}(t)$ all have been given in Eqs. (4.1)–(4.9). The last term t^{rm} has the same meaning and value as in Eqs. (4.39) and (4.40).

The generalized cost of passengers is defined as the weighted sum of the waiting time for dispatching, waiting time for vehicle coming, waiting time to get on board, the in-vehicle travel time, and the trip payment. Let σ_{iv}^{r} denote the e-hailing passenger's value of time of in-vehicle state, σ_{wt}^{r} denote the e-hailing passengers' value of waiting state. Since travelers typically place a higher value on waiting time, we assume σ_{wt}^{r} is greater than σ_{iv}^{r}. Let $f_{ij}(t)$ and $f_{jj}(t)$ denote the fare rates for trips starting from region i or j per unit time. The trip cost $C_{ij}^{r}(t)$ and $C_{jj}^{r}(t)$, starting from region i or j at time t, are respectively modeled as:

$$C_{ij}^{r}(t) = (f_{ij}(t) + \sigma_{iv}^{r}) \cdot (t_{ij}^{o}(t) + t^{rm}) + \sigma_{wt}^{r} \cdot (w_{ij}^{p}(t) + t_{ji}^{d}(t) + t_{i}^{b}(t)), \tag{4.54}$$

$$C_{jj}^{r}(t) = (f_{jj}(t) + \sigma_{iv}^{r}) \cdot (t_{jj}^{o}(t) + t^{rm}) + \sigma_{wt}^{r} \cdot (w_{jj}^{p}(t) + t_{jj}^{d}(t) + \hat{t}_{j}^{b}), \tag{4.55}$$

We assume a fixed commission rate ϕ, which denotes that a passenger will be charged $1+\phi$ of the drivers' wage while the extra will be the commission to the e-hailing platform. Therefore $f_{ij}(t)$ and $f_{jj}(t)$ are formulated as:

$$f_{ij}(t) = (1+\phi) \cdot g_{ji}(t), \tag{4.56}$$

$$f_{jj}(t) = (1+\phi) \cdot g_{jj}(t). \tag{4.57}$$

Then we proceed to model the passenger demand. Let $q_{ij}(t)$ and $q_{jj}(t)$ denote the exogenous total travel demand rate within regions i and j heading to region j at time t constituting all travel modes where the e-hailing is a travel choice among the set of travel modes. The total travel demand rate is assumed to be independent of e-hailing dynamics yet time-varying, while the demand rates of e-hailing maybe very sensitive to the change of dynamic traffic speed or perceived travel cost. This is more likely to happen especially when the traffic congestion is highly intensive in region i. Generally speaking, the less perceived travel cost of e-hailing service, the higher passenger demand for e-hailing vehicles can be expected. To take this fact into account, we assume that travel demand arrival rate is a function of the perceived generalized travel cost. Then the time varying e-hailing passenger demand arrival rates in both regions at time t can be formulated as:

$$q_{ij}^{A,r}(t) = q_{ij}(t) \cdot A^r(C_{ij}^r(t)), \tag{4.58}$$

$$q_{jj}^{A,r}(t) = q_{jj}(t) \cdot A^r(C_{jj}^r(t)), \tag{4.59}$$

where $0 \leq A^r \leq 1$, and $\frac{\partial A^r}{\partial C^r} \leq 0$ because more passengers enter the e-hailing market as the trip cost decreases.

After the passenger demand has arrived, the number of passengers waiting will keep accumulating. Due to longer waiting times and other reasons, passengers may switch to other modes of transportation. As we focus on e-hailing service bilateral dynamics, we don't use a discrete choice model to account the effect of other available modes of transportation. In the similar way, we assume that there exists an exit queuing rate $q_{ij}^{E,r}(t)$ and $q_{jj}^{E,r}(t)$ of passenger demand in e-hailing market, as a function of the perceived generalized travel cost, to denote the number of passengers who choose to switch to other modes of transportation to leave the region. The time varying e-hailing passenger demand exit queuing rates of both regions at time t, as a

Table 4.1 Travel demand distribution pattern of e-hailing vehicles in regions i and j

From / To	Demand surge region$i$	Normal region$j$
Demand surge region$i$	0	0
Normal region$j$	p_{ij}^r	p_{jj}^r

Table 4.2 E-hailing supply distribution pattern of regions i and j

From / To	Demand surge region$i$	Normal region$j$
Demand surge region$i$	0	n_{ji}^v
Normal region$j$	0	n_{jj}^v

proportion of the waiting passenger number in the market, $p_{ij}^r(t)$ and $p_{jj}^r(t)$, can be formulated as:

$$q_{ij}^{E,r}(t) = p_{ij}^r(t) \cdot E^r(C_{ij}^r(t)), \tag{4.60}$$

$$q_{jj}^{E,r}(t) = p_{ij}^r(t) \cdot E^r(C_{jj}^r(t)), \tag{4.61}$$

where $0 \leq E^r \leq 1$, and $\frac{\partial E^r}{\partial C^r} \geq 0$ because more passengers exit the e-hailing market as the trip cost increases.

As we assume once the passenger has been assigned an order, s/he is recognized has been served because we don't consider the order cancellation. Therefore the number of unserved passenger demand at time t in regions i and j can be formulated as:

$$p_{ij}^r(t) = \int_0^t [q_{ij}^{A,r}(s) - q_{ij}^{E,r}(s) - d_{ji}(s)]ds, \tag{4.62}$$

$$p_{jj}^r(t) = \int_0^t [q_{jj}^{A,r}(s) - q_{ij}^{E,r}(s) - d_{jj}(s)]ds. \tag{4.63}$$

4.3.3 Driver passenger dispatching

In this subsection, we introduce the driver-passenger dispatching scheme. We follow the same pattern in Subsection 3.1.2 in Chapter 3 to model the matching rate. When a passenger demand surge event occurs within region i, the demand/supply pattern undergoes rapid changes, and the system may struggle to maintain steady-state equilibrium conditions. From the perspective of passengers, they will make reasonable choices and leave crowded areas as quickly as possible to avoid potential danger. E-hailing drivers typically have the capacity to

carry only one passenger at a time. We assume that the dispatching rate in this bilateral market is mostly determined by the smaller value between the number of vacant e-hailing vehicles available for dispatching and the number of passengers waiting for dispatching. In most cases, this smaller value is the number of vacant e-hailing vehicles available for dispatch. This assumption is reasonable because the number of vacant vehicles can be fully regulated by the platform to cope with changes in system's supply and demand, but passenger demand cannot be directly regulated. Therefore, the number of vacant e-hailing vehicles can directly reflect the dispatching rate. We have defined $p_{ij}^r(t)$ and $p_{jj}^r(t)$ as the e-hailing passenger demand in regions i and j and heads towards region j respectively. We also have defined $n_{ji}^v(t)$ and $n_{jj}^v(t)$ as the number of vacant e-hailing vehicles in region j with the serving willingness of regions i and j respectively. The demand and supply distribution pattern of e-hailing service in both regions are defined in Table 4.1 and Table 4.2. Following we model the dispatching rate. As the e-hailing supply $n_{ji}^v(t)$ will serve the travel demand $p_{ij}^r(t)$, and the e-hailing supply $n_{jj}^v(t)$ will serve the travel demand $p_{jj}^r(t)$, then dispatching rate $d_{ji}(t)$ and $d_{jj}(t)$ of regions i and j at time t should satisfy the following condition:

$$d_{ji}(t) = \min\left\{n_{ji}^v(t), p_{ij}^r(t)\right\}, \tag{4.64}$$

$$d_{jj}(t) = \min\left\{n_{jj}^v(t), p_{jj}^r(t)\right\}. \tag{4.65}$$

The total dispatching rate in region j, $d_j(t)$ can be formulated as:

$$d_j(t) = d_{ji}(t) + d_{ji}(t). \tag{4.66}$$

To make the correlations in our proposed e-hailing market more clearly, Figure 4.4 demonstrates a better and systematical understanding. Dashed box denotes the exogenous variables and solid line box denotes the endogenous box. The adjustment of drivers' wage of e-hailing service will affect drivers' perceived utility. Together with the exogenously given vacant e-hailing vehicle supply, drivers will form their own serving willingness and the number of vacant vehicles will be given. Effected by drivers' wage change, the passengers' fare will be changed. Later on passengers will have a perceived cost. Given the external total demand rate, passengers' demand arrival and exit rates of e-hailing service will be decided. Both of the number of waiting passenger demand and vacant vehicles will affect the e-hailing dispatching rate, further to affect the dynamic traffic evolution. In turn, the traffic evolution will affect the drivers'

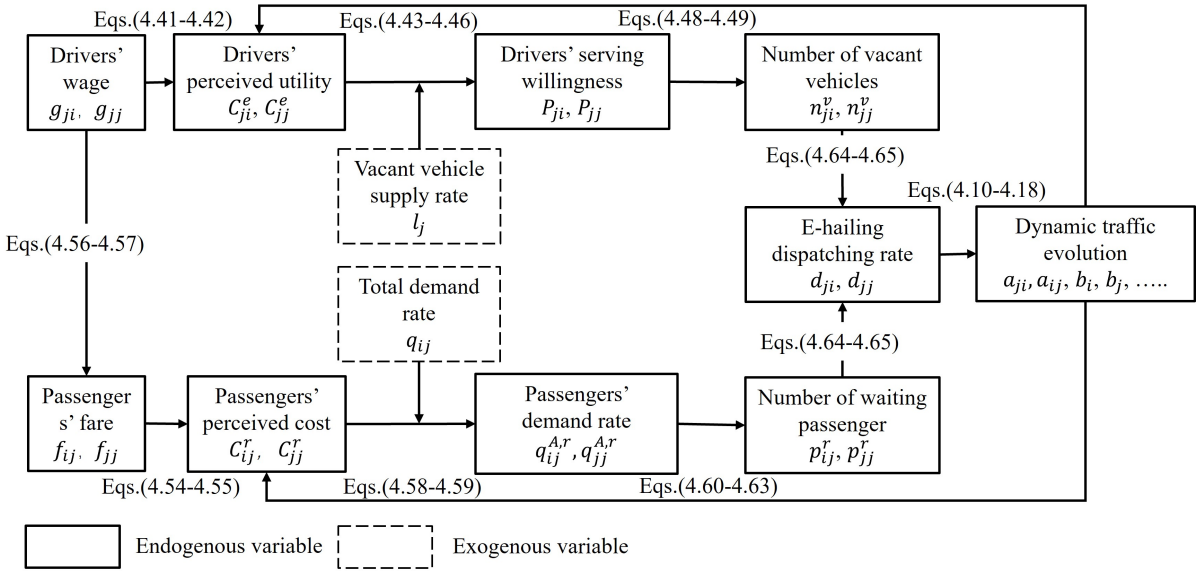

Figure 4.4 Correlations in our proposed e-hailing market

perceived utility and passengers' perceived cost. The correlations in both regions will follow this pattern. As shown in Figure 4.4, drivers' wage plays an important role in influencing both supply and demand, further in deciding the dispatching rate and traffic evolution. For sake of realizing a desired evacuation performance and appropriate operating efficiency of e-hailing vehicles, we aim to build a bridge between e-hailing dispatching rate and drivers' wage in the next Section 4.4. This strategy can capture the feedback from the bilateral market and the traffic evolution, to guide the price optimization of e-hailing platform, and form a closed loop for this framework.

4.4 Region-Dependent Price Optimization of E-hailing Platform under Mass Gathering Events

In this section, based on the above empirical evidence given in Subsection 4.1.1, we model the passenger evacuation dynamics in Subsection 4.4.1 and solve region-dependent pricing optimization problem in Subsection 4.4.2 to find the price that can realize optimal traffic performance.

4.4.1 Passenger evacuation dynamics during mass gathering events

There are a huge amount of passengers waiting for transportation from region i to region j after a mass gathering event or metro disruption. After the vehicles being dispatched and entering the demand surge region, e-hailing vehicles will first move towards passengers to stop

and load passengers. After e-hailing vehicles getting loaded, the vehicle will leave this region and the number of waiting passengers within the region decreases. Other available modes of transportation will also follow this similar pattern to transport the waiting passenger away from the demand surge region. To simplify this effect on overall evacuation performance, we assume a constant passenger sharing rate of all other modes from region i to region j as h_{ij}^{other}. Since each e-hailing vehicle always serves one passenger, so that $a_{ij}(t)$ can be used to record how many passengers have been transported out of this demand surge region by e-hailing service at time t. Let $Q(t)$ be the cumulative number of passengers that have been transported out of the area at time t, i.e.,

$$Q(t) = \int_0^t (a_{ij}(s) + h_{ij}^{other})ds. \tag{4.67}$$

When all of Q passengers are evacuated from the demand surge region i, the evacuation is considered to be completed. We also record the dynamic evolution of the traffic system during the entire evacuation process. Each passenger in the simulation wants to evacuate from the demand surge region as soon as possible. We assume that a total number of Q_{ij} passengers are accumulated within the region i and waiting for transportation at time $t = 0$. Let T be the total time it takes for all passengers to be evacuated, then T satisfies:

$$Q(T) = Q_{ij}. \tag{4.68}$$

Based on the above dynamic passenger evacuation model, we can simulate the dynamic traffic conditions and passenger evacuation process. However the above equations are all described in continuous-time form. Thereby we divide time into discrete units with time interval Δt, i.e., $t = \{0, \Delta t, 2\Delta t, ..., k\Delta t, ...\}$ in our simulation experiment. The integration of any function $y(x)$ from 0 to t is then approximated by:

$$\int_0^{k\Delta t} y(s)ds = \sum_0^k y(k\Delta t)\Delta t. \tag{4.69}$$

Let $N_i(0)$ and $N_j(0)$ be the initial e-hailing vehicle accumulation within each region at $k = 0$. From the above discussion, given $N_i(k\Delta t)$ and $N_j(k\Delta t)$ at the beginning of the kth interval, we can determine the vehicle speed $v_i(k\Delta t)$ and $v_j(k\Delta t)$ from Eqs. (4.35) and (4.36). By taking record of the total travel distance of vehicles at the beginning of the kth interval, we can determine the arrival rate, parking rate, boarding rate, outflow rate and trip completion rate of

each state of e-hailing vehicles at the end of the kth interval (or equivalently, the beginning of the $(k+1)$th interval) according to Eqs. (4.10)–(4.18), and the number of passengers evacuated according to Eq. (4.67). And based on the value of $a_{ji}((k+1)\Delta t), b_i((k+1)\Delta t), a_{ij}((k+1)\Delta t)$ and $o_i((k+1)\Delta t)$, we can further determine the e-hailing vehicle accumulation of each state in each region in the $(k+1)$th interval from Eqs. (4.19)–(4.30).

Based on the above dynamic passenger evacuation model, we can simulate the dynamic traffic conditions and passenger evacuation process to demonstrate the impacts of e-hailing services on the passenger evacuation efficiency.

4.4.2 Region-dependent price optimization problem

E-hailing platforms, as bilateral markets, balance passenger demand and driver supply via dynamic fare and wage adjustments. This mechanism guides passengers to better transportation options and encourages drivers to relocate for higher wages, enhancing service efficiency. In high-demand areas, surge pricing attracts more drivers, but research in Nicholas (2016) found it doesn't significantly boost drivers' willingness due to high time costs. This highlights traditional surge pricing's limitations, potentially worsening traffic and reducing service efficiency. To solve this, this study proposes a region-based pricing optimization, inspired by Lei et al. (2020)'s path pricing. By adjusting path prices, service providers guide passengers through high-demand areas, optimizing vehicle distribution. Focusing on driver behavior, providers can increase wages in high-demand areas to attract more drivers, optimizing supply distribution without direct scheduling intervention.

The optimization objectives based on region-dependent pricing strategy mainly include two aspects: first, improving the evacuation efficiency of demand surge region; second, improving the quality of service. By dynamically adjusting passenger fares and driver wages, e-hailing platforms can effectively balance supply and demand and alleviate the impact of surging demand on traffic flow. Inspired by Liu and Geroliminis (2017), we propose a concise and effective adaptive pricing scheme to dynamically adjust the drivers' wage in both regions, based on the updated information observed in the time-variant traffic system. We present the detailed formulation regarding the adaptive pricing in the following. We start from $g_{jj}(t)$ to firstly ensure the vacant e-hailing vehicles' dispatching rate in the two-region transportation system. Our aim of the adaptation of wage $g_{jj}(t)$ is to realize the dispatching rate in region j $d_j(t)$ can reach our

desired level d_j^*. The dynamic wage in region j at time $t+1$ is then updated by the following:

$$g_{jj}(t+1) = g_{jj}(t) - g_{jj,0} \cdot \max\left\{0, d_j(t) - d_j^*\right\} + g_{jj,0} \cdot \max\left\{0, d_j^* - d_j(t)\right\}, \quad (4.70)$$

where $g_{jj,0}$ is a coefficient for adjusting the wage $g_{jj}(t)$ and d_j^* is the optimal value of the dispatching rate in region j. For a given target d_j^*, this strategy updates the wage $g_{jj}(t)$ adaptively to drive the wage $g_{jj}(t)$ to reach the objective. The working rule is like: if $d_j(t)$ never exceeds the critical value d_j^*, which means the vehicles that are dispatched to region j is insufficient, second term will be zero, and the third term then will be strictly positive to increase the wage $g_{jj}(t)$, in order to attract more drivers to serve the region j. However, if $d_j(t)$ exceeds the critical value d_j^*, which means the vehicles dispatched to region j is the excessive, the second term will be positive, and the third term will be zero. Therefore wage $g_{jj}(t)$ will be decreased to prevent drivers from serving the region j. The optimal value d_j^* is decided by two portions, $d_j^* = d_{jj}^* + d_{ji}^*$. The first is the optimal dispatching rate to serve region j, d_{jj}^*, which will be given according to the historical traffic data to ensure the e-hailing service's operation efficiency in region j as usual. The second portion is the optimal e-hailing vehicles dispatching rate to region i, d_{ji}^*, which will be elaborated in the following.

Then we adjust the $g_{ji}(t)$ to make the $d_{ji}(t)$ close to our desired value d_{ji}^*. The decision of d_{ji}^* can be referred to Section 4.1.1. The value d_{ji}^t will convert to $a_{ji}(t)$ as Eq. (4.10) shows. Therefore, the decision of the optimal value d_{ji}^* can be referred to Section 4.1.1. It is reasonable to set the target dispatching rate d_{ji}^* as the same value as the optimal inflow rate a_r^*. We have confirmed in Section 4.1.1 that this target value can effectively improve the performance of system traffic flow and reach the minimum of total evacuation time. Therefore the wage $g_{ji}(t)$ should be set to realize no additional congestion delay and no systematical waste of roadway capacity. What's more, this target value is dependent on the traffic performance, therefore it is robust enough facing the varying e-hailing market's dynamics such as demand and supply. The dynamic wage in region i at time $t+1$ is then updated by the following:

$$g_{ji}(t+1) = g_{ji}(t) - g_{ji,0} \cdot \max\left\{0, d_{ji}(t) - d_{ji}^*\right\} + g_{ji,0} \cdot \max\left\{0, d_{ji}^* - d_{ji}(t)\right\}, \quad (4.71)$$

where $g_{ji,0}$ is a coefficient for adjusting the wage $g_{ji}(t)$. The second term on the right side is used to eliminate time duration with excessive driver to be dispatched to region j. The third term on the right side is used to avoid overpricing and underutilization of system capacity, which can

denote vacant e-hailing vehicles that can be dispatched to region i without causing accumulation to go beyond critical values and additional congestion delay. For a given target e-hailing vehicle dispatching rate in region i, this strategy updates the wage $g_{ji}(t)$ adaptively to drive the wage $g_{ji}(t)$ to reach the objective. The working rule is like: if $d_{ji}(t)$ never exceeds the critical value d^*_{ji}, the second term will be zero, and the third term then will be strictly positive to increase the wage $g_{ji}(t)$, in order to attract more drivers to serve the demand surge region. However, if $d_{ji}(t)$ exceeds the critical value d^*_{ji}, the second term will be positive, and the third term will be zero. Therefore wage $g_{ji}(t)$ will be reduced in order to stifle the drivers from serving the demand surge region. In summary, we design a method that first ensures the total supply of idle vehicles in both regions, and further ensures the supply of idle vehicles in a single region. To attract increased number of vacant e-hailing vehicles to this two-region system, $g_{jj}(t)$ should be increased firstly compared with other regions. To attract the increased number of vacant e-hailing vehicles to region i, $g_{ji}(t)$ should be increased further compared with $g_{jj}(t)$. Both of $g_{ji}(t)$ and $g_{jj}(t)$ are based on feedback-based adaptation.

In order to examine the effectiveness of this pricing strategy, we compare it with a two-region undifferentiated static wage rate strategy, which is as follows: $g_{ij}(t) = g_{jj}(t) = g$, for $t \in \{0, T\}$. This strategy resembles the solution of equilibrium-based modeling approach of the e-hailing market. For intuitive differentiation, we name this undifferentiated static pricing strategy for short as 'USP'. We name our proposed region-dependent dynamic pricing strategy for short as 'RDP'.

4.5 Numerical Examples

4.5.1 Numerical settings

The case study designates an urban two-region system, which includes the city center region i and its periphery region j, which is equivalent to $Z = 18$ times of region i, as schematically shown in Figure 4.2(b). The selection of this scale size is based on the fact that e-hailing platforms often match vehicles within 2 kilometers. Therefore, we define the distance between vehicles entering area j and the center of region i as 2 kilometers. For e-hailing vehicles that are matched to region i, we define the total distance from the matched e-hailing vehicle to the successful arrival of passengers as 2 kilometers, of which 1500 meters will travel in region j and 500 meters will travel in region i. After completing the passenger boarding, the first 500 meters will travel in region i, and the remaining 1500 meters will travel in region j before leav-

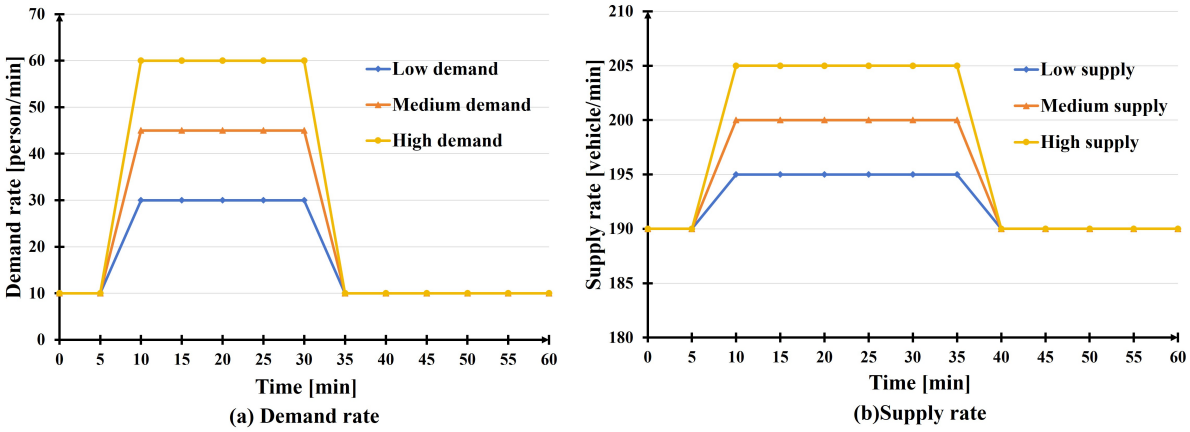

Figure 4.5 Demand and supply settings in numerical examples.

ing the two-region system. For the e-hailing vehicles that are matched to region j, we define the average distance from being matched to successfully arriving at the passenger and successfully picking up the passenger and leaving two-region system as 2 kilometers. We first specify the functional forms and parameter values necessary for numerical experiments. Without loss of generality, we assume both regions follow the well-defined relationship in MFD. The functional form of speed-accumulation relationship of regions i and j follow:

$$v_i(N_i) = v_i^f \cdot \exp\left\{-0.6 \cdot \left(\frac{N_i}{N_i^{opt}}\right)^2\right\}, \tag{4.72}$$

$$v_j(N_j) = v_j^f \cdot \exp\left\{-0.6 \cdot \left(\frac{N_j}{N_j^{opt}}\right)^2\right\}, \tag{4.73}$$

where v_i^f, v_j^f is the free flow speed of both regions and N_i^{opt} is the optimal vehicle accumulation of region i, N_j^{opt} is the optimal vehicle accumulation of region j, which that can maximize the vehicle production of this region.

The functional forms of $A_r(C^r)$ and $E_r(C^r)$ follow:

$$A_r(C^r) = 0.2 \cdot C^{r-0.5}, \tag{4.74}$$

$$E_r(C^r) = 0.2 \cdot C^{r0.5}. \tag{4.75}$$

In the following, we attempt to examine how different arrivals of passengers and drivers in the system impact both bilateral dynamics in e-hailing service's market and the traffic conditions. Figure 4.5 illustrates the demand (passengers) $q_{ij}(t)$, and supply (drivers), $l_j(t)$ of the

market in this two-region system during the evacuation period for different cases. Due to the different scale of the urgent events in practical cases, we consider different amount of total passenger evacuation demand rates in region i, $q_{ij}(t)$. Therefore we propose three levels: low, medium and high demand in region i, as presented in Figure 4.5(a). As the figure shows, we all assume a extreme period of demand located in the first half of the evacuation process. In Figure 4.5(a), the whole modeling duration is equal to 1 h. The demand in region i firstly stabilizes at 10 person/minute and then has a high demand duration starting from 5th min and dropping back to normal state at 35th min, which simulates the surged demand. The demands during the extreme period keep at 30, 45 and 60 person/minute for low, medium and high demand cases respectively. Referring to historical data, statistical information of similar events, we set the total evacuation passenger number Q_{ij} as 5000, 6000, 7000 respectively for these three low, medium and high demand cases. When all of Q_{ij} passengers are evacuated from the demand surge region i, the evacuation is considered to be completed. Finally region i's demand drops back to normal state 10 person/minute. However, not all of the demand will join the e-hailing market. The actual arrival rate of passengers depends on the time-variant perceived cost.

And then we proceed to give the vacant e-hailing vehicle supply rate to region j, $l_j(t)$, which will serve both region i's demand $q_{ij}(t)$ and region j's demand $q_{jj}(t)$. When the demand surges in the e-hailing system, e-hailing service providers always can schedule vehicles supply to areas with expected high demand to better meet the demand in practical case. Therefore, we propose to test three different levels of vehicle supply to region j, $l_j(t)$: low, medium and high supply, which indicates that e-hailing platform's different actions facing the surged demand. The three levels of vehicle supply are shown Figure 4.5(b). For comparison, we set the low level and high level cases to verify their impact on the traffic performance and e-hailing service quality.

However, this vacant e-hailing supply is just exogenously given by the platform. Simply increasing the total vacant e-hailing supply is not necessarily effective in resolving the spatiotemporal imbalance of supply and demand. How to allocate this supply into the two-region system as we desired and realize the optimal evacuation performance are dependent on the adaptive pricing scheme we proposed.

Simulation is conducted in a virtual environment. The time point at which simulation data is generated from $t = 0$ till the fixed number of passengers has been completely evacuated. The setup of parameters for the MFDs of regions, the two-region transportation system, the e-hailing market and the passengers in the evacuation process and the pricing strategies are respectively

Table 4.3 Parameters settings for the MFDs of regions

Parameter	Value	Unit
Free flow speed in region $i(v_i^f)$	12.5	m/s
Free flow speed in region $j(v_j^f)$	12.5	m/s
Driving distance of dispatched e-hailing vehicles within the region j moving towards region $i(l_j^{d1})$	1500	m
Driving distance of dispatched e-hailing vehicles within the region j moving towards region $j(l_j^{d2})$	2000	m
Driving distance of dispatched e-hailing vehicles within the region i (l_i^d)	500	m
Driving distance of occupied e-hailing vehicles moving in region j from the region i (l_j^{o1})	1500	m
Driving distance of occupied e-hailing vehicles within the region j moving towards region $j(l_j^{o2})$	2000	m
Driving distance of occupied e-hailing vehicles within the region i (l_i^o)	500	m
Vehicle boarding time in region $j(\hat{t_j^b})$	10	s

Table 4.4 Parameters setting for the two-region transportation system

Parameter	Value	Unit
Total number of other types of vehicles besides e-hailing vehicles in region $i(n_i^{other})$	140	veh
Total number of other types of vehicles besides e-hailing vehicles in region $j(n_j^{other})$	2250	veh
Optimal vehicle accumulation of region $i(N_i^{opt})$	340	veh
Optimal vehicle accumulation of region $j(N_j^{opt})$	6120	veh
Jam vehicle accumulation of region $i(N_i^{jam})$	1×10^3	veh
Jam vehicle accumulation of region $j(N_j^{jam})$	1.8×10^4	veh
Relative size difference coefficient between region j and region $i(Z)$	18	

summarized in Tables 4.3–4.6.

In the following, the simulation results are demonstrated in three aspects, which are effectiveness analysis of region-dependent wage strategy in Subsection 4.5.2, influence of passenger demand in Subsection 4.5.3 and influence of vehicle supply in Subsection 4.5.4. We finally provide a discussion on the impact of RDP on e-hailing platforms in Subsection 4.5.5.

4.5.2 Effectiveness of region-dependent wage strategy

To reveal the effect our proposed RDP on coordinating and allocating resources, we display the dynamic change of $g_{ji}(t)$ and $g_{jj}(t)$, under different levels of passenger demand and vehicle supply. In Figure 4.6, each row represents one level of passenger demand and each column represents one level of e-hailing vehicle supply. The red curve represents the driver wage rate serving region i, while the blue curve represents the driver wage rate serving region j. Comparing the three figures in each column, as the change of three demand levels, there is not much

Table 4.5 Parameters settings for the e-hailing market and the passengers in the evacuation process

Parameter	Value	Unit
Passenger's monetary value of waiting time(σ_{wt}^r)	30	¥/h
Passenger's monetary value of in-vehicle travel time (σ_{iv}^r)	20	¥/h
E-hailing driver's time-unit operating cost(σ^e)	60	¥/h
Passenger's average remaining trip time after leaving region j(t^{rm})	0.3	h
Commission rate(ϕ)	15%	
Dispersion parameter of e-hailing drivers' choice of serving different region(η)	0.15	
Passenger sharing rate of all other modes from region i to region j(h_{ij}^{other})	1.8	pax
Sampling time	1	s

Table 4.6 Parameters setting for the pricing strategies

Parameter	Value	Unit
Optimal e-hailing vehicles dispatching rate to serve region j(d_j^*)	200	veh/min
Coefficient for adjusting the wage $g_{ji}(t)$ ($g_{ji,0}$)	3×10^{-3}	
Coefficient for adjusting the wage $g_{jj}(t)$ ($g_{jj,0}$)	3×10^{-3}	
Undifferentiated wage rate of two regions (g)	0.03	¥/s

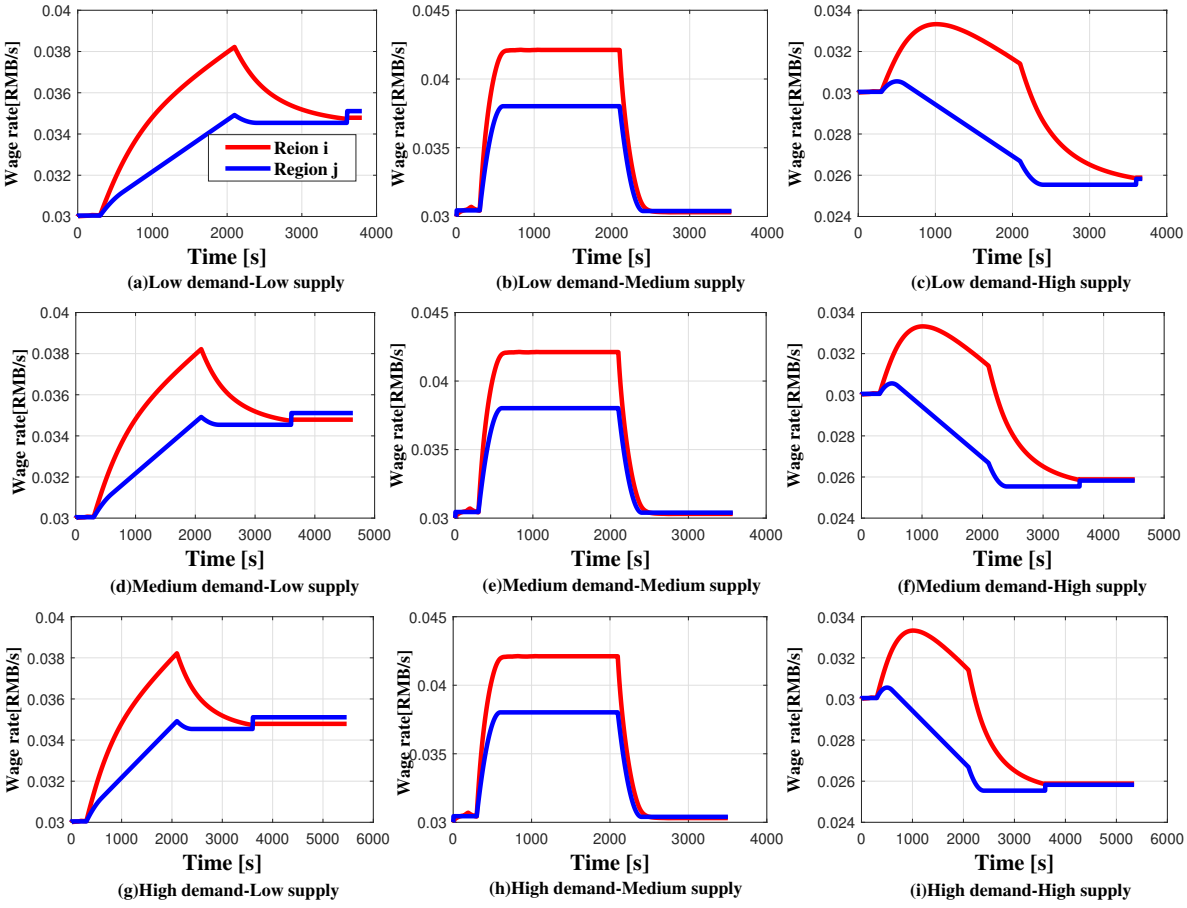

Figure 4.6 The outputs of the proposed region-dependent pricing strategy.

difference in the trend of the wage rate in regions i and j. It is because the vehicle supply is fixed, the trend of the wage rate used for vehicle supply allocation owns the same pattern. The fluctuation trend of wage rates is determined by the changing pattern of vehicle supply over time. It is depicted that significant change can always be observed at the time $t = 600s$ and $t = 2100s$, which is consistent with the 10 mins and 35 mins in Figure 4.5(b). Due to other modes of passenger sharing, passenger demand will not be fully shared by e-hailing service. However, the higher the demand, the longer the evacuation time will be used to complete the larger number of passengers. However, comparing the three figures in each row, as the change of three levels of vehicle supply, the trend of wage rate will undergo significant changes. This is because the vehicle supply mainly determines the total capacity, furthermore vehicle resources are allocated through the proposed region-dependent pricing strategy. Therefore, under different levels of vehicle supply, the wage rate will generate different forms to regulate resource allocation.

As the Figure 4.6(a),(d) and (g) show, under the low level of vehicle supply, the wage rate will increase from $t = 0s$ to $t = 2000s$. This is because the supply has been in a shortage, RDP needs to increase the wage constantly to attract drivers to meet passengers' needs. The wage rates in both regions are rising, but region i is rising faster than region j due to the need to attract more drivers to offer a higher service density to assist in passenger evacuation. The highest point reaches around $t = 2000s$, with region i around 0.038 and region j around 0.035, denoting increases of 26% and 16% respectively. After $t = 2000s$, the demand in region i will slowly decrease, and dispatching and evacuation will also enter the latter half. With less demand, the wage rate in region i will slowly fall back to 0.035. The wage rate of region j remains stable at 0.035. After experiencing a demand surge in both regions, the final wage rates increase 16% compared to the initial wage rate due to insufficient supply. This proves that under the demand surge, insufficient supply requires wage increase, to increase the attractiveness of the region and attract more vehicle supply to serve for it.

As the Figure 4.6(b),(e) and (h) show, under the medium level of vehicle supply, the wage rates in both regions first increase to attract more drivers. After the supply stabilizes at the peak value, the wage rates will also stabilize at the peak values 0.043 and 0.037 for both region, denoting increases of 43% and 23% respectively. This process will last from $t = 600s$ to $t = 2000s$. As the evacuation gradually ends, the supply gradually decreases and the both of wage rates will return to the initial level.

As the Figure 4.6(c),(f) and (i) show, under the high level of vehicle supply, the wage rate in region i will first increase when the vehicle supply is insufficient from $t = 0s$ to $t = 600s$, in order to attract more drivers. After the wage rate in region i reaches the peak point 0.033 around $t = 1000s$, due to excessive supply, the wage rate starts decreasing from then on, preventing drivers from continuing to provide service. The wage rate in region j keeps decreasing during this process. Finally, wage rates in both regions will stabilize at the minimal level 0.026, which denotes a decrease of 13% compared with the initial wage rate. This proves that under the demand surge, excessive supply requires price decreases, to decrease the attractiveness of the region and prevent more vehicle supply to serve for it. In summary, we can conclude that compared to demand, regulating the vehicle supply is more critical and it directly affects the platform's pricing strategy. If the vehicle supply can be appropriately provided, the wage rate can be well stabilized under any level of surged passenger demand.

To evaluate the evacuation performance and traffic condition, the total evacuation time ranks first. We firstly show the total evacuation time under three different levels of demand and three different levels of e-hailing vehicle supply, to examine the effectiveness of our proposed region-dependent strategy compared with USP. See Table 4.7, each row represents one level of passenger demand and each column represents one level of e-hailing vehicle supply. Both of the total evacuation times under USP case and RDP case are provided. It is evident that under any level of passenger demand or vehicle supply, RDP will always lead to a shorter evacuation time than USP, thanks to its better capability of resource allocation. When the vehicle supply is fixed, the less the demand, the shorter the total evacuation time. But when the demand level is fixed, the medium level will result in the shortest evacuation time, which is consistent with the results that we have previously verified in Section 4.1.1. A low level of vehicle supply will lead to insufficient transportation capacity, while high level can also lead to redundant servable vehicles and reduce evacuation efficiency. In the case of medium level, as demand increases, the effect of RDP on shortening the total evacuation time becomes more significant compared to USP. The results clearly indicate the effectiveness of RDP on improving the evacuation performance.

To verify the effectiveness of our proposed pricing scheme from other perspectives besides total evacuation time, we try to check whether the two goals have been achieved as our expectation. In Table 4.8, we select some variables that have a direct driving effect on the evacuation efficiency and e-hailing's service quality. We compare them under both USP and RDP strategies, along with their average values and units, focusing on the medium level of passenger

Table 4.7 Total evacuation times under both USP and RDP. Time expressed in seconds.

Demand level	Low supply		Medium supply		High supply	
	USP	RDP	USP	RDP	USP	RDP
Low demand	3975	3868	3908	3803	3783	3537
Medium demand	4808	4601	4741	4636	4514	3671
High demand	5641	5435	5575	5470	5347	3804

Table 4.8 Comparison of key indicators under both USP and RDP.

Strategy	T(s)	$\bar{g}_{ji}$ (¥/s)	$\bar{g}_{jj}$ (¥/s)	$\bar{w}^p_{ij}$(s)	$\bar{w}^p_{jj}$(s)	$\bar{C}^r_{ij}$(¥)	$\bar{C}^r_{jj}$(¥)	$\bar{C}^e_{ji}$(¥)	$\bar{C}^e_{jj}$(¥)
USP	4514	0.03	0.03	900	50	52	52	15	15
RDP	3671	0.042	0.037	450	35	73	64	30	25
Change	-18%	+40%	+23%	-50%	-30%	+40%	+23%	+50%	+66%

demand and high level of e-hailing vehicle supply. The percentage changes of RDP with respect to USP are also given. The most evident fact is that the total evacuation time of region i under RDP case decreases 18% compared to USP. The mechanism behind this is that through the means of increasing the wage rates by 40% and 23% of serving regions i and j, the average passengers' waiting times for dispatching in both regions decrease 50% and 30%, which greatly facilitates the efficiency operation of the e-hailing market as well as the traffic system. The increase of wage rates further lead to the increase of average generalized cost of e-hailing passengers (40% and 23%) and generalized wage of e-hailing drivers (50% and 66%) in regions i and j. This demonstrates that RDP greatly promotes the stability and efficiency of traffic conditions during evacuation, by the way of increasing prices. The platform use this mechanism to influence the choices of drivers and passengers, for sake of effectively balancing the supply and demand relationship in the e-hailing market as the regulator.

Next, we examine the impact of USP and RDP strategies on traffic conditions and e-hailing service quality under different levels of passenger demand and e-hailing vehicle supply.

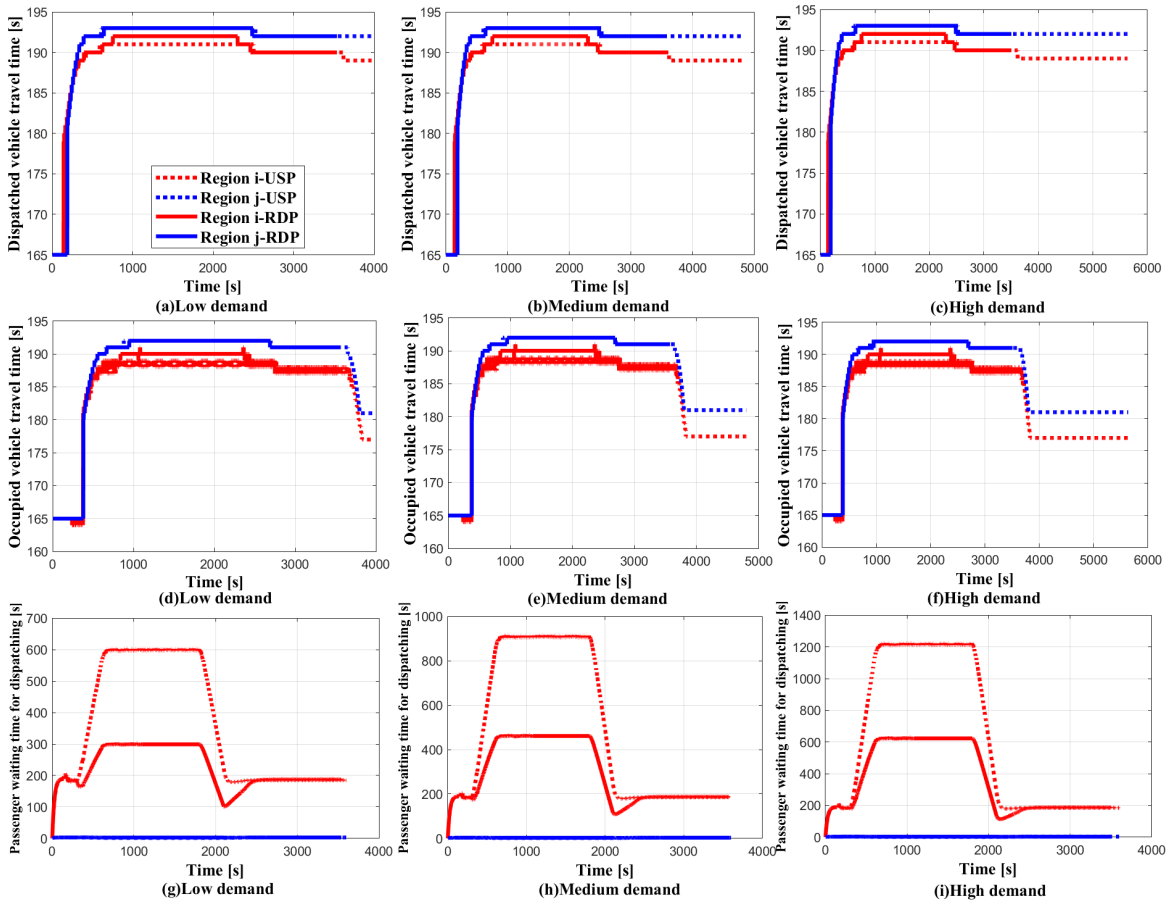

Figure 4.7 Evolution of system state under different passenger demands.

4.5.3 Influence of passenger demand

We fix the vehicle supply at a medium level and verifies the impact of three different levels of passenger demand on traffic conditions and the quality of e-hailing services.

We first explore the dynamics of traffic system under different demands, displaying the dispatched vehicles travel time, occupied vehicles travel time and the passenger waiting time for dispatching. Each row represents one variable and each column represents one level of passenger demand. For the following figures, the dashed curves illustrates USP, and the solid lines represent RDP. The red curve represents the driver wage rate serving region i, while the blue curve represents the driver wage rate serving region j. Details are referred to the legends. Figure 4.7(a)–(f) show that under the all three demand levels, the dispatched vehicle travel time and occupied vehicle travel time will be relatively stable at around 190s in both regions. This is because the vehicle supply is fixed, which will not lead to significant changes in traffic conditions and travel time. However, the passenger waiting time for dispatching will undergo significant

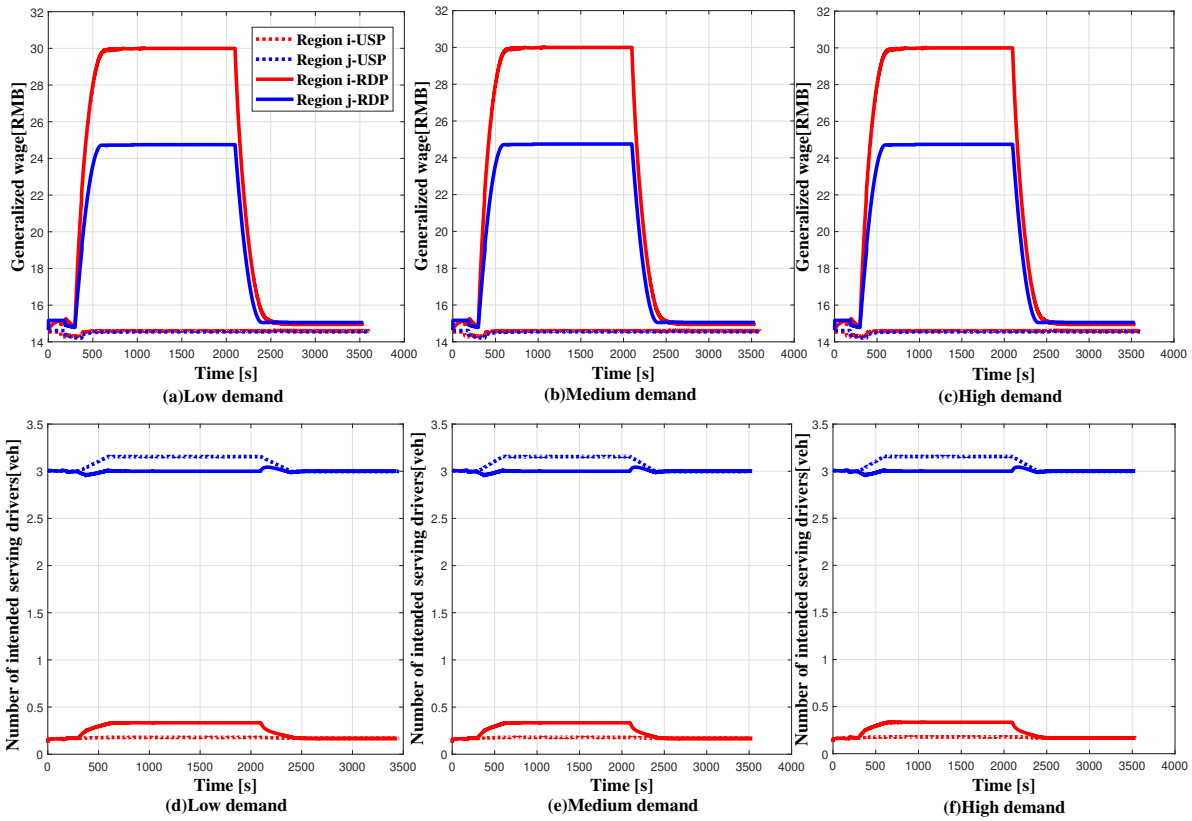

Figure 4.8 Evolution of e-hailing market under different passenger demands.

changes due to different demands, as shown in Figure 4.7(g)–(i). In the case of low demand, the average waiting time for dispatching under USP case is at 600s(10 mins) and under RDP case is at 300s(5 mins), a decrease of 50%. In the case of medium demand, the average waiting time for dispatching under USP case is at 900s(15 mins) and under RDP case is at 450s(7.5 mins), a decrease of 50% as well. In the case of high demand, the average waiting time for dispatching under USP case is at 1200s(20 mins), and under RDP case is at 60s(10 mins), reducing by 50% also. To summarize, there are significant decreases in all three demand levels. This demonstrates the significant effect of our proposed RDP in shortening the passengers' waiting time for dispatching and improving the quality of e-hailing services. The passengers' waiting time for dispatching in region j will remain at a relatively low level under both strategy.

In terms of the e-hailing service quality, we consider the service quality from the perspectives of drivers and passengers. We first investigate the evolution of the e-hailing market from driver side. Figure 4.8 shows driver related indicators, including generalized wage and the number of intended serving drivers in both regions. Since the vehicle supply is fixed, both the generalized wage and the number of intended serving driver remain unchanged, indicating that the driver

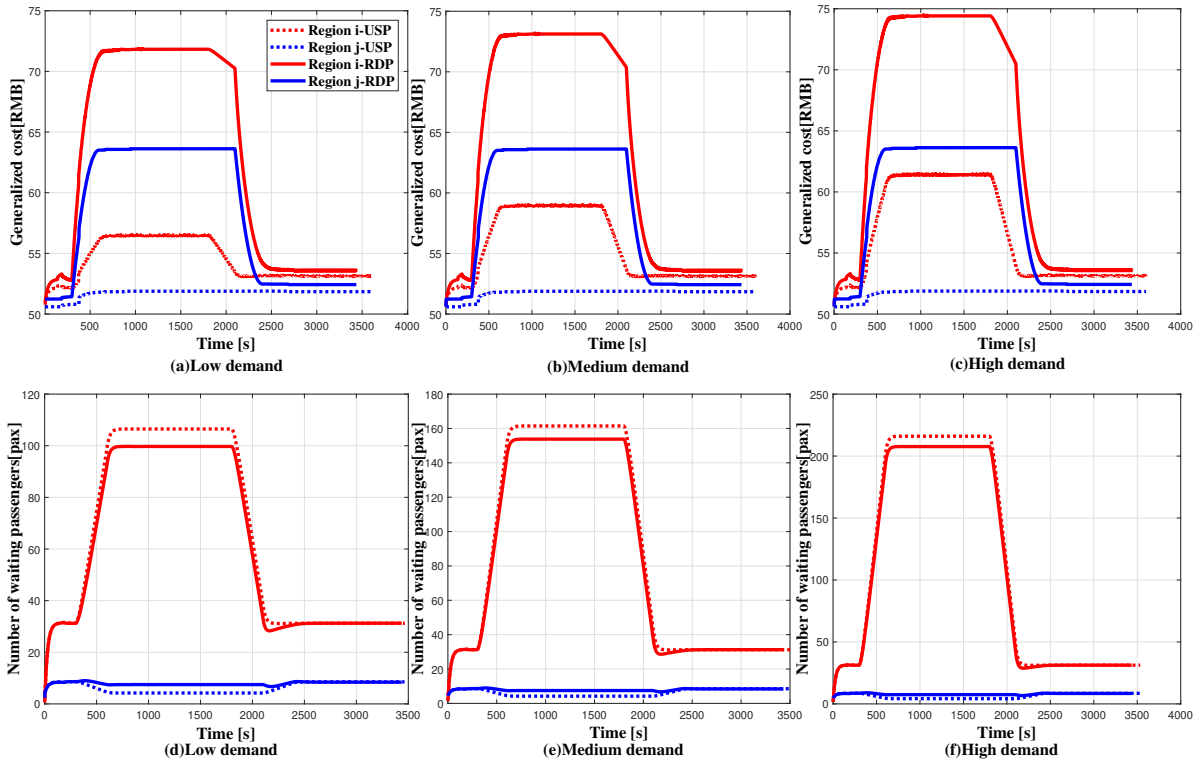

Figure 4.9 Evolution of e-hailing market under different passenger demands.

related indicators are insensitive to the change of demand. In the case of USP, the generalized wages are all around 15 serving both regions. However, in the case of RDP, the generalized wage of serving region i will first increase to 30 at $t = 600s$ and then remain stable at this value till $t = 2100s$. Finally it drops back to the initial value when $t = 2500s$. The generalized wage of serving region j shows similar patterns. The only major difference is that the peak value will remain stable at around 25. This confirms that RDP can help drivers improve their income. In terms of the number of intended serving drivers, RDP can lead to appropriately increase of the driver number in region i and reduce the number in region j, which reflects its beneficial role in capacity allocation to more needed region.

Hereafter we further explore the dynamics of e-hailing market from passenger side, under different demands. Figure 4.9 shows the passenger related indicators, including the generalized cost and total unserved passenger demand in both regions. Depicted in Figure 4.9(a)–(c), as the demand increases, under USP case, the generalized cost in region i will increase from 52 to 62 during the peak hour. Under RDP case, the generalized cost in region i also increases, though it keeps at high values but the increase is not as significant as USP, rising from 72 to 75. This clearly indicates that with the increase of passenger demand, the generalized cost will

increase inevitably due to the more competitive situation among passengers. The generalized cost in region j does not show significant changes under the both two pricing strategies. Shown in Figure 4.9(d)–(f), as the demand increases, the number of waiting passenger during the peak hour will sharply increase to 100, 150, 200 respectively for the three levels. However, due to the increase in generalized cost under RDP case, the number of waiting passenger will decrease a little bit compared to USP. Analyzing the dynamics of the e-hailing market from the passenger's perspective under various demand scenarios offers valuable insights, yet potential limitations or variations might arise in different contexts. For instance, in regions where e-hailing services are newly introduced or have low adoption rates, passenger behavior and demand patterns could vary significantly from those in well-established markets. Cultural and individual preferences can influence passengers' sensitivity to price changes and their willingness to wait. Therefore, future research should be tailored to specific contexts to offer more universally applicable insights into the e-hailing market dynamics.

4.5.4 Influence of e-hailing vehicle supply

We further explore the impact of three different levels of e-hailing vehicle supply on traffic conditions and e-hailing service quality, using USP and RDP strategies respectively, under the premise of a medium level of passenger demand. Based on the above settings, a new set of experimental simulation analysis is conducted.

Re-displaying the figures like Figure 4.7, Figure 4.10 displays that under all three levels of vehicle supply in the same sequences. Figure 4.10(a)–(f) show that under the three levels of vehicle supply, the dispatched travel time and occupied travel time will be relatively stable at around 190s in both regions. This is because although the vehicle supply has changed, it will not cause a significant decrease in speed, thereby it will not greatly affect traffic conditions and the travel time. However, as depicted in Figure 4.10(g)–(i), changes in vehicle supply do result great difference in passenger waiting time for dispatching, especially to region i. In the case of low level of vehicle supply, the average passenger waiting time for dispatching under USP case in region i is at 920s and under RDP case is 500s, a decrease of 46%. In the case of medium level of vehicle supply, the average passenger waiting time for dispatching under USP case is 900s and under RDP case is 450s, a decrease of 50%. In the case of high level of vehicle supply, the average passenger waiting time for dispatching under USP case is 720s, and under RDP case is 460s, reducing by 36%. Significant decreases are found in all three levels of vehicle supply and

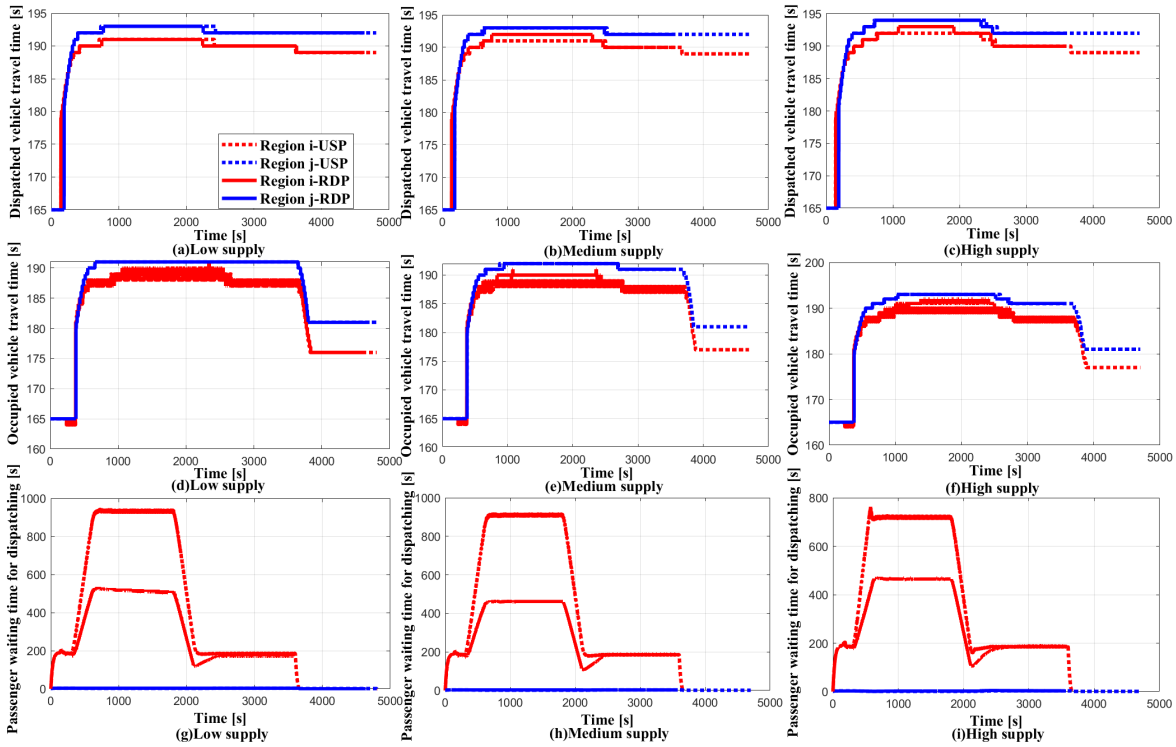

Figure 4.10 Evolution of system state under different vehicle supplies.

a most decrease is found under the case of medium level of vehicle supply. This is because RDP allocates more vehicle supplies to region i, thus increasing the dispatching rate and reducing the passengers' waiting time for dispatching. This demonstrates the significant effect of our proposed RDP in improving the quality of e-hailing services. The passengers' waiting time for dispatching in region j will remain at a relatively low level during this time period. Several potential limitations or variations could emerge in different contexts. For instance, the type of vehicles in the fleet (e.g., electric vs. traditional fuel, autonomous vs. human-driven) and technological advancements can affect the overall performance and applicability of the RDP strategy. Future research can be tailored to provide more insights into the effectiveness of fleet management strategies.

We then investigate the evolution of the e-hailing market from driver side. Re-displaying the figures like Figure 4.8, Figure 4.11 displays that under all three levels of vehicle supply. Under USP case, the generalized wages remain stable at 15 for both regions. However, under RDP case, it can be clearly found that the trend of generalized wage is the same as the wage rate depicted in Figure 4.6. As shown in Figure 4.11(a), in the case of low level of vehicle supply, the generalized wage of serving region i under RDP case will first increase to 25 at $t = 2100$, and then keeps decreasing and remains stable around 20 at $t = 3500$. The generalized wage of

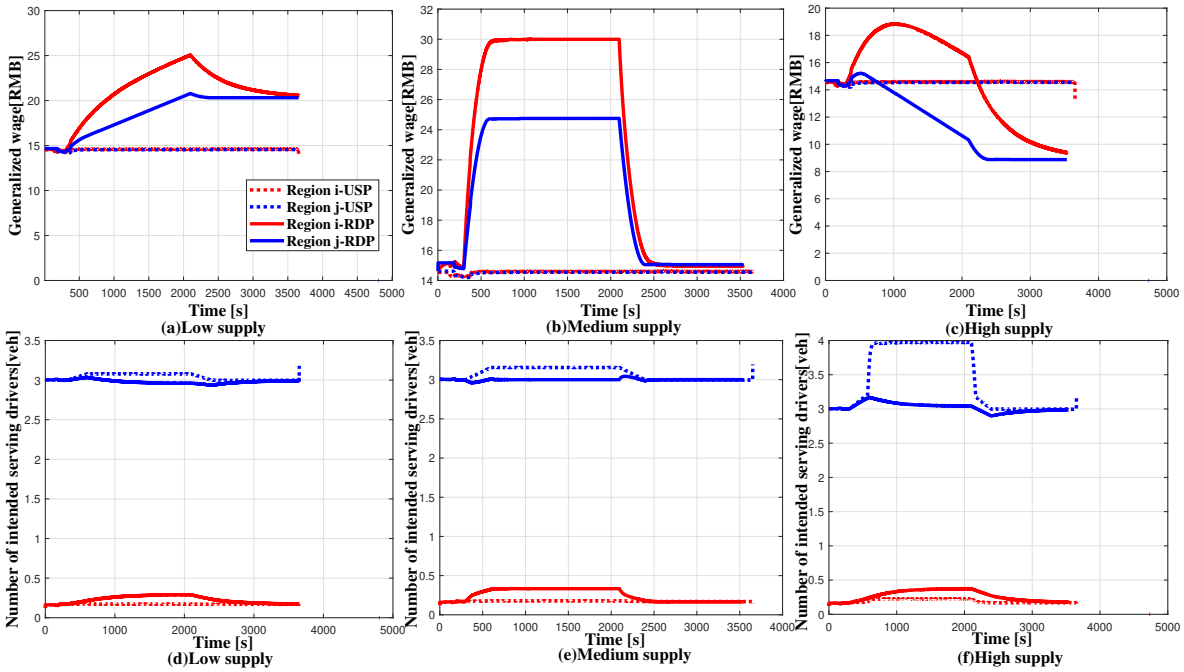

Figure 4.11 Evolution of e-hailing market under different vehicle supplies.

serving region j under RDP case will first increase to 20 at $t = 2100$, and then keep stable at this value till $t = 3500$. The final generalized wages in both regions increase 33% compared to the initial generalized wages due to insufficient supply. As shown in Figure 4.11(b), in the case of medium level of vehicle supply, the generalized wage of serving region i under RDP case will first increase to 30 at $t = 600$, and then keep stable till $t = 2100s$ and finally fall back to initial value of 15 at $t = 2500$. The generalized wage of serving region j owns the same trend as region i, and peak value keeps stable at 30. As shown in Figure 4.11(c), in the case of high level of vehicle supply, the generalized wage of serving region i under RDP case will first increase to 19 at $t = 900$. After reaching the peak point, due to excessive supply, the generalized wage will keep decreasing to 9 at $t = 3500s$, preventing drivers from continuing to provide service. The generalized wage in region j keeps decreasing during this process and also finally stabilizes at 9 at $t = 3500s$. The final generalized wages in both regions decrease 40% compared to the initial generalized wages due to redundant supply. Therefore, it proves that the platform needs to carefully plan how much vehicle supply to provide. If the capacity is insufficient, the generalized wage needs to continuously increase and drivers satisfaction towards the platform may be ensured. However, if the capacity is excessive, the generalized wage needs to be lowered, which causes a decrease in drivers' satisfaction, and may

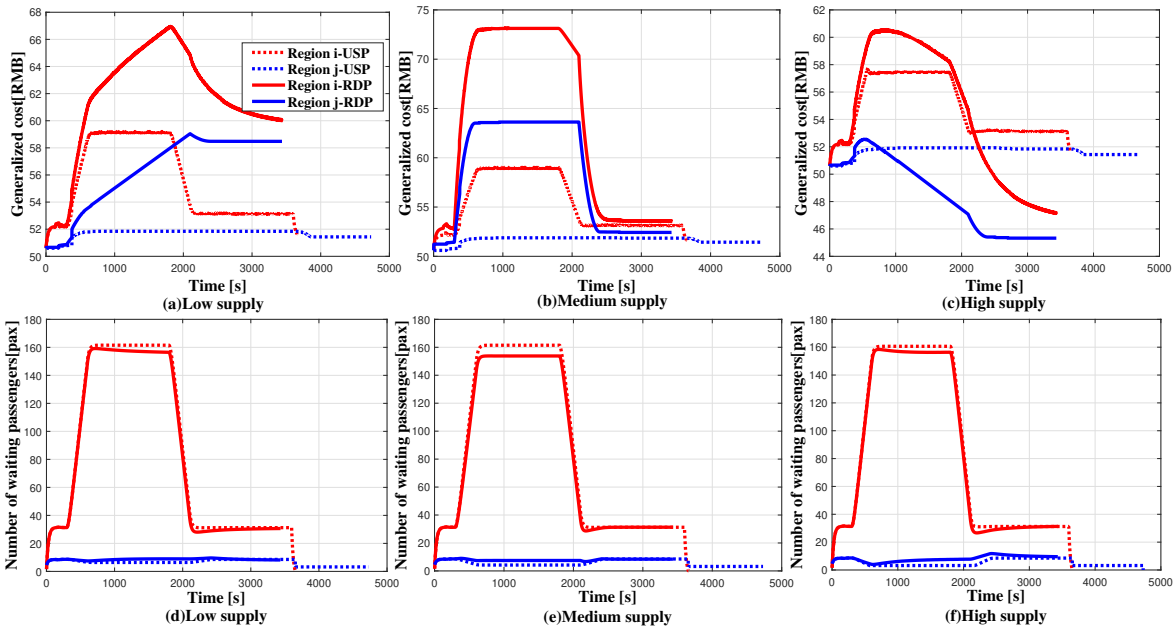

Figure 4.12 Evolution of e-hailing market under different vehicle supplies.

even lead to other long-term negative impacts such as driver withdrawal from the platform. This demonstrates the importance of developing a reasonable level of vehicle supply. If the vehicle supply can be appropriate provided, the generalized wage of drivers can be well stabilized, which ensure the drivers' sustainable serving willingness in the platform. In terms of the number of intended drivers depicted in Figure 4.11(d)–(f), RDP will help to appropriately increase the number of intended drivers in region i and reduce the number in region j. This is because region i needs a higher service density for evacuating passengers, which reflects its role in allocating capacity to more needed regions. However, with advances in e-hailing technology, such as improved passenger-driver matching algorithms or the introduction of autonomous vehicles, variations in the market dynamics may exist under the RDP strategy.

However, we also need to explore the impact of different levels of vehicle supply from passenger side. Re-displaying the figure like Figure 4.9, Figure 4.12 displays that under all three levels of vehicle supply. In Figure 4.12(a)–(c), under the USP, as the vehicle supply increases, the generalized cost in region i will slightly decrease and the generalized wage of region j keeps stable at 52. Under RDP case, it clearly indicates that under all three levels of vehicle supply, the trend of generalized cost is also the same as the wage rate depicted in Figure 4.6. As depicted in Figure 4.12(a), when the vehicle supply is insufficient, the generalized cost in region i continues to increase from $t = 0s$ to $t = 2000s$, reaching a maximum value of 67.

As the demand decreases, due to the gradual decrease of wage rate, the generalized cost also gradually decreases to 60 at $t = 3500s$. The generalized cost in region j increases from $t = 0s$ to $t = 2000s$, reaching a maximum value of 58, and keep stable at this value till the end. The final generalized costs in both regions increase around 18% compared to the initial generalized cost due to insufficient vehicle supply. As depicted in Figure 4.12(b), when the vehicle supply is appropriately given, the generalized cost in region i increases from $t = 0s$ and reaches a maximum value of 73 at $t = 600s$. After that, the generalized cost in region i stabilizes at this value till $t = 2100s$. Finally the generalized cost gradually decreases to the initial value at $t = 2500s$. The generalized cost in region j has the similar trend as region i, reaching a maximum value of 64 during the peak hour. As depicted in Figure 4.12(c), when the vehicle supply is over estimated, the generalized cost in region i continues to increase from $t = 0s$ to $t = 600s$, reaching a maximum value of 60. As the vehicle supply is excessive, the wage rates are gradually decreasing, and the generalized cost also gradually decreases to 48 at $t = 3500s$. The generalized cost in region j decreases from $t = 0s$ to $t = 2500s$, reaching a minimum value of 46, and keeps stable at this value till the end. The final generalized costs in both regions increase around 6% compared to the initial generalized cost due to excessive supply. This also indicates that appropriate setting of vehicle supply will affect the perceived service quality of passengers. If the vehicle supply is insufficient, the generalized cost needs to be continuously increased and passengers' satisfaction towards the platform can be weakened. However, if the vehicle supply is excessive, it will attract more passengers to join the platform, making it difficult to operate smoothly. Besides, the generalized wage needs to be lowered, which is not consistent with the platform's sustainable development. If the vehicle supply can be appropriately given, the generalized cost of passengers can be well stabilized as well, which ensure the passengers' stable use and long-term enrollment in the platform. In terms of the number of waiting passengers depicted in Figure 4.12(d)–(f), as the demand is fixed, the number of waiting passenger remains almost unchanged with the increasing of vehicle supply. However, due to the increase of generalized cost under RDP case, the number of waiting passenger will be slightly declined compared to USP. In reality, the existence and competitive landscape of alternative transportation modes (such as bus) may affect the effectiveness of the RDP strategy. The results may be different in markets with fierce competition with other transportation options.

To summarize, the change in vehicle supply will have an impact on both the driver's wage and the passenger's cost, affecting bilateral dynamics, as shown in Figure 4.11 and Figure 4.12.

The generalized cost and wage have similar trends, both of which are determined by the wage rate depicted in Figure 4.6. However, if only the demand level is changed, the impact on the driver side is unnoticeable, as shown in Figure 4.8 and Figure 4.9. Therefore, it further confirms the necessity and effectiveness of proposing a pricing strategy to regulate the traffic performance and e-hailing service quality from the driver side. Moreover, we accurately characterize the impact of supply and demand on pricing strategies and passenger evacuation efficiency. Based on this, we make it possible to further verify the impact of some indirect variables such as weather condition and media impact.

Taking into account the traffic flow dynamics of demand surge areas, we design a moderate and efficient e-hailing pricing strategy, while ensuring that demand surge region can attract the necessary number of vehicles to support evacuation and avoid causing traffic congestion. This highlights the importance of dynamic resource allocation, particularly in transportation supply management during emergencies. It emphasizes the need for accurate understanding of e-hailing supply and demand dynamics in different regions to formulate effective pricing strategies. In the face of increasingly frequent large passenger flow events, the proposed pricing strategy can effectively help e-hailing platforms to adjust the perceived utility of drivers and the perceived cost of passengers, thereby affecting their behavior and ultimately affecting dispatching and evacuation efficiency. The effectiveness of such strategies in balancing supply and demand relationships is well confirmed. In real-world application and management, more flexible price adjustment methods can be used, such as passenger taxi discounts and driver order rewards. It is reported that these methods have been used by Didi in dealing with large passenger flow transportation after the concert. These methods have greatly shortened the average waiting time of passengers, reduced the risk of exposure to passengers, and improved the quality of service. This not only promotes the stability and efficiency of traffic conditions during evacuation, but also alleviates the waiting anxiety of passengers. Policymakers can leverage these findings to develop adaptive policies that enhance the resilience of urban transportation systems, ensuring better coordination between traffic regulators and e-hailing platforms.

4.5.5 Discussion on the impact of RDP on e-hailing platforms

The region-dependent pricing optimization strategy for e-hailing services is reasonable in theory, but in practice it is necessary to balance the needs of multiple stakeholders, especially in the coordination between e-hailing platforms and transportation departments.

Although transportation departments may hope that e-hailing platforms will fully obey their guidance in emergency situations to ensure public safety and evacuation efficiency, e-hailing platforms, as a commercial entity, must also consider overall profits. When calculating the matching rate, e-hailing platforms should not only consider the guidance of the transportation department, but also combine their own operating costs, driver income, passenger payment ability, and market demand to formulate a comprehensive pricing strategy. Completely ignoring the profit orientation may lead to platform sustainability issues and may even reduce the enthusiasm of drivers, thereby affecting evacuation efficiency. In this case, the transportation department and e-hailing platforms should reach a solution through negotiation that can improve evacuation efficiency while ensuring commercial viability. This approach balances the interests of all parties in practice and is an effective evacuation strategy.

If we want to make e-hailing platforms obey the guidance of traffic management departments, especially in emergency evacuations or other special situations, we can ensure that e-hailing platforms can maintain consistency with the government's evacuation strategy in specific situations through economic subsidies, policy support, and signing cooperation agreements, thereby better serving the overall interests of the public and society.

4.6 Concluding Remarks

Based on the concept of the MFD, this chapter proposes a mathematical model to depict the time-varying evolution of e-hailing vehicles within a two-region transportation system using a trip-based manner. Given the imbalanced spatial distribution of e-hailing vehicle supplies resulting from sudden large passenger flows, we incorporate bilateral dynamics, including drivers' repositioning decisions, passengers' demand dynamics, and dispatching processes between these two parties. To facilitate the e-hailing platform in effectively managing an appropriate vehicle supply for swift evacuation, we propose a region-dependent pricing strategy (RDP) by adjusting e-hailing drivers' per unit time wages in different regions to incentivize their service willingness. Through simulation experiments, we confirm that, irrespective of passenger demand and vehicle supply levels, RDP consistently leads to a shorter total evacuation time, more stable traffic conditions, and reduced passenger waiting times for dispatching. In contrast, the static pricing strategy lacks the ability to distinguish between the two regions, hindering the allocation of additional vehicle supply to the more critical area. The evident superiority of the region-dependent pricing strategy lies in its significant advantage in mitigating

regional demand-supply imbalances. However, an exploration of the dynamics of the e-hailing market reveals that RDP results in higher drivers' generalized wages and passengers' generalized costs. Furthermore, our analysis verifies that changes in supply exert a more critical role than demand. Regulating the supply from the driver side can lead to substantial changes in the bilateral e-hailing market and traffic performance. Appropriately provided the vehicle supply for serving an extreme event can stabilize both drivers' and passengers' generalized wages. This underscores that RDP, acting as a regulator by increasing prices, influences the choices of drivers and passengers, effectively balancing the supply and demand relationship in the e-hailing market, and promoting the stability and efficiency of traffic conditions during evacuation. These designed cases aim to assist in traffic management during emergency situations and provide insights into optimizing the operation of the e-hailing market. Drawing lessons from the results of different cases, researchers can determine that our proposed pricing strategy is a impactful tool and serves as guidance for urban traffic operation and management administrations in formulating dispatching policies for e-hailing systems.

CHAPTER 5 BOARDING SPACE DESIGN PROBLEM WITH BUS AND E-HAILING SERVICES CONSIDERING EVACUATION EFFICIENCY AND SAFETY

With the rapid expansion of cities, the contradiction between the limited road infrastructure and the growing demand for transportation has become increasingly acute. In order to enhance the convenience of commuting, expanding the range of travel choices has become an urgent task. Therefore, it is crucial to achieve effective integration between different transportation modes. This requires us to deeply analyze the operational characteristics of various modes of transportation, including passenger carrying capacity, driving behavior (including speed and distance traveled), travel time, and whether they follow established schedules. Meanwhile, while introducing new modes of transportation can improve system performance, it may also lead to increased operating costs and potential safety hazards. Therefore, when optimizing the transportation system, we must seek a reasonable balance between improving user convenience and controlling operating costs. By comprehensively considering the above factors, more efficient, flexible, and safe traffic management can be achieved to better cope with the challenges brought by urbanization.

This chapter models the evacuation dynamics and performance through a three dimensional macroscopic fundamental diagram, and comprehensively evaluates the generalized cost of completing evacuation in the transportation system. In addition to the travel and operating costs of passengers, the research innovatively incorporates safety costs into the total cost, focusing on two common safety issues in real-life scenarios: pedestrian vehicle conflict and pedestrian conflict. This study analyzes four boarding space configuration scenarios within the transportation system and compares them through numerical analysis. The results show that neglecting operating costs may lead to higher safety costs, while fully focusing on overall safety during evacuation can significantly reduce total costs. From the perspective of passengers, strengthening transportation infrastructure can reduce travel costs. In addition, this chapter also explores the additional complexity that e-hailing services bring to the transportation system, quantifies the monetary and safety costs of e-hailing services under high passenger flow conditions, and provides a basis for optimizing traffic management.

The remainder of the chapter is organized as follows. Section 5.1 provides the research as-

sumptions and problem description. Section 5.2 describes the evacuation framework in this 3D-MFD system, which guides our empirical methodology. Section 5.3 models the three types of cost of this transportation system. Section 5.4 models and compares four scenarios under specific design of this transportation system. Section 5.5 examines the methodology by conducting numerical experiments. Section 5.6 concludes.

5.1 Problem Setup and Assumption

We also consider the passenger evacuation situation when travel demand surges following a mass gathering event or metro disruption. The transportation system is a bi-modal system with e-hailing services and buses, each with its own passenger loading capacity. Extraneously given e-hailing and bus supply will be continuous provided to deal with the passenger demand, until it is sufficient to transport all Q passengers out of the region.

Using the three-dimensional vehicle macroscopic fundamental diagram (3D-vMFD), we describe the vehicle dynamics in the mixed traffic environment, including the relationship between the average speed and vehicle accumulation for both e-hailing vehicles and public buses. By dividing the system into inbound and outbound directions, we define the e-hailing trip into three phases: the first stage is to enter the pick-up phase, the second stage is to stop and wait for passengers to board, and the third stage is to pick up passengers and leave the area. We define the spatial average speeds for the inbound and outbound directions respectively by use of the representation of MFD. Adopting a trip-based MFD model to study the vehicle evacuation dynamics, satisfies the first-in-first-out (FIFO) assumption.

We assume the total generalized cost of the transportation system can be approximated as a combination of the passengers' trip cost, the transportation system operating cost and the safety cost. Passengers are price-sensitive and they will choose travel modes based on perceived cost, which includes monetary and time costs. As e-hailing service possesses the characteristic of pre-book, we assume once the vacant e-hailing supply has been assigned a passenger, this trip has began and the passenger will not cancel this order.

5.2 Evacuation Dynamics and Performance

5.2.1 Evacuation system dynamics

This section models a bi-modal transportation system with an aggregate approach, characterizing traffic dynamics in urban areas during rush-hour evacuations prompted by events like mass gatherings or metro disruptions. It simulates scenarios where numerous passengers are waiting to be evacuated from the demand surge region, each seeking to exit the evacuation system as soon as possible. Passengers' will make a mode choice between two available modes: e-hailing service (denote as r) and bus (denote as p). A three-dimensional vehicular MFD (3D-vMFD) relating the accumulation of e-hailing vehicles and buses is adopted to depict vehicle dynamics with mixed traffic. The mean speed of the e-hailing vehicles, v_r, is expressed as a linear function of the accumulation of e-hailing vehicles, n_r, the accumulation of buses, n_p as follows,

$$v_r\left(n_r, n_p\right) = \beta_{r,0} + \beta_{r,r} \cdot n_r + \beta_{p,r} \cdot n_p. \tag{5.1}$$

where the constant $\beta_{r,0}$ in the Eq.(5.1) corresponds to the free-flow speed of the e-hailing vehicles. The coefficients $\beta_{r,r}$ and $\beta_{p,r}$ represent the marginal effect of e-hailing vehicle and bus on the e-hailing vehicle's mean speed, i.e. , the amount by which the free flow speed of the e-hailing vehicle is reduced by adding a vehicle of each mode. Similarly, the speed of buses is defined as:

$$v_p\left(n_r, n_p\right) = \beta_{p,0} + \beta_{r,p} \cdot n_r + \beta_{p,p} \cdot n_p, \tag{5.2}$$

where the constant $\beta_{p,0}$ in the Eq.(5.2) corresponds to the free-flow speed of the buses. The coefficients $\beta_{r,p}$ and $\beta_{p,p}$ represent the marginal effect of each mode on bus mean speed.

It should be admitted that the demand-surge area is generally not homogeneously congested. As all vehicles will change their direction from driving in to leaving the area after passengers get on-board, we divide the system into two directions. Therefore we define $v^{in}(t)$ and $v^{out}(t)$ as the space mean speed in in-direction and out-direction at time t, where the relationship between vehicle speed and vehicle accumulation in both two directions, for both modes, will also follow the 3D-MFD relationship stated above. To investigated the vehicle evacuation dynamics, we model a dynamic system using trip-based MFD model. The adoption of trip-based MFD model makes the vehicle follow first-in-first-board and first-in-first-out assumptions, enabling us to trace the dynamic traffic conditions.

We describe the entire evacuation process starting from the process of vehicles entering the region. We define $v_r^{in}(t)$ and $v_p^{in}(t)$ as the driving speed of e-hailing vehicles and bus in in-direction at time t. From the perspective of vehicular dynamics, it drives in in-direction with the 'dispatched' state to pick up passengers. Therefore we use d to represent this dispatched state. Then the driving times for both modes at dispatched state starting at time t, i.e., $t_r^d(t)$ and $t_p^d(t)$, should satisfy the following conditions:

$$\int_t^{t+t_r^d(t)} v_r^{in}(s)ds = l_r^d, \tag{5.3}$$

$$\int_t^{t+t_p^d(t)} v_p^{in}(s)ds = l_p^d, \tag{5.4}$$

where l_r^d and l_p^d denote the average distance for vehicles' dispatched state, which starts from inflowing this area to arriving the passenger boarding area.

Following process is passengers' boarding process (e-hailing passenger offline meeting and bus passenger loading process), which we use b to represent. The e-hailing boarding process can be divided into two processes, which are (1) e-hailing driver waiting for parking ($b1$) and (2) parked to wait passengers ($b2$). The respective boarding times for both modes at time t are represented as $t_r^{b1}(t)$ and $t_r^{b2}(t)$, and the sum of which equal $t_r^b(t)$. In terms of bus, its boarding process is also divided into two processes, which are (1) waiting for parking and (2) passenger loading and unloading. Similarly, we use $b1, b2$ to represent the corresponding process. The respective times at time t are represented as $t_p^{b1}(t)$ and $\tilde{t}_p^{b2}$, and the sum of which equals $t_p^b(t)$. To this end, the total boarding times for both modes $t_r^b(t)$ and $t_p^b(t)$ should be formulated as:

$$t_r^b(t) = t_r^{b1}(t) + t_r^{b2}(t), \tag{5.5}$$

$$t_p^b(t) = t_p^{b1}(t) + \tilde{t}_p^{b2}. \tag{5.6}$$

We assume that the passenger loading time is an increasing function of bus average loaded passenger number a_p, which is always the maximum passenger capacity under massive evacuations. As we consider a_p as a constant, $\tilde{t}_p^{b2}$ is a constant as well. The determinations of $t_p^{b1}(t)$, $t_r^{b1}(t)$ and $t_r^{b2}(t)$ will be elaborated specifically in the following.

The final process is vehicles' out-direction driving process. From the perspective of e-hailing vehicle, it drives in out-direction with the occupied state to transport the passenger out of the demand surge area. We define $v_r^{out}(t)$ and $v_p^{out}(t)$ as the driving speed of e-hailing vehicles

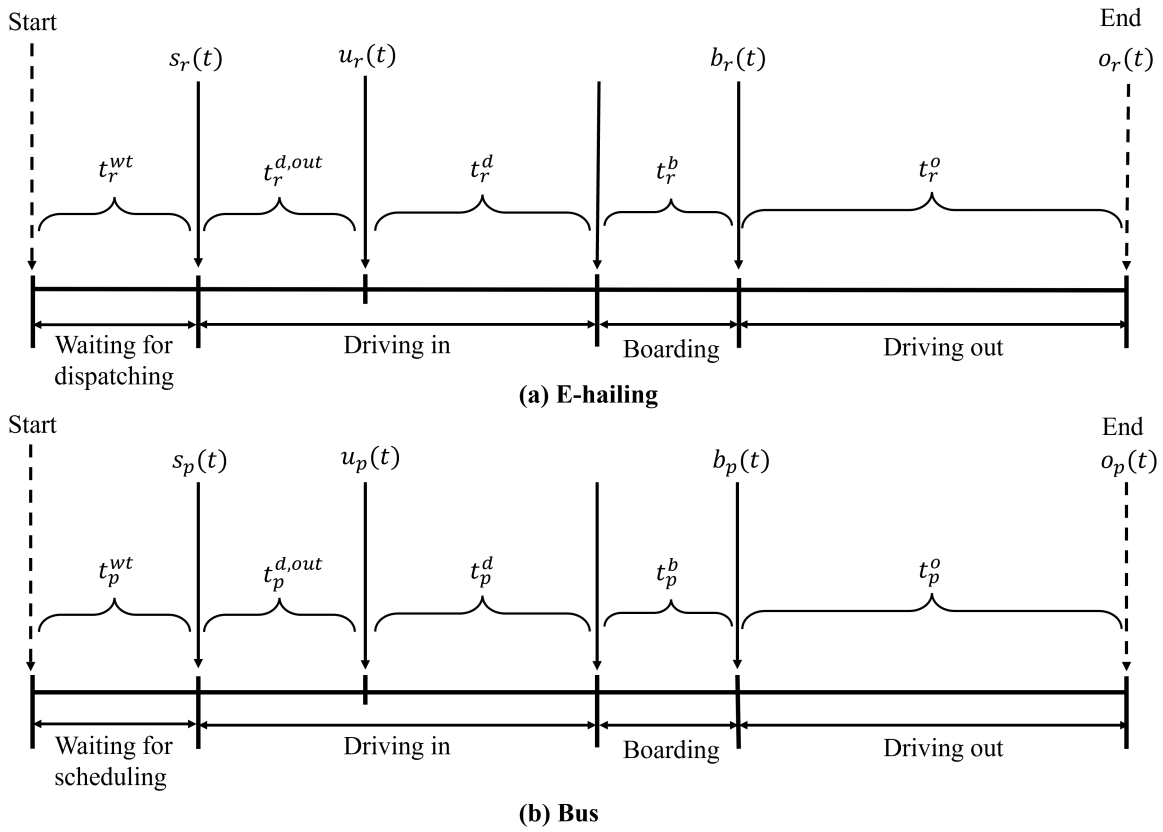

Figure 5.1 The trip duration of each type of vehicles within the transportation system.

and bus in out-direction at time t. From the same definition of like $t_r^d(t)$ and $t_p^d(t)$, we use o to represent this process and define $t_r^o(t)$ and $t_p^o(t)$ as the time it takes to drive an average distance l_r^o and l_p^o with passengers on-board to leave the area at time t. Based on which, $t_r^o(t)$ and $t_p^o(t)$ must satisfy the following conditions:

$$\int_{t+t_r^v(t)+t_r^b(t)}^{t+t_r^v(t)+t_r^b(t)+t_r^o(t)} v_r^{out}(s)ds = l_r^o, \tag{5.7}$$

$$\int_{t+t_p^v(t)+t_p^b(t)}^{t+t_p^v(t)+t_p^b(t)+t_p^o(t)} v_p^{out}(s)ds = l_p^o. \tag{5.8}$$

In summary, the vehicle states for both modes are categorized as: driving in, waiting to board, and driving out. The dynamic system meticulously tracks the state of each trip at every moment. Those three states for both two types of vehicles can be clearly represented in Figure 3.1. All of the e-hailing vehicles (or buses) that are in their drive-in process and follow the Eq.(5.3)(or Eq.(5.4)) at time t, will be cumulatively counted as the number $n_r^{in}(t)$(or $n_p^{in}(t)$); in their wait-to-board process and follow the Eq.(5.5)(or Eq.(5.6)) at time t, will be cumulatively counted as

the number $n_r^{wb}(t)$(or $n_p^{wb}(t)$); in their drive-out process and follow the Eq.(5.7)(or Eq.(5.8)) at time t, will be cumulatively counted as the number $n_r^{out}(t)$(or $n_p^{out}(t)$). To summarize, the total e-hailing vehicles $n_r(t)$ and bus number $n_p(t)$ within the demand surge area at time t can be formulated as:

$$n_r(t) = n_r^{in}(t) + n_r^{wb}(t) + n_r^{out}(t), \tag{5.9}$$

$$n_p(t) = n_p^{in}(t) + n_p^{wb}(t) + n_p^{out}(t). \tag{5.10}$$

Based on Eq. (5.9) (or Eq. (5.10)), we can replace the $n_r(t)$ (or $n_p(t)$) in Eq. (5.1) (or Eq. (5.2)) with $n_r^{in}(t)$ and $n_r^{out}(t)$ (or $n_p^{in}(t)$ and $n_p^{out}(t)$), to calculate the speed of e-hailing vehicles (or buses) in both in and out directions. We assume the wait-to-board vehicles generate negligible effect on the speeds in both in and out directions.

5.2.2 Evacuation performance

We assume extraneously given e-hailing and bus supply rates $s_r(t)$, $s_p(t)$, which is continuous to be provided to gradually deal with the passenger demand until it is sufficient to transport all passengers out of the region. As shown in Figure 5.1, given constant e-hailing and bus coming time on the way before getting into the demand surge area $\tilde{t}_r^{d,out}$ and $\tilde{t}_p^{d,out}$, we have the e-hailing vehicle and bus inflow rates $u_r(t)$ and $u_p(t)$ as follow,

$$u_r(t + \tilde{t}_r^{d,out}) = s_r(t), \tag{5.11}$$

$$u_p(t + \tilde{t}_p^{d,out}) = s_p(t). \tag{5.12}$$

Provided the two types of vehicle's in-direction driving time $t_r^d(t)$, $t_p^d(t)$, and parking and boarding time $t_r^b(t)$, $t_p^b(t)$, the e-hailing vehicle boarding rate $b_r(t)$ and bus boarding rate $b_p(t)$ can be formulated as:

$$b_r(t + \tilde{t}_r^{d,out} + t_r^d(t) + t_r^b(t)) = s_r(t), \tag{5.13}$$

$$b_p(t + \tilde{t}_p^{d,out} + t_p^d(t) + t_p^b(t)) = s_p(t). \tag{5.14}$$

Provided the on-the-trip time $t_r^o(t)$ and $t_p^o(t)$, the e-hailing and bus outflow rates $o_r(t)$ and $o_p(t)$ can be formulated as:

$$o_r(t + \tilde{t}_r^{d,out} + t_r^d(t) + t_r^b(t) + t_r^o(t)) = s_r(t), \tag{5.15}$$

$$o_p(t + \tilde{t}_p^{d,out} + t_p^d(t) + t_p^b(t) + t_p^o(t)) = s_p(t). \tag{5.16}$$

And then we use the outflow rates to denote the passenger evacuation efficiency. We denote a_r and a_p as the average number of on-board passenger per vehicle. Let $Q_{out}(t)$ be the cumulative number of passengers that have been transported out of the area at time t, then we have,

$$Q_{out}(t) = \int_0^t a_r \cdot o_r(s) + a_p \cdot o_p(s) ds. \tag{5.17}$$

We assume that a total number of Q passengers are accumulated and waiting for transportation at time $t = 0$. Accordingly, the total number of waiting passengers $n^{rm}(t)$ that haven't gotten on board at time t, should be given as:

$$n^{rm}(t) = Q - \int_0^t a_r \cdot b_r(s) + a_p \cdot b_p(s) ds. \tag{5.18}$$

Embedded into the dynamic traffic system, passengers will experience each process illustrated in Subsection 5.2.1 before leaving this demand surge area.

When all of Q passengers are evacuated from the demand surge region, the evacuation is considered to be completed. We also record the dynamic evolution of the traffic system during the entire evacuation process. Let T be the total time it takes for all passengers to be evacuated, then T satisfies:

$$Q_{out}(T) = Q. \tag{5.19}$$

As the waiting passengers gradually leaves the demand surge area and the whole evacuation is completed, the passenger number evacuated by both modes R_r and R_p will be finally decided by the total evacuation time T, can be formulated as:

$$R(T) = R(R_r(T), R_p(T)). \tag{5.20}$$

We denote $E_r(T)$ and $E_p(T)$ as the total number of e-hailing vehicles and bus scheduled for the evacuation under the total evacuation time T, which is determined by the simulation. Provided the average passenger number of per e-hailing vehicle a_r and per bus a_p, $E_r(T)$ and $E_p(T)$ should be formulated as:

$$E_r(T) = \frac{R_r(T)}{a_r}, \tag{5.21}$$

$$E_p(T) = \frac{R_p(T)}{a_p}. \tag{5.22}$$

5.3 Generalized Cost of the Bi-modal Transportation System

5.3.1 Users' cost

5.3.1.1 Passengers' mode choice and trip cost

The traffic performance affects traffic participants' decisions. The generalized cost of using both modes for traveling in the system is approximated on an aggregated level, which basically depends on the mode of transportation that users choose for their trips. In the above Subsection 5.2.1, we make a use of the MFD model to capture the effect on the average speed and the outflow of the system. We denote the each e-hailing trip as $N_r \in \{1, R_r(T)\}$ and each bus trip as $N_p \in \{1, R_p(T)\}$. Besides, we denote $t_r^{wt}(N_r)$ and $t_p^{wt}(N_p)$ as e-hailing passengers' waiting time for dispatching and bus passenger experienced headway. Based on the above stated variables, we can summarize the e-hailing and bus passengers' average travel time from the start to leaving the demand surge area of each trip N_r, N_p as:

$$t_r(N_r) = t_r^{wt}(N_r) + \tilde{t}_r^{d,out} + t_r^d(N_r) + t_r^b(N_r) + t_r^o(N_r), \tag{5.23}$$

$$t_p(N_p) = t_p^{wt}(N_p) + \tilde{t}_p^{d,out} + t_p^d(N_p) + t_p^b(N_p) + t_p^o(N_p). \tag{5.24}$$

In Eq. (5.23), the passengers' waiting time for dispatching $t_r^{wt}(t)$ is obtained by the demand and supply in the e-hailing market. We assume that once the e-hailing passenger has been assigned an driver, they will not change and quit mode choice process. We denote $d_r(t)$ as the e-hailing passenger demand rate at time t, which will be given in the following. Therefore the number of waiting passengers for e-hailing service who haven't been assigned an order at time t, can be formulated as:

$$n_r^{wt}(t) = \int_0^t a_r \cdot [d_r(s) - s_r(s)]ds. \tag{5.25}$$

We denote $n_p^{rm}(t)$ as the total remaining passenger number for bus at time t, which will be elaborated in the following. Given the average passenger number of per e-hailing vehicle a_r and per bus a_p, together with the vehicle supply rates, $s_r(t)$ and$s_p(t)$, the average expected waiting time for dispatching $t_r^{wt}(N_r)$ for passenger N_r and the average experienced headway $t_p^{wt}(N_p)$ for passenger N_p at time t, can be formulated as:

$$t_r^{wt}(N_r) = \frac{n_r^{wt}(t)}{2 \cdot a_r \cdot s_r(t)}, \tag{5.26}$$

$$t_p^{wt}(N_p) = \frac{n_p^{rm}(t)}{2 \cdot a_p \cdot s_p(t)}. \tag{5.27}$$

Based on the estimated time they will experienced in their trips as above, passengers evaluate their time-variant generalized cost to make a mode choice. This generalized cost is evaluated based on the sum of time cost (waiting time for vehicle coming, waiting time for getting on board, the in-vehicle travel time and so on), trip fare based on the on-trip time and discomfort cost. We let f_p denote the bus trip fare, θ_p as the discomfort cost of bus and f_r as the per unit time ride fare for trips. Let σ^{iv} denote the passenger's value of time of in-vehicle state, σ^{wt} denote the passengers' value of waiting time. Since travelers typically place a higher value on waiting time, we define σ^{wt} is greater than σ^{iv}. The e-hailing trip cost $c_r(N_r)$ of each trip N_r and bus trip cost $c_p(N_p)$ of each trip N_p, are respectively modeled as:

$$c_r(N_r) = (f_r + \sigma^{iv}) \cdot t_r^o(N_r) + \sigma^{wt} \cdot (t_r^{wt}(N_r) + \tilde{t}_r^{d,out} + t_r^d(N_r) + t_r^b(N_r)), \tag{5.28}$$

$$c_p(N_p) = f_p + \sigma^{iv} \cdot t_p^o(N_p) + \sigma^{wt} \cdot (t_p^{wt}(N_p) + \tilde{t}_p^{d,out} + t_p^d(N_p) + t_p^b(N_p)) + \theta_p. \tag{5.29}$$

Assuming a flexibility of mode choice for users, we utilize a logit model to allocate the overall travel demand between e-hailing vehicles and buses, relying on the average generalized cost (disutility) associated with each mode. We assume η as the dispersion parameter reflecting passengers' uncertainty towards the utility of choosing different modes of transportation. The passenger choosing probability for both modes at time t can be formulated as:

$$P_r(t) = \frac{exp\{-\eta \cdot c_r(t)\}}{exp\{-\eta \cdot c_r(t)\} + exp\{-\eta \cdot c_p(t)\}}, \tag{5.30}$$

$$P_p(t) = \frac{exp\{-\eta \cdot c_p(t)\}}{exp\{-\eta \cdot c_r(t)\} + exp\{-\eta \cdot c_p(t)\}}. \tag{5.31}$$

Then we proceed to model the passenger demand for both modes. Let $d(t)$ denote the exogenous total passenger demand rate at time t, which is highly relied on the total demand Q. We assume a total demand time series distribution function $D(t)$ with respect to time t, which discrete the total demand Q into different time moment as $d(t)$, i.e.,

$$d(t) = Q \cdot D(t). \tag{5.32}$$

Thereby the time varying passenger demand rates for both modes at time t can be formulated

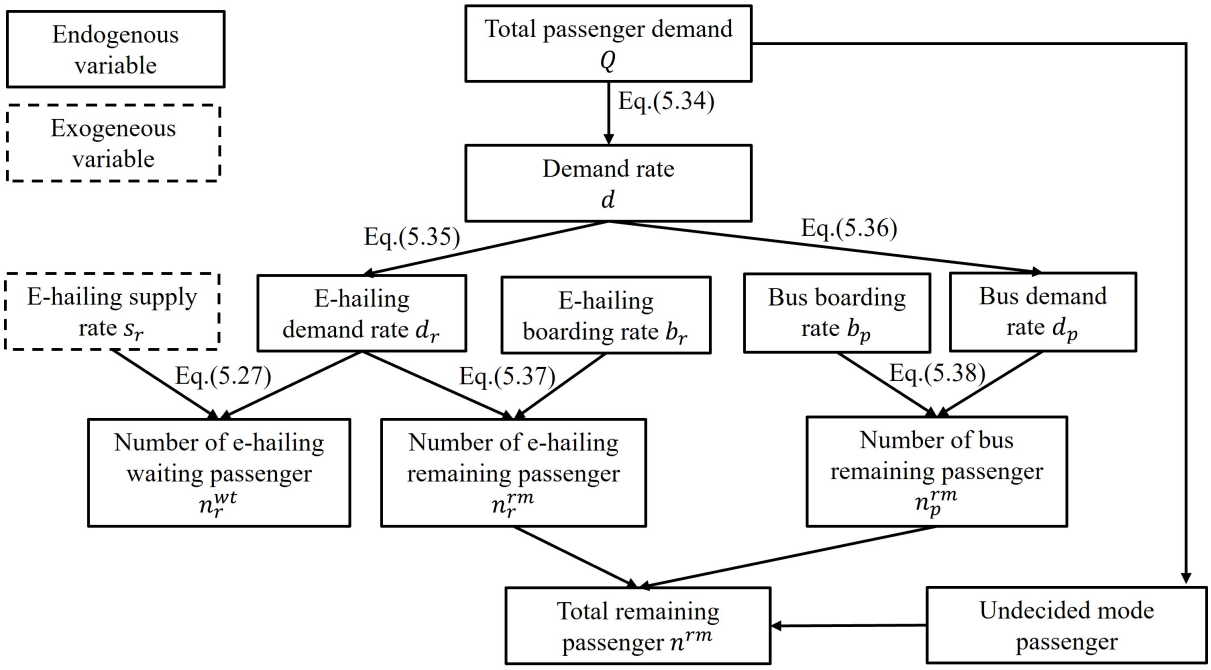

Figure 5.2 Passenger mode choice and remaining passenger update structure.

as:

$$d_r(t) = d(t) \cdot P_r(t), \tag{5.33}$$

$$d_p(t) = d(t) \cdot P_p(t), \tag{5.34}$$

where $d_r(t)$ and $d_p(t)$ are assumed to have included the newly join in passengers and exit waiting passengers.

Therefore the number of the remaining e-hailing/bus passenger in the market at time t can be formulated as:

$$n_r^{rm}(t) = \int_0^t a_r \cdot [d_r(s) - b_r(s)]ds, \tag{5.35}$$

$$n_p^{rm}(t) = \int_0^t a_r \cdot [d_p(s) - b_p(s)]ds. \tag{5.36}$$

It is important to note that except $n_r^{rm}(t)$ and $n_p^{rm}(t)$, there are still a portion of passengers in $n^{rm}(t)$ that haven't made the mode choice. In remaining e-hailing passengers, $n_r^{rm}(t)$, a proportion of them are waiting to be matched while the rest proportion have finalized their driver however they are still waiting in this system to wait to be picked up. This passenger mode choice and remaining passenger update structure can be clearly represented in Figure 5.2. As e-hailing service possesses the characteristic of pre-book, once the vacant e-hailing supply has been assigned a passenger, we can regard this trip has began. However bus doesn't own

this characteristic, only when bus passengers finish getting on board, we can regard this trip has began. From Eqs. (5.25) and (5.36), given an supply rates for e-hailing $s_r(t)$ and boarding rate for bus $b_p(t)$, the passengers will start their trips and the vehicles will start to participate within this system. When the total evacuation ends, the total travel costs for e-hailing passengers and bus passengers in this system, denoted as C_r and C_p, can be expressed as the total $R_r(T)$ and $R_p(T)$ trips' cost, respectively,

$$C_r = \sum_{N_r=1}^{R_r(T)} c_r(N_r), \tag{5.37}$$

$$C_p = \sum_{N_p=1}^{R_p(T)} c_p(N_p). \tag{5.38}$$

5.3.1.2 E-hailing platform's cost

Similar to other users (i.e. passengers) in the evacuation system, e-hailing platform contributes to overall system dynamics and travel costs. In this sense, e-hailing platforms can also be seen as users participating in evacuation systems, just like passengers. The total cost of e-hailing platforms (C_e) can be expressed as a summation $E_r(T)$ trips' cost. The cost for scheduling one e-hailing vehicles can be divided into two parts: (1) the average wage offered to the drivers per unit time c_r^w, and (2) the fixed scheduling cost c_r^s per unit time, including fuel cost, vehicle depreciation, and all other indirect costs happened during this service time period. Besides, the revenue (negative cost) from the fare collection is assumed to be f_r per unit time. All the costs are only counted when the e-hailing vehicle is in the occupied state. Therefore, the scheduling cost(/revenue) of each e-hailing trip $N_e \in \{1, E_r(T)\}$ can be expressed as follows:

$$c_e(N_e) = (c_r^w + c_r^s - f_r) \cdot t_r^o(N_e). \tag{5.39}$$

Therefore, the total scheduling cost(/revenue) of the evacuation can be expressed as total $E_r(T)$ trips' cost as follows:

$$C_e = \sum_{N_e=1}^{E_r(T)} c_e(N_e). \tag{5.40}$$

E-hailing passengers, bus passengers, and e-hailing platform are defined as the three participants in the transportation system, who together constitute the users of the transportation system. Therefore the total users' cost C_U includes e-hailing users' travel cost C_r, bus users'

travel cost C_p and e-hailing platform's cost C_e:

$$C_U = C_r + C_p + C_e. \tag{5.41}$$

5.3.2 Operating cost

Similar to the e-hailing platform, buses also facilitate the evacuation process by providing transportation services. However, buses are part of a public transportation system that is centrally controlled and managed by the transportation authority. Therefore, the total scheduling cost of buses are incorporated into the aggregated operating costs of the evacuation system. We assume that the transportation authority has the cost c_p^s once they schedule one bus to help evacuation, which includes the costs associated with total vehicle miles traveled, drivers' wage, fuel cost, vehicle depreciation, and all other indirect costs happened during this service time period. Assuming the fare collection from each bus passenger is f_p, the cost C_O^P of scheduling all $E_p(T)$ buses can be formulated as:

$$C_O^P = (c_p^s - f_p \cdot a_p) \cdot E_p(T). \tag{5.42}$$

In terms of road space management, normally, the space allocation decides service frequency, further decides the passengers accessibility and passenger ridership towards this service. This can further influence the driving speed or travel demand of this mode under steady-state. However, under the urgent case like massive evacuations, both of the allocation of road space and service supply rates are preset by the transport authority, which will not be affected the adaptable regulatory. Passengers make mode choice based on their time-variant perceived travel cost for sake of rapidly leaving this area. Therefore, we treat both space allocation and supply rate as exogenous. However, the road space management expense spent on arrangement and instruction should be considered, due to the higher requirement for rapid massive evacuation.

Unlike other existing studies that often focus on the allocation of roadway space for specific mode, the allocation of boarding space is more important in the case of massive evacuation. Because compared with driving on the roadway, such drop-off/pickup stays greatly affect the boarding efficiency of passengers, which further influence the evacuation performance. This road space management expense varies from traffic authority's decisions on how to set system's space allocation, which can be analytically approximated based on the configuration settings of the transportation system. We assume the management expense of per unit roadway space as

m_L, per unit bus boarding space as m_p and per unit e-hailing boarding space as m_r. Therefore the total road space management expense C_O^R can be expressed as:

$$C_O^R = m_L \cdot S_L + m_p \cdot S_p + y_r \cdot m_r \cdot S_r, \tag{5.43}$$

where S_L, S_p and S_r respectively denote the roadway space, bus boarding space and e-hailing boarding space within this transportation system. In this formula, y_r indicates whether or not the e-hailing boarding space is set. If it is set, $y_r = 1$. If not, $y_r = 0$. The specific road space management expense C_O^R will be elaborated in different settings in next section.

Therefore, both of bus scheduling cost C_O^P and road space management cost C_O^R together constitute the total operating cost C_O, i.e.,

$$C_O = C_O^P + C_O^R. \tag{5.44}$$

5.3.3 Safety cost

In this urgent situation after mass gathering events, we consider two types of safety cost that related to conflicts, which are pedestrian-vehicle conflicts and pedestrian-pedestrian conflicts.

5.3.3.1 Between pedestrians and vehicles

Waiting passengers must navigate through vehicles with the presence of e-hailing services, because they will navigate in different directions to locate their designated vehicles. A significant amount of research has been conducted to assess pedestrian safety during interactions with vehicles. We set two factors that collectively influence conflict risk as: average minimum distance (DS) and average relative speed (SP). The proposed two indicators focus on predicting critical traffic conflicts, based on the collective effect of selected safety indicators.

In a limited congested region, we define the vehicle and pedestrian conflicts will happen within roadway space S_L, which denotes the space occupied by routes in a transportation system, excluding areas designated for vehicle stopping or waiting. The likelihood of conflicts occurring when people move within an area depends more on the nearest vehicle, as conflicts can only occur when the distance between the pedestrian and the vehicle is close enough. To capture this local characteristic, we denote the average distance from each passenger to the nearest vehicle at time t as $DS_{v,p}(t)$, to estimate the probability of conflict occurrence:

$$DS_{v,p}(t) = \frac{1}{2}\sqrt{\frac{S_L}{n_r^{wb}(t)}} \tag{5.45}$$

where $n_r^w b(t)$ denotes the number of e-hailing vehicles that are slow-moving/parked on the road. We multiply $1/2$ as the empirical adjustment coefficient. Eq.(5.45) indicates that the average distance from each passenger to the nearest vehicle mainly depends on the sparsity of the vehicle distribution within roadway space, rather than the number of people.

We denote $v_r^{b1}(t)$ as the slow-moving speed of e-hailing vehicles at time t when they intend to find vacant parking spaces, which is of a discount of the in-direction driving speed at time t, i.e., $v_r^{b1}(t) = k_1 \cdot v_r^{in}(t)$. We denote $v_{v,p}^{wk}(t)$ as walking speed of pedestrians navigating through vehicles at time t. It is assumed that passengers' walking speed is decided by their perception of the distance with vehicles. When the distance is far, they may speed up their pace to walk as quickly as possible. When it is close, causing people a sense of oppression or anxiety, they may slow down and walk to ensure their own safety. The pedestrians' walking speed at time t can be formulated as: $v_{v,p}^{wk}(t) = k_2 \cdot DS_{v,p}(t)$, where k_2 represents the speed change corresponding to a unit distance, measured in seconds.

Under the assumption that both passengers and vehicles are evenly distributed and move independently and randomly, the estimation formula for the average relative speed is:

$$SP_{v,p}(t) = 0.85 \cdot \sqrt{\left(\mathrm{v}_r^{b1}(\mathrm{t})\right)^2 + \left(\mathrm{v}_{v,p}^{wk}(\mathrm{t})\right)^2} \tag{5.46}$$

Eq.(5.46) indicates that if people and cars are randomly and uniformly distributed in a two-dimensional area, and the direction of speed is independently and uniformly distributed on $[0, 2\pi]$, then the expected relative speed can be calculated using geometric relationships. The difference in direction (through angle difference) does not contribute to the average relative speed. However, in our research context, we assume the speed direction of people is evenly distributed at $[0, 2\pi]$ (as pedestrians have a very flexible direction of movement) and the speed direction of cars is evenly distributed at $[0, \pi]$ (as vehicles are prohibited driving in the opposite direction). Therefore, we multiply 0.85 as the empirical adjustment parameter.

The Logit model is widely used to calculate the probability of conflicts between people and vehicles, and is a common method in traffic safety analysis (Amini et al., 2022, 2024). The core idea is to predict the probability of an event occurring through a set of characteristic variables such as traffic flow, speed, distance, etc. Given the thresholds leading to conflicts as $DS_{v,p}^*$ and

$SP^*_{v,p}$, we define the probability of vehicle-pedestrian conflicts at time t as:

$$P_{v,p}(t) = \frac{1}{1 + \exp\left(-\left(\alpha_1 + \alpha_2 \cdot \frac{DS_{v,p}(t)}{DS^*_{v,p}} + \alpha_3 \cdot \frac{SP_{v,p}(t)}{SP^*_{v,p}}\right)\right)} \tag{5.47}$$

where α_1, α_2 and α_3 are all coefficients of the conflict probability function and estimated based on the related studies. The ratio form of various factors (such as $\frac{DS_{v,p}(t)}{DS^*_{v,p}}$ and $\frac{SP_{v,p}(t)}{SP^*_{v,p}}$)can be understood as quantifying the difference between the current state and the critical state. This means that if the current state is close to the threshold, the probability value will be greater; On the contrary, the probability is smaller. Eq. (5.47) measures the dynamic impact of traffic conditions on conflict probability.

To compute the expected safety cost caused by pedestrians-vehicle conflicts, we multiply this probability by the average cost of an event of pedestrian-vehicle conflict $\phi_{v,p}$. For passenger N_r, the safety cost of navigating through vehicles $c_S^{v,p}(N_r)$ at time t is formulated as follow:

$$c_S^{v,p}(N_r) = \phi_{v,p} \cdot P_{v,p}(t). \tag{5.48}$$

The total vehicle-pedestrian cost is the summation of the total $R_r(T)$ trips' cost, which is formulated as:

$$C_S^{v,p} = \sum_{N_r=1}^{R_r(T)} c_S^{v,p}(N_r). \tag{5.49}$$

5.3.3.2 Between pedestrians

In most urgent cases, pedestrians will tumble, push and squeeze within the crowds, besides interacting with automobiles. Similarly, we model the conflicts between pedestrians in a same way as pedestrian-vehicle conflicts, setting average minimum distance and average relative speed as the two factors influencing conflicts. The difference lies in classifying this pedestrian-pedestrian conflicts as two types: between e-hailing passengers and between bus passengers.

All of the pedestrian-pedestrian conflicts for e-hailing vehicles (or buses) will happen among the remaining passengers $n_r^{rm}(t)$ (or $n_p^{rm}(t)$) at time t. This occurs within its boarding space S_r (or S_p), which denotes the space for vehicles to park or wait. The average distances between remaining waiting passengers for both modes at time t are defined as:

$$DS^r_{p,p}(t) = \frac{1}{2}\sqrt{\frac{S_r}{n_r^{rm}(t)}}, \tag{5.50}$$

$$DS^{p}_{p,p}(t) = \frac{1}{2}\sqrt{\frac{S_p}{n^{rm}_p(t)}}. \tag{5.51}$$

We denote $SP^{r}_{p,p}(t)$ and $SP^{p}_{p,p}(t)$ as the relative speed between e-hailing and bus waiting passengers walking within the boarding space at time t, $v^{wk}_{p,p,r}(t)$ and $v^{wk}_{p,p,p}(t)$ as the walking speed of passengers moving through each other for e-hailing and bus at time t. The pedestrian walking speed is decided by their perception of the distance with other pedestrian. Therefore, walking speeds of e-hailing and bus passengers can be formulated as: $v^{wk}_{p,p,r}(t) = k \cdot DS^{r}_{p,p}(t)$ and $v^{wk}_{p,p,p}(t) = k \cdot DS^{p}_{p,p}(t)$, where k has the same meaning and value as in Subsection.5.3.3.1. Then the average relative speeds between e-hailing and bus waiting passengers at time t can be formulated as,

$$SP^{r}_{p,p}(t) = 0.85 \cdot v^{wk}_{p,p,r}(t), \tag{5.52}$$

$$SP^{p}_{p,p}(t) = 0.85 \cdot v^{wk}_{p,p,p}(t). \tag{5.53}$$

Same as above, by setting thresholds leading to conflicts $DS^{*}_{p,p}$ and $SP^{*}_{p,p}$, we define the probability of pedestrian-pedestrian conflicts at time t for both modes as:

$$P^{r}_{p,p}(t) = \frac{1}{1 + \exp\left(-\left(\alpha_1 + \alpha_2 \cdot \frac{DS^{r}_{p,p}(t)}{DS^{*}_{p,p}} + \alpha_3 \cdot \frac{SP^{r}_{p,p}(t)}{SP^{*}_{p,p}}\right)\right)} \tag{5.54}$$

$$P^{p}_{p,p}(t) = \frac{1}{1 + \exp\left(-\left(\alpha_1 + \alpha_2 \cdot \frac{DS^{p}_{p,p}(t)}{DS^{*}_{p,p}} + \alpha_3 \cdot \frac{SP^{p}_{p,p}(t)}{SP^{*}_{p,p}}\right)\right)} \tag{5.55}$$

To calculate the expected safety cost caused by pedestrians-pedestrian conflicts, we multiply the probability by the average cost of a event of pedestrian-pedestrian conflict $\phi_{p,p}$. Therefore, the safety costs of navigating through other pedestrians, $c^{p,p,r}_{S}(N_r)$ and $c^{p,p,p}_{S}(N_p)$, for each e-hailing/bus passenger N_r and N_p at time t are expressed as follow:

$$c^{p,p,r}_{S}(N_r) = \phi_{p,p} \cdot P^{r}_{p,p}(t), \tag{5.56}$$

$$c^{p,p,p}_{S}(N_p) = \phi_{p,p} \cdot P^{p}_{p,p}(t). \tag{5.57}$$

The total costs for pedestrian-pedestrian conflicts for e-hailing/bus mode, $C^{p,p,r}_{S}$ and $C^{p,p,p}_{S}$, are the summations of total $R_r(T)$ and $R_p(T)$ trips' cost, which can be formulated as:

$$C^{p,p,r}_{S} = \sum_{N_r=1}^{R_r(T)} c^{p,p,r}_{S}(N_r), \tag{5.58}$$

$$C_S^{p,p,p} = \sum_{N_p=1}^{R_p(T)} c_S^{p,p,p}(N_p). \tag{5.59}$$

Therefore the total safety cost, including vehicle-pedestrian conflict costs and pedestrian-pedestrian conflict costs, can be formulated as:

$$C_S = C_S^{v,p} + C_S^{p,p,r} + C_S^{p,p,p}, \tag{5.60}$$

where the first term and second term in the right side in Eq. (5.60) will be applied to e-hailing passengers and the third term is applied to bus passengers. This indicates that the availability of e-hailing will also bring more potential danger on pedestrians.

To summarize, the total generalized cost of the transportation system C, can be approximated as a combination of the users' cost C_U, operating cost C_O, and safety cost C_S as follows:

$$C = (1 - \beta_S) \cdot (C_U + C_O) + \beta_S \cdot C_S, \tag{5.61}$$

where β_S represent the relative importance of safety costs in the generalized cost function of transportation systems from the perspective of traffic managers. This is to emphasize the safety cost and enable it to be quantified. When designing a transportation system, it is crucial to strike a balance between the efficiency, economy, and safety concerns, and to minimize the overall generalized cost.

5.4 Boarding Space Design of the Bi-modal Transportation System

The effect of the vehicle-passenger offline boarding process greatly decides system's efficiency and performance. Considering the users' cost, operating cost and safety cost of the transportation system, we plan to adjust the space allocation among S_L, S_p and S_r to obtain an optimal design. We formulate the problem as four prevalent transportation system scenarios in an urban region, as shown in Figure 5.3. The difference between these four scenarios lies in the road space configuration. When characterizing the time cost in different scenarios, we specially model the two sub processes in the boarding process. Different parking space designs allow us to depict both modes' boarding time in detail.

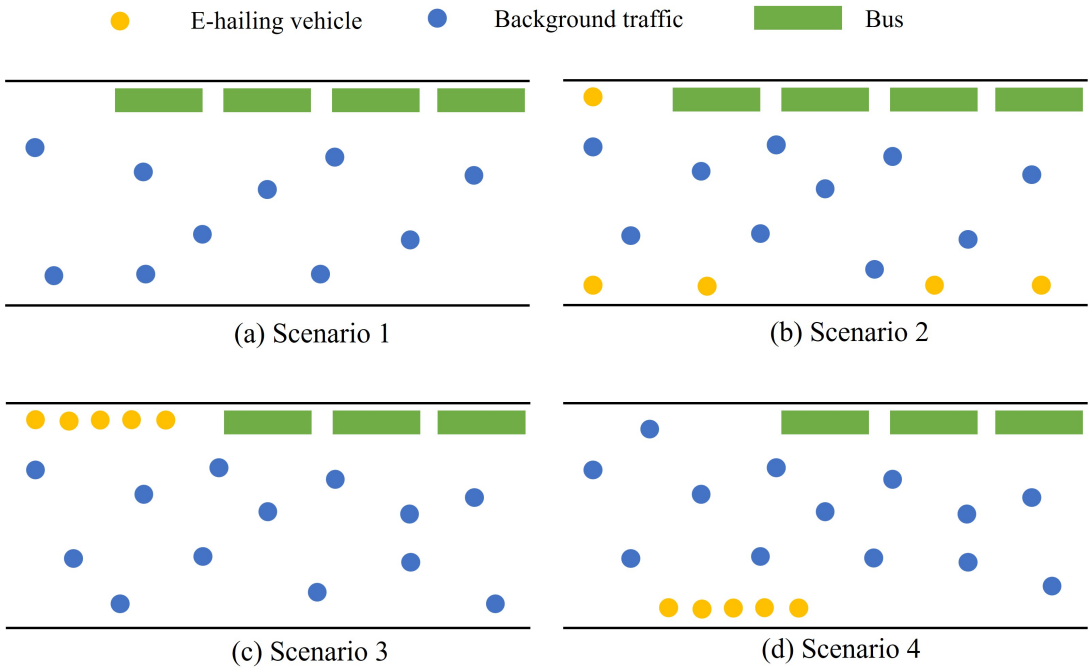

Figure 5.3 Boarding space configurations in four scenarios.

5.4.1 Scenario 1: only bus service

In Scenario 1, we consider the case where there is only bus service. Bus service serves as the only factor that affects the dynamics in the urban region and the modal split doesn't exist naturally. According to the infrastructure setting of the system, the bus parking capacity, which denotes the maximal bus number that allowed to be parked at the station, can be given as:

$$F_p^S = \frac{S_p}{L_p}, \tag{5.62}$$

where L_p denotes the length of per bus.

Provided the fixed bus loading and unloading time t_p^{b2} and the bus supply rate $s_p(t)$, the arrived bus number at bus station at time t can be given as:

$$F_p^A(t) = \left\lceil t_p^{b2} \cdot s_p(t) \right\rceil. \tag{5.63}$$

If the arrived bus number exceeds the bus parking capacity, bus passengers' perceived waiting time to park at time t is $\frac{1}{2} \cdot (F_p^A(t) - F_p^S) \cdot \tilde{t}_p^{b2}$. Otherwise, bus passengers' perceived waiting time to park at time t equals zero. Translated into notations, we have:

$$t_p^{b1}(t) = \begin{cases} \frac{1}{2} \cdot (F_p^A(t) - F_p^S) \cdot \tilde{t}_p^{b2} & \text{if } F_p^S(t) < F_p^A(t)\,; \\ 0 & \text{otherwise}\,. \end{cases} \tag{5.64}$$

The costs within this system are all related to bus. We denote the total road space in this region as S, which is composed with bus boarding space S_p^1 and roadway space S_L^1. Besides bus passengers' perceived cost and bus operating cost, the safety cost between bus passengers' conflicts $C_S^{p,p,p}$ can be decided by Eq. (5.59). The total road space management expense under Scenario 1 $C_{O,1}^R$ can be formulated as:

$$C_{O,1}^R = m_L \cdot S_L^1 + m_p \cdot S_p^1. \tag{5.65}$$

5.4.2 Scenario 2: both modes are available with no dedicated boarding space for e-hailing service

In Scenario 2, to account for the interaction between automobiles and transit vehicles in the mixed bi-modal system, both of e-hailing and bus service are available, and there is no dedicated boarding space of e-hailing service. E-hailing vehicles will use curbside spaces for parking. The determination of bus experienced waiting time to park follows Scenario 1. As e-hailing boarding space can't accurately figured out, we can refer to Subsection 3.1.1 in Chapter 3 for a comprehensive explanation to model the waiting time to park $t_r^{b1}(t)$ and parked time $t_r^{b2}(t)$. The parameter settings also follow Chapter 3. Therefore the e-hailing passengers' experienced boarding time can be given.

We denote the total road space in this region S is divided as bus boarding space S_p^2 and roadway space S_L^2. Besides passengers' perceived cost and operating cost for both modes, two types of safety cost, $C_S^{v,p}$ and $C_S^{p,p,p}$, exist and can be determined. Since we assume that there is no dedicated boarding space of e-hailing service, we consider that all waiting passengers are navigating through parked e-hailing vehicles to search for the reserved vehicle more quickly. Therefore we do not consider conflicts between e-hailing passengers and passengers. However, such vehicle-pedestrian conflicts can be more serious because larger and more dispersed parking areas can lead to more parked vehicles and more disordered pedestrian movements.

The total road space management expense under Scenario 2 can be formulated as:

$$C_{O,2}^R = m_L \cdot S_L^2 + m_p \cdot S_p^2. \tag{5.66}$$

5.4.3 Scenario 3: both modes are available with independent but co-located boarding spaces

In Scenario 3, we consider the case where both modes are available with independent but co-located boarding spaces in this evacuation system. This means boarding spaces of both modes are adjacent, which is consistent with real case. The determination of bus experienced waiting time to park will be the same as Scenario 1.

According to the infrastructure setting, the e-hailing parking capacity, which denotes the maximal number that allowed to be parked at the boarding space, can be given as:

$$F_r^S = \frac{S_r}{L_r}, \tag{5.67}$$

where L_r denotes the length of per e-hailing vehicle. Different from Scenario 2, the parked vehicle number should be limited by parking capacity.

Given the e-hailing vehicle supply rate $s_r(t)$, the arrived number of e-hailing vehicle at boarding space can be given as:

$$F_r^A(t) = \left\lceil t_r^{b2}(t) \cdot s_r(t) \right\rceil . \tag{5.68}$$

If there is no more available parking space, the e-hailing vehicle can't park and wait for passengers. If the arrived e-hailing vehicle number exceeds the e-hailing parking capacity, the vehicle parked time (/passengers' offline checking time) is the time of passenger checking F_r^S parked vehicles. Otherwise, the vehicle parked time at time t is the time of passenger checking $F_r^A(t)$ parked vehicles. Therefore, $t_r^{b2}(t)$ should be written as:

$$t_r^{b2}(t) = \begin{cases} \frac{1}{2} \cdot F_r^S \cdot t_{chk} & \text{if } F_r^S < F_r^A(t)\,; \\ \frac{1}{2} \cdot F_r^A(t) \cdot t_{chk} & \text{otherwise}\,. \end{cases} \tag{5.69}$$

If the arrived number of e-hailing vehicle exceeds the e-hailing parking capacity, passengers' perceived waiting time to park at time t is $\frac{1}{2} \cdot (F_r^A(t) - F_r^S) \cdot t_r^{b2}(t)$. Otherwise, passengers' perceived waiting time to park at time t equals zero. Translated into notations,

$$t_r^{b1}(t) = \begin{cases} \frac{1}{2} \cdot (F_r^A(t) - F_r^S) \cdot t_r^{b2}(t) & \text{if } F_r^S < F_r^A(t)\,; \\ 0 & \text{otherwise}\,. \end{cases} \tag{5.70}$$

The specifically set boarding area of e-hailing service can make the vehicle-passenger offline searching more orderly. Passengers' moving directions will be reduced, thereby the conflicts will be less. Passengers are protected from moving in different directions and they are no longer interferes with the flow of automobiles. The cost $C_S^{v,p}$ is eliminated. However, as the boarding space are shared by both modes, the waiting passengers for both modes are highly compacted and the danger of tumbling will increase. All of the remaining passengers will condense within the boarding space.

We denote the total road space in this region S is divided as bus boarding space S_p^3, e-hailing boarding space S_r^3 and roadway space S_L^3. We denote $v_{p,p}^{wk}(t)$ as walking speed of passengers move through each other for both modes at time t, which can be formulated as: $v_{p,p}^{wk}(t) = k \cdot DS_{p,p}(t)$. Similar with Subsection 5.3.3.2, we redefine the integrated average minimum distance and relative speed at time t as the following form:

$$DS_{p,p}(t) = \frac{1}{2}\sqrt{\frac{S_r^3 + S_p^3}{n^{rm}(t)}} \tag{5.71}$$

$$SP_{p,p}(t) = 0.85 \cdot v_{p,p}^{wk}(t). \tag{5.72}$$

The conflict probability at time t can be formulated as:

$$P_{p,p}(t) = \frac{1}{1 + \exp\left(-\left(\alpha_1 + \alpha_2 \cdot \frac{DS_{p,p}(t)}{DS_{p,p}^*} + \alpha_3 \cdot \frac{SP_{p,p}(t)}{SP_{p,p}^*}\right)\right)}. \tag{5.73}$$

Served as the only element of C_S and applied to all $N_{all} \in \{1, Q\}$ passengers, the cost $c_S^{p,p}(N_{all})$ is defined as:

$$c_S^{p,p}(N_{all}) = \phi_{p,p} \cdot P_{p,p}(t). \tag{5.74}$$

The total cost for pedestrian-pedestrian conflicts $C_S^{p,p}$ is the summation of total Q trips' cost as follows:

$$C_S^{p,p} = \sum_{N_{all}=1}^{Q} c_S^{p,p}(N_{all}). \tag{5.75}$$

The total road space management expense under Scenario 3 can be formulated as:

$$C_{O,3}^R = m_L \cdot S_L^3 + m_p \cdot S_p^3 + m_r \cdot S_r^3. \tag{5.76}$$

5.4.4 Scenario 4: both modes are available with independent and separated boarding spaces

In Scenario 4, we consider the case where both of e-hailing and bus service are available and with dedicated boarding space. E-hailing vehicles' boarding space is separated with bus station within this evacuation system. In this scenario, the waiting time to park and parked time for buses and e-hailing vehicles all follow the same modeling approach as in Scenario 3.

We denote the total road in this region S is divided as bus boarding space S_p^4, e-hailing boarding space S_r^4 and roadway space S_L^4. The vehicle-pedestrian cost $C_S^{v,p}$ doesn't exist in Scenario 4. Besides passengers' perceived cost and operating cost for both modes, both of the costs $C_S^{p,p,r}$ and $C_S^{p,p,p}$ can be separately given.

Furthermore, the total road space management expense under Scenario 4 can be formulated as:

$$C_{O,4}^R = m_L \cdot S_L^4 + m_p \cdot S_p^4 + m_r \cdot S_r^4. \tag{5.77}$$

5.4.5 Summary and comparison of four scenarios

To clearly illustrate the above four formulated scenarios, we compare and summarize their connections and differences. A comparison of cost elements in four scenarios is clearly presented in Table 5.1. Scenario 1 represents the simplest case with only buses present. Although Scenario 1 doesn't simulate a bi-modal system, it provides the a vivid comparison with the addition of the e-hailing mode. In Scenario 2, a basic framework is introduced where passengers have the option to choose between two available modes to leave this demand surge area. With the incorporation of e-hailing services, additional costs arise, including the e-hailing platform's cost and safety cost. Due to the interaction between pedestrians and vehicles in the e-hailing mode, two types of safety costs exist, which are pedestrian-pedestrian conflicts and pedestrian-vehicle conflicts. In Scenario 3, changes occur in certain components of passengers' perceived travel time due to the system configurations setting, such as e-hailing parked time and waiting time for parking e-hailing vehicles. Due to dedicated boarding space for both modes, only the risk of integrated pedestrian-pedestrian conflicts exists, while the risk of pedestrian-vehicle conflicts is eliminated. In Scenario 4, building upon the road space configurations of Scenario 3, a special setting creates separate pedestrian-pedestrian conflicts for both modes. Finally, the road space management expenses vary in different scenarios due to the different settings.

Table 5.1 Cost element comparison under four different scenarios.

Scenario	Bus service related costs		E-hailing service related costs		Safety costs		
	Users' cost	Operating cost	Users' cost	Operating cost	Vehicle passenger conflict	Bus passengers' conflict	E-hailing passengers' conflict
Scenario 1	✓	✓				✓	
Scenario 2	✓	✓	✓	✓	✓	✓	
Scenario 3	✓	✓	✓	✓			✓
Scenario 4	✓	✓	✓	✓		✓	✓

5.5 Numerical Experiments and Analysis

5.5.1 Numerical settings

The case study designates a bi-modal transportation system for massive evacuation regarding safety concerns. We first specify the functional forms and parameter values necessary for numerical experiments. The functional form between total demand Q and time discrete demand $D(t)$ follows a normal distribution. And the whole modeling duration is equal to 1 hour. The e-hailing vehicle and bus supply rates $s_r(t)$ and $s_p(t)$ start from 5th minute, keep at this level to 35th minute and finally drop back to 0. E-hailing vehicle and bus supply rates keep at 0.3 veh/s and 0.05 veh/s during the time period. Simulation is conducted in a virtual environment. The time point at which simulation data is generated from $t = 0$ till the fixed number of passengers has been completely evacuated. The additional setup of parameters for the 3D-MFD transportation system, the evacuation process, passengers' safety cost and in four scenarios are respectively summarized in Tables 5.2–5.5.

The rest of this section describes the experiment results, which is divided into two parts. Subsection 5.5.2 displays the variations of the transportation system's costs, considering different values for system's total demand and safety weight factor in four scenarios from the system's perspective. Subsection 5.5.3 demonstrates the variations of a trip's average cost, considering the same factors as above from the passengers' perspective. Subsection 5.5.4 provides discussions and policy implications.

Table 5.2 Parameters settings for the 3D-MFD transportation system

Parameter	Value	Unit
Free-flow speed of the e-hailing vehicles($\beta_{r,0}$)	11	m/s
Free-flow speed of the buses($\beta_{p,0}$)	8	m/s
Marginal effect of bus on the e-hailing vehicles mean speed($\beta_{p,r}$)	-0.014	
Marginal effect of bus on the bus mean speed($\beta_{p,p}$)	-0.0072	
Marginal effect of e-hailing vehicles on the bus mean speed($\beta_{r,p}$)	-2.07×10^{-4}	
Marginal effect of e-hailing vehicles on the e-hailing vehicles mean speed($\beta_{r,r}$)	-4.07×10^{-4}	
Average distance for e-hailing vehicles starting from inflowing this area to arriving the passenger boarding area(l_r^d)	500	m
Average distance for bus starting from inflowing this area to arriving the passenger boarding area(l_p^d)	500	m
Average distance for e-hailing vehicles starting from passenger boarding area to outflowing the area(l_r^o)	500	m
Average distance for bus starting from the passenger boarding area to outflowing the area(l_p^o)	500	m

Table 5.3 Parameters settings for the evacuation process

Parameter	Value	Unit
Average bus occupied passenger number(a_p)	50	person
Average e-hailing vehicle occupied passenger number(a_r)	1	person
E-hailing coming time on the way before getting into the demand surge area ($\tilde{t}_r^{d,out}$)	120	s
Bus coming time on the way before getting into the demand surge area ($\tilde{t}_p^{d,out}$)	180	s
Bus passenger loading time($\tilde{t}_p^{b2}$)	180	s
Passenger's value of time of in-vehicle state(σ^{iv})	20	¥/h
Passenger's value of time of waiting(σ^{wt})	30	¥/h
Mode choice parameter of the passengers (η)	-0.05	
Discomfort cost of taking bus(θ_p)	3	¥
Unit time fare for each e-hailing passenger (f_r)	100	¥/h
Fare for each bus passenger (f_p)	3	¥
Unit time wage offered to the e-hailing drivers (c_r^w)	80	¥/h
Unit time fixed scheduling cost of per e-hailing vehicle (c_r^s)	40	¥/h
Per bus scheduling cost (c_p^s)	200	¥

Note: ¥100 = $ 13.9

Table 5.4 Parameters settings for passengers' safety cost

Parameter	Value	Unit
Average cost of a event of pedestrian-vehicle conflict($\phi_{v,p}$)	1000	¥
Average cost of a event of pedestrians conflict($\phi_{p,p}$)	300	¥
Coefficient of the conflict probability function(α_1)	0.15	
Coefficient of the conflict probability function(α_2)	0.15	
Coefficient of the conflict probability function(α_3)	2	
Probability that the pedestrian and the vehicle are moving in the same direction($m_{v,p}$)	0.5	
Probability that the pedestrians are moving in the same direction($m_{p,p}$)	0.5	
Threshold of average distance in vehicle-pedestrian conflicts($DS^*_{v,p}$)	1.5	m
Threshold of conflict speed in vehicle-pedestrian conflicts($SP^*_{v,p}$)	1	m/s
Threshold of average distance in pedestrian-pedestrian conflicts($DS^*_{p,p}$)	1.5	m
Threshold of conflict speed in pedestrian-pedestrian conflicts($SP^*_{p,p}$)	1	m/s
Parameter in pedestrian walking speed function(k)	0.4	

Table 5.5 Parameters settings in four scenarios

Parameter	Value	Unit
Per unit of roadway space management expense (m_L)	20	¥/m^2
Per unit of bus boarding space management expense (m_p)	40	¥/m^2
Per unit of e-hailing boarding space management expense (m_r)	50	¥/m^2
Sampling time	60	s
Cruising for parking discount parameter(γ)	0.6	
Roadway space in Scenarios 1 and 2(S^1_L, S^2_L)	8850	m^2
Bus boarding space in Scenarios 1 and 2(S^1_p, S^2_p)	150	m^2
Roadway space in Scenarios 3 and 4(S^3_L, S^4_L)	8700	m^2
E-hailing boarding space in Scenarios 3 and 4(S^3_r, S^4_r)	300	m^2
Bus boarding space in Scenarios 3 and 4(S^3_p, S^4_p)	300	m^2
Length of each bus(L_p)	12	m
Length of each e-hailing vehicle(L_r)	5	m

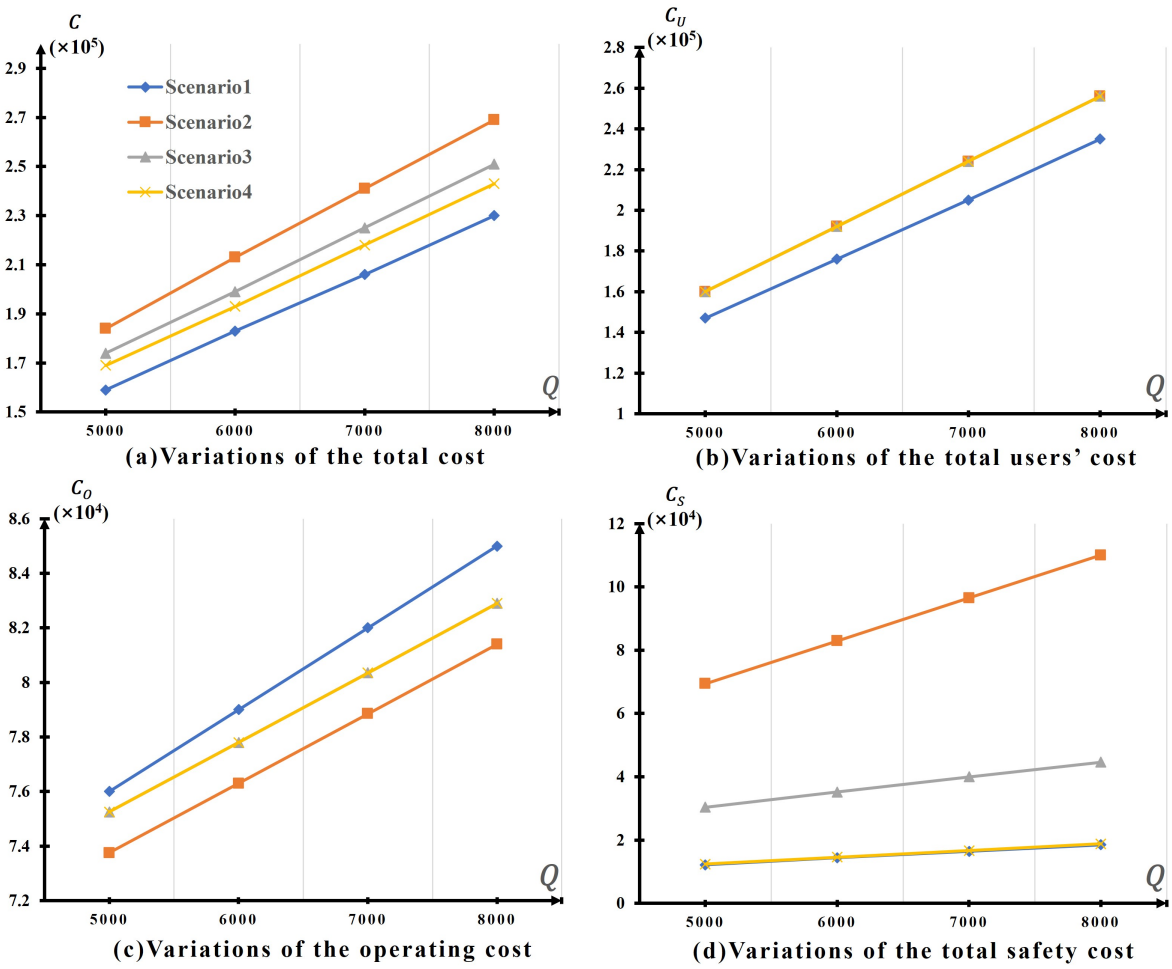

Figure 5.4 Variations of transportation system's costs considering different total passenger demand.

5.5.2 Variations of transportation system's cost

We conduct sensitivity analysis to illustrate the impact of total demand Q and safety weight factor β_S on a transportation system under four scenarios. Setting $\beta_S = 0.3$, we first explore the total demand ranging from 5000 to 8000 to observe the fluctuations in following variables, including (1) total user's cost; (2) operating cost; (3) safety cost and (4) total cost, as shown in Figure 5.4(a)–(d). Across all scenarios, these costs escalate with increasing demand. In Figure 5.4(a), total costs surge with demand, with Scenario 2 exhibiting the swiftest ascent, peaking at 2.69×10^5 when demand hits 8000. Subsequent rankings in cost escalation are Scenario 3, Scenario 4, and the lowest being Scenario 1. The minimal total cost can always be found in Scenario 4 under any level of total demand, except for Scenario 1 since it is not a bi-modal system. Figure 5.4(b) depicts total users' cost. Only Scenario 1 has a marginally lower value compared to the other three scenarios. Figure 5.4(c) highlights Scenario 1's highest operating cost, contrasting with Scenario 2, which boasts the lowest operating cost. Scenario 3 and 4 share identical operating costs. Across all four scenarios, total operating costs rise in the same trend with increasing demand. Regarding total safety costs illustrated in Figure 5.4(d), Scenario 2 has a notably higher safety cost than the others. As demand escalates from 5000 to 8000, its safety cost surges from 6.94×10^4 to 1.1×10^5. Scenario 3 follows, increasing from 3.04×10^4 to 4.46×10^4. Scenarios 1 and 4 exhibit negligible safety cost increases, underscoring system security robustness when facing passenger demand. Analyzing Figure 5.4, we observe Scenario 2 experiencing the highest and swiftest total cost escalation, primarily attributed to surging safety costs as the total demand increases. Combining Figures 5.4(c) and (d), it is reasonable to conclude this is due to lack of operating cost. In contrast, Scenario 1 prioritizes elevated operating costs for efficient and secure evacuation, resulting in lower safety cost and the lowest total cost. Comparing Scenarios 3 and 4, despite similar total users' cost and operating cost, Scenario 4 has lower safety cost and slower increasing speed with rising demand.

In our total cost function (5.61), we introduce β_S as a safety weight factor, enabling a balance between travel efficiency and safety as perceived by traffic regulators. This factor integrates travel time and safety components within the transportation system's cost function. We conduct additional experiments to assess safety's impact on overall cost across four scenarios and discern a safety-time trade-off. These experiments explore variations in the transportation system's total cost with different values of the safety weight factor, ranging from 0 to 0.45 to examine traffic regulators' emphasis on safety, under a constant passenger demand of 6000.

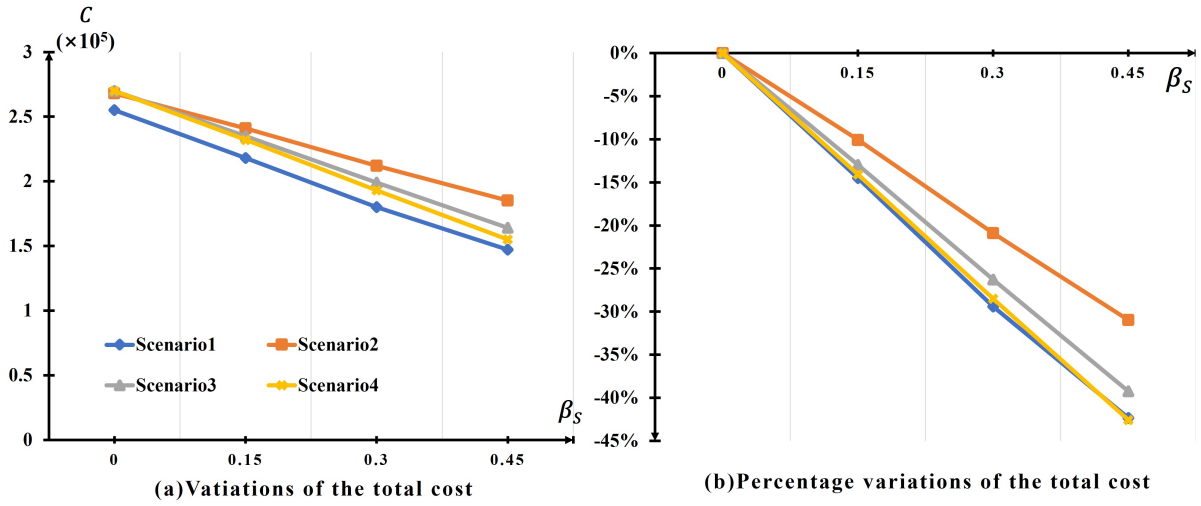

Figure 5.5 Variations of the transportation system's total cost considering β_S.

As depicted in Figure 5.5, increasing β_S reflects heightened safety awareness among traffic managers, leading to decreased total cost. Notably, in Figure 5.5(a), Scenario 1 exhibits the swiftest decrease, followed by Scenario 4, while Scenario 2 experiences the slowest reduction. Comparing percentage reductions in total cost relative to $\beta_S = 0$ in Figure 5.5(b), it's evident that at $\beta_S = 0.45$, Scenarios 1 and 4 demonstrate a 42% decrease, outperforming Scenario 2's 30% reduction. This underscores the effectiveness of Scenarios 1 and 4 in ensuring evacuation system safety.

We specifically compare scenarios with $\beta_S = 0$ and $\beta_S = 0.3$ to highlight the disparity between perceived ($\beta_S = 0$) and actual ($\beta_S = 0.3$) total cost across four scenarios. The setting $\beta_S = 0$ denotes safety receives negligible attention from traffic regulators. As depicted in Figure 5.6, Scenario 4 exhibits the most substantial reduction in total cost, while Scenario 2 sees the least reduction. The superiority of Scenario 4 should be underscored in reducing system's total cost, especially when safety considerations weigh heavily in regulators' decisions on transportation system design.

5.5.3 Variations of trip's average cost

While assessing the overall effectiveness of the evacuation from the transportation system's viewpoint is crucial, evaluating its utility from the passengers' perspective holds equal significance in crafting an efficient evacuation plan. Passenger perception primarily revolves around the experienced travel and safety costs throughout their evacuation journey, as these costs directly impact their experience. Passengers distinguish these costs differently based on their

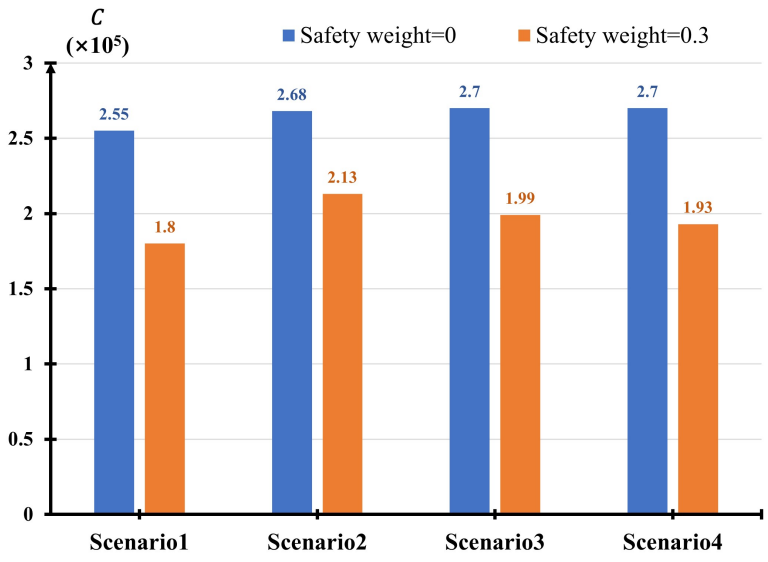

Figure 5.6 Comparisons of the perceived ($\beta_S = 0$) and actual ($\beta_S = 0.3$) transportation system's total costs.

mode of transportation. Similar to considering the total transportation system's cost, we introduce relative importance factors denoted by β_s to gauge safety cost perception. This factor combines travel time and safety considerations in the cost function representing an individual's evacuation trip. Consequently, we define two variables, c_r^A and c_p^A, representing the average perceived costs for each e-hailing and bus trip respectively, aiding in capturing passengers' actual experiences during evacuation. They can be given as:

$$c_r^A(N_r) = (1 - \beta_s) \cdot c_r(N_r) + \beta_s \cdot (c_S^{v,p}(N_r) + c_S^{p,p,r}(N_r)) \tag{5.78}$$

$$c_p^A(N_p) = (1 - \beta_s) \cdot c_p(N_p) + \beta_s \cdot c_S^{p,p,p}(N_p) \tag{5.79}$$

Unlike Eqs. (5.28) and (5.29) where passengers determine their mode choice, each passenger encounters two additional safety costs in the e-hailing mode and one additional safety cost in bus mode. Thus, the actual perceived cost differs from the expected cost during mode choice. Special cases should be noted that c_r^A doesn't exist in Scenario 1, $c_S^{p,p,r}(N_r)$ doesn't exist in Scenario 2. In Scenario 3, $c_S^{v,p}(N_r)$ does not exist whereas $c_S^{p,p}(N_{all})$ exists for all e-hailing and bus passengers. In Scenario 4, $c_S^{v,p}(N_r)$ doesn't exist whereas pedestrian-pedestrian conflicts exist for separate e-hailing and bus passengers. In Figure 5.7, we illustrate the variations in average trip cost for both bus and e-hailing modes across different total passenger demands from 5000 to 8000, with $\beta_s = 0.3$. In all scenarios, the average cost of per trip remains stable as total passenger demand increases, only spotting a slight decrease for bus with rising demand.

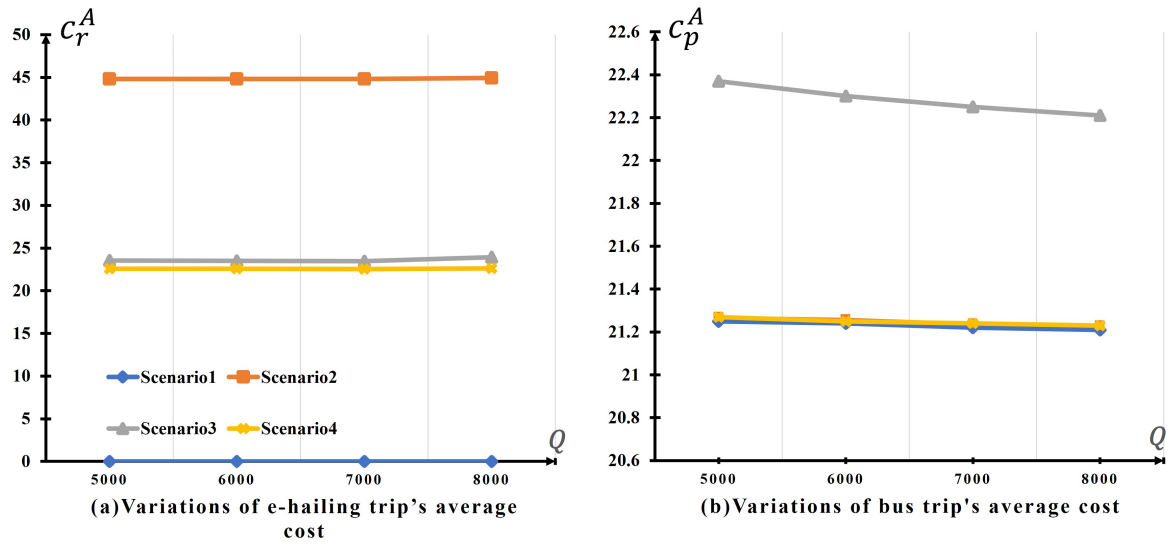

Figure 5.7 Variations of a trip's average cost for both modes considering different total passenger demand.

As depicted in Figure 5.7(a), the average cost per e-hailing trip in Scenarios 3 and 4, which implement separate infrastructure for passengers and vehicles, is notably lower than that in Scenario 2. This reduction is attributed to the significant decrease in passenger safety costs. Conversely, in Scenario 3, where e-hailing and bus stations are not separated, the average cost per bus trip, as shown in Figure 5.7(b), is higher due to increased safety risks. The average cost per bus trip in the other three scenarios remains relatively unchanged.

We conduct a supplementary series of experiments to explore the influence of safety on overall trip cost and seek a balance between safety and time. Figure 5.8 illustrates the fluctuation of trip average costs for both modes across various safety weight factors. Maintaining a constant total passenger demand of 6000, we vary β_s from 0 to 0.45 to examine passengers' safety awareness. The $\beta_s = 0$ case serves as a reference to depict the percentage change in trip average costs. As depicted in Figures 5.8(a) and (b), as β_s increases from 0 to 0.45, only Scenario 2 witnesses a surge in e-hailing trip average costs by over 60%. Conversely, both Scenario 3 and Scenario 4 experience a decline, with Scenario 4 showing the most notable decrease by over 40%. This underscores the significance of prioritizing passenger safety during evacuation. Passengers' trip cost will be significantly reduced with placing sufficient consideration on self safety issue during evacuation like Scenario 3 and 4. In Figures 5.8(c) and (d), regarding the average cost of bus trips, an increase in β_s correlates with a decrease in total average cost across the four scenarios. Notably, Scenario 3 exhibits the slowest decline at 35%, attributed to the heightened risk associated with the absence of distinct bus and e-hailing stations. The other

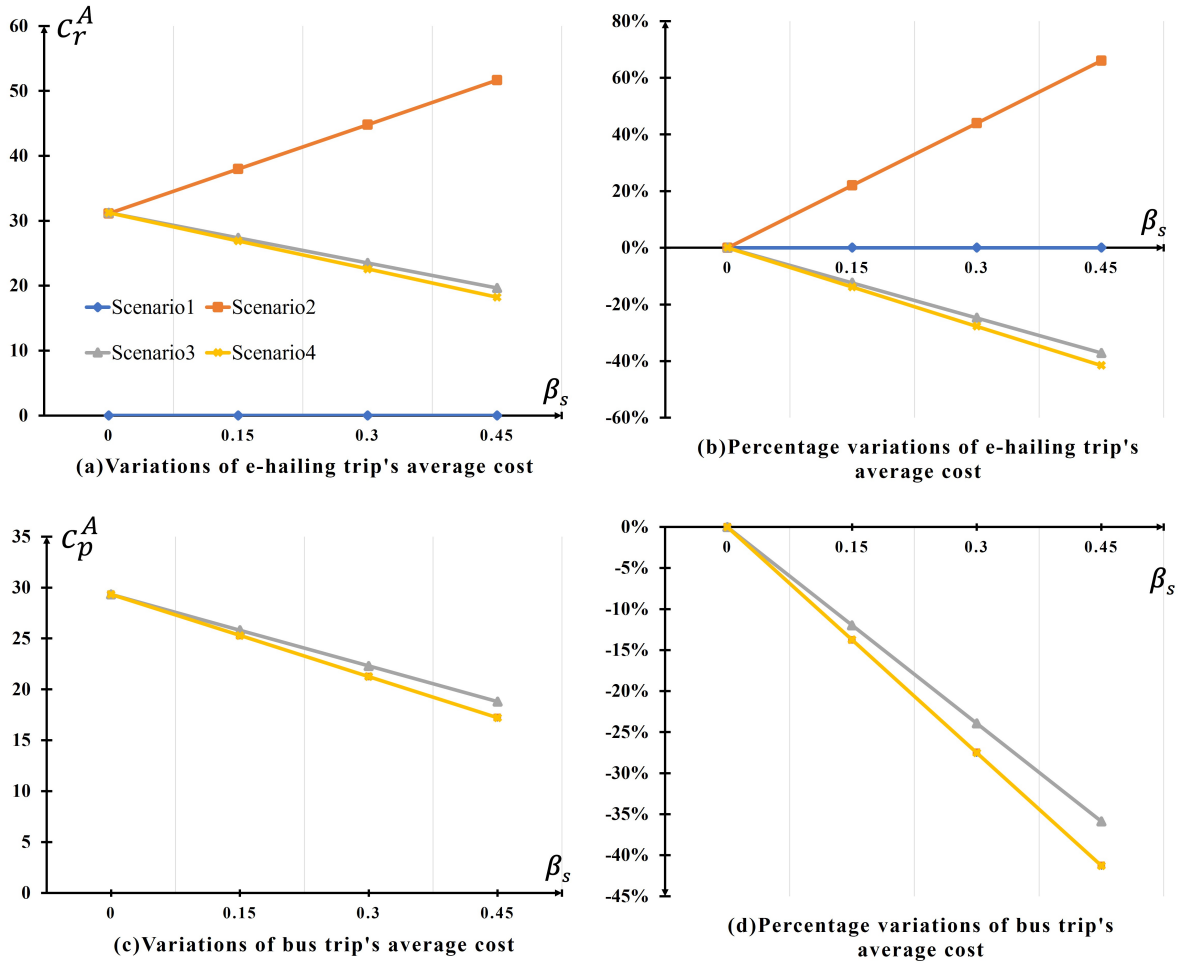

Figure 5.8 Variations of the trip's average cost for both modes considering different β_s.

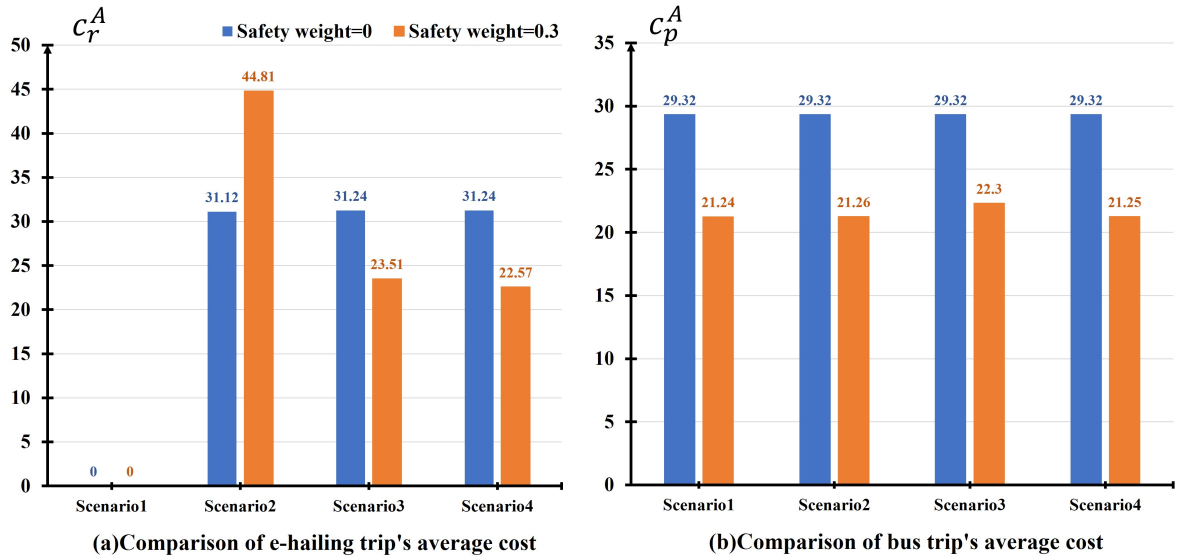

Figure 5.9 Comparisons of the perceived ($\beta_s = 0$) and actual ($\beta_s = 0.3$) trip's average costs for both modes.

three scenarios witness reductions of approximately 41%. This underscores the importance of safety-conscious measures, suggesting a greater necessity for protective transportation facilities when passengers have a stronger sense of safety.

To further illustrate the impact of considering safety costs, we compare the perceived costs $c_r(N_r)$ and $c_p(N_p)$ when $\beta_s = 0$ with the actual costs $c_r^A(N_r)$ and $c_p^A(N_p)$, when $\beta_s = 0.3$ for both modes across four scenarios. In Figure 5.9(a), the e-hailing trip's average cost notably increases from 31.12 to 44.81 in Scenario 2 as β_s rises from 0 to 0.3, highlighting a significant escalation. Conversely, in Scenario 4, the e-hailing trip's average cost decreases from 31.24 to 22.57 with the same increase in β_s, indicating a considerable reduction. As shown in Figure 5.9(b), the average cost of bus trips decreases across all four scenarios as β_s increases from 0 to 0.3. Among these, Scenario 3 exhibits the slowest decline, from 29.32 to 22.33, while the decrease in the other scenarios is more significant. These findings confirm the superiority of Scenario 4 in reducing trip average cost, which can apply to both e-hailing and bus mode.

In essence, while optimizing the transportation system reduces overall costs, its effects on passengers' average trip costs vary. Notably, Scenario 4 stands out for its ability to minimize both total and perceived trip costs, mainly by reducing safety cost. Through numerical experiments, its resilience to heightened passenger demand is evident. Thus, implementing suitable traffic infrastructures benefits both pedestrians and vehicles, ensuring smooth and safe operations of bi-modal transportation systems during emergencies. Considering the impact of total

demand and safety weight factors, four scenarios are compared from the perspective of total system cost and passenger perceived cost. However, other factors need to be considered in practical applications, such as passenger preferences, vehicle supply rates, number of passengers per vehicle, unit time cost, road system configuration, etc. These factors may generate variations in different contexts. In addition to system costs and passengers' trip costs, other costs need to be considered as well in reality, such as environmental costs and costs related to social equity.

5.5.4 Discussions and policy implications

In densely populated urban areas, it is significant to optimize both public and private transportation services to ensure efficient traffic flow. Through the above analysis, we can conclude that Scenario 4 is the optimal boarding space design for rapid and safe evacuations among the four scenarios. In this scenario, e-hailing vehicles are specifically equipped with independent boarding spaces, which is consistent with the traditional taxi stands. They all follow the pattern of passengers queuing up to board, and drivers queuing up to pick up passengers. A distinct comparison can be given, where Scenario 2 represents the normal e-hailing service and Scenario 4 represents the traditional taxi service. In Figs 5.7–5.9, we display the monetary and safety costs that Scenario 2 and 4 bring to passengers under evacuations. Therefore from passengers' perspective, facing evacuations, Scenario 2 brings them a longer trip time especially for the longer offline boarding time, and an extra part of safety cost due to vehicle-pedestrian conflicts. Scenario 4 helps to shorten their offline boarding time and only brings them negligible safety cost due to pedestrians conflicts. The results confirm that, with people's increased safety awareness and greater total passenger demand, passengers will have a greater preference for Scenario 4's settings. The offline boarding pattern of e-hailing service under evacuations can follow the traditional taxi stand service, which shows a higher level of order and stability.

From the perspective of the design of boarding spaces in different modes of the entire transportation system, the applicability and generalizability of setting 'separate and independent boarding spaces for different transportation modes' in Scenario 4 can be confirmed by real practices in many countries or cities. For example:

(1) In Singapore, major public transportation transfer stations such as Changi Airport, Marina Bay, and the city center implement dedicated boarding and alighting areas: buses, taxis, and shared mobility vehicles have different boarding and alighting areas to avoid confusion.

Pedestrian paths are also planned to ensure a rational flow of passengers. The government stipulates the priority of vehicle types, with priority given to bus routes, followed by taxis, and limited time stops for shared travel vehicles.

(2) In London, there are separate boarding points for buses, taxis, and private vehicles located near major stations such as King's Cross. The subway entrance is separated from the bus stop, while providing seamless pedestrian access. The transportation department will use AI and CCTV technology to monitor the traffic flow in the boarding space in real time to prevent congestion.

Many other large cities such as Tokyo, Hong Kong, and New York have also followed this design concept, which confirms its ability to adapt to different urban transportation environments and needs, providing an efficient operational framework for high passenger flow situations.

The proposed boarding space layout decision for bus and e-hailing services is reasonable in theory, but in practice it is necessary to balance the needs of multiple stakeholders, especially in the coordination between e-hailing platforms and transportation departments. During peak passenger demand, e-hailing drivers aim to take as many trips as possible to maximize their earnings. As a result, they may be reluctant to follow the designated fixed parking spots and instead choose to stop closer to the passengers' location or in other non-designated areas to save time and increase pick-up efficiency. To address this issue, the transportation management department can take measures on both the platform and passenger sides. By collaborating with e-hailing platforms, financial subsidies can incentivize platforms to better align with transportation policies, encouraging them to implement stricter measures to guide drivers in following the rules. On the passenger side, guidance and incentives can be introduced. Passengers can be directed to fixed pick-up points for boarding and drop-off, with clear prompts in the application. If passengers comply with the rules, they can be rewarded with points or vouchers, reducing violations caused by passenger behavior.

5.6 Concluding Remarks

To balance efficiency, economy, and safety concerns, this study conducts boarding space design in a bi-modal transportation system for massive gathering events, when both of bus and e-hailing service are available. Using MFD-representations, we aggregately assess the generalized cost of this transportation system by modelling the evacuation system dynamics and performance. Besides users' cost and operating cost, we innovatively introduce a safety im-

portance factor and incorporate the safety cost into the total cost. We specifically address two common safety concerns that frequently occurs in real scenarios, which are pedestrian-vehicle conflicts and pedestrian-pedestrian conflicts. To obtain the design with the minimal total cost, we compare and analyze four key scenarios with different boarding space configurations in the transportation system, employing a numerical illustration for comparison. Simulations indicate that from transportation system's perspective, a lack of operating cost can lead to higher safety costs. However, by placing sufficient emphasis on overall safety during evacuation, the total cost can be effectively reduced. Implementing suitable infrastructure to segregate vehicles and pedestrians, along with establishing dedicated stations for different transportation modes, can notably reduce both safety and total costs. Secondly, from a passenger's perspective, improved protective traffic infrastructure can lower trip costs, especially when passengers prioritize personal safety. The implementation of suitable traffic infrastructures benefits both pedestrians and vehicles, ensuring the effective operation of a bi-modal transportation system during urgent events. Thirdly, this study explores the additional complexity brought by e-hailing service, particularly regarding the heightened risk of pedestrian incidents. The monetary and safety costs that e-hailing service brings to passengers are quantified in face of a surge in demand. The design with minimal total cost of this bi-modal transportation system is found, where both modes are available with independent boarding space. It helps transportation system planners to have a clear understanding towards the impact of boarding space design on system's performance. We also discuss the insights of e-hailing offline boarding pattern under evacuations and provide some policy implications. These insights offer valuable guidance to optimize overall system efficiency for coordinating with large-scale evacuation events. The potential lies in that traffic management strategies can be integrated for urban planning and design purposes.

CHAPTER 6 CONCLUSIONS AND RECOMMENDATIONS

In this chapter, a detailed overview of the outcomes outlined in this thesis is first provided (Section 6.1). Then the recommendation for future studies is presented (Section 6.2).

6.1 Overview and Research Contributions

The thesis addresses three problems of e-hailing service's application under demand surge after mass gathering events: the e-hailing vehicles' control problem within a single-region transportation system considering e-hailing service's impact on traffic conditions, the e-hailing service's pricing problem within a two-region transportation system taking into account traffic flow dynamics modelling and e-hailing market's bilateral dynamics, and the boarding space design problem within a bi-modal evacuation transportation system.

Chapter 3 tackles the passenger evacuation process modelling and vehicle control problem. Firstly, it introduces a model to investigate and uncover the impacts of e-hailing services on urban traffic in a unique scenario where a substantial number of passengers await pick-up within a confined area following a mass-gathering event. Notably, this work is the first to address the prolonged offline passenger-driver searching time inherent to this specific scenario, incorporating the dynamic offline passenger-driver searching process. Secondly, the proposed model in this chapter captures the dynamics of passenger evacuation in a bi-modal system, illustrating the double-edged effects of e-hailing services on evacuation efficiency. The simulation results derived from this model contribute to a deeper understanding of how e-hailing vehicles influence passenger evacuation efficiency during demand-surge events. Thirdly, building upon the dynamic model, this chapter proposes two feedback based perimeter control strategies that control the total inflow rate of e-hailing vehicles and background traffic based on the vehicle accumulation and the number of parked vehicles within the area respectively. The effectiveness of these two strategies are demonstrated through simulations. Importantly, these controllers can effectively improve the evacuation efficiency in the presence of e-hailing vehicles, as well as being practical and straightforward to implement in real-world scenarios, providing a valuable tool for traffic regulators to expedite the passenger evacuation process after mass-gathering events.

Chapter 4 makes an extension for the study in Chapter 3 such that a two-region model is considered. Firstly, this study introduces an enhanced response framework tailored for traffic

regulators and e-hailing platforms facing sudden large traffic flows. To account for the impact of the demand surge region on the normal region, we propose a mathematical model that portrays the time-varying evolution of e-hailing vehicles within a two-region transportation system, adopting a trip-based approach. This model effectively captures the time-dependent transitions between trip phases and the interactions between both regions. Secondly, this study uses dynamic traffic flow modeling of the transportation system to describe the time-varying dynamics of demand and supply for e-hailing services. This involves modeling the decisions of drivers regarding repositioning and the dynamics of passengers' demand. These elements contribute to estimating the number of passengers waiting for e-hailing services and the availability of vacant e-hailing vehicles during demand surge scenarios. This information is instrumental in regulating dispatching rates in both regions. Thirdly, this study proposes an adaptive region-dependent driver wage mechanism and a vehicle dispatching strategy. This strategic approach optimizes the distribution of e-hailing vehicle supply, enhancing passenger evacuation efficiency in the demand surge region while maintaining a satisfactory service level in the normal region. Positioned as a leader, the e-hailing service providers guide drivers' and passengers' behaviors in the market. We assess our proposed model and region-dependent pricing strategy across varying levels of passenger demand and vehicle supply, scrutinizing traffic performance and e-hailing service quality. This thorough investigation explores how diverse arrivals of passengers and drivers influence both traffic conditions and bilateral dynamics within the e-hailing service market. These factors collectively impact the overall evacuation efficiency of the system. The simulation results affirm the efficacy of our proposed region-dependent pricing strategies in minimizing evacuation time in the demand surge region and ensuring service quality in both regions. This offers valuable insights for formulating pricing and scheduling strategies during demand-surge events.

Chapter 5 deals with the design of boarding space in a bi-modal evacuation system. Firstly, based on a non-equilibrium model, we characterize the spatiotemporal dynamics and stochastic variability in a transportation systems. In the context of the sudden high passenger flow, a transportation system design based on a non-equilibrium model is more suitable for making short-term responses and adjustments facing special events, while time-invariant static equilibrium models are not capable of analyzing such policies. Secondly, our contribution lies in designing an optimized boarding space in a transportation system that integrates both e-hailing and bus services as a bi-modal system. This integration involves analyzing the operational

and financial characteristics of different modes to design and plan a comprehensive transportation system. Under our setting of passenger demand surge, we consider boarding space design of different modes in the transportation system. We especially aim to take the effect of this vehicle-passenger offline boarding process into consideration, because this critical process plays an important part in deciding the transportation system's efficiency and transportation modes' performance. The primary objective during such a massive evacuation is to efficiently and safely move the large passenger flow out of the demand surge region. This can facilitate the synergistic operation of various transportation modes, offering a more inclusive range of transportation choices. Thirdly, we emphasize the risks of accidents and casualties resulting from pedestrian accumulation under expeditious passenger evacuation. Previously, the risk of accidents and casualties due to pedestrian congestion was a key motivator for quick passenger evacuation. Exploring how e-hailing services increase the risk of crowd disasters is a compelling research topic that warrants further investigation. In the case of evacuation after mass gathering events, pedestrian movements could be more complicated and disordered, potentially leading to increasing danger. What's more, the availability of e-hailing services introduces new risks. Therefore, when designing systems for mass gathering events, decisions should prioritize not only efficiency but also safety. Our innovative approach incorporates safety costs into the overall utility assessment of the evacuation system, introducing a safety importance factor to address pedestrian-vehicle conflicts in crowd disasters. In summary, this study helps transportation system planners to have a clear understanding towards the impact of boarding space design on system's performance during demand-surge events, which presents a compelling and meaningful avenue for exploration.

The three chapters investigated in the thesis help e-hailing platforms and traffic authorities address the decision-making challenges caused by demand surge after mass gathering events.

6.2 Recommendations for Future Studies

In this section, several possible future research directions are highlighted. Several research directions related to the limitations of the three chapters can be investigated in future studies.

(1) Research directions concerning the common limitations of the investigated studies

First, all of the three studies investigate the traffic dynamics under the assumption that the relationship between the accumulation and speed of vehicles in a region follows a well-defined MFD relationship. Changes in the proportion of vehicle types caused by different types of ve-

hicles do not undermine the assumption of uniformity in traffic conditions, thus not causing significant changes in MFD shape. Future research can relax these assumptions to be more realistic and adapt to complex system conditions and nonlinear dynamic evolution. Secondly, the data from simulation examples were used in the research, but there is a lack of validation in actual scenarios. The next step can be to conduct on-site verification research in real scenarios, such as collaborating with transportation operators to pilot the scheduling of large passenger flow events. Exploring new sources of data, such as mobile location data and big data from e-hailing platforms, is also a meaningful attempt. Subsequent research can apply more comprehensive datasets or combine multiple data sources to improve the accuracy and robustness of model predictions, providing basic support for field research. Thirdly, the model or method proposed in our research is effective in small-scale testing, but difficult to scale in large-scale networks or complex scenarios. Therefore, subsequent research can develop new methods to make them applicable to complex optimization problems in large-scale multimodal networks.

(2) Research directions regarding the specific limitations of the investigated studies

For the study in Chapter 3, we modelled the e-hailing passenger-driver offline meeting time based on artificial assumptions about the driver parking and passenger searching process. In reality, these assumptions may or may not hold true. To establish a genuine relationship between bilateral searching time and the number of (online-matched) passenger-driver pairs within an area with dense traffic and populations, further experiments and/or simulation studies should be conducted.

For the study in Chapter 4, this study proposed a region-based driver wage scheme designed to improve evacuation efficiency within the region while ensuring normal service levels outside the region during demand surges. This innovative approach paves the way for future research to explore flexible passenger pricing mechanisms in e-hailing services, such as time-based or distance-based pricing. Additionally, examining the relationship between these pricing mechanisms and driver compensation will be crucial for adapting e-hailing services to varying market demands and supply conditions. Future studies could investigate the impact of dynamic pricing and compensation mechanisms on service quality and system efficiency, building directly on the insights provided by this chapter.

For the study in Chapter 5, we primarily focused on e-hailing and buses as the main modes of transportation in a bi-modal system, traditional taxis also play a crucial role in passenger evacuation. Incorporating traditional taxi services into the model and comparing them with

smartphone-based e-hailing applications in terms of pricing, pickup patterns, and wait times could yield valuable insights. This comparison could help in understanding the complementarities and trade-offs between different modes of transportation.

(3) Research directions reflected in the literature review

Firstly, almost all the existing studies in the field of emergency traffic evacuation focus on modeling and control, and have not yet systematically explored the dynamic characteristics of passenger behavior from a social psychological perspective. One of the next possible major research directions would be the combination of traffic dynamics with the social effects, which would induce more decision-making regarding group influence on evacuation choices, real-time information dissemination, and collective behavior patterns under stress. Such efforts could lead to the development of more robust, adaptive, and human-centered evacuation frameworks for large-scale emergencies.

Secondly, a promising future research direction lies in the study of coordinated dispatching strategies for multimodal transportation systems during large passenger flow events. Specifically, the integration of public transportation and ride-hailing services presents significant potential for enhancing evacuation efficiency. For example, bus services can be utilized to transport passengers from densely populated event areas to designated transfer hubs, where ride-hailing services can then be deployed to provide flexible and distributed onward transportation. Such a hierarchical approach requires in-depth investigation into the dynamic allocation of resources, optimization of transfer hub locations, and real-time scheduling algorithms that account for passenger demand variability, traffic conditions, and service capacity limitations.

Last but not the least, for the road priority problem, little attention has been paid on the dynamic allocation of for different vehicle types during large passenger flow events. Prioritizing vehicles such as buses, e-hailing services, and emergency vehicles based on occupancy rates, service roles, and demand patterns could significantly enhance evacuation efficiency. This research would focus on optimizing road space allocation through real-time control algorithms and balancing trade-offs between efficiency, fairness, and user satisfaction. Such efforts could provide a foundation for developing adaptive and equitable traffic management strategies tailored to multimodal evacuation scenarios.

APPENDIX A NOTATIONS FOR CHAPTER 3

Q	Total number of passengers
u_p	Arrival rate of bus
u_r	Arrival rate of e-hailing vehicle
u_b	Arrival rate of background traffic
C_{max}	Maximum boundary capacity
l_r^v	The average driving distances of e-hailing vehicles in vacant state
l_p^v	The average driving distances of buses in vacant state
l_r^o	The average driving distances of e-hailing vehicles in occupied state
l_p^o	The average driving distances of buses in occupied state
l_b	The average travelling distance of background traffic
θ	Trip proportion of background trips
N^{pk}	Total number of curbside parking spaces within the area
n_r^{pk}	The number of parked e-hailing vehicles
q	Probability of success in each trial
l_r^c	E-hailing vehicle cruising for parking distance
d	The average distance between two neighbouring parking spaces
t_{chk}	average time for passengers to check one vehicle
α	Vehicle and passenger distribution parameter
v^d	Speed of vehicles driving in direction $d \in \{in, out\}$
A_r	E-hailing vehicles' arrival rate at the platform's searching radius
b_r	Boarding rates of e-hailing vehicle
b_p	Boarding rates of buses
p_r	Parking rate of e-hailing vehicles
o_r	Outflow rates of e-hailing vehicle
o_b	Outflow rates of background traffic
o_p	Outflow rates of buses
Q^{rm}	The number of waiting passengers who haven't been assigned vacant vehicles or gotten on buses

P_p	Passengers' choice probability of bus
P_r	Passengers' choice probability of e-hailing
W_r	Perceived generalized trip cost of taking e-hailing vehicle
W_p	Perceived generalized trip cost of taking bus
Q_r^{rm}	Intended passengers number of e-hailing
Q_p^{rm}	Intended passengers number of bus
w_r^{rp}	E-hailing passengers' perceived waiting time for response
w_r^{wt}	E-hailing passengers' perceived time for rest duration
f_r	Average trip payment for the e-hailing service
β	Value of time
$\tilde{t}_r$	The driving time from being assigned an order to arriving the boundary of the demand surge area
t_r^v	Vacant driving time of e-hailing
t_r^c	Cruising for parking time of e-hailing
t_r^s	Checking time of e-hailing
t_r^o	Occupied driving time of e-hailing
w_p^{av}	Bus headway of 'arriving' the boundary of the demand surge area
w_p^{rt}	Bus passengers' 'rest' trip time
θ_p	Discomfort cost of taking bus
f_p	Average bus trip fare
$\bar{u}_p$	The average bus arrival rate at the boundary of the demand surge area during the past k minutes
C_p	Bus's passenger capacity when it is fully loaded
t_p^v	Vacant driving time of e-hailing
$\tilde{t}_p$	The bus's passenger loading time
t_r^o	Occupied driving time of e-hailing
M_r	The cumulative number of passengers successfully matched by e-hailing platform
M_p	The cumulative number of passengers successfully on boarded by bus
m_r	Matching rate of e-hailing passenger
m_p	Boarding rate of bus passenger
γ	Cruising speed discount parameter

ϕ	Passenger boarding speed
n_r^{in}	The e-hailing vehicle accumulation that into the passenger-waiting area
n_r^{out}	The e-hailing vehicle accumulation that out of the passenger-waiting area
n_p^{in}	The bus accumulation that into the passenger-waiting area
n_p^{out}	The bus accumulation that out of the passenger-waiting area
n_b^{in}	The background traffic accumulation that into the passenger-waiting area
n_b^{out}	The background traffic accumulation that out of the passenger-waiting area
P	System production
e	Passenger evacuation rate
Q_r	Cumulative passenger number transported by e-hailing
Q	Cumulative total passenger number transported
S_r	The proportion of passengers evacuated by e-hailing vehicles
n_{jam}^{in}	Jam accumulation of the 'in' direction
n_{opt}^{in}	The optimal accumulation of the 'in' direction that maximizes the production
C	Boundary capacity
I	Maximally allowed inflow rate of e-hailing vehicles and background traffic under the perimeter control strategy
$\bar{u}_r$	The actual inflow rates of e-hailing vehicles
$\bar{u}_p$	The actual inflow rates of bus
$\bar{u}_b$	The actual inflow rates of background traffic
W_r	The number of waiting e-hailing vehicles
W_p	The number of waiting bus
W_b	The number of waiting background traffic
$\tilde{u}_r$	The arrival rates of e-hailing vehicles at the gating position
$\tilde{u}_b$	The arrival rates of background traffic at the gating position
$\tilde{u}_p$	The arrival rates of buses at the gating position
$\bar{n}^{in}$	Desired vehicle accumulation of the 'in' direction
σ	Control threshold
K_P	Non-negative proportional gain
K_I	Non-negative integral gain
$\hat{I}_1$	Maximally allowed inflow rate of e-hailing vehicles and background traffic under the perimeter control strategy 1

$\hat{I}_2$	Maximally allowed inflow rate of e-hailing vehicles and background traffic under the perimeter control strategy 2
$\bar{n}_r^{pk}$	Target level for the number of parked vehicles within the area

APPENDIX B NOTATIONS FOR CHAPTER 4

a_r	Boundary arrival rate
$\bar{a}_r$	Boundary allowed inflow rate after perimeter control
T^1	Total evacuation time and total vehicle boundary queuing time at demand surge region boundary under case 1
T_q^1	Total vehicle boundary queuing time at demand surge region boundary under case 1
T^2	Total evacuation time and total vehicle boundary queuing time at demand surge region boundary under case 2
T_q^2	Total vehicle boundary queuing time at demand surge region boundary under case 2
a_r^*	Optimal inflow rate
T^*	Minimal total evacuation time
t_{jij}^d	The e-hailing driving time of the trips that is dispatched from region j and drives towards region i, which has not crossed the border and currently is driving in region j
t_{jii}^d	The e-hailing driving time of the trips that is dispatched from region j and drives towards region i, which has crossed the border and currently is driving in region i
t_{jj}^d	E-hailing driving time of the trips that is dispatched from region j and drives towards region j to pick up passenger
l_j^{d1}	Mean value dispatched trip length in region j and heading to region i
l_j^{d2}	Mean value dispatched trip length in region j and heading to region j
l_i^d	Mean value dispatched trip length in region i
v_i	Speed of vehicles driving in region i
v_j	Speed of vehicles driving in region j
t_{ji}^d	The total time of driving from region j to i with dispatched state
t_i^{cr}	Cruising for parking time of vehicles driving in region i
t_i^{pk}	Parking time of vehicles in region i

t_i^b	Total boarding time of e-hailing vehicles in region i
$\hat{t}_j^b$	Total boarding time of e-hailing vehicles in region j
l_i^o	Mean value occupied trip length in region i
t_{iji}^o	The e-hailing driving time of the trips that is occupied from region i and drives towards region j, which has not crossed the border and currently is driving in region j
t_{ijj}^o	The e-hailing driving time of the trips that is occupied from region i and drives towards region j, which has crossed the border and currently is driving in region j
t_{jj}^o	E-hailing driving time of the trips that is occupied from region j and drives towards region j
l_j^{o1}	Mean value occupied trip length in region j and starting from region i
l_j^{o2}	Mean value occupied trip length in region j and starting from region j
t_{ij}^o	The total time of driving from region i to j with occupied state
d_j	Total dispatching rate in region j
d_{ji}	Dispatching rate distributed to region i
d_{jj}	Dispatching rate distributed to region j
a_{ji}	Border arrival rate from region j to i
r_i	Cruising for parking rate in region i
p_i	Parking rate in region i
b_i	Boarding rate in region i
a_{ij}	Border arrival rate from region i to j
s_j	Passenger pick-up point arrival rate in region j
b_j	Boarding rate in region j
o_i	Outflow rate from region i
o_j	Outflow rate from region j
n_{jij}^d	Number of dispatched vehicle in region j that has been dispatched to region i, which has not crossed the border and currently in region j
n_{jii}^d	Number of dispatched vehicle in region j that has been dispatched to region i, which has crossed the border and currently in region i
n_i^{pk}	Parked e-hailing vehicles number in region i
n_i^b	Total boarding e-hailing vehicles number in region i

n_{iji}^{o}	The number of occupied vehicle in region i and drives towards region j, which has not crossed the border and currently in region i
n_{ijj}^{o}	The number of occupied vehicle in region i and drives towards region j, which has crossed the border and currently in region j
l_j	Total e-hailing vehicle supply rate to this two-region system
n_j^v	Number of vacant vehicle supply in region j
n_{jj}^{d}	The number of dispatched vehicle starting from region j and keeping running in region j
n_j^b	The number of boarding state vehicles in region j
n_{jj}^{o}	The number of occupied vehicle starting from region j
n_j^d	The total number of dispatched vehicles in region j
n_j^o	The total number of occupied vehicles in region j
n_i^d	The total number of dispatched vehicles in region i
n_i^o	The total number of occupied vehicles in region i
n_i	The total number of e-hailing vehicles in region i
n_j	The total number of e-hailing vehicles in region j
n_i^{other}	The total number of other types of vehicle besides e-hailing vehicles in region i
n_j^{other}	The total number of other types of vehicle besides e-hailing vehicles in region j
N_i	The total number of vehicles in region i
N_j	The total number of vehicles in region j
w_{ji}^{e}	The waiting time of vacant vehicles to be dispatched a new passenger from region j to region i
w_{jj}^{e}	The waiting time of vacant vehicles to be dispatched a new passenger from region j to region j
t_i^e	The e-hailing driver's total driving time of per trip that picks up passenger from region i
t_j^e	The e-hailing driver's total driving time of per trip that picks up passenger from region j
t^{rm}	The average remaining trip time in the outside region after the e-hailing vehicle has left region j

C_{ji}^{e}	The trip utility of serving region i
C_{jj}^{e}	The trip utility of serving region j
g_{ji}	Wage rate offered to the drivers who serve region i
g_{jj}	Wage rate offered to the drivers who serve region j
σ_e	Drivers' time-unit operating cost
e_{ji}	Drivers' per unit time earning of serving region i
e_{jj}	Drivers' per unit time earning of serving region j
Z	Size difference coefficient between regions i and j
z	Each subregion in region j
η	Dispersion parameter reflecting e-hailing drivers' uncertainty towards the utility of serving different region(/subregion)
P_{ji}	Idle drivers serving region i
P_{jj}^{z}	Idle drivers serving Z subregions in region j
q_{ij}^{r}	Passenger demand for e-hailing in region i
q_{jj}^{r}	Passenger demand for e-hailing in region j
w_{ij}^{p}	Passengers' expected waiting time in region i heading to region j
w_{jj}^{p}	Passengers' expected waiting time in region j heading to region j
t_{i}^{r}	The passengers' average travel time in region i
t_{j}^{r}	The passengers' average travel time in region j
σ_{iv}^{r}	E-hailing passenger's value of time of in-vehicle state
σ_{wt}^{r}	E-hailing passenger's value of time of waiting state
C_{ij}^{r}	E-hailing passenger's trip cost starting from region i
C_{jj}^{r}	E-hailing passenger's trip cost starting from region j
f_{ij}	Fare rates for trips starting from region i
f_{jj}	Fare rates for trips starting from region j
ϕ	Platform commission rate
q_{ij}	Total travel demand rate within region i heading to region j
q_{jj}	Total travel demand rate within region j heading to region j
$q_{ij}^{A,r}$	E-hailing passenger demand arrival rate within region i
$q_{jj}^{A,r}$	E-hailing passenger demand arrival rate within region j
$q_{ij}^{E,r}$	E-hailing passenger demand exit queuing rate within region i
$q_{jj}^{E,r}$	E-hailing passenger demand exit queuing rate within region j

p_{ij}^r	Waiting passenger number in region i
p_{jj}^r	Waiting passenger number in region j
h_{ij}^{other}	Passenger sharing rate of all other modes from region i to region j
Q	The cumulative number of passengers that have been transported out of the area
Q_{ij}	Total number of passengers are accumulated within the region i and waiting for transportation
$g_{ij,0}$	The coefficient for adjusting the wage g_{ij}
$g_{jj,0}$	The coefficient for adjusting the wage g_{jj}
d_j^*	The optimal value of the dispatching rate in region j
d_{ji}^*	The optimal value of the dispatching rate distributed to region i

APPENDIX C NOTATIONS FOR CHAPTER 5

$\beta_{r,0}$	The free-flow speed of the cars
$\beta_{p,0}$	The free-flow speed of the buses
$\beta_{r,r}$	The marginal effect of car on the car mean speed
$\beta_{p,r}$	The marginal effect of bus on the car mean speed
$\beta_{r,p}$	The marginal effect of car on the bus mean speed
$\beta_{p,p}$	The marginal effect of bus on the bus mean speed
n_p	The accumulation of buses
n_r	The accumulation of cars
v_r	The mean speed of the cars
v_p	The mean speed of the buses
v_r^{in}	The driving speed of e-hailing vehicles in in-direction
v_r^{out}	The driving speed of e-hailing vehicles in out-direction
v_p^{in}	The driving speed of buses in in-direction
v_p^{out}	The driving speed of buses in out-direction
t_r^d	The e-hailing vehicle driving time of dispatched state
t_p^d	The buses driving time before loading passengers
l_r^d	The e-hailing vehicle driving distance of dispatched state
l_p^d	The buses driving distance before loading passengers
t_r^{b1}	The e-hailing driver waiting for parking
t_r^{b2}	The e-hailing driver parked time to wait passengers
t_p^{b1}	The bus driver waiting for parking
t_p^{b2}	The bus driver passengers loading time
a_p	The bus average loaded passenger number
a_r	The e-hailing average loaded passenger number
t_r^o	The passenger on-board driving time of e-hailing vehicles
t_p^o	The passenger on-board driving time of buses
l_r^o	The e-hailing vehicle driving distance of occupied state
l_p^o	The buses driving distance after loading passengers

n_p^{in}	The in-direction accumulation of buses
n_p^{wb}	The wait for boarding accumulation of buses
n_p^{out}	The out-direction accumulation of buses
n_r^{in}	The in-direction accumulation of e-hailing vehicles
n_r^{wb}	The wait for boarding accumulation of e-hailing vehicles
n_r^{out}	The out-direction accumulation of e-hailing vehicles
$t_r^{d,out}$	E-hailing vehicles' coming time on the way before getting into the demand surge region
$t_p^{d,out}$	Buses' coming time on the way before getting into the demand surge region
s_r	The e-hailing supply rate
s_p	The bus supply rate
u_r	The e-hailing inflow rate
u_p	The bus inflow rate
b_r	The e-hailing boarding rate
b_p	The bus boarding rate
o_r	The e-hailing outflow rate
o_p	The bus outflow rate
Q_{out}	The cumulative number of passengers that have been transported out of the area
Q	The total number of passengers accumulated and waiting for transportation
R_r	The evacuated passenger number by e-hailing vehicles
R_p	The evacuated passenger number by bus
T	The total evacuation time
E_r	The total e-hailing vehicle number scheduled for the evacuation
E_p	The total bus number scheduled for the evacuation
C	Total generalized cost of the transportation system
C_U	Users' cost in the transportation system
C_O	Operating cost of the transportation system
C_S	Safety cost of the transportation system
β_S	The relative importance factors of safety cost in the generalized cost function of the transportation system from the perspective of traffic administrators
c_r	Perceived travel cost of each e-hailing trip

c_p	Perceived travel cost of each bus trip
C_r	E-hailing users' total perceived travel cost
C_p	Bus users' total perceived travel cost
C_e	E-hailing platform's total cost
t_p	The buses' passenger average experienced travel time from the start to leaving the demand surge area
t_r	The e-hailing passenger average experienced travel time from the start to leaving the demand surge area
N_r	The e-hailing trip number
N_p	The bus trip number
D	The total demand time series distribution function
d	The total passenger demand rate
d_r	The e-hailing passenger demand rate
d_p	The bus passenger demand rate
n_r^{wt}	The number of waiting passengers for e-hailing service
t_r^{wt}	The passengers' expected waiting time for dispatching
n_p^{rm}	The number of remaining passengers for bus
n_r^{rm}	The number of remaining passengers for e-hailing
n^{rm}	The total number of remaining passengers
t_p^{wt}	The bus passenger experienced headway
θ_p	The discomfort cost of bus
f_p	Average bus trip fare
f_r	Unit time fare for e-hailing passenger
σ^{iv}	The passenger's value of time of the in-vehicle state
σ^{wt}	The passenger's value of time of the waiting
P_p	The passenger choosing probability of bus
P_r	The passenger choosing probability of e-hailing
η	The dispersion parameter reflecting passengers' uncertainty towards the utility of choosing different modes of transportation
c_e	The cost for scheduling one e-hailing vehicles
c_r^w	The wage offered to the drivers per unit time
c_r^s	The fixed scheduling cost for every minute

c_p^s	The cost of scheduling each bus
C_O^P	Total bus scheduling cost
C_O^R	Total road space management expense
S_L	Roadway space
v_r^{b1}	The slow-moving speed of e-hailing vehicles
$DS_{v,p}$	The average minimum distance between passenger and vehicles
$SP_{v,p}$	The relative conflicting speed between vehicles and passengers
$v_{v,p}^{wk}$	The walking speed of passengers navigating through e-hailing vehicles
$m_{v,p}$	Probability that the pedestrian and the vehicle are moving in the same direction
$DS_{v,p}^*$	The threshold of average minimum distance between passenger and vehicles
$SP_{v,p}^*$	The threshold of relative conflicting speed between vehicles and passengers
$P_{v,p}$	The probability of pedestrian-vehicle conflicts
$\phi_{v,p}$	The average cost of a event of pedestrians-vehicle conflict
$c_S^{v,p}$	The safety cost of each pedestrians-vehicle conflict
$C_S^{v,p}$	The total safety cost of pedestrians-vehicle conflict
$DS_{p,p}^r$	The average minimum distance between e-hailing passengers
$SP_{p,p}^r$	The conflicting speed between e-hailing passengers
$v_{p,p,r}^{wk}$	The walking speed of passengers navigating rhtough each other for e-hailing vehicle
$m_{p,p}$	Probability that pedestrians are moving in the same direction
$P_{p,p}^r$	The probability of conflicts between e-hailing passengers
$c_S^{p,p,r}$	The safety cost of each e-hailing passengers conflict
$C_S^{v,p}$	The total safety cost of e-hailing passengers conflict
$DS_{p,p}^p$	The average minimum distance between bus passengers
$SP_{p,p}^p$	The relative conflicting speed between bus passengers
$v_{p,p,p}^{wk}$	The walking speed of passengers navigating through each other for bus
$P_{p,p}^p$	The probability of conflicts between bus passengers
$c_S^{p,p,p}$	The safety cost of each bus passengers conflict
$C_S^{p,p,p}$	The total safety cost of bus passengers conflict
$\phi_{p,p}$	The average cost of a event of pedestrians-pedestrian conflict
$DS_{p,p}^*$	The threshold of average minimum distance between passengers
$SP_{p,p}^*$	The threshold of relative conflicting speed between passengers

α_1,α_2,α_3	Coefficients of the conflict probability function
S_r	The boarding space for e-hailing
S_p	The boarding space for bus
m_L	Per unit of roadway space management expense
m_p	Per unit of bus boarding space management expense
m_r	Per unit of e-hailing boarding space management expense
F_p^S	The bus parking capacity
L_p	The length of each bus
F_p^A	The arrived bus number at the bus station
F_r^S	The e-hailing vehicles parking capacity
L_r	The length of each e-hailing vehicle
F_r^A	The arrived e-hailing vehicles number
S	The total road space in this region
S_p^1	The boarding space for bus under Scenario 1
S_L^1	The roadway space under Scenario 1
S_r^2	The boarding space for e-hailing under Scenario 2
S_p^2	The boarding space for bus under Scenario 2
S_L^2	The roadway space under Scenario 2
S_r^3	The boarding space for e-hailing under Scenario 3
S_p^3	The boarding space for bus under Scenario 3
S_L^3	The roadway space under Scenario 3
S_r^4	The boarding space for e-hailing under Scenario 4
S_p^4	The boarding space for bus under Scenario 4
S_L^4	The roadway space under Scenario 4
$C_{O,1}^R$	The total road space management expense under Scenario 1
$C_{O,4}^R$	The total road space management expense under Scenario 4
$C_{O,4}^R$	The total road space management expense under Scenario 4
$C_{O,4}^R$	The total road space management expense under Scenario 4
$DS_{p,p}$	The average minimum distance between passengers
$SP_{p,p}$	The average relative speed between passengers
$v_{p,p}^{wk}$	The walking speed of pedestrians
$P_{p,p}$	The probability of conflicts between passengers

$c_S^{p,p}$	The safety cost of each pedestrians conflict
$C_S^{p,p}$	The total safety cost of pedestrians conflict
c_r^A	Passengers' average actual perceived costs for each e-hailing trip during their evacuation
c_p^A	Passengers' average actual perceived costs for each bus trip during their evacuation
β_s	Relative importance factors of safety cost in the actual perceived cost from the perspective of each passenger

REFERENCES

Aalami, S. and Kattan, L. (2020). Fairness and efficiency in pedestrian emergency evacuation: Modeling and simulation. *Safety science*, 121:373–384.

Aalipour, A., Kebriaei, H., and Ramezani, M. (2019). Analytical optimal solution of perimeter traffic flow control based on mfd dynamics: A pontryagin's maximum principle approach. *IEEE Transactions on Intelligent Transportation Systems*, 20(9):3224–3234.

Abdel-Aty, M. A. and Radwan, A. E. (2000). Modeling traffic accident occurrence and involvement. *Accident Analysis & Prevention*, 32(5):633–642.

Aboudolas, K. and Geroliminis, N. (2013). Perimeter and boundary flow control in multi-reservoir heterogeneous networks. *Transportation Research Part B: Methodological*, 55:265–281.

AFP (2023). Yemen stampede during charity distribution kills 85. https://www.france24.com/en/live-news/20230420-yemen-stampede-during-charity-distribution-kills-85. Accessed 25-March-2024.

Agatz, N. A., Erera, A. L., Savelsbergh, M. W., and Wang, X. (2011). Dynamic ride-sharing: A simulation study in metro atlanta. *Transportation Research Part B: Methodological*, 45(9):1450–1464. Select Papers from the 19th ISTTT.

Amini, R. E., Abouelela, M., Dhamaniya, A., Friedrich, B., and Antoniou, C. (2024). A game-theoretic approach for modelling pedestrian–vehicle conflict resolutions in uncontrolled traffic environments. *Accident Analysis & Prevention*, 203:107604.

Amini, R. E., Yang, K., and Antoniou, C. (2022). Development of a conflict risk evaluation model to assess pedestrian safety in interaction with vehicles. *Accident Analysis & Prevention*, 175:106773.

Amini, S., Papapanagiotou, E., and Busch, F. (2016). Traffic management for major events. *Digital Mobility Platforms and Ecosystems*, page 187.

Amirgholy, M. and Gonzales, E. J. (2016). Demand responsive transit systems with time-dependent demand: User equilibrium, system optimum, and management strategy. *Transportation Research Part B: Methodological*, 92:234–252. Within-day Dynamics in Transportation Networks.

Amirgholy, M., Shahabi, M., and Gao, H. O. (2017). Optimal design of sustainable transit systems in congested urban networks: A macroscopic approach. *Transportation Research Part E: Logistics and Transportation Review*, 103:261–285.

Ampountolas, K., Zheng, N., and Geroliminis, N. (2017). Macroscopic modelling and robust control of bi-modal multi-region urban road networks. *Transportation Research Part B: Methodological*, 104:616–637.

Arnott, R. (2013). A bathtub model of downtown traffic congestion. *Journal of Urban Eco-*

nomics, 76:110–121.

Arnott, R. and Williams, P. (2017). Cruising for parking around a circle. *Transportation Research Part B: Methodological*, 104:357–375.

Austroads (2010). Balancing traffic density in a signalised network.

Ban, X., Dessouky, M., Pang, J.-S., and Fan, R. (2019a). A general equilibrium model for transportation systems with e-hailing services and flow congestion. *Transportation Research Part B: Methodological*, 129:273–304.

Ban, X. J., Dessouky, M., Pang, J.-S., and Fan, R. (2019b). A general equilibrium model for transportation systems with e-hailing services and flow congestion. *Transportation Research Part B: Methodological*, 129:273–304.

BangkokPost (2022). Indonesia football riot, which led to 132 deaths, caused by police tear gas. https://www.bangkokpost.com/sports/2414618/indonesia-football-riot-which-led-to-132-deaths-caused-by-police-tear-gas. Accessed 25-March-2024.

Barmpounakis, E. and Geroliminis, N. (2020). On the new era of urban traffic monitoring with massive drone data: The pneuma large-scale field experiment. *Transportation Research Part C: Emerging Technologies*, 111:50–71.

BBC (2010). Swaying footbridge 'triggered deadly cambodia stampede'. https://www.bbc.com/news/world-asia-pacific-11827313. Accessed 25-November-2024.

BBC (2017). Morocco food stampede kills 15. https://www.bbc.com/news/world-africa-42044887. Accessed 25-November-2024.

Beojone, C. V. and Geroliminis, N. (2021). On the inefficiency of ride-sourcing services towards urban congestion. *Transportation Research Part C: Emerging Technologies*, 124:120890.

Beojone, C. V. and Geroliminis, N. (2023a). A dynamic multi-region mfd model for ride-sourcing with ridesplitting. *Transportation Research Part B: Methodological*, 177:102821.

Beojone, C. V. and Geroliminis, N. (2023b). Relocation incentives for ride-sourcing drivers with path-oriented revenue forecasting based on a markov chain model. *Transportation Research Part C: Emerging Technologies*, 157:104375.

Bharadwaj, S., Ballare, S., and Chandel, M. K. (2017). Impact of congestion on greenhouse gas emissions for road transport in mumbai metropolitan region. *Transportation Research Procedia*, 25:3538–3551. World Conference on Transport Research - WCTR 2016 Shanghai. 10-15 July 2016.

Bretherton, D., Bowen, G., and Wood, K. (2002). *EFFECTIVE URBAN TRAFFIC MANAGEMENT AND CONTROL - SCOOT VERSION 4.4*. EFFECTIVE URBAN TRAFFIC MANAGEMENT AND CONTROL - SCOOT VERSION 4.4.

Castillo, J. C., Knoepfle, D., and Weyl, G. (2017). Surge pricing solves the wild goose chase. In *Proceedings of the 2017 ACM Conference on Economics and Computation*, EC '17, page 241–242, New York, NY, USA. Association for Computing Machinery.

Chen, C., Sun, H., Lei, P., Zhao, D., and Shi, C. (2021a). An extended model for crowd evac-

uation considering pedestrian panic in artificial attack. *Physica A: Statistical Mechanics and its Applications*, 571:125833.

Chen, J., Shi, T., and Li, N. (2021b). Pedestrian evacuation simulation in indoor emergency situations: Approaches, models and tools. *Safety science*, 142:105378.

Chen, L. and Miller-Hooks, E. (2012). Resilience: An indicator of recovery capability in intermodal freight transport. *Transportation Science*, 46(1):109–123.

Chen, M., Chen, L., and Miller-Hooks, E. (2007). Traffic signal timing for urban evacuation. *Journal of Urban Planning and Development*, 133(1):30–42.

Chen, X., Li, H., Miao, J., Jiang, S., and Jiang, X. (2017). A multiagent-based model for pedestrian simulation in subway stations. *Simulation Modelling Practice and Theory*, 71:134–148.

Chen, Y. Z., Shen, S. F., Chen, T., and Yang, R. (2014). Path optimization study for vehicles evacuation based on dijkstra algorithm. *Procedia Engineering*, 71:159–165. 2013 International Conference on Performance-based Fire and Fire Protection Engineering, Wuhan (ICPFFPE 2013).

Chiabaut, N. (2015). Evaluation of a multimodal urban arterial: the passenger macroscopic fundamental diagram. *Transportation Research Part B: Methodological*, 81:410–420.

Chiabaut, N., Xie, X., and Leclercq, L. (2014). Performance analysis for different designs of a multimodal urban arterial. *Transportmetrica B: Transport Dynamics*, 2:229–245.

ChinaDaily (2015). 36 killed, 47 injured in new year stampede in shanghai. https://www.chinadaily.com.cn/china/2015-01/01/content_19211508_2.htm. Accessed 25-November-2024.

Choudhary, A. and Gokhale, S. (2016). Urban real-world driving traffic emissions during interruption and congestion. *Transportation Research Part D: Transport and Environment*, 43:59–70.

Christofa, E., Papamichail, I., Skabardonis, and A. (2013). Person-based traffic responsive signal control optimization. *IEEE transactions on intelligent transportation systems*, 14(3):1278–1289.

Christofa, E., Ampountolas, K., and Skabardonis, A. (2016a). Arterial traffic signal optimization: A person-based approach. *Transportation Research Part C Emerging Technologies*, 66(May):27–47.

Christofa, E., Ampountolas, K., and Skabardonis, A. (2016b). Arterial traffic signal optimization: A person-based approach. *Transportation Research Part C: Emerging Technologies*, 66:27–47.

Christofa, E. and Skabardonis, A. (2011). Traffic signal optimization with application of transit signal priority to an isolated intersection. *Transportation Research Record*, 2259(1):192–201.

Clewlow, R. R. and Mishra, G. S. (2017). Disruptive transportation: The adoption, utilization, and impacts of ride-hailing in the united states. Technical report, Institute of Transportation Studies, UC Davis.

Code, L. S. (2012). Nfpa 101 life safety code.

Daganzo, C. F. (1981). *EQUILIBRIUM MODEL FOR CARPOOLS ON AN URBAN NETWORK*. EQUILIBRIUM MODEL FOR CARPOOLS ON AN URBAN NETWORK.

Daganzo, C. F. (2007). Urban gridlock: Macroscopic modeling and mitigation approaches. *Transportation Research Part B: Methodological*, 41(1):49–62.

Daganzo, C. F., Gayah, V. V., and Gonzales, E. J. (2011). Macroscopic relations of urban traffic variables: Bifurcations, multivaluedness and instability. *Transportation Research Part B: Methodological*, 45(1):278–288.

Daganzo, C. F., Gayah, V. V., and Gonzales, E. J. (2012). The potential of parsimonious models for understanding large scale transportation systems and answering big picture questions. *EURO Journal on Transportation and Logistics*, 1(1):47–65.

Di, X. and Ban, X. J. (2019). A unified equilibrium framework of new shared mobility systems. *Transportation Research Part B: Methodological*, 129:50–78.

Di, X., Ma, R., Liu, H. X., and Ban, X. J. (2018a). A link-node reformulation of ridesharing user equilibrium with network design. *Transportation Research Part B: Methodological*, 112:230–255.

Di, Z., Yang, L., Qi, J., and Gao, Z. (2018b). Transportation network design for maximizing flow-based accessibility. *Transportation Research Part B: Methodological*, 110:209–238.

Ding, H., Zhang, Y., Zheng, X., Yuan, H., and Zhang, W. H. (2018). Hybrid perimeter control for two-region urban cities with different states. *IEEE Transactions on Control Systems Technology*, 26(6):2049–2062.

Djavadian, S. and Chow, J. Y. (2017). An agent-based day-to-day adjustment process for modeling 'mobility as a service' with a two-sided flexible transport market. *Transportation Research Part B: Methodological*, 104:36–57.

Ercolano, J. (2008). Pedestrian disaster preparedness and emergency management of mass evacuations on foot: State-of-the-art and best practices. *Journal of Applied Security Research*, 3(3-4):389–405.

Fosgerau, M. (2015). Congestion in the bathtub. *Economics of Transportation*, 4(4):241–255.

Fruin, J. J. (1971). Pedestrian planning and design. Technical report.

Fu, H., Liu, N., and Hu, G. (2017). Hierarchical perimeter control with guaranteed stability for dynamically coupled heterogeneous urban traffic. *Transportation Research Part C: Emerging Technologies*, 83:18–38.

Geroliminis, N. (2015). Cruising-for-parking in congested cities with an mfd representation. *Economics of Transportation*, 4:156–165.

Geroliminis, N. and Daganzo, C. F. (2008). Existence of urban-scale macroscopic fundamental diagrams: Some experimental findings. *Transportation Research Part B: Methodological*, 42(9):759–770.

Geroliminis, N., Haddad, J., and Ramezani, M. (2012). Optimal perimeter control for two

urban regions with macroscopic fundamental diagrams: A model predictive approach. *IEEE Transactions on Intelligent Transportation Systems*, 14(1):348–359.

Geroliminis, N., Zheng, N., and Ampountolas, K. (2014). A three-dimensional macroscopic fundamental diagram for mixed bi-modal urban networks. *Transportation Research Part C: Emerging Technologies*, 42:168–181.

Godfrey, J. (1969). The mechanism of a road network. *Traffic Engineering & Control*, 8(8).

Gonzales, E. J. and Daganzo, C. F. (2012). Morning commute with competing modes and distributed demand: User equilibrium, system optimum, and pricing. *Transportation Research Part B: Methodological*, 46(10):1519–1534.

Green, L. V. and Kolesar, P. J. (2004). Anniversary article: Improving emergency responsiveness with management science. *Management Science*, 50(8):1001–1014.

Gu, Z., Li, Y., Saberi, M., Rashidi, T. H., and Liu, Z. (2023). Macroscopic parking dynamics and equitable pricing: Integrating trip-based modeling with simulation-based robust optimization. *Transportation Research Part B: Methodological*, 173:354–381.

Gu, Z., Najmi, A., Saberi, M., Liu, W., and Rashidi, T. H. (2020). Macroscopic parking dynamics modeling and optimal real-time pricing considering cruising-for-parking. *Transportation Research Part C: Emerging Technologies*, 118:102714.

Haddad, J. (2015). Robust constrained control of uncertain macroscopic fundamental diagram networks. *Transportation Research Part C: Emerging Technologies*, 59:323–339. Special Issue on International Symposium on Transportation and Traffic Theory.

Haddad, J. (2017a). Optimal coupled and decoupled perimeter control in one-region cities. *Control Engineering Practice*, 61:134–148.

Haddad, J. (2017b). Optimal perimeter control synthesis for two urban regions with aggregate boundary queue dynamics. *Transportation Research Part B: Methodological*, 96:1–25.

Haddad, J. and Geroliminis, N. (2012). On the stability of traffic perimeter control in two-region urban cities. *Transportation Research Part B: Methodological*, 46(9):1159–1176.

Haddad, J. and Mirkin, B. (2016). Adaptive perimeter traffic control of urban road networks based on mfd model with time delays. *International Journal of Robust and Nonlinear Control*, 26(6):1267–1285.

Haddad, J., Ramezani, M., and Geroliminis, N. (2013). Cooperative traffic control of a mixed network with two urban regions and a freeway. *Transportation Research Part B: Methodological*, 54:17–36.

Haddad, J. and Shraiber, A. (2014). Robust perimeter flow control design for an urban region. *Transportation Research Part B: Methodological*, 68:315–332.

Haddad, J. and Zheng, Z. (2020). Adaptive perimeter control for multi-region accumulation-based models with state delays. *Transportation Research Part B: Methodological*, 137:133–153. Advances in Network Macroscopic Fundamental Diagram (NMFD) Research.

Haghani, M., Sarvi, M., and Shahhoseini, Z. (2020). Evacuation behaviour of crowds under

high and low levels of urgency: Experiments of reaction time, exit choice and exit-choice adaptation. *Safety Science*, 126:104679.

Hajiahmadi, M., Haddad, J., De Schutter, B., and Geroliminis, N. (2015). Optimal hybrid perimeter and switching plans control for urban traffic networks. *IEEE Transactions on Control Systems Technology*, 23(2):464–478.

Hakkert, A. S. and Mahalel, D. (1978). Estimating the number of accidents at intersections from a knowledge of the traffic flows on the approaches. *Accident Analysis & Prevention*, 10(1):69–79.

He, F. and Shen, Z.-J. M. (2015). Modeling taxi services with smartphone-based e-hailing applications. *Transportation Research Part C: Emerging Technologies*, 58:93–106.

He, F., Wang, X., Lin, X., and Tang, X. (2018). Pricing and penalty/compensation strategies of a taxi-hailing platform. *Transportation Research Part C: Emerging Technologies*, 86:263–279.

He, M., Chen, C., Zheng, F., Chen, Q., Zhang, J., Yan, H., and Lin, Y. (2021). An efficient dynamic route optimization for urban flooding evacuation based on cellular automata. *Computers, Environment and Urban Systems*, 87:101622.

HEI (2010). Traffic-related air pollution: A critical review of the literature on emissions, exposure, and health effects. *Health Effects Institute*.

Helbing, D. and Mukerji, P. (2012). Crowd disasters as systemic failures: analysis of the love parade disaster. *EPJ Data Science*, 1(1):1–40.

Hoffmann, K., Ipeirotis, P., and Sundararajan, A. (2016). Ridesharing and the use of public transportation.

Hsieh, Y.-H., Ngai, K. M., Burkle, F. M., and Hsu, E. B. (2009). Epidemiological characteristics of human stampedes. *Disaster Medicine and Public Health Preparedness*, 3(4):217–223.

Hu, J., Park, B. B., and Lee, Y.-J. (2016). Transit signal priority accommodating conflicting requests under connected vehicles technology. *Transportation research, Part C. Emerging technologies*, 69C(Aug.):173–192.

Hu, X., Lin, W., Wang, J., and Jiang, J. (2022). Choice of ride-hailing or traditional taxi services: From travelers' perspectives. *Research in Transportation Business & Management*, 43:100788.

Ibeas, Á., dell'Olio, L., Alonso, B., and Sainz, O. (2010). Optimizing bus stop spacing in urban areas. *Transportation Research Part E: Logistics and Transportation Review*, 46(3):446–458.

Ihssian, A. and Ismail, K. (2023). Modelling pedestrian safety at urban intersections using user perception. *Accident Analysis & Prevention*, 180:106912.

Ikeda, Y. and Inoue, M. (2016). An evacuation route planning for safety route guidance system after natural disaster using multi-objective genetic algorithm. *Procedia Computer Science*, 96:1323–1331. Knowledge-Based and Intelligent Information & Engineering Systems: Proceedings of the 20th International Conference KES-2016.

Ingole, D., Mariotte, G., and Leclercq, L. (2020). Perimeter gating control and citywide dy-

namic user equilibrium: A macroscopic modeling framework. *Transportation Research Part C: Emerging Technologies*, 111:22–49.

Irannezhad, E. and Mahadevan, R. (2022). Examining factors influencing the adoption of solo, pooling and autonomous ride-hailing services in australia. *Transportation Research Part C: Emerging Technologies*, 136:103524.

Jahangiri, A., Afandizadeh, S., and Kalantari, N. (2011). The optimization of traffic signal timing for emergency evacuation using the simulated annealing algorithm. *Transport*, 26(2):133–140.

Jaydarifard, S., Behara, K., Baker, D., and Paz, A. (2024). Driver fatigue in taxi, ride-hailing, and ridesharing services: a systematic review. *Transport Reviews*.

Jin, J. G., Tang, L. C., Sun, L., and Lee, D.-H. (2014). Enhancing metro network resilience via localized integration with bus services. *Transportation Research Part E: Logistics and Transportation Review*, 63:17–30.

Jin, J. G., Teo, K. M., and Odoni, A. R. (2016). Optimizing bus bridging services in response to disruptions of urban transit rail networks. *Transportation Science*, 50(3):790–804.

Ke, J., Cen, X., Yang, H., Chen, X., and Ye, J. (2019). Modelling drivers' working and recharging schedules in a ride-sourcing market with electric vehicles and gasoline vehicles. *Transportation Research Part E: Logistics and Transportation Review*, 125:160–180.

Ke, J., Zheng, H., Yang, H., and Chen, X. M. (2017). Short-term forecasting of passenger demand under on-demand ride services: A spatio-temporal deep learning approach. *Transportation Research Part C: Emerging Technologies*, 85:591–608.

Kepaptsoglou, K. and Karlaftis, M. (2009). Transit route network design problem: Review. *Journal of Transportation Engineering*, 135(8):491–505.

Kershner, I., Nagourney, E., and Ives, M. (2021). Stampede at israel religious celebration kills at least 45. https://www.nytimes.com/2021/04/29/world/middleeast/israel-mount-meron-stampede.html. Accessed 25-March-2024.

Keyvan-Ekbatani, M., Kouvelas, A., Papamichail, I., and Papageorgiou, M. (2012). Exploiting the fundamental diagram of urban networks for feedback-based gating. *Transportation Research Part B: Methodological*, 46(10):1393–1403.

Keyvan-Ekbatani, M., Papageorgiou, M., and Knoop, V. L. (2015). Controller design for gating traffic control in presence of time-delay in urban road networks. *Transportation Research Part C: Emerging Technologies*, 59:308–322. Special Issue on International Symposium on Transportation and Traffic Theory.

Kim, B. (2022). Over 150 dead in crowd crush in itaewon halloween festivities. https://world.kbs.co.kr/service/news_view.htm?lang=e&Seq_Code=173416. Accessed 25-March-2024.

Kim, K. M., Hong, S.-P., Ko, S.-J., and Kim, D. (2015). Does crowding affect the path choice of metro passengers? *Transportation Research Part A: Policy and Practice*, 77:292–304.

Knoop, V., Hoogendoorn, S., and Van Lint, J. (2012). Routing strategies based on macroscopic

fundamental diagram. *Transportation Research Record*, 2315(1):1–10.

Kouvelas, A., Lioris, J., Fayazi, S. A., and Varaiya, P. (2014). Maximum pressure controller for stabilizing queues in signalized arterial networks. *Transportation Research Record*, 2421(1):133–141.

Kouvelas, A., Saeedmanesh, M., and Geroliminis, N. (2017). A linear formulation for model predictive perimeter traffic control in cities. *IFAC-PapersOnLine*, 50:8543–8548.

Kraidi, R. and Evdorides, H. (2020). Pedestrian safety models for urban environments with high roadside activities. *Safety Science*, 130:104847.

Krausz, B. and Bauckhage, C. (2012). Loveparade 2010: Automatic video analysis of a crowd disaster. *Computer Vision and Image Understanding*, 116(3):307–319.

Lamotte, R. and Geroliminis, N. (2018). The morning commute in urban areas with heterogeneous trip lengths. *Transportation Research Part B: Methodological*, 117:794–810. TRB:ISTTT-22.

Lamotte, R., Murashkin, M., Kouvelas, A., and Geroliminis, N. (2018). Dynamic modeling of trip completion rate in urban areas with mfd representations.

Leclercq, L., Sénécat, A., and Mariotte, G. (2017). Dynamic macroscopic simulation of on-street parking search: A trip-based approach. *Transportation Research Part B: Methodological*, 101:268–282.

Lei, C., Jiang, Z., and Ouyang, Y. (2020). Path-based dynamic pricing for vehicle allocation in ridesharing systems with fully compliant drivers. *Transportation Research Part B: Methodological*, 132:60–75. 23rd International Symposium on Transportation and Traffic Theory (ISTTT 23).

Li, M., Di, X., Liu, H. X., and Huang, H.-J. (2020a). A restricted path-based ridesharing user equilibrium. *Journal of Intelligent Transportation Systems*, 24(4):383–403.

Li, X., Li, Q., Xu, X., Xu, D., and Zhang, X. (2018). A novel approach to developing organized multi-speed evacuation plans. *Transactions in GIS*, 22(5):1205–1220.

Li, Y. and Liu, Y. (2021). Optimizing flexible one-to-two matching in ride-hailing systems with boundedly rational users. *Transportation Research Part E: Logistics and Transportation Review*, 150:102329.

Li, Y., Liu, Y., and Xie, J. (2020b). A path-based equilibrium model for ridesharing matching. *Transportation Research Part B: Methodological*, 138:373–405.

Liu, Q. (2018). The effect of dedicated exit on the evacuation of heterogeneous pedestrians. *Physica A: Statistical Mechanics and its Applications*, 506:305–323.

Liu, W. and Geroliminis, N. (2016). Modeling the morning commute for urban networks with cruising-for-parking: An mfd approach. *Transportation Research Part B: Methodological*, 93:470–494.

Liu, W. and Geroliminis, N. (2017). Doubly dynamics for multi-modal networks with park-and-ride and adaptive pricing. *Transportation Research Part B: Methodological*, 102:162–179.

Liu, Y. and Li, Y. (2017). Pricing scheme design of ridesharing program in morning commute problem. *Transportation Research Part C: Emerging Technologies*, 79:156–177.

Loder, Allister and, A. L., Menendez, M., and Axhausen, K. W. (2017). Empirics of multimodal traffic networks – using the 3d macroscopic fundamental diagram. *Transportation Research Part C: Emerging Technologies*, 82:88–101.

Long, J., Tan, W., Szeto, W., and Li, Y. (2018). Ride-sharing with travel time uncertainty. *Transportation Research Part B: Methodological*, 118:143–171.

Lu, W. and Quadrifoglio, L. (2019). Fair cost allocation for ridesharing services – modeling, mathematical programming and an algorithm to find the nucleolus. *Transportation Research Part B: Methodological*, 121:41–55.

Marcianò, F. A., Musolino, G., and Vitetta, A. (2015). Signal setting optimization on urban road transport networks: The case of emergency evacuation. *Safety Science*, 72:209–220.

Mariotte, G., Leclercq, L., and Laval, J. A. (2017). Macroscopic urban dynamics: Analytical and numerical comparisons of existing models. *Transportation Research Part B: Methodological*, 101:245–267.

Mascia, M., Hu, S., Han, K., North, R., Van Poppel, M., Theunis, J., Beckx, C., and Litzenberger, M. (2017). Impact of traffic management on black carbon emissions: a microsimulation study. *Networks and Spatial Economics*, 17:269–291.

Matherly, D., Langdon, N., Wolshon, B., Murray-Tuite, P., Renne, J., Thomas, R., Mobley, J., and Reinhardt, K. (2014). *A guide to regional transportation planning for disasters, emergencies, and significant events*. Number Project 20-59 (42).

Matherly, D., Murray-Tuite, P., and Wolshon, B. (2015). Traffic management for planned, unplanned, and emergency events. *Traffic Engineering Handbook: Institute of Transportation Engineers*, pages 599–636.

Menelaou, C., Kolios, P., Timotheou, S., Panayiotou, C., and Polycarpou, M. (2017). Controlling road congestion via a low-complexity route reservation approach. *Transportation Research Part C: Emerging Technologies*, 81:118–136.

Menelaou, C., Timotheou, S., Kolios, P., Panayiotou, C. G., and Polycarpou, M. M. (2019). Minimizing traffic congestion through continuous-time route reservations with travel time predictions. *IEEE Transactions on Intelligent Vehicles*, 4(1):141–153.

Mileti, D. S. and Sorensen, J. H. (1990). Communication of emergency public warnings: A social science perspective and state-of-the-art assessment.

Mohajerpoor, R., Saberi, M., Vu, H. L., Garoni, T. M., and Ramezani, M. (2020). H∞ robust perimeter flow control in urban networks with partial information feedback. *Transportation Research Part B: Methodological*, 137:47–73. Advances in Network Macroscopic Fundamental Diagram (NMFD) Research.

Murashkin, M. (2021). The influence of trip length distribution on urban traffic in network-level models. page 124.

Najmi, A., Rey, D., and Rashidi, T. H. (2017). Novel dynamic formulations for real-time ride-sharing systems. *Transportation Research Part E: Logistics and Transportation Review*, 108:122–140.

Nicholas, C. (2016). Experimentation in a ridesharing marketplace.

Nie, Y. M. (2017). How can the taxi industry survive the tide of ridesourcing? evidence from shenzhen, china. *Transportation Research Part C: Emerging Technologies*, 79:242–256.

Nourinejad, M. and Ramezani, M. (2020). Ride-sourcing modeling and pricing in non-equilibrium two-sided markets. *Transportation Research Part B: Methodological*, 132:340–357.

Ommeren, J. N., McIvor, M., Mulalic, I., and Inci, E. (2021). A novel methodology to estimate cruising for parking and related external costs. *Transportation Research Part B: Methodological*, 145:247–269.

Ommeren, J. N., Wentink, D., and Rietveld, P. (2012). Empirical evidence on cruising for parking. *Transportation Research Part A: Policy and Practice*, 46:123–130.

Osama, A. and Sayed, T. (2017). Investigating the effect of spatial and mode correlations on active transportation safety modeling. *Analytic Methods in Accident Research*, 16:60–74.

Parr, S. A. and Kaisar, E. (2011). Critical intersection signal optimization during urban evacuation utilizing dynamic programming. *Journal of Transportation Safety & Security*, 3(1):59–76.

Paudel, D. and Das, T. K. (2023). Infrastructure planning for ride-hailing services using shared autonomous electric vehicles. *International Journal of Sustainable Transportation*, 17(10):1139–1154.

Pereira, R. H., Herszenhut, D., Saraiva, M., and Farber, S. (2024). Ride-hailing and transit accessibility considering the trade-off between time and money. *Cities*, 144:104663.

Perry, R. W. and Lindell, M. K. (2003). Preparedness for emergency response: Guidelines for the emergency planning process. *Disasters*, 27(4):336–350.

Ramezani, M., Haddad, J., and Geroliminis, N. (2015). Dynamics of heterogeneity in urban networks: aggregated traffic modeling and hierarchical control. *Transportation Research Part B: Methodological*, 74:1–19.

Ramezani, M. and Nourinejad, M. (2018). Dynamic modeling and control of taxi services in large-scale urban networks: A macroscopic approach. *Transportation Research Part C: Emerging Technologies*, 94:203–219.

Rashidi, E., Parsafard, M., Medal, H., and Li, X. (2016). Optimal traffic calming: A mixed-integer bi-level programming model for locating sidewalks and crosswalks in a multimodal transportation network to maximize pedestrians' safety and network usability. *Transportation Research Part E: Logistics and Transportation Review*, 91:33–50.

Ren, G., Huang, Z., Cheng, Y., Zhao, X., and Zhang, Y. (2013). An integrated model for evacuation routing and traffic signal optimization with background demand uncertainty. *Journal*

of Advanced Transportation, 47(1):4–27.

Reuters (2019). Five people killed in stampede at algiers rap concert. https://www.reuters.com/article/world/five-people-killed-in-stampede-at-algiers-rap-concert-idUSKCN1VD015/. Accessed 25-November-2024.

Ribeiro, M. D., Lucchesi, S. T., Larranaga, A. M., Lavieri, P. S., and Cheng, Y.-T. (2024). Analyzing the relationship between bus and ride-hailing use in a large emerging economy city: A bivariate ordered probit model application. *Journal of Public Transportation*, 26:100084.

Saberi, M., Hamedmoghadam, H., Ashfaq, M., Hosseini, S. A., Gu, Z., Shafiei, S., Nair, D. J., Dixit, V., Gardner, L., Waller, S. T., and González, M. C. (2020). A simple contagion process describes spreading of traffic jams in urban networks. *Nature Communications*, 11.

Saeedmanesh, M. and Geroliminis, N. (2016). Clustering of heterogeneous networks with directional flows based on "snake" similarities. *Transportation Research Part B: Methodological*, 91:250–269.

Santos, D. O. and Xavier, E. C. (2013). Dynamic taxi and ridesharing: A framework and heuristics for the optimization problem. In *Twenty-Third International Joint Conference on Artificial Intelligence*.

Schaller, B. (2017). Unsustainable? the growth of app-based ride services and traffic, travel and the future of new york city. *Schaller Consulting*.

Seriani, S. and Fernandez, R. (2015). Pedestrian traffic management of boarding and alighting in metro stations. *Transportation Research Part C: Emerging Technologies*, 53:76–92.

Shahhoseini, Z. and Sarvi, M. (2019). Pedestrian crowd flows in shared spaces: Investigating the impact of geometry based on micro and macro scale measures. *Transportation Research Part B: Methodological*, 122:57–87.

Shahparvari, S., Abbasi, B., Chhetri, P., and Abareshi, A. (2019). Fleet routing and scheduling in bushfire emergency evacuation: A regional case study of the black saturday bushfires in australia. *Transportation Research Part D: Transport and Environment*, 67:703–722.

Shandilya, S. (2024). Hathras satsang stampede: Over 130 died at religious congregation in uttar pradesh; a look at similar incidents in past. https://english.jagran.com/india/hathras-satsang-stampede-people-died-during-congregation-by-vishwa-hari-bhole-baba-a-look-at-similar-incidents-in-past-10170988. Accessed 25-March-2024.

Shen, Y., Liao, J., Zheng, N., Cui, Z., Guo, Z., and Shan, W. (2023). Aggregated modeling for multimodal traffic flow and dispatching control in urban road networks with ride-sharing services. *Journal of Transportation Engineering, Part A: Systems*, 149(12):04023115.

Shiwakoti, N., Liu, Z., Hopkins, T., and Young, W. (2013). An overview on multimodal emergency evacuation in an urban network. In *Australasian Transport Research Forum*, pages 1–10.

Shoup, D. C. (2006). Cruising for parking. *Transport Policy*, 13:479–486.

Sirmatel, I. I. and Geroliminis, N. (2020). Nonlinear moving horizon estimation for large-scale

urban road networks. *IEEE Transactions on Intelligent Transportation Systems*, 21(12):4983–4994.

Sirmatel, I. I. and Geroliminis, N. (2021). Stabilization of city-scale road traffic networks via macroscopic fundamental diagram-based model predictive perimeter control. *Control Engineering Practice*, 109:104750.

Sirmatel, I. I., Tsitsokas, D., Kouvelas, A., and Geroliminis, N. (2021). Modeling, estimation, and control in large-scale urban road networks with remaining travel distance dynamics. *Transportation Research Part C: Emerging Technologies*, 128:103157.

Sivakumaran, K., Li, Y., Cassidy, M., and Madanat, S. (2014). Access and the choice of transit technology. *Transportation Research Part A: Policy and Practice*, 59:204–221.

Smith, A. (2013). India temple stampede: Death toll reaches 115 as rescue operation ends. https://www.nbcnews.com/news/world/india-temple-stampede-death-toll-reaches-115-rescue-operation-ends-flna8c11388181. Accessed 25-November-2024.

Still, G. K. (2000). *Crowd dynamics*. PhD thesis, University of Warwick UK.

Su, H., Wang, X., Liu, W., Zhang, X., and Xu, M. (2024a). Modelling and accelerating the passenger evacuation process in a bi-modal system with bus and e-hailing modes after mass gathering events. *Travel Behaviour and Society*, 35:100713.

Su, H., Xu, M., Wang, X., and Zhang, X. (2024b). A region-dependent e-hailing service pricing strategy for rapid massive evacuation. *Transportation Research Part D: Transport and Environment*, 136:104399.

Su, J. and Sze, N. (2022). Safety of walking trips accessing to public transportation: A bayesian spatial model in hong kong. *Travel Behaviour and Society*, 29:125–135.

Sun, X., Wandelt, S., Hansen, M., and Li, A. (2017). Multiple airport regions based on inter-airport temporal distances. *Transportation Research Part E: Logistics and Transportation Review*, 101(MAY):84–98.

Szeto, W. and Wu, Y. (2011). A simultaneous bus route design and frequency setting problem for tin shui wai, hong kong. *European Journal of Operational Research*, 209(2):141–155.

Tamakloe, R., Hong, J., Tak, J., and Park, D. (2021). Finding evacuation routes using traffic and network structure information. *Transportation Research Part D: Transport and Environment*, 95:102853.

TheGuardian (2021). Astroworld: deaths of 10 people at houston concert ruled accidental. https://www.theguardian.com/music/2021/dec/16/astroworld-festival-deaths-ruled-accidental. Accessed 25-March-2024.

Tong, L., Zhou, X., and Miller, H. J. (2015). Transportation network design for maximizing space–time accessibility. *Transportation Research Part B: Methodological*, 81:555–576.

Tsitsokas, D., Kouvelas, A., and Geroliminis, N. (2023). Two-layer adaptive signal control framework for large-scale dynamically-congested networks: Combining efficient max pressure with perimeter control. *Transportation Research Part C: Emerging Technologies*,

152:104128.

Uber (2018). How surge pricing works. *Uber*.

Vermuyten, H., Beliën, J., De Boeck, L., Reniers, G., and Wauters, T. (2016). A review of optimisation models for pedestrian evacuation and design problems. *Safety science*, 87:167–178.

Wang, D., Miwa, T., and Morikawa, T. (2022). Interrelationships between traditional taxi services and online ride-hailing: empirical evidence from xiamen, china. *Sustainable Cities and Society*, 83:103924.

Wang, H. and Yang, H. (2019). Ridesourcing systems: A framework and review. *Transportation Research Part B: Methodological*, 129:122–155.

Wang, J.-P., Ban, X., and Huang, H.-J. (2019). Dynamic ridesharing with variable-ratio charging-compensation scheme for morning commute. *Transportation Research Part B: Methodological*, 122:390–415.

Wang, X., Agatz, N., and Erera, A. (2018). Stable matching for dynamic ride-sharing systems. *Transportation Science*, 52(4):850–867.

Wang, X., He, F., Yang, H., and Gao, H. O. (2016). Pricing strategies for a taxi-hailing platform. *Transportation Research Part E: Logistics and Transportation Review*, 93:212–231.

Wang, X., Liu, W., Yang, H., Wang, D., and Ye, J. (2020). Customer behavioural modelling of order cancellation in coupled ride-sourcing and taxi markets. *Transportation Research Part B: Methodological*, 132:358–378.

Wang, X., Wang, J., Guo, L., Liu, W., and Zhang, X. (2021). A convex programming approach for ridesharing user equilibrium under fixed driver/rider demand. *Transportation Research Part B: Methodological*, 149:33–51.

Wang, Y., Lv, C., Nie, Q., and Liu, H. (2024a). Analyzing the impact of road accidents on carbon dioxide emissions in freeway traffic: A simulation and statistical modeling approach. *Sustainability*, 16(5).

Wang, Z., Ke, J., and Li, S. (2024b). Planning and operation of ride-hailing networks with a mixture of level-4 autonomous vehicles and for-hire human drivers. *Transportation Research Part C: Emerging Technologies*, 160:104541.

Wardrop, J. G. (1952). Road paper. some theoretical aspects of road traffic research. *Proceedings of the Institution of Civil Engineers*, 1(3):325–362.

Wei, B., Saberi, M., Zhang, F., Liu, W., and Waller, S. T. (2020). Modeling and managing ridesharing in a multi-modal network with an aggregate traffic representation: a doubly dynamical approach. *Transportation Research Part C: Emerging Technologies*, 117:102670.

Wong, K., Wong, S., and Yang, H. (2001). Modeling urban taxi services in congested road networks with elastic demand. *Transportation Research Part B: Methodological*, 35(9):819–842.

Wong, K., Wong, S., Yang, H., and Wu, J. (2008). Modeling urban taxi services with mul-

tiple user classes and vehicle modes. *Transportation Research Part B: Methodological*, 42(10):985–1007.

Wood, K., Bretherton, D., Maxwell, A., Smith, K., and Bowen, G. (2002). Improved traffic management and bus priority with scoot. *Trl Staff Paper Pa*.

Xiao, D., Ding, H., Sze, N., and Zheng, N. (2024). Investigating built environment and traffic flow impact on crash frequency in urban road networks. *Accident Analysis & Prevention*, 201:107561.

Xie, W., Lee, E. W. M., Li, T., Shi, M., Cao, R., and Zhang, Y. (2021). A study of group effects in pedestrian crowd evacuation: Experiments, modelling and simulation. *Safety Science*, 133:105029.

Xu, H., Ordóñez, F., and Dessouky, M. (2015a). A traffic assignment model for a ridesharing transportation market. *Journal of Advanced Transportation*, 49(7):793–816.

Xu, H., Pang, J.-S., Ordóñez, F., and Dessouky, M. (2015b). Complementarity models for traffic equilibrium with ridesharing. *Transportation Research Part B: Methodological*, 81:161–182.

Xu, K., Saberi, M., and Liu, W. (2022). Dynamic pricing and penalty strategies in a coupled market with ridesourcing service and taxi considering time-dependent order cancellation behaviour. *Transportation Research Part C: Emerging Technologies*, 138:103621.

Xu, Z., Yin, Y., and Ye, J. (2019). On the supply curve of ride-hailing systems. *Transportation Research Procedia*, 38:37–55. Journal of Transportation and Traffic Theory.

Yang, H., Leung, C. W., Wong, S., and Bell, M. G. (2010). Equilibria of bilateral taxi–customer searching and meeting on networks. *Transportation Research Part B: Methodological*, 44(8):1067–1083.

Yang, H., Shao, C., Wang, H., and Ye, J. (2020). Integrated reward scheme and surge pricing in a ridesourcing market. *Transportation Research Part B: Methodological*, 134:126–142.

Yang, H. and Wong, S. (1998). A network model of urban taxi services. *Transportation Research Part B: Methodological*, 32(4):235–246.

Yang, H., Wong, S., and Wong, K. (2002). Demand–supply equilibrium of taxi services in a network under competition and regulation. *Transportation Research Part B: Methodological*, 36(9):799–819.

Yang, H. and Yang, T. (2011). Equilibrium properties of taxi markets with search frictions. *Transportation Research Part B: Methodological*, 45(4):696–713.

Yi, J., Pan, S., and Chen, Q. (2020). Simulation of pedestrian evacuation in stampedes based on a cellular automaton model. *Simulation Modelling Practice and Theory*, 104:102147.

Yildirimoglu, M., Ramezani, M., and Geroliminis, N. (2015). Equilibrium analysis and route guidance in large-scale networks with mfd dynamics. *Transportation Research Procedia*, 9:185–204.

Zakharenko, R. (2016). The time dimension of parking economics. *Transportation Research Part B: Methodological*, 91:211–228.

Zeng, M., Wang, M., Chen, Y., and Yang, Z. (2021). Dynamic evacuation optimization model based on conflict-eliminating cell transmission and split delivery vehicle routing. *Safety Science*, 137:105166.

Zha, L., Yin, Y., and Yang, H. (2016). Economic analysis of ride-sourcing markets. *Transportation Research Part C: Emerging Technologies*, 71:249–266.

Zhai, G., Xie, K., Yang, H., and Yang, D. (2023). Are ride-hailing services safer than taxis? a multivariate spatial approach with accommodation of exposure uncertainty. *Accident Analysis & Prevention*, 193:107281.

Zhang, F. and Liu, W. (2020). Responsive bus dispatching strategy in a multi-modal and multi-directional transportation system: A doubly dynamical approach. *Transportation Research Part C: Emerging Technologies*, 113:21–37.

Zhao, C., Liao, F., Li, X., and Du, Y. (2021). Macroscopic modeling and dynamic control of on-street cruising-for-parking of autonomous vehicles in a multi-region urban road network. *Transportation Research Part C: Emerging Technologies*, 128:103176.

Zheng, N. and Geroliminis, N. (2013). On the distribution of urban road space for multimodal congested networks. *Transportation Research Part B: Methodological*, 57:326–341.

Zheng, N. and Geroliminis, N. (2016). Modeling and optimization of multimodal urban networks with limited parking and dynamic pricing. *Transportation Research Part B: Methodological*, 83:36–58.

Zhong, R., Chen, C., Huang, Y., Sumalee, A., Lam, W., and Xu, D. (2018a). Robust perimeter control for two urban regions with macroscopic fundamental diagrams: A control-lyapunov function approach. *Transportation Research Part B: Methodological*, 117:687–707. TRB:ISTTT-22.

Zhong, R., Huang, Y., Chen, C., Lam, W., Xu, D., and Sumalee, A. (2018b). Boundary conditions and behavior of the macroscopic fundamental diagram based network traffic dynamics: A control systems perspective. *Transportation Research Part B: Methodological*, 111:327–355.

Zuniga-Garcia, N., Tec, M., Scott, J. G., Ruiz-Juri, N., and Machemehl, R. B. (2020). Evaluation of ride-sourcing search frictions and driver productivity: A spatial denoising approach. *Transportation Research Part C: Emerging Technologies*, 110:346–367.

Zuo, J., Shi, J., Li, C., Mu, T., Zeng, Y., and Dong, J. (2021). Simulation and optimization of pedestrian evacuation in high-density urban areas for effectiveness improvement. *Environmental Impact Assessment Review*, 87:106521.